

DEVELOPMENT OF NOVEL POLY(GLYCIDOL) HYDROGELS FOR APPLICATIONS IN  
REGENERATIVE MEDICINE AND DRUG DELIVERY

By

Dain Bridgeon Beezer

Dissertation

Submitted to the Faculty of the  
Graduate School of Vanderbilt University  
in partial fulfillment of the requirement  
for the degree of

DOCTOR OF PHILOSOPHY

in

Chemistry

August 31, 2017

Nashville, Tennessee

Approved:

Eva M. Harth, Ph.D.

Jeffrey N. Johnston, Ph.D.

Brian O. Bachmann, Ph.D.

Ned A. Porter, Ph.D.

To my amazing parents, Valrie and Chester,  
and  
my beloved wife Ysanne, for their constant support and unconditional love.

## ACKNOWLEDGEMENT

I would like to thank my PhD advisor, Professor Eva Harth, for supporting and encouraging me during these past four years. Professor Harth is one of the most lively, enthusiastic, and energetic persons I have ever known and I hope to someday be able to inspire students as well as she can. I am eternally grateful for her scientific advice, knowledge and many insightful discussions and suggestions over the years. I also would like to thank the members of the Harth Research Laboratory, for their support and encouragement over the years. These are some of the most talented people I have had the opportunity to work with and I am grateful for all the knowledge I gained through all the collaborative work we have done.

I would also like to thank the members of my PhD committee, Professors Jeffrey Johnston, Brian Bachmann, and Ned Porter, for their helpful career advice and suggestions in general. I also thank my collaborators Bradly Baer and Brian O'Grady for their help and instruction with the mechanical characterization of my hydrogels, and Dr. Don Stec for his help with NMR characterizations.

A solid support system is important to surviving and staying in grad school, so special thanks to my wife, Ysanne, who has been and will undoubtedly continue to be in the future, a constant source of inspiration, strength, encouragement and love. I am also very grateful to my mom and dad for seeing the potential I had in me, believing in me and never giving up on me.

Finally, I would like to say thank you to the Chemistry Department and everyone else who helped in enriching my thoughts, guiding my ideas and refining my path. I will be forever grateful to you.

## TABLE OF CONTENTS

	Page
DEDICATION .....	ii
ACKNOWLEDGEMENTS .....	iii
LIST OF TABLES .....	vi
LIST OF FIGURES .....	vii
LIST OF SCHEMES.....	xi
Chapter	
I. INTRODUCTION .....	1
Dissertation Overview .....	10
References.....	13
II. SYNTHESIS AND CHARACTERIZATION OF BRANCHED POLY(GLYCIDOL) ...	17
Introduction .....	17
Results and Discussion .....	28
Sn(OTf) <sub>2</sub> -Mediated Ring-Opening Polymerization of Glycidol.....	28
Optimization of Reaction Conditions .....	29
Characterization via NMR, GPC and MALDI-ToF MS.....	30
SEC/MALDI-ToF Mass Spectrometry Study of Branched Poly(glycidol).....	39
Cytotoxicity of Branched Poly(glycidol).....	43
Conclusion .....	45
Experimental .....	46
References.....	55
III. SYNTHESIS AND CHARACTERIZATION OF BRANCHED POLY(GLYCIDOL) DERIVATIVES .....	58
Introduction.....	58
Results and Discussion .....	64
Synthesis of Thiol-Functionalized Branched Poly(glycidol).....	66
Synthesis of Alkene-terminated Branched Poly(glycidol) .....	71
Synthesis of Acrylate-Functionalized Poly(glycidol).....	74
Synthesis of Aminoxy-Functionalized Branched Poly(glycidol). .....	76



	Synthesis of Keto-Functionalized Branched Poly(glycidol).....	85
	Cytotoxicity of Branched Poly(glycidol) Derivatives .....	89
	Conclusion .....	91
	Experimental .....	92
	References.....	106
IV.	<b>SYNTHESIS AND CHARACTERIZATION OF NOVEL POLY(GLYCIDOL) HYDROGELS .....</b>	<b>110</b>
	Introduction.....	110
	Results and Discussion .....	116
	Synthesis of Poly(glycidol) Hydrogels by Oxime Click Chemistry .....	117
	Mechanical Studies of Poly(glycidol) Oxime Hydrogels .....	123
	Tailoring and Optimizing the Elasticity and Strength of the Poly(glycidol) Oxime Hydrogels .....	129
	Biodegradation studies of Poly(glycidol) Oxime Hydrogels.....	137
	Oxidative Degradation.....	137
	Enzymatic Degradation.....	139
	Hydrolytic Degradation .....	140
	Biocompatibility Studies of Poly(glycidol) Oxime Hydrogels.....	142
	Swelling Studies of Poly(glycidol) Oxime Hydrogels.....	143
	Protein Release from Poly(glycidol) Hydrogels.....	144
	Conclusion .....	147
	Experimental .....	148
	References.....	154
V.	<b>CONCLUDING REMARKS AND FUTURE DIRECTIONS.....</b>	<b>160</b>
	General Discussion and Conclusion .....	160
	Future Directions .....	166
	Photoacid-Mediated Ring-Opening Polymerization of Glycidol Driven by Visible Light.....	166
	Poly(glycidol)-based Cartilage Scaffolds with Tunable Mechano-Responsive Behavior .....	167
	References.....	169

## LIST OF TABLES

Table	Page
I-1. Table highlighting the comparison of current hydrogel technologies to the proposed hydrogel technology.....	9
II-1. Interpretation of the inverse gated (IG) proton-decoupled <sup>13</sup> C NMR (CD <sub>3</sub> OD) of poly(glycidol).....	33
II-2. Showing results from the <sup>13</sup> C NMR, MALDI-TOF MS and GPC. ....	34
II-3. Showing results from the <sup>13</sup> C NMR, MALDI-TOF and GPC. ....	38
II-4. SEC analysis of semi-branched poly(glycidol) fractions showing a comparison between using polystyrene and polyethylene glycol calibration versus absolute molar-mass calibration with MALDI-ToF MS.....	41
II-5. Summary of characterization data for optimum branched poly(glycidol) synthesis. ....	42
II-6. Summary of characterization data for semi-branched poly(glycidol) synthesis.....	49
II-7. Interpretation of the inverse gated (IG) proton-decoupled <sup>13</sup> C NMR of several branched poly(glycidol) samples.....	51
III-1. Distribution of primary and secondary hydroxy groups in polyglycidol calculated from <sup>13</sup> C NMR structural data and measured from <sup>29</sup> Si NMR of the trimethylsilyl ethers of polyglycidol. ....	65
III-2. Synthesis of 3-mercaptopropionyl polyglycidol by a modified fisher esterification route. Table showing the targeted composition and the actual composition of thiol-terminated branched poly(glycidol) determined by <sup>1</sup> H NMR. ....	70
III-3. Showing the targeted functionalization and the actual functionalization of branched poly(glycidol) determined by <sup>1</sup> H NMR. ....	73
V-1. Mechanical properties of PEG-based hydrogels in compression studies.. ....	162
V-2. Table highlighting the comparison of current hydrogel technologies to the novel branched poly(glycidol) hydrogel technology.....	165

## LIST OF FIGURES

Figure	Page
I-1. Showing the various forms of poly(glycidol) architectures. ....	3
I-2. Showing the synthesis of hydrogel via alkene polymerization of acrylate-functionalized poly(glycidol- <i>co</i> -ethylene glycol) multiarm star polymer. ....	5
I-3. Poly(glycidol) hydrogels by radical polymerization or photopolymerization of methacrylated poly(glycidol).....	6
I-4. Synthesis of poly(glycidol) hydrogels through the reaction of epichlorohydrin with L-lactic acid, followed by hydrolysis, polymerization, and crosslinking reactions. ....	7
I-5. Poly(glycidol) hydrogel via polyaddition crosslinking of polyepoxides followed by epoxide hydrolysis.....	8
I-6. Showing an overview of dissertation research.....	10
I-7. Proposed structure of branched poly(glycidol). ....	11
I-8. Functional polyglycidol building blocks “Legos”, with amino-oxy (AO-PG) and keto-functionalized AO-PG to form networks in water in 1-2 minutes via oxime “click” chemistry..	12
II-1. Poly(glycidol) sulfates as heparin analogs.....	26
II-2. <sup>1</sup> H NMR (CD <sub>3</sub> OD) showing copolymerization of glycidol and tetrahydrofuran and the formation of acetals when precipitated in acetone.....	29
II-3. <sup>1</sup> H NMR (CD <sub>3</sub> OD) of poly(glycidol) showing the incorporation of isoamyl alcohol.....	30
II-4. Illustrations of the different structural units present in poly(glycidol) and their respective <sup>13</sup> C NMR assignments (CD <sub>3</sub> OD, ppm). ....	31
II-5. <sup>13</sup> C NMR (CD <sub>3</sub> OD) of poly(glycidol) showing structural assignment of the carbons. ....	32
II-6. MALDI-ToF mass spectra of poly(glycidol) obtained from the Sn(OTf) <sub>2</sub> mediated polymerization with isoamyl alcohol (IAOH). ....	36
II-7. Showing decrease in macrocyclic species as the rate of addition is decreased. (top) slow monomer addition at 0 °C, (middle) slow monomer addition at 25 °C, (bottom) slow monomer addition at 25 °C with a syringe pump and mechanical stirrer. ....	37

II-8. SEC chromatograph of semi-branched poly(glycidol) homopolymer. The insets display the SEC chromatograms (bottom) and the MALDI-ToF MS spectra (top) of the selected fractions.	40
II-9. SEC calibration curves obtained with polystyrene standards, polyethylene glycol standards and SEC/MALDI-ToF fractions (24-27). This illustrates that PEG standards are suitable enough for relative molar-mass determination of semi-branched poly(glycidol) by SEC, while polystyrene standards are not ideal.	42
II-10. MTT assay of branched poly(glycidol) against NIH 3T3 cells for 24 hrs.	43
II-11. LIVE/DEAD staining of NIH 3T3 cells in contact with PEG and poly(glycidol) (5 mg/mL). (left) PEG, (middle) poly(glycidol), (right) control.	44
II-12. Showing GPC chromatograph of different semi-branched Poly(glycidol)s.	50
II-13. MALDI-ToF MS analysis of semi-branched poly(glycidol) samples. PGly-2 (Top-right), PGly-5 (top-left) and PGly-2 magnified portion (bottom-center).	50
II-14. The inverse-gated proton decoupled $^{13}\text{C}$ NMR for samples PGly-2, PGly-3 and PGly-4 showing the methine carbon of the Linear 1,3 structural unit as the reference for integration.	51
II-15. $^1\text{H}$ NMR (Top) and Inverse-gated proton decoupled $^{13}\text{C}$ NMR (bottom) spectra of PGly-5 in $\text{DMSO-}d_6$ .	52
III-1. $^{29}\text{Si}$ NMR (501 MHz, $(\text{CD}_3)_2\text{SO}$ ) of the trimethylsilyl ethers of poly(glycidol).	65
III-2. $^1\text{H}$ NMR (400 MHz, $\text{CD}_3\text{OD}$ ) of thiol-terminated branched poly(glycidol) derivatives.	68
III-3. $^1\text{H}$ NMR (400 MHz, $\text{CD}_3\text{OD}$ ) of the alkene-terminated derivative of poly(glycidol).	72
III-4. GPC chromatograph showing the evolution of molecular weight during the esterification of poly(glycidol) with acrylic acid.	74
III-5. $^1\text{H}$ NMR (400 MHz, $(\text{CD}_3)_2\text{SO}$ ) of acrylate-terminated branched polyglycidol.	75
III-6. Mitsunobu reaction of branched poly(glycidol) with N-hydroxyphthalimide.	78
III-7. SEC chromatographs of branched poly(glycidol) functionalized with N-hydroxyphthalimide. Analysis was carried out in DMF (LiBr) at 45 °C. The plot of $M_n$ vs time shows changes in molecular weight and molecular weight distribution over the course of the reaction.	79
III-8. $^1\text{H}$ NMR (400 MHz, $(\text{CD}_3)_2\text{SO}$ ) of branched poly(glycidol) functionalized with N-hydroxy phthalimide.	80

III-9. Hydrazinolysis of the branched poly(glycidol) N-oxyphthalimide derivatives to provide aminoxy functionalized poly(glycidol).....	82
III-10. <sup>1</sup> H NMR (top) and GPC (bottom) of aminoxy-functionalized branched poly(glycidol)	84
III-11. GPC monitoring of the synthesis of keto-functionalized branched poly(glycidol) showing no change in molecular weight or molecular weight distribution after 30 min of reaction time..	86
III-12. GPC traces of keto-functionalized branched poly(glycidol). .....	87
III-13. <sup>1</sup> H NMR (400 MHz, (CD <sub>3</sub> ) <sub>2</sub> SO) of branched poly(glycidol) functionalized with levulinic acid.....	88
III-14. Cytotoxicity of aminoxy and keto-ester functionalized poly(glycidol)s. ....	89
IV-1. Dual drug delivery system. The MEK loaded nanosponges and the growth factor stabilized in the bPG “matrix” results in the only successful callus formation and bone strength of all treatment groups.....	113
IV-1. Dual drug delivery system. The MEK loaded nanosponges and the growth factor stabilized in the bPG “matrix” results in the only successful callus formation and bone strength of all treatment groups.....	116
IV-2. Formation of 20% and 60% bPG hydrogels showing changes in crosslinking density. ....	120
IV-3. Showing the influence of degrees of functionalization of gelation kinetics at pH 7.4. Higher degree of functionalization increases the rate of gelation.....	121
IV-4. pH dependence of hydrogel gelation kinetics determined by rheometry. ....	122
IV-5. Scanning electron microscopy (SEM) images of various poly(glycidol) hydrogel formulations. ....	123
IV-6. Stress/strain data for the poly(glycidol) oxime hydrogel formulations at pH 7.4. ....	125
IV-7. Stress/strain data for three poly(glycidol) oxime hydrogel formulations at pH 9. ....	126
IV-8. Stress/strain data for poly(glycidol) hydrogel showing comparison of 30/60% hydrogel with previous hydrogel formulations. ....	128
IV-9. Stress/strain data for the 10 wt.% poly(glycidol) oxime hydrogel.....	129
IV-10. Stress/strain data for poly(glycidol) hydrogels made with silica nanoparticles incorporated .....	130

IV-11. Showing formation of physically crosslinked network consisting of poly(glycidol) poly(ethylene glycol) and silica nanoparticles via the tilt vial method. ....	131
IV-12. Stress/strain data for the 60% AO-PG with 2 and 4 kDa Keto-PEG hydrogels.....	133
IV-13. Stress/strain curves for poly(glycidol)-PEG Hydrogels.....	134
IV-14. Stress/strain data for 60% poly(glycidol)-PEG hydrogel with 10 wt.% silica.....	135
IV-15. Stress/strain data for 30% poly(glycidol)-PEG hydrogels with and without silica nanoparticles. ....	136
IV-16. Oxidative degradation of poly(glycidol) hydrogels .....	138
IV-17. Showing the enzymatic degradation of various poly(glycidol) hydrogels with 1 U/mL cholesterol esterase. ....	140
IV-18. Hydrolytic degradation of poly(glycidol) oxime hydrogels in PBS buffer pH 7.4. ....	141
IV-19. Changes in mass during hydrolytic degradation of poly(glycidol) oxime hydrogels .....	142
IV-20. Fluorescent image showing LIVE/DEAD staining of the encapsulated NIH 3T3 cell after 24 h in swollen 20% poly(glycidol) hydrogel.....	143
IV-21. Showing the ratio of swelling of poly(glycidol) hydrogels.....	144
IV-22. Showing the release of lysozyme from polyglycidol hydrogel in PBS buffer 7.4 at 37 °C. ....	146
V-1. (a) Nucleophilic base-catalyzed reaction between an alkyne and thiol; (b) Schematic of PEG precursors synthesized for crosslinking; and (c) Schematic of exemplar hydrogel networks. Ref. 10.....	164
V-2. Synthesis and photochemical reaction of the protonated merocyanine (MEH) photoacid 1. ....	166
V-3. Development of poly(glycidol) hydrogels for cartilage tissue engineering. ....	167

## LIST OF SCHEMES

Scheme	Page
II-1. Sandler and Berg proposed mechanism for the anionic polymerization of glycidol.....	18
II-2. Vandenberg proposed mechanism for the anionic ring opening polymerization of glycidol. .....	19
II-3. Synthesis of linear poly(glycidol) via anionic polymerization.....	20
II-4. Formation of macrocyclic polymers via anionic intramolecular ring-opening. ....	21
II-5. Active chain end mechanism for the polymerization of glycidol. ....	22
II-6. Chain transfer reaction via ACE mechanism during polymerization of glycidol.....	22
II-7. Activated monomer mechanism for the polymerization of glycidol. ....	23
II-8. Ratio of the rate constants for the polymerization of epichlorohydrin via AM and ACE mechanism. ....	24
II-9. Competition between IAOH and glycidol for activated epoxide intermediate.....	34
II-10. Proposed mechanism for the intramolecular macrocyclization of poly(glycidol) initiated by glycidol .....	35
III-1. Synthesis of poly(glycidol) sulfate and poly(glycidol) carboxylate.....	60
III-2. Synthesis of linear esterified poly(glycidol).....	61
III-3. Synthesis of poly(glycidol) phosphonate and phosphonic acid derivatives. ....	61
III-4. Poly(glycidol) supported Suzuki coupling applied to the synthesis of biphenylaldehyde ..	62
III-5. Some postpolymerization modification of polyglycidol reported to date. ....	63
III-6. Synthesis of thiol-disulfide reagent for thiol functionalization of branched poly(glycidol)	66
III-7. Reduction of the thiol-disulfide poly(glycidol) derivative to form a thiol-terminated branched poly(glycidol) derivative. ....	67
III-8. Synthesis of thiol-terminated branched polyglycidol via nucleophilic acyl substitution....	67

III-9. Synthesis of thiol-terminated branched poly(glycidol) by Steiglich esterification. ....	69
III-10. Esterification of 3-thoxy-1,2-propanediol .....	71
III-11. Mitsunobu reaction of 3-ethoxy-1,2-propanediol followed by hydrazinolysis .....	77
III-12. Synthesis of keto-functionalized branched poly(glycidol) via esterification with levulinic acid.....	85
IV-1. Reaction of aminoxy bPG with 1,4-cyclohexanedione to form hydrogels .....	118
IV-2. Showing the combination of the aminoxy and the ketone derivative of branched bPG to form a network via Oxime Click chemistry.....	119
V-1. Synthesis and Encapsulation of MSCs within RGD-functionalized Oxime-Crosslinked PEG hydrogels. Adopted from ref. 1.....	163



# CHAPTER I

## INTRODUCTION

The ability to tune the properties of a material to meet the needs of a complex biological system is a key goal in biomaterials engineering.<sup>1-3</sup> Polymeric networks are an important class of materials that have shown great promise towards fulfilling this goal.<sup>4-6</sup> They include nanoparticles, microparticles, nanogel, and hydrogels. For the past decade, research into these polymeric networks has drastically increased and as a result this class of materials has found use in biomedical applications ranging from scaffolds for tissue engineering<sup>7-11</sup> to carriers for drug delivery.<sup>12-14</sup> For many of these biological applications, tailoring the physical properties (e.g. swelling and elasticity) of the polymeric network is essential to respond to the demands of a particular biological environment or to yield a desired cellular response.<sup>15</sup> For example, polymeric networks with different stiffness can support the migration and differentiation of stem cells while the swelling ability of a polymeric network at different temperatures can impact the controlled release ability of drugs from vesicles. Furthermore, other properties such as the biocompatibility and biodegradability of the polymeric network is essential for the polymeric biomaterial to be successfully implemented into a biological environment. Polymeric biomaterials in which these properties can be readily tuned are essential to the advancement of this area.

Hydrogels are water-swollen polymeric networks capable of absorbing large quantities of water and biological fluids while maintaining a distinct three-dimensional structure.<sup>11</sup> Hydrogels are attractive synthetic materials for biomedical applications due to their extracellular matrix-like properties, which includes high water content, low stiffness, and high mass transport.<sup>16</sup> So far, a variety of polymeric hydrogels have found applications in drug release,<sup>17-18</sup> cell delivery

scaffolds,<sup>19</sup> functional tissues,<sup>20</sup> and wound dressings.<sup>21</sup> Some of the hydrogels used in these applications are prepared from naturally derived polymers. However, due to numerous limitations of natural polymers, such as high cost, batch-to-batch variation, possible adverse immune responses, and risk of contamination, many applications are best served by using hydrogels made with completely synthetic polymers.<sup>22</sup> To achieve hydrogel formation, the synthetic polymer must be rapidly and effectively crosslinked in a manner that is not detrimental to the survival and proliferation of living systems. The crosslinked, three-dimensional structure is key to the ultimate applications of hydrogel.

The most studied polymeric hydrogels are based on poly(lactic-glycolic acid),<sup>23</sup> a hydrolytically degradable polymer that affords some degree of stiffness and a surface well suited for cell growth and tissue regeneration. However, the degradation of these hydrogels leads to localized acidity issues and the rigidity of the system limits the potential applications in most regenerative medicine and drug delivery applications.<sup>24</sup> Hence many research groups are currently designing hydrogels that can degrade into inert products, in addition to possessing all the other essential properties of an artificial biomaterial.

Poly(glycidol) (PG), sometimes referred to as poly(glycerol), is a flexible, functionalizable, hydrophilic aliphatic polyether-polyol synthesized from the ring-opening polymerization of glycidol (2,3-epoxy-1-propanol) and exhibits varying polymeric architectures. PG has been synthesized in four main forms i.e. linear, branched or semi-branched, hyperbranched, and dendritic (Figure I-1). PG consist of an inert polyether-backbone with functional hydroxy groups along the polymer backbone and at every branch-end.<sup>25-27</sup> This structural feature resembles the well-known poly(vinyl alcohol) (PVA) and poly(ethylene glycol) (PEG) that are accepted for various applications. Furthermore, PG has been found to have very good biocompatibility based

on a variety of in vitro and in vivo assays.<sup>28-32</sup> The polyether-backbone of branched poly(glycidol) (*bPG*) and its branched functional architecture makes it an attractive alternative polymer for many biomedical applications. Additionally, the hydrophilicity in combination with its polyhydroxy functionalities makes *bPG* very suitable for the design of hydrogels. An anticipated advantage of *bPG* over existing hydrogel precursors is the low viscosity of the hydrogel precursors in water.<sup>33-</sup><sup>34</sup> This can lead to gels with high solid contents and consequently excellent mechanical properties. Additionally, *bPG* would be an ideal polymer for the design of injectable hydrogels that can be delivered inside the body in a minimally invasive way (i.e. non-surgical procedures such as injection).<sup>9</sup>

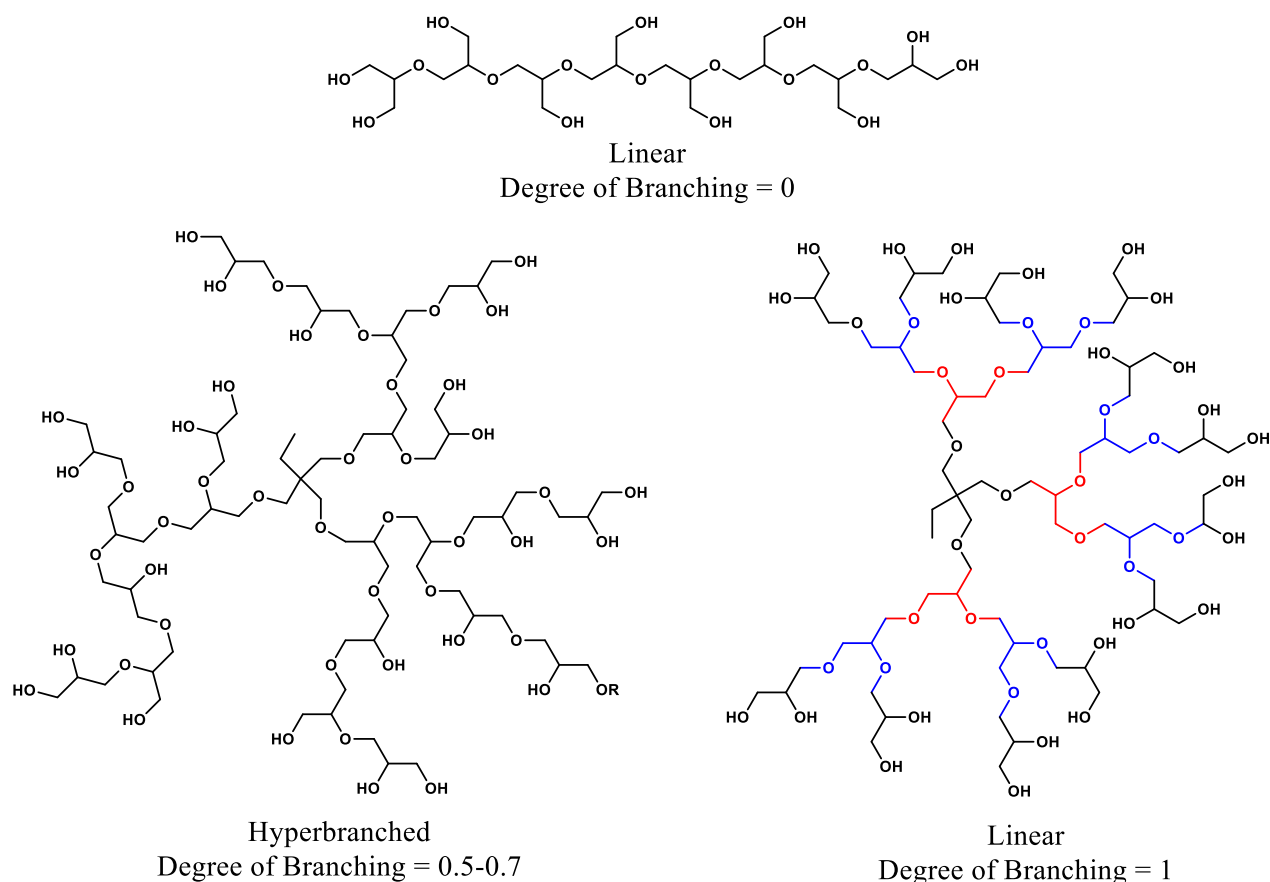


**Figure I-1.** Showing the various forms of poly(glycidol) architectures.

Branched poly(glycidol) offers some additional significant advantages over their linear counterpart (e.g. poly(lactic-glycolic acid), poly(vinyl alcohol) and poly(ethylene glycol)). *bPG* has increased functionality due to its branched polyether polyol structure, and possesses different physiochemical properties. In comparison to linear polymers, *bPG* has a large number of functional groups available for crosslinking reactions in a small volume. This leads to the formation of more crosslinking points with respect to molecular weight when compared to linear polymer of the same molecular weight. As a result, hydrogels with a higher crosslinking density can be formed. Furthermore, the unique branching of *bPG* will result in hydrogels with a homogeneous structure. Such structures cannot be obtained with linear polymers.<sup>35-37</sup>

Despite the many advantages of branched poly(glycidol), its application to the synthesis of hydrogels has been limited. The first poly(glycidol) based hydrogels were reported in 2001. Knischka and others<sup>38</sup> synthesized a series of functionalizable hydrogels based on poly(ethylene glycol) and poly(glycidol) (Figure I-2). These hydrogels showed excellent suitability towards cell growth. Later, Kim and others<sup>39-40</sup> used hyperbranched poly(glycidol) (*hbPG*) to form hydrogel films, by crosslinking the polymer with glutaraldehyde and some small molecule dicarboxylic acid (e.g. glutaric acid). These hydrogels were not ideal for biomedical application due to the toxicity of glutaraldehyde, very low water content, and high temperatures need for crosslinking. It should be noted however that they were able to increase the water content of the hydrogel by using PEG-dicarboxylic acid instead of glutaric acid. The increase in water content was attributed to the hydrophilicity of PEG in the network. Hennink and coworkers<sup>41</sup> later reported a less invasive synthesis of *hbPG* hydrogels. They first derivatized the *hbPG* with methacrylate groups then employed two different methods for hydrogel synthesis (Figure I-3). They use radical polymerization with potassium peroxydisulfate (KPS) and *N,N,N',N'*-tetramethylethylenediamine

(TMEDA) as initiator and catalyst respectively. They also used photopolymerization with Irgacure 2959 as the photoinitiator. While these hydrogels were developed with biomedical application in mind, the impact of gelation condition on a biological environment was not explored.

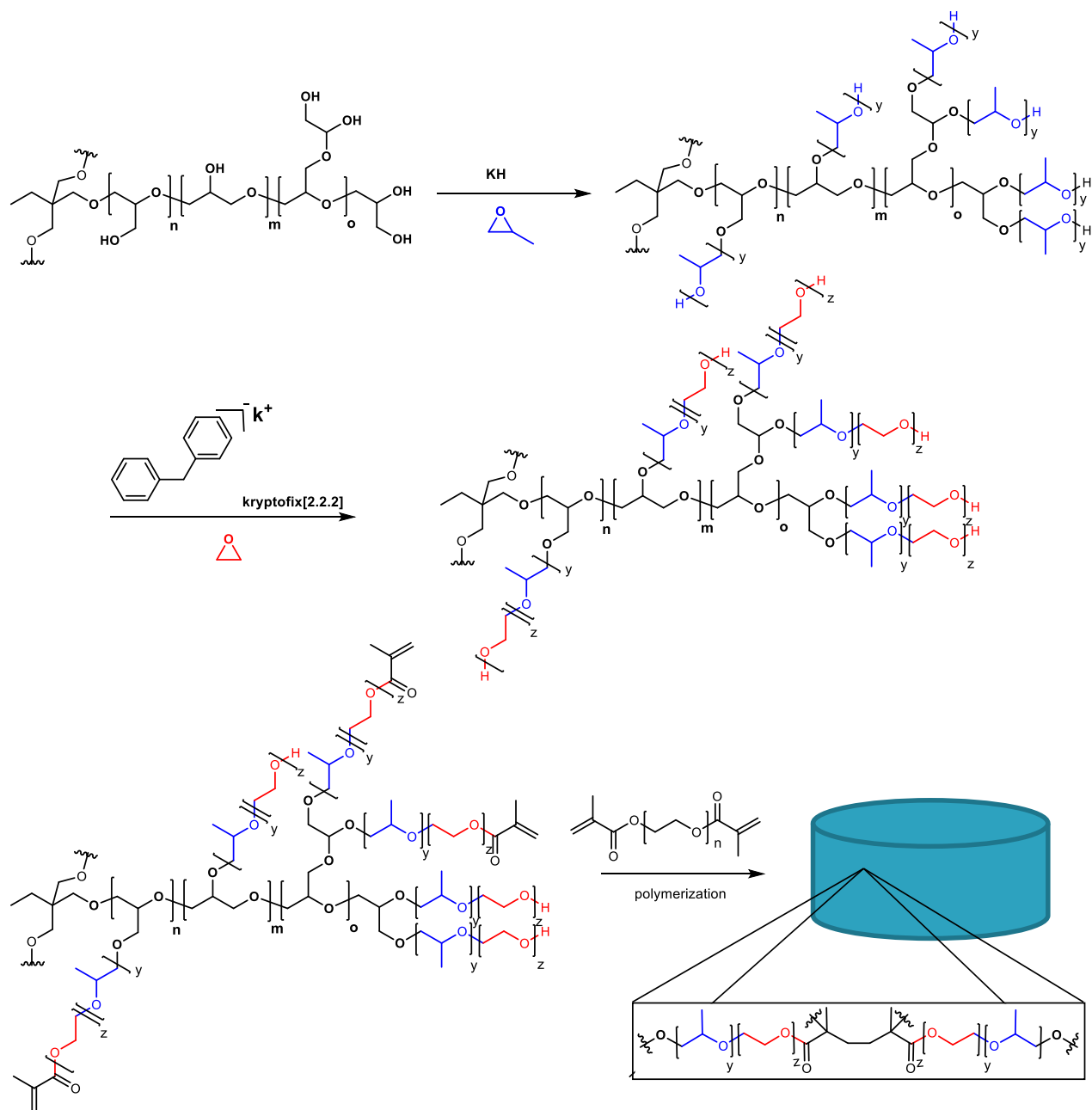


**Figure I-2.** Showing the synthesis of hydrogel via alkene polymerization of acrylate-functionalized poly(glycidol-*co*-ethylene glycol) multiarm star polymer.

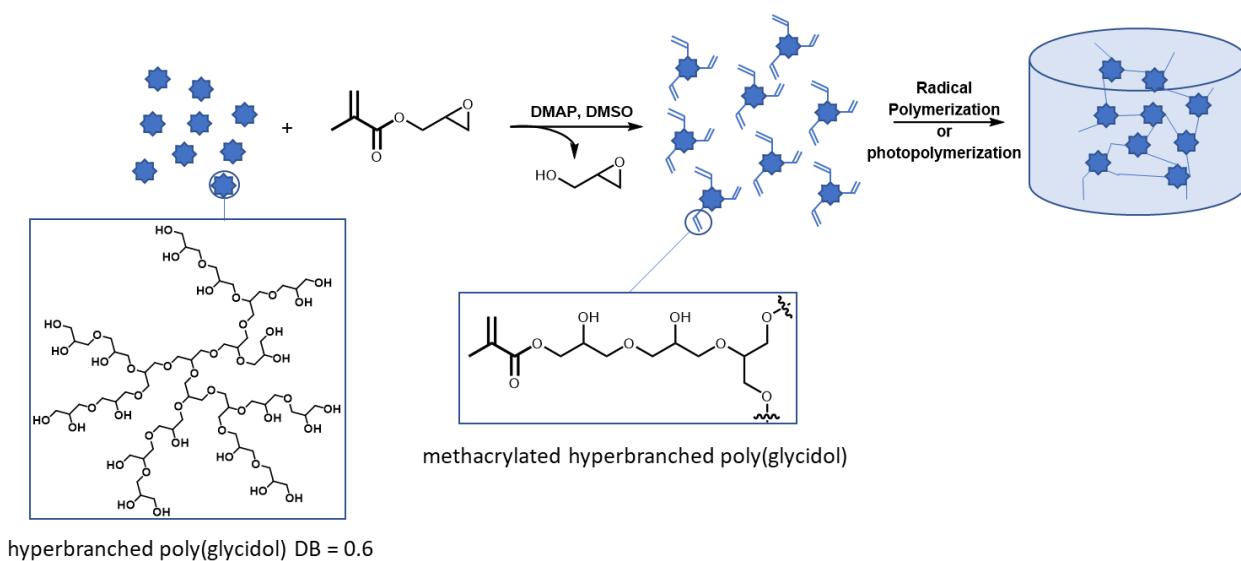


**Figure I-3.** Poly(glycidol) hydrogels by radical polymerization or photopolymerization of methacrylated poly(glycidol)

In 2009, the first pH-responsive *hbPG*-based hydrogel was reported by Yang and coworkers.<sup>42</sup> The pH-responsive hydrogels were synthesized through the reaction of epichlorohydrin with L-lactic acid in the presence of sodium hydroxide and cetyltrimethylammonium bromide as a phase transfer catalyst at room temperature (Figure I-4). While the resulting hydrogel possesses pH-responsive behavior which has numerous applications in drug delivery, the extensive synthesis and energy consuming purifications would prevent its implementation in biomedical devices. Shortly afterwards, Steinhilber and coworkers<sup>43</sup> reported the preparation of disulfide crosslinked *hbPG* hydrogel by the ring-opening crosslinking polymerization of glycerol and PEG polyepoxides and  $\text{Na}_2\text{S}_2$  (Figure I-5). While these hydrogels can serve as drug delivery scaffolds, their elaborate preparation procedure will not allow for cell encapsulation and hence these hydrogels are limited to applications in drug delivery. Dube and coworkers<sup>44-45</sup> reported another example of *hbPG* hydrogels synthesized by ring-opening crosslinking polymerization. They first synthesized *hbPG* from glycerol and used it to make

hydrogel through the use of anionic ring-opening crosslinking polymerization with a polyepoxide crosslinker. The hydrogel takes approximately 48 h to synthesize, which is not ideal for application in regenerative medicine. Furthermore, given the limited stability of some biologically active drugs, this preparation would only be applicable to a limited class of bioactive molecules.

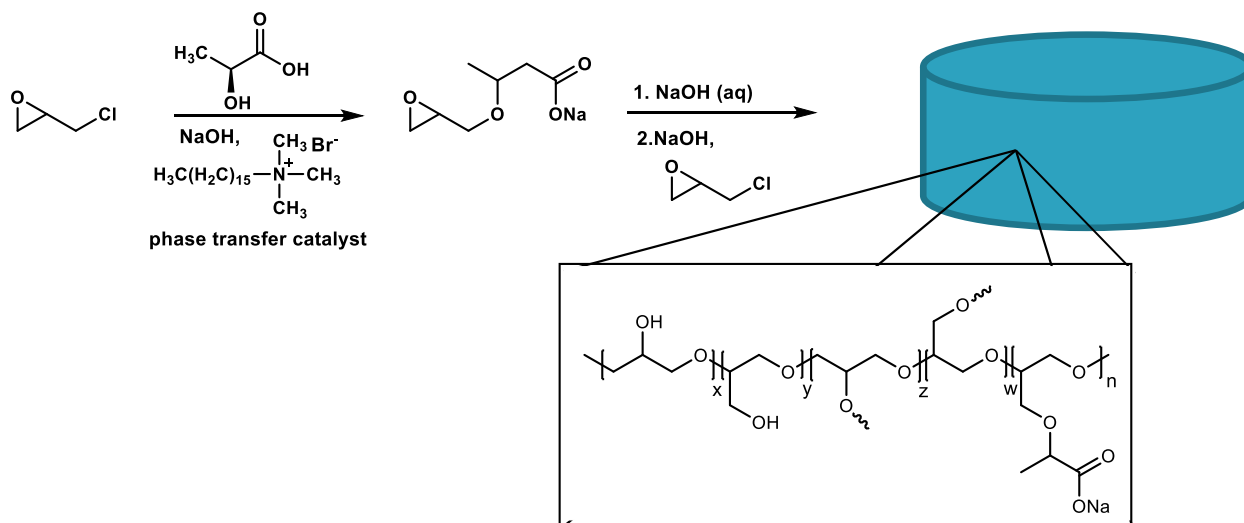


**Figure I-4.** Synthesis of poly(glycidol) hydrogels through the reaction of epichlorohydrin with L-lactic acid, followed by hydrolysis, polymerization, and crosslinking reactions.

The hydroxyl group chemistry used to crosslink or functionalize the *hbPGs* in the above-cited articles is based on epoxide-containing agents. These commonly used epoxides are highly toxic.<sup>46</sup> Furthermore, radical polymerization or photopolymerization when applied is performed by adding initiators and catalysts. If these residues are not removed with great thoroughness, they will be released into biological systems, causing a detrimental effect on living organisms. Although *hbPG* have excellent biocompatibility, the crosslinking protocol reported so far involves toxic byproducts which creates the need for exhaustive purification. Hence novel hydrogel forming reactions are needed to expand the application of *hbPG* hydrogels for regenerative medicine and drug delivery applications.

In recent years, a few reports have emerged to address these concerns. In 2013, Shchipunov and coworkers<sup>47</sup> reported the synthesis of *hbPG* hydrogels through biomimetic mineralization.

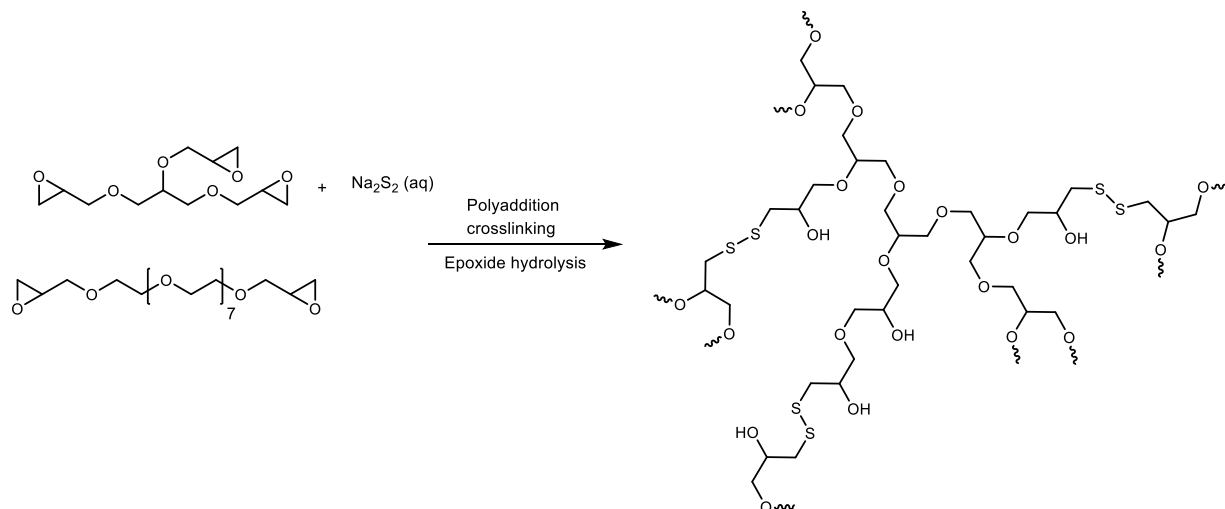


**Figure I-5.** Poly(glycidol) hydrogel via polyaddition crosslinking of polyepoxides followed by epoxide hydrolysis.

They combined *hbPG* with a special biocompatible silica precursor, tetrakis(2-hydroxyethyl) orthosilicate (THEOS). While they were able to achieve hydrogel formation under ambient conditions without the need for heat, organic solvent, catalyst, and acid or base, a large amount (50 wt.%) of THEOS was needed for gelation to occur in 10-15 minutes. In 2014, Haag and coworkers,<sup>48</sup> produced the first example of an enzymatically crosslinked *hbPG* hydrogel. *hbPG* was first functionalized with phenol group. Then the enzyme horseradish peroxidase (HRP) was used in the presence of hydrogen peroxide to catalyzed the oxidative coupling of the phenol groups to form a hydrogel within 10-15 min. The cytocompatibility of this hydrogel was also evaluated and reported. Cell viability ranged from 51-61 % relative to control. This was attributed to the cell-repellent properties of *hbPG*. When a cell-attachment promoting compound was added, cell viability increased to 98%. This is the first example of a cell study for not only *hbPG* hydrogels



but for hydrogel made by enzymatic oxidative crosslinking. Furthermore, these examples represent the most promising *hbPG* hydrogels reported to date.

Despite the advances mentioned above, there still exist a need for a more robust *hbPG* hydrogels which are fully capable to extending the applications of *hbPG* in regenerative medicine applications. We propose to address this need by employing the use of Click chemistry to fabricated poly(glycidol) hydrogels. Click chemistry reactions are high yielding, highly atom efficient reaction which results in the formation of stable bonds in a biorthogonal manner.<sup>49</sup> The use of click chemistry in the synthesis of poly(glycidol) hydrogels have been largely unexplored, however we envision that the advantages of Click chemistry combined with the advantages of poly(glycidol) will give advanced materials for applications in regenerative medicine and drug delivery (Table I-1).

**Table I-1.** Table highlighting the comparison of current hydrogel technologies to the proposed hydrogel technology.

Current Hydrogel Technologies	<i>Hydrogel Properties</i>	Proposed Hydrogel Technology
COMPARISON OF TECHNOLOGY		
Too high and non-tailorable	<u>Swellability</u>	Tailorable
Alkene and epoxide containing agents	<u>Crosslinkers</u>	Clickable groups
hydroxyl group chemistry or radical polymerization	<u>Crosslinking Mechanism</u>	Click chemistry
low strength and stiffness	<u>Mechanical Properties</u>	High strength and elasticity
Toxic byproducts hinder cell encapsulation	<u>Biocompatibility</u>	non-toxic byproducts
non-tailorable	<u>Crosslinking Density</u>	Tailorable

## Dissertation Overview

The aim of this work is to fabricate a series of cytocompatible poly(glycidol) hydrogels where the crosslinking systems integrates a hydrolysable degradable bond and crosslinking occurs under ambient conditions in a fast, efficient, and biorthogonal manner. For application in regenerative medicine or tissue engineering, the hydrogels need to be able to support long term tissue regeneration by being degraded and remodeled so that cells can migrate and form new extracellular matrix. Additionally, the hydrogels need to possess mechanical properties similar to those of native tissues.

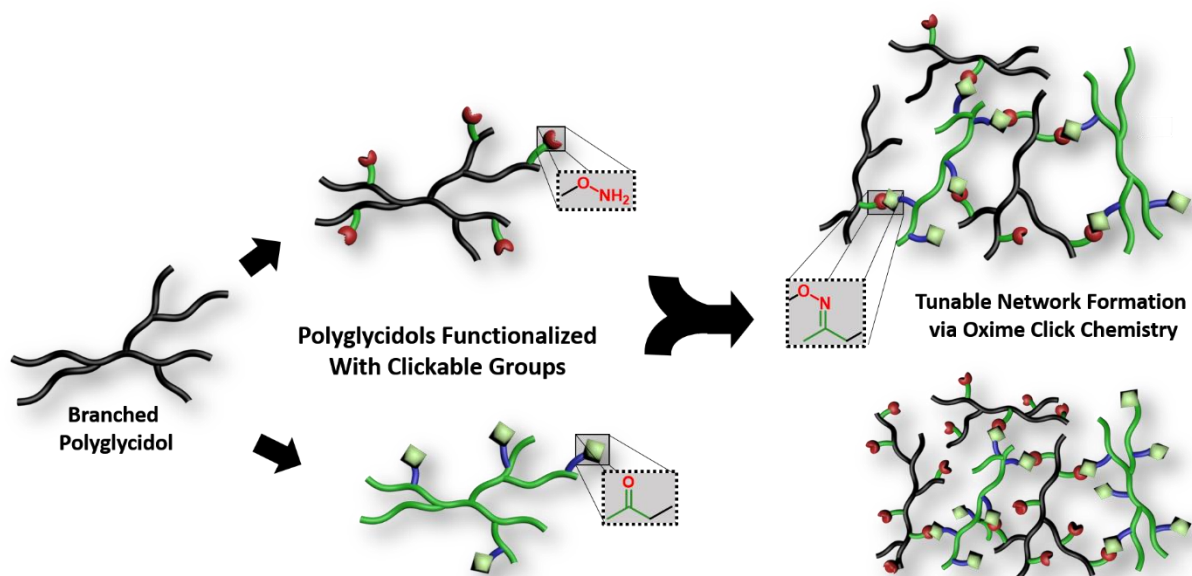


**Figure I-6.** Showing an overview of dissertation research.

Efforts towards the synthesis of poly(glycidol) hydrogels started with the synthesis of branched poly(glycidol) (Figure I-7). Branched poly(glycidol) is different from hyperbranched systems in that it possesses a more linear structure. By using tin triflate ( $\text{Sn}(\text{OTf})_2$ ) to mediate the cationic ring-opening polymerization of glycidol, we were able to access well-defined branched poly(glycidol) for use in the synthesis of hydrogels. The lower branching will open up the

structure, allowing more hydroxyl groups to be available for functionalization. Chapter II focuses on the work done to optimize polymerization conditions and methods developed to characterize the obtained branched poly(glycidol).

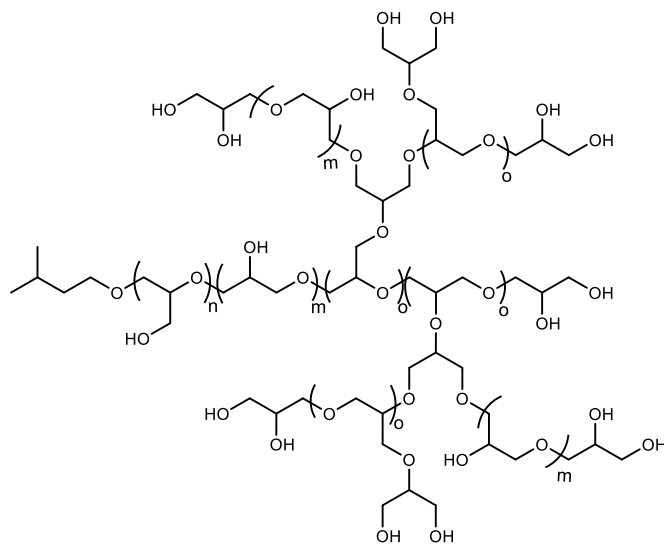


**Figure I-7.** Proposed structure of branched poly(glycidol).

Branched poly(glycidol) (*bPG*) was then subjected to a number of different functionalization reactions. Initially we wanted to synthesize precursors for the thiol-ene click reaction. Therefore, the ene-ester and thiol derivative of *bPG* was synthesized and characterized. However, due to the limited solubility of ene-ester derivative, an alternate functionality was needed. Hence, the synthesis of the acrylate derivative of *bPG* was explored. However, isolation was difficult as the polymer crosslinked during isolation and purification. We then turned our attention to the oxime-click reaction. For this reaction, we needed an aminoxy and a ketone functionalized *bPG*. We were able to successfully synthesize and characterize both derivatives needed for hydrogel formation via oxime Click chemistry. Furthermore, the cytotoxicity of the functionalized polyglycidols were investigated and found to have comparable biocompatibility to polyethylene glycol. Chapter III covers details about this study.

Chapter IV chronicles the synthesis and characterization of novel *b*PG hydrogel via oxime Click reaction (Figure I-8). The oxime reaction proved to be a versatile method of creating *b*PG hydrogel networks with properties well suited for applications in regenerative medicine and tissue engineering. The combination of the two highly branched components together with the variation in functionality showed a remarkable effect on its mechanical properties with surprisingly high strength and stiffness. These findings demonstrate the advantages of *b*PG in contrast to linear PEG and PVA, where network densities cannot be easily adjusted and high strength materials cannot be formed. Other properties which were investigated included water swelling ratios and degradability which were found to be easily tuned by varying the degree of functionality in each functional polymer.

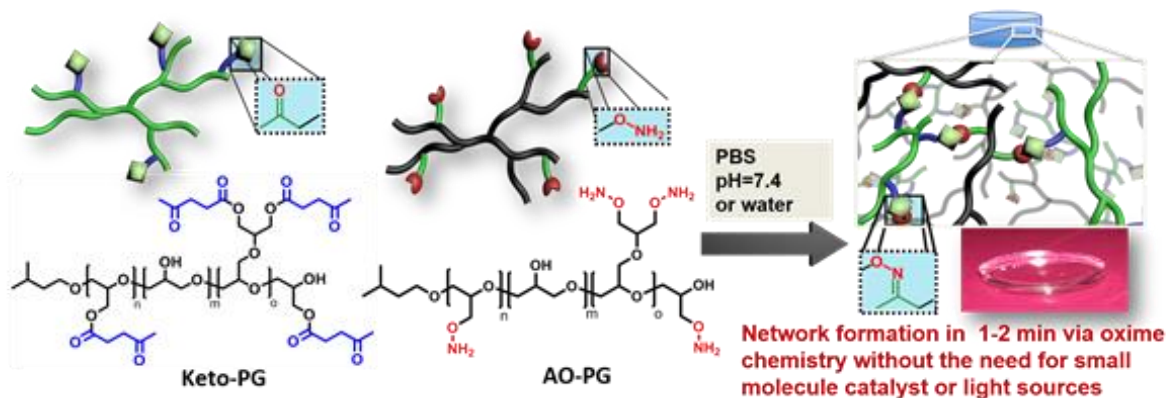


**Figure I-8.** Functional polyglycidol building blocks “Legos”, with amino-oxime (AO-PG) and keto-functionalized AO-PG to form networks in water in 1-2 minutes via oxime “click” chemistry.

## REFERENCES

1. Langer, R.; Tirrell, D. A., Designing materials for biology and medicine. *Nature* **2004**, *428* (6982), 487-492.
2. Hutmacher, D. W., Scaffolds in tissue engineering bone and cartilage. *Biomaterials* **2000**, *21* (24), 2529-2543.
3. Elsabahy, M.; Wooley, K. L., Design of polymeric nanoparticles for biomedical delivery applications. *Chemical Society Reviews* **2012**, *41* (7), 2545-2561.
4. Appel, E. A.; del Barrio, J.; Loh, X. J.; Scherman, O. A., Supramolecular polymeric hydrogels. *Chemical Society Reviews* **2012**, *41* (18), 6195-6214.
5. Hoffman, A. S., Hydrogels for biomedical applications. *Advanced Drug Delivery Reviews* **2002**, *54* (1), 3-12.
6. Sun, J. Y.; Zhao, X. H.; Illeperuma, W. R. K.; Chaudhuri, O.; Oh, K. H.; Mooney, D. J.; Vlassak, J. J.; Suo, Z. G., Highly stretchable and tough hydrogels. *Nature* **2012**, *489* (7414), 133-136.
7. Pina, S.; Oliveira, J. M.; Reis, R. L., Natural-Based Nanocomposites for Bone Tissue Engineering and Regenerative Medicine: A Review. *Advanced Materials* **2015**, *27* (7), 1143-1169.
8. Annabi, N.; Tamayol, A.; Uquillas, J. A.; Akbari, M.; Bertassoni, L. E.; Cha, C.; Camci-Unal, G.; Dokmeci, M. R.; Peppas, N. A.; Khademhosseini, A., 25th Anniversary Article: Rational Design and Applications of Hydrogels in Regenerative Medicine. *Advanced Materials* **2014**, *26* (1), 85-124.
9. Yang, J. A.; Yeom, J.; Hwang, B. W.; Hoffman, A. S.; Hahn, S. K., In situ-forming injectable hydrogels for regenerative medicine. *Progress in Polymer Science* **2014**, *39* (12), 1973-1986.
10. Slaughter, B. V.; Khurshid, S. S.; Fisher, O. Z.; Khademhosseini, A.; Peppas, N. A., Hydrogels in Regenerative Medicine. *Advanced Materials* **2009**, *21* (32-33), 3307-3329.
11. Van Vlierberghe, S.; Dubruel, P.; Schacht, E., Biopolymer-Based Hydrogels As Scaffolds for Tissue Engineering Applications: A Review. *Biomacromolecules* **2011**, *12* (5), 1387-1408.
12. Lin, C. C.; Anseth, K. S., PEG Hydrogels for the Controlled Release of Biomolecules in Regenerative Medicine. *Pharmaceutical Research* **2009**, *26* (3), 631-643.
13. Qiu, Y.; Park, K., Environment-sensitive hydrogels for drug delivery. *Advanced Drug Delivery Reviews* **2012**, *64*, 49-60.

14. Qiu, Y.; Park, K., Environment-sensitive hydrogels for drug delivery. *Advanced Drug Delivery Reviews* **2001**, *53* (3), 321-339.
15. Xia, T. T.; Liu, W. Q.; Yang, L., A review of gradient stiffness hydrogels used in tissue engineering and regenerative medicine. *Journal of Biomedical Materials Research Part A* **2017**, *105* (6), 1799-1812.
16. Tibbitt, M. W.; Anseth, K. S., Hydrogels as Extracellular Matrix Mimics for 3D Cell Culture. *Biotechnology and Bioengineering* **2009**, *103* (4), 655-663.
17. Li, Z. Q.; Guan, J. J., Thermosensitive hydrogels for drug delivery. *Expert Opinion on Drug Delivery* **2011**, *8* (8), 991-1007.
18. Hoare, T. R.; Kohane, D. S., Hydrogels in drug delivery: Progress and challenges. *Polymer* **2008**, *49* (8), 1993-2007.
19. Dhandayuthapani, B.; Yoshida, Y.; Maekawa, T.; Kumar, D. S., Polymeric Scaffolds in Tissue Engineering Application: A Review. *International Journal of Polymer Science* **2011**, *2011*, 19.
20. Lutolf, M. P.; Hubbell, J. A., Synthetic biomaterials as instructive extracellular microenvironments for morphogenesis in tissue engineering. *Nature Biotechnology* **2005**, *23* (1), 47-55.
21. Boateng, J. S.; Matthews, K. H.; Stevens, H. N. E.; Eccleston, G. M., Wound healing dressings and drug delivery systems: A review. *Journal of Pharmaceutical Sciences* **2008**, *97* (8), 2892-2923.
22. Mazunin, D.; Broguiere, N.; Zenobi-Wong, M.; Bode, J. W., Synthesis of Biocompatible PEG Hydrogels by pH-Sensitive Potassium Acyltrifluoroborate (KAT) Amide Ligations. *ACS Biomaterials Science & Engineering* **2015**, *1* (6), 456-462.
23. Howard, D.; Buttery, L. D.; Shakesheff, K. M.; Roberts, S. J., Tissue engineering: strategies, stem cells and scaffolds. *Journal of Anatomy* **2008**, *213* (1), 66-72.
24. Kim, I.; Byeon, H. J.; Kim, T. H.; Lee, E. S.; Oh, K. T.; Shin, B. S.; Lee, K. C.; Youn, Y. S., Doxorubicin-loaded highly porous large PLGA microparticles as a sustained-release inhalation system for the treatment of metastatic lung cancer. *Biomaterials* **2012**, *33* (22), 5574-5583.
25. Sunder, A.; Mulhaupt, R.; Frey, H., Hyperbranched polyether-polyols based on polyglycerol: Polarity design by block copolymerization with propylene oxide. *Macromolecules* **2000**, *33* (2), 309-314.
26. Garamus, V. M.; Maksimova, T. V.; Kautz, H.; Barriau, E.; Frey, H.; Schlotterbeck, U.; Mecking, S.; Richtering, W., Hyperbranched polymers: Structure of hyperbranched polyglycerol and amphiphilic poly(glycerol ester)s in dilute aqueous and nonaqueous solution. *Macromolecules* **2004**, *37* (22), 8394-8399.

27. Wan, D. C.; Li, Z. Y.; Huang, J. L., Synthesis of a new type of core-shell particle from hyperbranched polyglycerol. *Journal of Polymer Science Part A: Polymer Chemistry* **2005**, *43* (22), 5458-5464.
28. Kainthan, R. K.; Gnanamani, M.; Ganguli, M.; Ghosh, T.; Brooks, D. E.; Maiti, S.; Kizhakkedathu, J. N., Blood compatibility of novel water soluble hyperbranched polyglycerol-based multivalent cationic polymers and their interaction with DNA. *Biomaterials* **2006**, *27* (31), 5377-5390.
29. Kainthan, R. K.; Janzen, J.; Kizhakkedathu, J. N.; Devine, D. V.; Brooks, D. E., Hydrophobically derivatized hyperbranched polyglycerol as a human serum albumin substitute. *Biomaterials* **2008**, *29* (11), 1693-1704.
30. Liu, Z. H.; Janzen, J.; Brooks, D. E., Adsorption of amphiphilic hyperbranched polyglycerol derivatives onto human red blood cells. *Biomaterials* **2010**, *31* (12), 3364-3373.
31. Li, S. D.; Constantinescu, I.; Guan, Q. N.; Kalathottukaren, M. T.; Brooks, D. E.; Nguan, C. Y. C.; Kizhakkedathu, J. N.; Du, C. G., Advantages of replacing hydroxyethyl starch in University of Wisconsin solution with hyperbranched polyglycerol for cold kidney perfusion. *Journal of Surgical Research* **2016**, *205* (1), 59-69.
32. Kainthan, R. K.; Janzen, J.; Levin, E.; Devine, D. V.; Brooks, D. E., Biocompatibility Testing of Branched and Linear Polyglycidol. *Biomacromolecules* **2006**, *7* (3), 703-709.
33. Sunder, A.; Krämer, M.; Hanselmann, R.; Mülhaupt, R.; Frey, H., Molecular Nanocapsules Based on Amphiphilic Hyperbranched Polyglycerols. *Angewandte Chemie International Edition* **1999**, *38* (23), 3552-3555.
34. Sunder, A.; Heinemann, J.; Frey, H., Controlling the growth of polymer trees: Concepts and perspectives for hyperbranched polymers. *Chemistry – A European Journal* **2000**, *6* (14), 2499-2506.
35. Matsunaga, T.; Sakai, T.; Akagi, Y.; Chung, U.-i.; Shibayama, M., Structure Characterization of Tetra-PEG Gel by Small-Angle Neutron Scattering. *Macromolecules* **2009**, *42* (4), 1344-1351.
36. Sakai, T.; Matsunaga, T.; Yamamoto, Y.; Ito, C.; Yoshida, R.; Suzuki, S.; Sasaki, N.; Shibayama, M.; Chung, U.-i., Design and Fabrication of a High-Strength Hydrogel with Ideally Homogeneous Network Structure from Tetrahedron-like Macromonomers. *Macromolecules* **2008**, *41* (14), 5379-5384.
37. Li, X.; Tsutsui, Y.; Matsunaga, T.; Shibayama, M.; Chung, U.-i.; Sakai, T., Precise Control and Prediction of Hydrogel Degradation Behavior. *Macromolecules* **2011**, *44* (9), 3567-3571.
38. Knischka, R.; Lutz, P. J.; Sunder, A.; Frey, H., Structured hydrogels based on poly(ethyleneoxide) multi-arm stars with hyperbranched polyglycerol core. *Abstracts of Papers of the American Chemical Society* **2001**, *221*, U438-U438.

39. Kim, B. S.; Im, J. S.; Baek, S. T.; Lee, J. O.; Azuma, Y.; Yoshinaga, K., Synthesis and characterization of crosslinked hyperbranched polyglycidol hydrogel films. *Journal of Macromolecular Science Part A* **2006**, *43* (4-5), 829-839.
40. Kim, B. S.; Im, J. S.; Baek, S. T.; Lee, J. O.; Sigeta, M.; Yoshinaga, K., Synthesis of polyglycidol hydrogel films crosslinked with carboxyl-terminated poly(ethylene glycol). *Polymer Journal* **2006**, *38* (4), 335-342.
41. Oudshoorn, M. H. M.; Rissmann, R.; Bouwstra, J. A.; Hennink, W. E., Synthesis and characterization of hyperbranched polyglycerol hydrogels. *Biomaterials* **2006**, *27* (32), 5471-5479.
42. Yang, X. G.; Liu, L. J., Synthesis and Characterization of Novel Polyglycerol Hydrogels Containing L-Lactic Acid Groups as Pendant Acidic Substituents: pH-Responsive Polyglycerol-Based Hydrogels. *Journal of Applied Polymer Science* **2009**, *112* (6), 3209-3216.
43. Steinhilber, D.; Haag, R.; Sisson, A. L., Multivalent, biodegradable polyglycerol hydrogels. *International Journal of Artificial Organs* **2011**, *34* (2), 118-122.
44. Salehpour, S.; Dube, M. A., Application Properties of Stimuli-Responsive Polyglycerol Hydrogels. *Journal of Macromolecular Science Part A* **2012**, *49* (2), 103-110.
45. Salehpour, S.; Zuliani, C. J.; Dube, M. A., Synthesis of novel stimuli-responsive polyglycerol-based hydrogels. *European Journal of Lipid Science and Technology* **2012**, *114* (1), 92-99.
46. Melnick, R. L., Carcinogenicity and mechanistic insights on the behavior of epoxides and epoxide-forming chemicals. *Carcinogenesis Bioassays and Protecting Public Health* **2002**, *982*, 177-189.
47. Postnova, I.; Silant'ev, V.; Kim, M. H.; Song, G. Y.; Kim, I.; Ha, C. S.; Shchipunov, Y., Hyperbranched polyglycerol hydrogels prepared through biomimetic mineralization. *Colloids and Surfaces B: Biointerfaces* **2013**, *103*, 31-37.
48. Wu, C. Z.; Strehmel, C.; Achazi, K.; Chiapisi, L.; Dervede, J.; Lensen, M. C.; Gradzielski, M.; Ansorge-Schumacher, M. B.; Haag, R., Enzymatically Cross-Linked Hyperbranched Polyglycerol Hydrogels as Scaffolds for Living Cells. *Biomacromolecules* **2014**, *15* (11), 3881-3890.
49. Kharkar, P. M.; Kiick, K. L.; Kloxin, A. M., Designing degradable hydrogels for orthogonal control of cell microenvironments. *Chemical Society Reviews* **2013**, *42* (17), 7335-7372.



## CHAPTER II

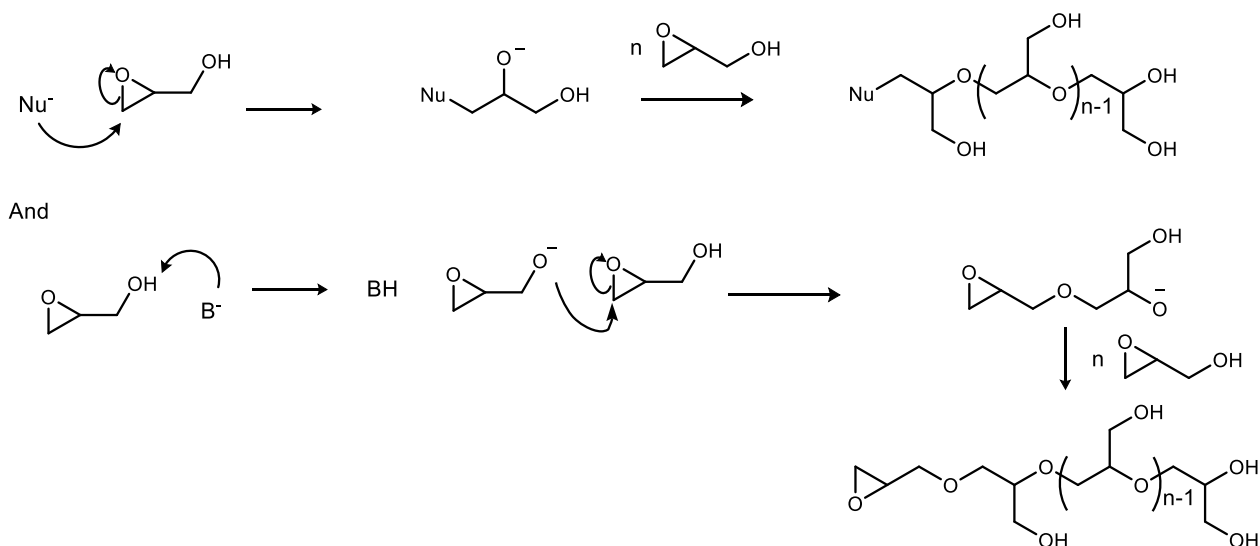
### SYNTHESIS AND CHARACTERIZATION OF BRANCHED POLY(GLYCIDOL)

#### INTRODUCTION

Poly(glycidol), sometimes referred to as poly(glycerol), is a flexible hydrophilic aliphatic polyether-polyol synthesized from the ring-opening polymerization of glycidol (2,3-epoxy-1-propanol) and exhibits varying polymeric architectures. Poly(glycidol) has been synthesized in three main forms i.e. linear, hyperbranched, and dendritic. Various groups have studied the polymerization of glycidol, a highly reactive hydroxy epoxide with latent AB<sub>2</sub> monomer structure, since the 1960s. Since then, two classes of polymerization have emerged based on the type of reagents used. They are anionic polymerization, which involves a base-catalyzed ring-opening polymerization and cationic polymerization, which involves an acid-catalyzed ring-opening polymerization.

Sandler and Berg<sup>1</sup> reported the first anionic polymerization of glycidol in 1966. Polymerizations were carried out at room temperature in the presence of triethylamine, pyridine, lithium hydroxide, potassium hydroxide, sodium hydroxide, sodium methoxide, sodium amide and other anionic catalyst. Conversions reported were greater than 70% for each catalyst used. They further suggested that the low molecular weight (~500 g/mol) polymer obtained by this method has a linear, regular structure and proposed two possible mechanistic routes for the likely course of the polymerization (Scheme II-1).

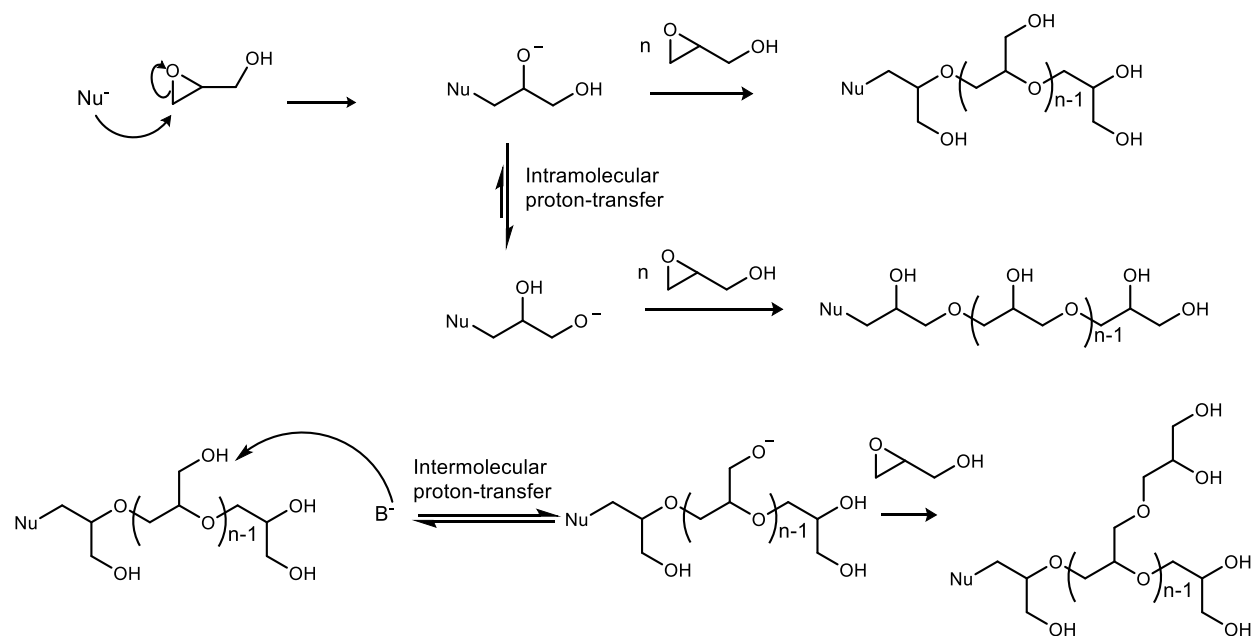
In 1985, Vandenberg reported on the anionic polymerization of glycidol using KOH as the catalyst.<sup>2</sup> In this work, he disputed claims made by Sandler and Berg about the structure of the



**Scheme II-1.** Sandler and Berg proposed mechanism for the anionic polymerization of glycidol.

polymer obtained. He showed that the polymer obtained when glycidol is polymerized with KOH has a complex branched structure and not linear, as proposed by Sandler and Berg. He gave detailed NMR evidence for the existence of the extensively branched structure and proposed that the branching originates from a rearrangement or transfer that occurs during the course of the polymerization (Scheme II-2).

Vandenberg applied his anionic polymerization protocol to the polymerization of glycidol trimethylsilyl (TMS) ether using potassium hydroxide (KOH) and potassium tert-butoxide (KOTBu). The product obtained with KOH was of low molecular weight and surprisingly branched in structure. This unexpected branching was a result of the hydrolysis of the trimethylsilyl group prior to polymerization. The observation of hexamethyldisiloxane and some trimethylsilanol confirmed these findings. When KOTBu was used, hydrolysis was substantially reduced, however significant amount of branching was still observed. Vandenberg proposed a mechanism for the formation of the branched structure during polymerization. This study concludes that the TMS

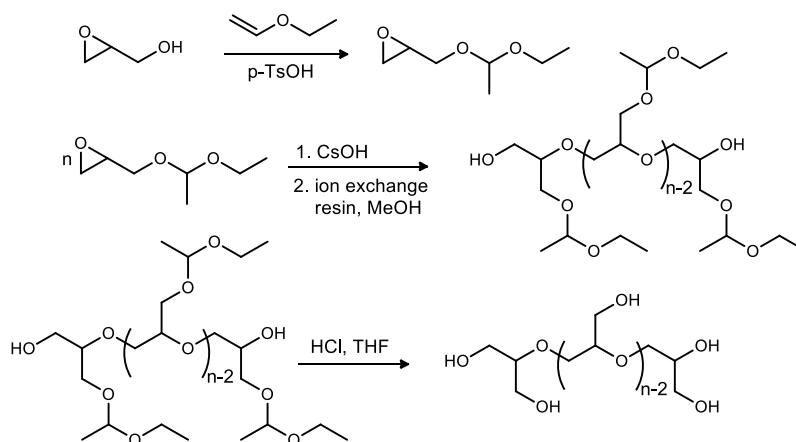


**Scheme II-2.** Vandenberg proposed mechanism for the anionic ring opening polymerization of glycidol.

group was not a viable protecting group for the synthesis of linear poly(glycidol), as it was not stable under polymerization conditions.

A few years later, Spassky and others<sup>3</sup> explored the polymerization of protected glycidol using anionic and coordination initiators (Scheme II-3). Glycidol, protected as its ethoxy ethyl ether, was subjected to polymerization with cesium hydroxide (CsOH). The polymer obtained had molecular weights as high as 30,000 g/mol with no observable cleavage of the protecting group. As a result, the polymer was linear in structure and soluble in non-polar organic solvents. Restoration of the hydroxyl groups was achieved by cleavage with acid. Stiriba et al<sup>4</sup> later reported a modified version of this synthetic scheme where they used KOtBu as the initiator instead of CsOH. Copolymers of ethylene oxide and ethoxy ethyl glycidyl ether were also synthesized by Spassky et al<sup>3</sup> using KOH as the catalyst thus further demonstrating the stability of the protecting

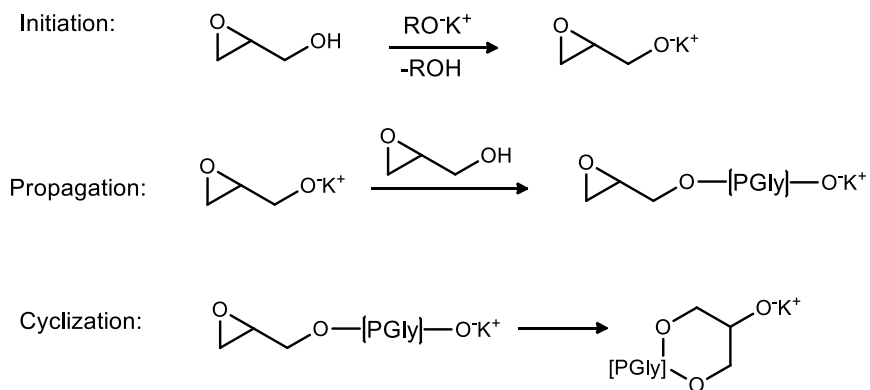
group under basic condition. This protecting group is now the most widely used for the synthesis of linear poly(glycidol).



**Scheme II-3.** Synthesis of linear poly(glycidol) via anionic polymerization

Sunder and coworkers<sup>5</sup> later demonstrated that hyperbranched poly(glycidol)s can be synthesized in a controlled manner by anionic ring opening polymerization using partially deprotonated (10% using potassium methylate) 1,1,1-tris(hydroxymethyl) propane (TMP) as the initiator. Here they reinforce the work of Vandenberg by demonstrating that there is fast proton exchange between the alkoxide ion and the hydroxyl group. This exchange is considerably faster than the chain growth, which consequently results in the multiplication of active centers giving rise to chain branching. Slow monomer additions (~ 4 mL/hr) was used to obtain highly branched polyether polyol with control over molecular weight, polydispersity and microstructure. The hyperbranched structure was characterized comprehensively by Frey and other.<sup>5</sup> It is worth mentioning that Sunder and coworkers discovered the existence of macrocyclic polymer formed by the intramolecular ring-opening polymerization of glycidol at high glycidol to initiator ratios

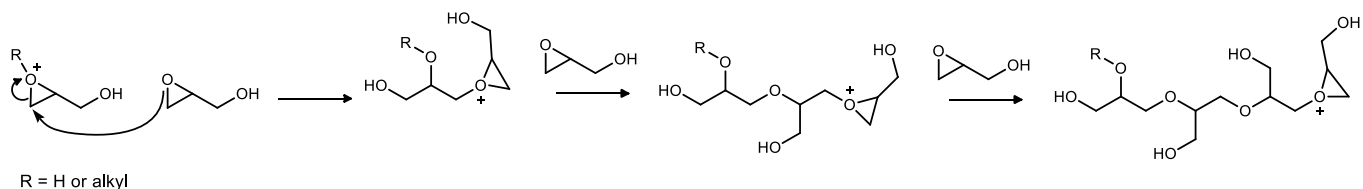
or in the absence of an initiator (Scheme II-4). Cyclization has the effect of broadening polydispersities and diminishing molecular weights.



**Scheme II-4.** Formation of macrocyclic polymers via anionic intramolecular ring-opening.

Copolymers of glycidol have also been synthesized by anionic ring-opening polymerization. Wilms and others<sup>6</sup> reported the synthesis of hyperbranched poly(ethylene glycol)-*co*-poly(glycidol) copolymers by anionic ring-opening polymerization. The obtained copolymers had moderate polydispersity (< 1.8), high molecular weight (up to 49,800 g/mol) and varying glycidol content. Schomer et al<sup>7</sup> also showed that glycidol can also be copolymerized with propylene oxide to give hyperbranched poly(propylene oxide) via anionic ring opening polymerization. Molecular weights ranged from 1200 to 2000 g/mol and the degree of branching was found to increase as the composition of glycidol in the copolymer increased.

Penczek and coworkers<sup>8</sup> reported the cationic ring-opening polymerization of glycidol. Lewis acid initiators (BF<sub>3</sub>·Et<sub>2</sub>O, SnCl<sub>4</sub>, HPF<sub>6</sub>·Et<sub>2</sub>O) was used to polymerize glycidol in bulk or in solution (using dichloromethane as the solvent). An inverse relationship was observed between temperature and molecular weights in addition to a high degree of polymerization and greater than 80% monomer conversion was also reported. Two competing propagating mechanisms was

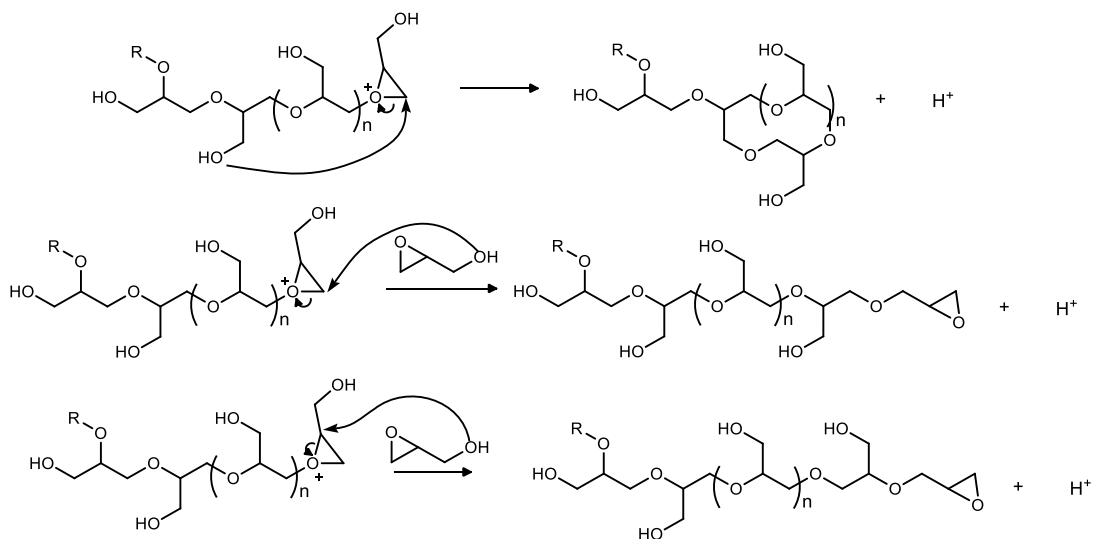


**Scheme II-5.** Active chain end mechanism for the polymerization of glycidol.

proposed: active chain end (ACE) mechanism and activated monomer mechanism (AM). The active chain end mechanism involves a nucleophilic attack of the glycidyl monomer on the tertiary oxonium ion active species (Scheme II-5).

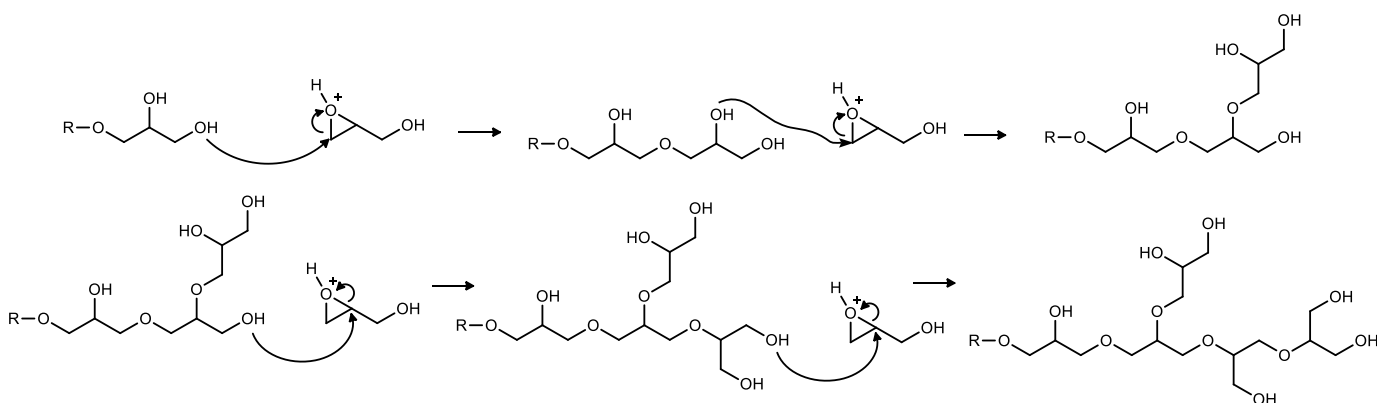
Polymerization of glycidol via the ACE mechanism should lead to a polymer with exclusively primary hydroxyl groups. Chain transfer reactions involving hydroxyl groups from monomer or polymer can also occur. Intramolecular chain transfer could result in cyclization, which would limit the molecular weight obtainable by cationic polymerization (Scheme II-6).

The activated monomer mechanism involves a nucleophilic attack of an oxygen atom of the hydroxyl group (at the electrically neutral polymer chain) on the  $\alpha$ -carbon atom of an oxonium



**Scheme II-6.** Chain transfer reaction via ACE mechanism during polymerization of glycidol.

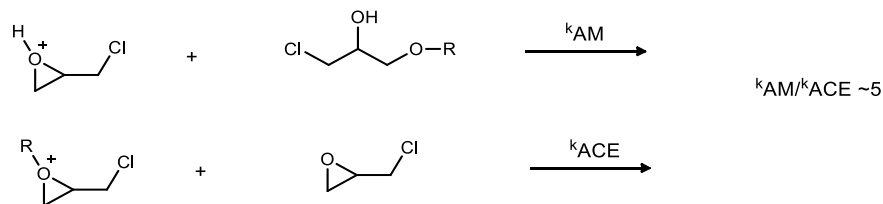
ion (the protonated monomer). If this mechanism is dominant, then chain propagation occurs by successive addition of activated (protonated) monomer to the terminal hydroxyl group of a growing polymer chain (Scheme II-7).



**Scheme II-7.** Activated monomer mechanism for the polymerization of glycidol.

Penczek and others carried out kinetic studies on the mechanism of polymerization of oxiranes.<sup>9</sup> They determined the ratio of rate constants for the reaction of activated oxiranes with hydroxyl groups and the oxirane ring oxygen (Scheme II-8). The ratio of the rate constants was found to be ~ 5:1 (hydroxyl to oxirane ring oxygen) for epichlorohydrin. Hence, when the hydroxyl end group of the polymer chain is more nucleophilic than that of the monomer, the AM mechanism can dominate over the ACE mechanism. This is desirable because cyclization, which occurs by the ACE mechanism, can be avoided.

In most cases, cationic polymerization of glycidol proceeds via both the AM and the ACE mechanism. Branched structures are formed from reaction of the protonated monomer with any hydroxyl group in the system (either at the chain end or in a linear repeating unit), whereas linear structures are formed by ACE-type propagation of the actively growing polymer chain. Dworak et



**Scheme II-8.** Ratio of the rate constants for the polymerization of epichlorohydrin via AM and ACE mechanism.

al. showed that there exist a dependence of the AM contribution on the type of catalyst used.<sup>10</sup> However, Kubisa<sup>11</sup> reasoned that quantification of the contribution of both mechanism is difficult due to changes in the concentration and reactivity of hydroxyl groups present in the monomer and the polymer during the course of the reaction. Despite this, it was deduced by Magnusson and Malmstrom<sup>12</sup> that contribution from the AM mechanism increases during the course of the polymerization. This was based on their observation that the content of branched units increases with increasing monomer conversion.

Various copolymer of glycidol have also been synthesized by cationic ring-opening polymerization. Royappa<sup>13</sup> reported the copolymerization of glycidol and epichlorohydrin with boron trifluoride catalyst. He observed that polymerization resulted in the formation of a block or graft copolymer, with evidence of some branching and the existence of small cyclic species. The molecular weight was found to vary inversely with the amount of water present. He went on to explore boron trifluoride-catalyzed copolymerization of glycidol with other nonpolar epoxide comonomer, namely isopropyl glycidyl ether, 1,2-epoxybutane, propylene oxide, and glycidyl phenyl ether.<sup>14-15</sup> These copolymers were all synthesized at room temperature open to the atmosphere. These products were proposed to consist of a hyperbranched poly(glycidol) core, incorporating various fractions of comonomer, with arms made from comonomer units. They all



were of low molecular weights and high molecular weight distribution. Both solubility and glass transition temperature were found to vary according to the proportion of comonomer units present in the copolymers.

Research interest in this class of polymers is perhaps motivated by their inherent biocompatibility. Poly(glycidol) is structurally similar to polyethylene glycol (PEG) which has been well studied and is widely used in the biomedical and pharmaceutical industry for the suppression of protein adsorption to surfaces in contact with bodily fluids<sup>16</sup> and for drug conjugation for increased solubility and bioavailability.<sup>17</sup>

The biocompatibility of poly(glycidol) was explored by Brooks and other<sup>18</sup> in 2006. These testing were conducted both *in vitro* and *in vivo*. The *in vitro* studies included hemocompatibility testing, complement activation, red blood cell aggregation, and cytotoxicity measurements among others. They also did comparative studies with some common biocompatible polymers currently in clinical use. Based on the results they obtained from these experiments they concluded that poly(glycidol) is highly biocompatible. Hyperbranched poly(glycidol) was tested for toxicity in mice and found to be well tolerated, even in high doses. That same year, Brooks et al reported the synthesis of high molecular weight hyperbranched poly(glycidol),<sup>19</sup> which was not available at the time. They later showed, via *in vitro*<sup>20</sup> and *in vivo*<sup>21</sup> studies, that these too were highly biocompatible.

Because of the biocompatibility of poly(glycidol), the use of some poly(glycidol) derivatives as biomaterials has been widely explored. One such example involves the hydrophobic modification of hyperbranched poly(glycidol) by the attachment of C18 alkyl groups followed by methoxy polyethylene glycol to a certain fraction of the polyether polyol OH groups.<sup>22</sup> These were synthesized in with varying composition. The resulting material was found to be non-toxic in mice,

and exhibits low intrinsic viscosities coupled with high water solubility. These properties amongst others, make this biomaterial an extremely promising candidate for use as human serum albumin (HSA) substitutes. Such a substitute would drastically reduce the risk of disease transmission making it a safe, inexpensive alternative.

Another example of the biomedical application of poly(glycidol) derivatives is the development of hyperbranched poly(glycidol) sulfates as alternatives to heparin, a highly sulfated natural glycosaminoglycan widely used as an injectable anticoagulant.<sup>23</sup> These hyperbranched poly(glycidol) sulfates can be conveniently prepared in a straightforward manner, which can be easily scaled up (Figure II-1). These poly(glycidol) sulfates were shown to exhibit both anticoagulant and anti-inflammatory activities that makes them promising candidates for the development of drugs to treat coagulation and inflammation that is typically seen in cardiovascular diseases and sepsis amongst others.

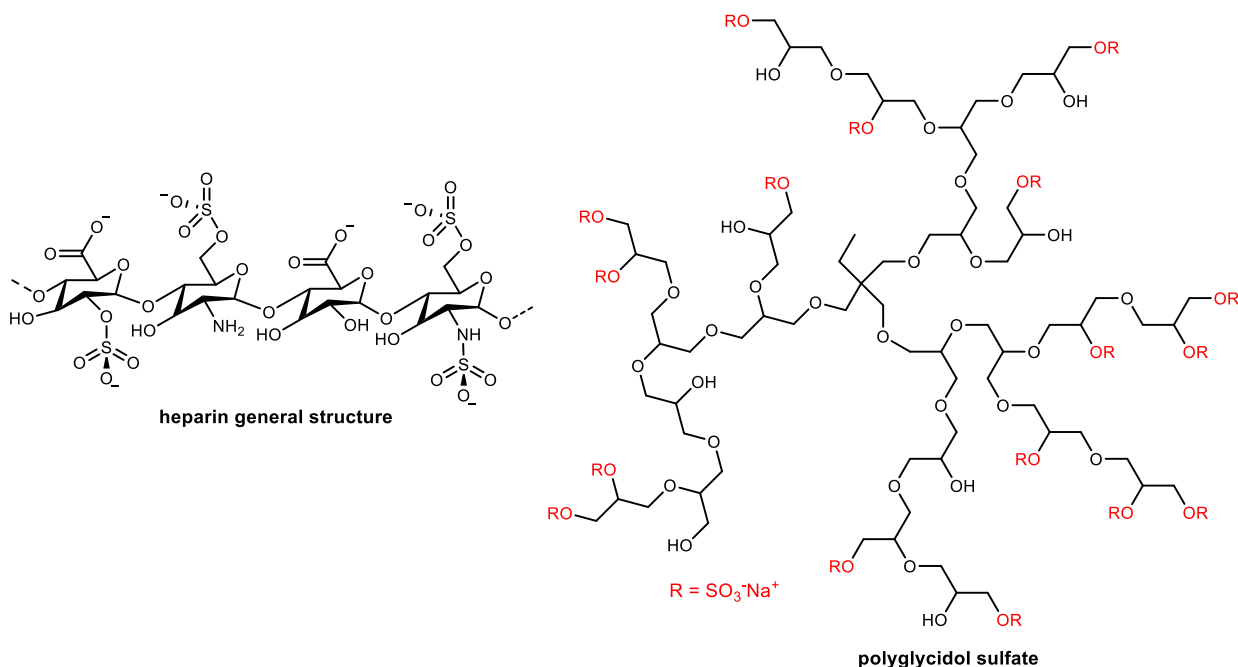


**Figure II-1.** Poly(glycidol) sulfates as heparin analogs.

Hyperbranched poly(glycidol) has also been used in the design and development of protein-resistant surfaces for medical devices or biosensors. Haag and others<sup>24</sup> showed that poly(glycidol) can be modified with a surface-active disulfide linker group. These can then be attached to a surface and subsequently self-assembled monolayers can be obtained. Further studies showed that these monolayers of the disulfide-functionalized poly(glycidol) effectively prevented the adsorption of protein onto gold used as the model surface. In a subsequent study by the same author, protein adsorption onto monoamino oligo(glycidol) self-assembled monolayers was systematically investigated to derive a structure-property relationship.<sup>25</sup> Co-polymers of glycidol and epichlorohydrin has been shown to be a viable component of coatings that has been applied to hydrophobic porous microscopic poly(styrene-divinylbenzene) beads. These coated beads are no longer hydrophobic and has been used to separate, purify and analyze a wide assortment of important biological molecules, most of which are soluble in aqueous media.

## RESULTS AND DISCUSSION

### **Sn(OTf)<sub>2</sub>-Mediated Ring-Opening Polymerization of Glycidol**

Despite many advances in the cationic polymerization of glycidol, there still exist a need for a catalyst that will allow for control over molecular weight, molecular weight distribution and polymer architecture. During our recent work on the tin triflate-catalyzed ring-opening polymerization of cyclic esters and carbonates,<sup>26</sup> it was observed that residual amounts of the catalyst react readily with epoxide groups. This prompted us to launch an investigation into the polymerization of glycidol catalyzed by tin triflate to see if this catalyst can offer control over molecular weight, polydispersity and microstructure. It was further envisioned that control over the branching of poly(glycidol) may lead to materials with properties that allow it to overcome the limitations of polyethylene glycol in protein therapeutics.<sup>27</sup>

Collado et al. demonstrated that tin triflate was an efficient and versatile catalyst for the highly regioselective opening of styrene oxide with aromatic amines.<sup>28</sup> Tin triflate was also found to catalyzed the opening of styrene oxide with aliphatic amines but in moderate to high yields and with less regioselectivity. Additionally, Dworak and coworker<sup>10</sup> investigated the ring opening of glycidol with either alcohols in the presence of boron trifluoride, and found that attack at the less hindered carbon of the epoxide was favored. We hypothesize that tin triflate might provide efficient activation of the epoxide, hence increasing the contribution of the ACE mechanism during the propagation of polymerization. Increase contribution of the ACE mechanism in a controlled manner, would result in a less branched polymer. This represent a novel approach to controlled

branching of poly(glycidol), as previous attempts were focus on the copolymerization of glycidol with its hydroxy-protected counterpart or a linear comonomer via anionic polymerization.<sup>5-7</sup>

### Optimization of Reaction Conditions

Our investigation began with the synthesis of poly(glycidol) using isoamyl alcohol as the initiator, tin triflate as the catalyst and tetrahydrofuran as the reaction medium. Glycidol was added dropwise at 0 °C and polymerization when to completion within 12 hrs. The crude polymer was diluted with methanol and isolated by precipitation in acetone. Analysis of the <sup>1</sup>H NMR revealed that the tetrahydrofuran copolymerizes with glycidol. Additionally, upon precipitation in acetone, acetal formation was observed (Figure II-2). As a result, bulk conditions were employed, and a

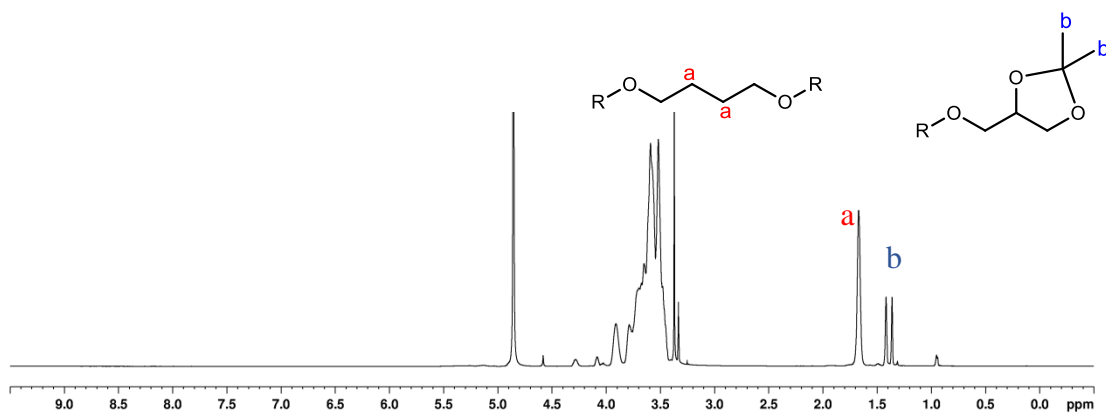


**Figure II-2.** <sup>1</sup>H NMR (CD<sub>3</sub>OD) showing copolymerization of glycidol and tetrahydrofuran and the formation of acetals when precipitated in acetone.

stoichiometric amount (with respect to the catalyst) of sodium bicarbonate in water and methanol was added to the reaction prior to precipitation in acetone. These optimizations resulted in pure poly(glycidol) (Figure II-3). <sup>13</sup>C NMR showed that no bicarbonate was present and <sup>19</sup>F NMR showed that no tin triflate was present in the final product.

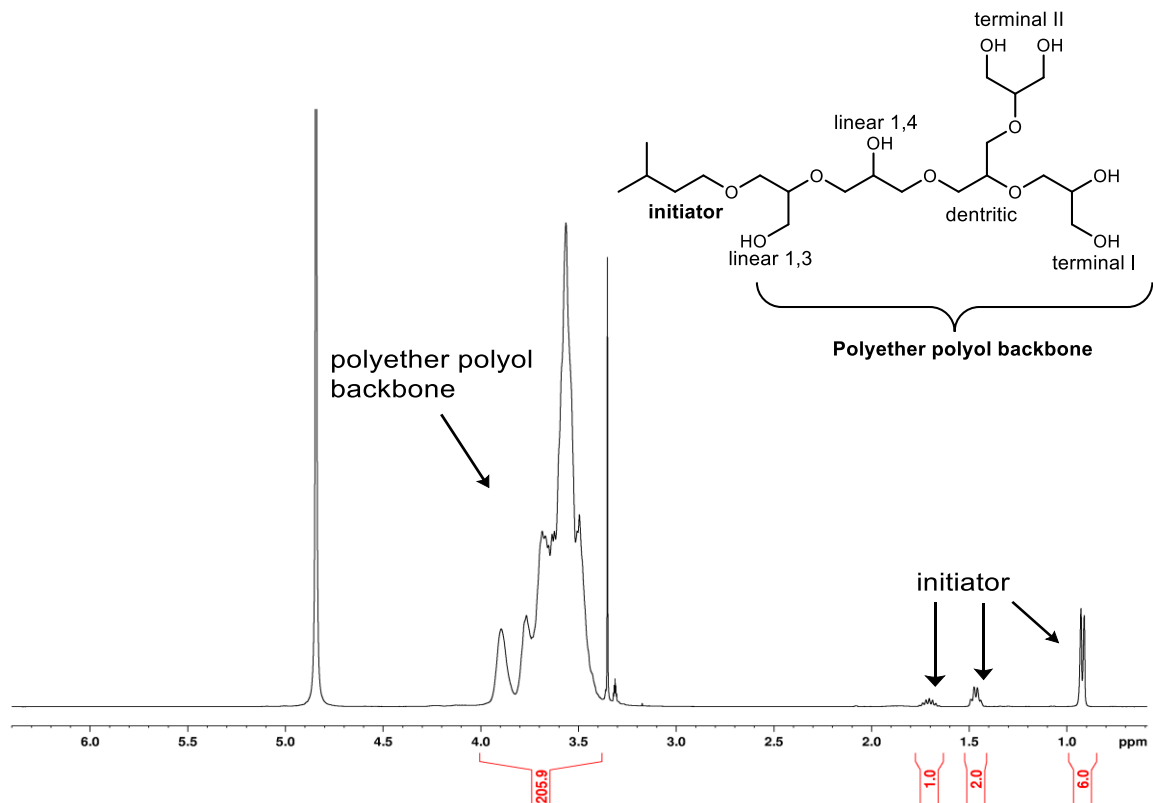


**Figure II-3.**  $^1\text{H}$  NMR ( $\text{CD}_3\text{OD}$ ) of poly(glycidol) showing the incorporation of isoamyl alcohol

### Characterization via NMR, GPC and MALDI-ToF MS

$^{13}\text{C}$  NMR gave detail information about the structural components of poly(glycidol). Vandenberg, Spassky, Dworak, and Frey gave the assignment of the signals in the  $^{13}\text{C}$  NMR spectrum. Based on their work the peak assignments for each structural unit are given in Figure II-4.

Quantitative  $^{13}\text{C}$  NMR can give details about the relative abundance of each structural unit present in poly(glycidol). Inverse-gated (IG) proton decoupled  $^{13}\text{C}$  NMR allows reliable integration of the signal intensity. To check the reliability of the  $^{13}\text{C}$  NMR data, the integration of the signal intensities was accessed to ensure that they reflect the fact that each structural unit has

one methane and two methylene carbons. Additionally, the sum of the dendritic units and the initiating hydroxyl unit should be equal to the number of terminal units present in a single polymer.

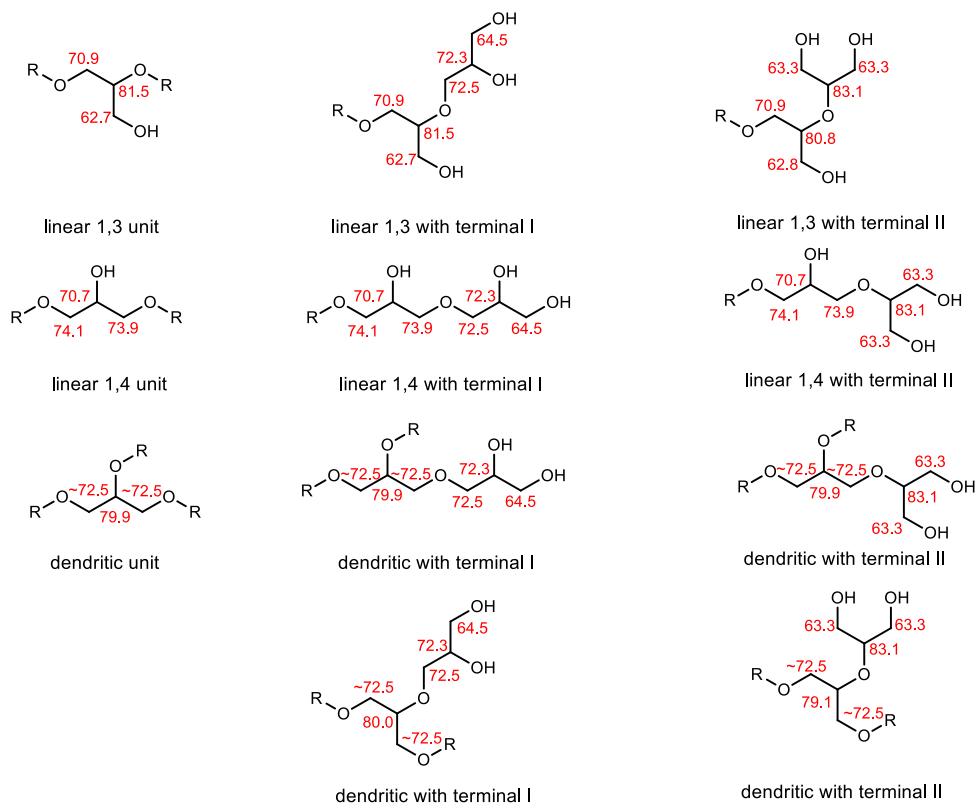


**Figure II-4.** Illustrations of the different structural units present in poly(glycidol) and their respective <sup>13</sup>C NMR assignments (CD<sub>3</sub>OD, ppm).

Initially, four different poly(glycidol) samples were prepared, each with differing molecular weight. PGly-1, PGly-2, and PGly-3a was synthesized on a 2g scale while PGly-3b was synthesized on a 5g scale. The successful synthesis of PGly-3b demonstrates the scalability of the reaction. Up to 15g has been attempted, however it was difficult to maintain control of the reaction. The results of the interpretation of the inverse-gated (IG) proton decoupled <sup>13</sup>C NMR spectra for these four different branched poly(glycidol) samples are summarized in Table II-1.

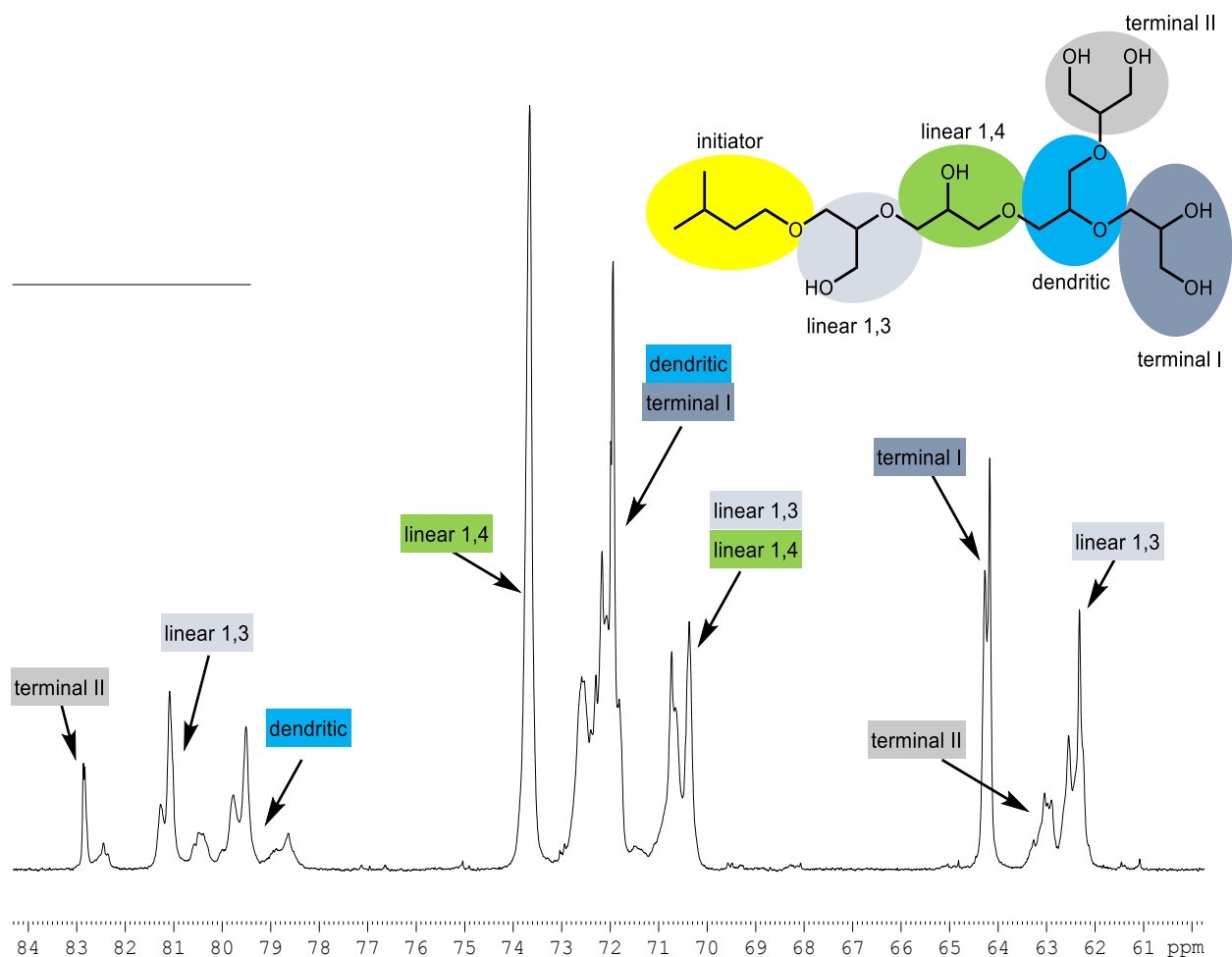


**Figure II-5.**  $^{13}\text{C}$  NMR ( $\text{CD}_3\text{OD}$ ) of poly(glycidol) showing structural assignment of the carbons.

It is important to note that the substructure of the peaks in the region 78.6-83.4 ppm is due to the different possible triads as well as the random distribution of units (Figure II-5). The relative abundance of linear 1,3 units is higher compared to hyperbranched poly(glycidol) synthesized by anionic polymerization. There does not seem to be a relationship between the molecular weight and the ratio of linear units. The increase amounts of linear 1,3 units is consistent with propagation via ACE and AM mechanism, where the more hindered carbon of the epoxide is attacked by the nucleophile. Linear 1,4 and dendritic units are produced exclusively by the AM mechanism.



**Table II-1.** Interpretation of the inverse gated (IG) proton-decoupled  $^{13}\text{C}$  NMR ( $\text{CD}_3\text{OD}$ ) of poly(glycidol).

Structural Unit	Chemical Shift (ppm)	Relative Integrals			
		PGly-1	PGly-2	PGly-3a	PGly-3b
<b>T<sub>2</sub> (CH)</b>	83.2-82.3	0.28	0.25	0.28	0.26
<b>L<sub>1,3</sub> (CH)</b>	81.6-80.2	1.00	1.00	1.00	1.00
<b>D (CH)</b>	80.2-78.1	0.92	0.94	0.96	1.02
<b>2 L<sub>1,4</sub> (CH<sub>2</sub>)</b>	74.1-73.2	2.57	2.60	2.58	2.65
<b>2 D (CH<sub>2</sub>), 2 T<sub>1</sub> (CH, CH<sub>2</sub>)</b>	72.9-71.6	4.33	4.17	4.27	4.22
<b>L<sub>1,3</sub> (CH<sub>2</sub>), L<sub>1,4</sub> (CH), I (CH<sub>2</sub>)</b>	71.2-69.8	2.20	2.04	2.11	2.27
<b>T<sub>1</sub> (CH<sub>2</sub>)</b>	64.5-63.9	1.02	1.06	1.00	0.95
<b>2 T<sub>2</sub> (CH<sub>2</sub>)</b>	63.5-62.7	0.51	0.49	0.50	0.50
<b>L<sub>1,3</sub> (CH<sub>2</sub>)</b>	62.7-61.8	1.19	1.25	1.24	1.17
<b>I (CH<sub>2</sub>)</b>	39.9-39.0	0.10	0.07	0.04	0.04
<b>I (CH)</b>	26.2-25.7	0.11	0.07	0.04	0.04
<b>2 I (CH<sub>3</sub>)</b>	23.3-22.7	0.20	0.14	0.08	0.08
Structural Unit	Relative abundance (%)				
<b>Linear 1,3 (L<sub>1,3</sub>)</b>	21.7	21.7	21.9	21.8	
<b>Linear 1,4 (L<sub>1,4</sub>)</b>	27.9	28.1	28.2	28.8	
<b>Dendritic (D)</b>	20.1	20.3	21.0	22.1	
<b>Terminal I (T<sub>1</sub>)</b>	22.1	22.9	21.8	20.7	
<b>Terminal II (T<sub>2</sub>)</b>	6.1	5.5	6.1	5.6	
<b>Initiator (I)</b>	2.2	1.5	0.9	0.9	

The degree of branching (DB) is a measure of the dendritic character of a polymer. It describes the branching structure of a polymer relative to a perfect dendrimer. For polymers with linear structure the DB is 0. Polymers with perfectly branched dendrimers has a DB of 1, while hyperbranched polymers typically exhibit a DB between 0 and 1 (DB of 0.5-0.66 is most often seen for hyperbranched poly(glycidol)).<sup>29</sup> The DB is calculated from the integration of signal intensities in the IG  $^{13}\text{C}$  NMR spectrum using the following equation derived by Holter and Frey.

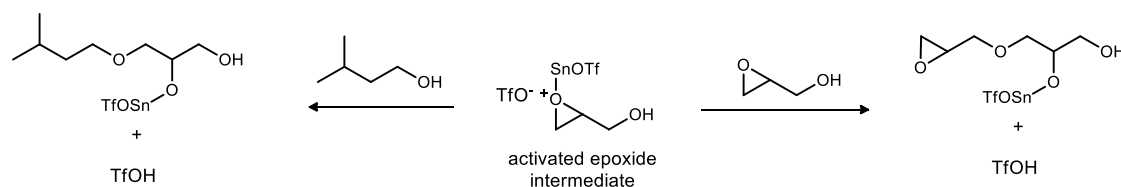
$$DB = \frac{2D}{2D + L_{1,3} + L_{1,4}}$$

DB represents degrees of branching,  $L_{1,3}$ ,  $L_{1,4}$ , and  $D$  represents the fractions of linear 1,3, linear 1,4 and dendritic units respectively. Table II-2 summarizes the DB calculated for the four different glycidol homopolymer synthesized by  $\text{Sn}(\text{OTf})_2$ -mediated ring-opening polymerization of glycidol.

**Table II-2.** Showing results from the  $^{13}\text{C}$  NMR, MALDI-TOF MS and GPC.

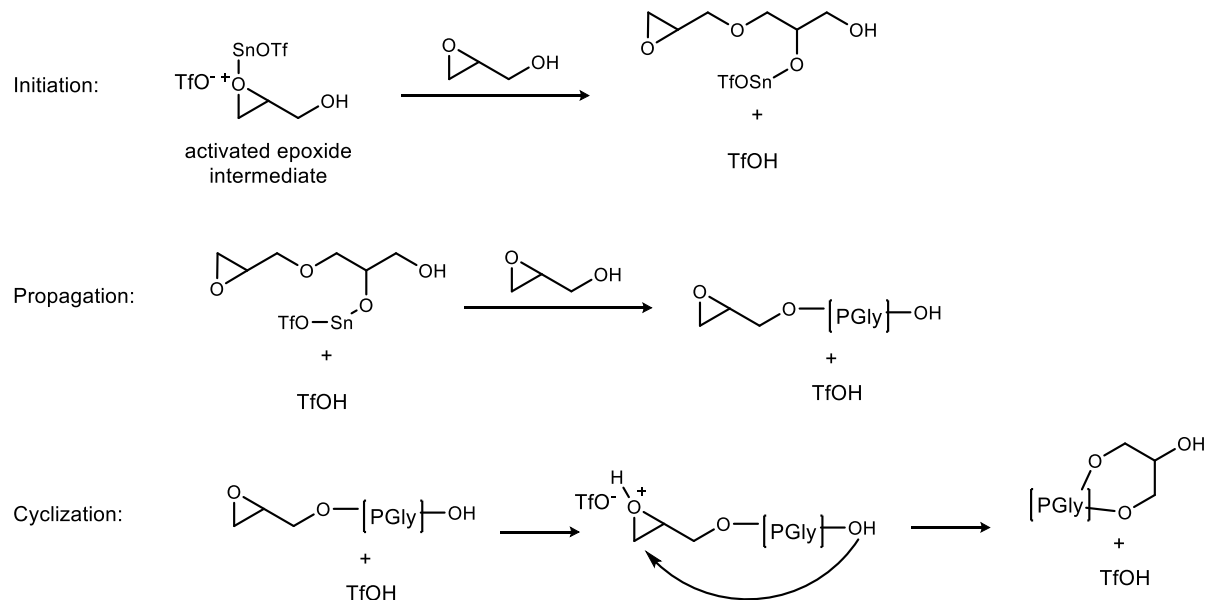
Sample	Degrees of branching	Desired molecular weight	Molecular weight by $^{13}\text{C}$ NMR	MALDI-TOF MS			GPC
				$M_n$	$M_w$	$M_w/M_n$	$M_w/M_n$
PGly-1	0.45	1000	3526	2429	2693	1.11	1.23
PGly-2	0.45	2000	4853	2041	2246	1.10	1.26
PGly-3a	0.46	3000	8224	2272	2567	1.13	1.23
PGly-3b	0.47	3000	8406	2914	3834	1.32	1.25

The degrees of branching for the poly(glycidol) samples analyzed varied from 0.45 to 0.47 indicating that there may be a proportional relationship between molecular weight and degrees of branching. The DB is also lower compared to poly(glycidol) prepared by anionic methods. The data presented in Table II-2 shows that the molecular weight calculated by NMR is significantly higher than the desired molecular weight. This would indicate that isoamyl alcohol (IAOH) might not be the sole initiator of glycidol polymerization. The molecular weight calculated from NMR also significantly differs from that seen in the MALDI-ToF mass spectroscopy. Analysis of the reaction mechanisms offered some explanation for this disparity. In the activated monomer



**Scheme II-9.** Competition between IAOH and glycidol for activated epoxide intermediate

mechanism, two alcohols compete to react with the activated monomer in the initiation step. The two competing alcohols are isoamyl alcohol and glycidol (Scheme II-9). Since glycidol is higher in concentration, it preferentially reacts in the initiation step. However, if this is the case, then the presence of an epoxide peak should be observed in the  $^1\text{H}$  and  $^{13}\text{C}$  NMR. Analysis of the NMR spectrums showed no epoxide peaks. This could be due to cyclization (Scheme II-10). Efforts were



**Scheme II-10.** Proposed mechanism for the intramolecular macrocyclization of poly(glycidol) initiated by glycidol

directed towards MALDI-ToF mass spectroscopy to look for evidence of the presence of two distinct type of polymer.

The MALDI-ToF spectrum shows a clearly distinct sub-distribution shifted by 14-16 mass units (Figure II-6). This difference in the mass corresponds to the difference between isoamyl alcohol and glycidol. This led to the conclusion that the observed sub-distribution results from polymers initiated from glycidol that then underwent macrocyclization by intramolecular ring-opening of the epoxide. Unfortunately, MALDI-ToF mass spectroscopy is the only analytical tool that allows for detection of the macrocycle. In light of this discovery, we start exploring ways to optimize reaction conditions that would eliminate the formation of polycyclic species, with good control over molecular weight. The consistently low molecular weight observed in the MALDI-ToF could be due to the relatively large amounts of initiation steps created by the large abundance of glycidol present in the reaction. Initially reactions were carried out at  $-10\text{ }^{\circ}\text{C}$ . This low

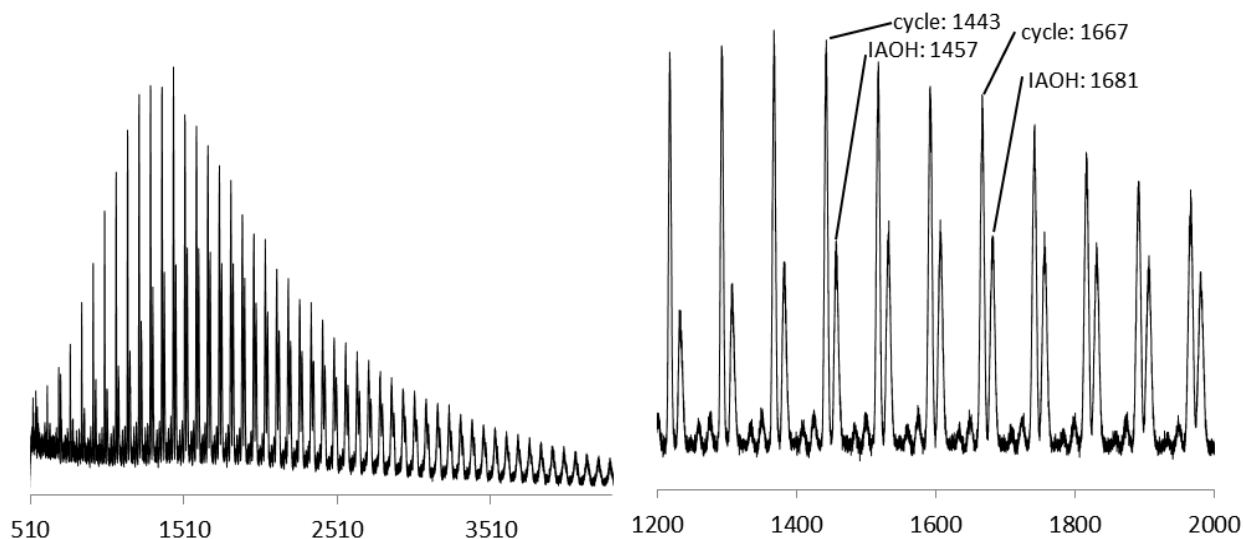


**Figure II-6.** MALDI-ToF mass spectra of poly(glycidol) obtained from the  $\text{Sn}(\text{OTf})_2$  mediated polymerization with isoamyl alcohol (IAOH).

temperature may have slowed the rate of initiation allowing for an increase in glycidol concentration during dropwise addition of glycidol. Upon increasing the reaction temperature to 0 °C and slowing the initial rate of addition of glycidol a significant decrease in the ratio of the macrocycle to the polymer was observed.

When the temperature was further raised from zero degrees to room temperature there was a considerable shift in the MALDI-ToF from being centered on 1500 Da at zero degree to being centered on 2000 Da at room temperature. Additionally, it was observed that the polycyclic species has decrease significantly (Figure II-7). Stirring with a magnetic stirrer was difficult and hence the reaction was difficult to control at 40 °C. Reaction conditions were optimized by designing a small-scale reactor employing the use of a mechanical stirrer and a syringe pump to control the rate of monomer addition. Using this reactor, polymerization under different reaction temperatures with different rates of monomer addition were explored and the results were summarized in Table II-3. Sample PGly-4 was synthesized at a temperature of 37 °C and a monomer addition rate of 0.1

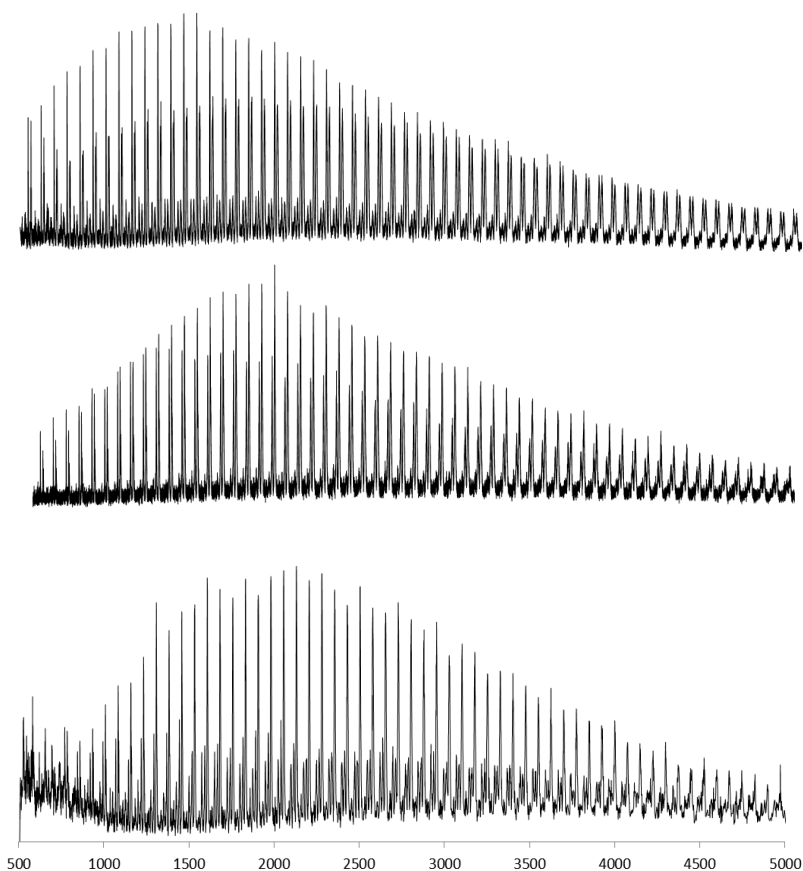


**Figure II-7.** Showing decrease in macrocyclic species as the rate of addition is decreased. (top) slow monomer addition at 0 °C, (middle) slow monomer addition at 25 °C, (bottom) slow monomer addition at 25 °C with a syringe pump and mechanical stirrer.

mL/hr. Despite a significant increase in the DB, the molecular calculated from NMR and MALDI-ToF were in closer agreement with the desired molecular weight. This trend continued when the temperature was lowered from 37 to 25 °C while keeping the addition rate of glycidol constant at 0.1 ml/hr. When the addition rate was increased to 0.2 ml/hr a significant decrease in the macrocyclic species was observed in the MALDI-ToF (Figure II-7). The desired molecular weight and the molecular weight calculated by NMR showed better agreement as a result of less macrocyclic species. This is evident in samples PGly-6 and PGly-7.

Sample	Temp / °C	% Yield	DB	Desired Mn	Mn by <sup>13</sup> C NMR	MALDI-ToF MS			GPC
						M <sub>n</sub>	M <sub>w</sub>	M <sub>w</sub> /M <sub>n</sub>	M <sub>w</sub> /M <sub>n</sub>
<b>PGly-4</b>	37	72	0.56	3000	4408	2232	2880	1.29	1.28
<b>PGly-5</b>	25	84	0.59	3000	3623	1416	1831	1.29	1.33
<b>PGly-6</b>	25	75	0.59	3000	3082	1943	2568	1.32	1.27
<b>PGly-7</b>	25	84	0.56	4000	3856	2353	3199	1.36	1.29
<b>PGly-8</b>	25	70	0.56	6000	4067	2012	2501	1.24	1.21
<b>PGly-9</b>	25	85	0.56	6000	3189	1963	2568	1.31	1.33
<b>PGly-10</b>	0-25	60	0.49	6000	7190	2199	2683	1.22	1.25

**Table II-3.** Showing results from the <sup>13</sup>C NMR, MALDI-TOF and GPC.

The ability to control molecular weight by changing the monomer to initiator ratio as well as the scalability of the reaction was explored in samples PGly-8 and PGly-9. Both reactions were carried out on a 6g scale with a desired molecular weight of 6000 g/mol. The molecular weight calculated from NMR and MALDI-ToF for these samples does not correspond to the desired molecular weight. This shows that reaction kinetics differ according to the size of the reaction. By adjusting the reaction parameters (PGly-10), better agreement between the desired molecular weight and the molecular weight calculated by NMR was observed. Additionally, the decrease in the DB with decreasing reaction temperature, suggest that there is a relationship between temperature and DB. The molecular weight calculated by MALDI differed from the molecular weight determined by NMR. This could be as a result of the broad molecular weight distribution.

MALDI-ToF MS is only accurate for polymers with very narrow molecular weight distribution (> 1.1). To investigate the accuracy of the MALDI-ToF, sample PGly-5 was separated into several fractions by size exclusion chromatography (SEC). Each fraction was then analyzed by MALDI-ToF MS. The results indicate that the molecular weight distribution observed by MALDI-ToF is not the actual molecular weight distribution for the polymer. SEC-MALDI-ToF

MS gives a better picture as each of the fractions analyzed had molecular weight distributions less than 1.1 (Figure II-8).

### **SEC/MALDI-ToF Mass Spectrometry Study of Branched Poly(glycidol)**

Gel permeation chromatography (GPC) analysis of branched poly(glycidol), calibrated with poly(styrene) standards, does not allow for accurate quantitative molecular weight determination due to differences in solvent/polymer interactions and hydrodynamic volume of branched poly(glycidol) compared to poly(styrene) polymer standards. Additionally, branched poly(glycidol) can aggregate or interact with the GPC column due to their large number of end groups. If no aggregation occurs, GPC can be used to determine the molecular weight distribution of poly(glycidol), provided a suitable polymer standard is used. Additionally, MALDI-ToF MS is only accurate for polymers with very narrow molecular weight distribution ( $> 1.1$ ). Hence while we were able to use these two independent methods to optimize the polymerization of glycidol, these methods could not be used to accurately characterize the molecular weight of the synthesized branched poly(glycidol).

The off-line coupling of SEC and MALDI-ToF MS is the best way to determine the absolute average molecular weight of branched poly(glycidol). This technique involves taking a polymer, that is too disperse for accurate MALDI-ToF MS analysis, and fractionating it with SEC in order to collect fractions with narrow molecular weight distribution. The fractions are then analyzed with by MALDI-ToF MS and used afterwards as standards for calibration of the GPC. This results in the absolute molecular weight determination of the polydisperse polymer.

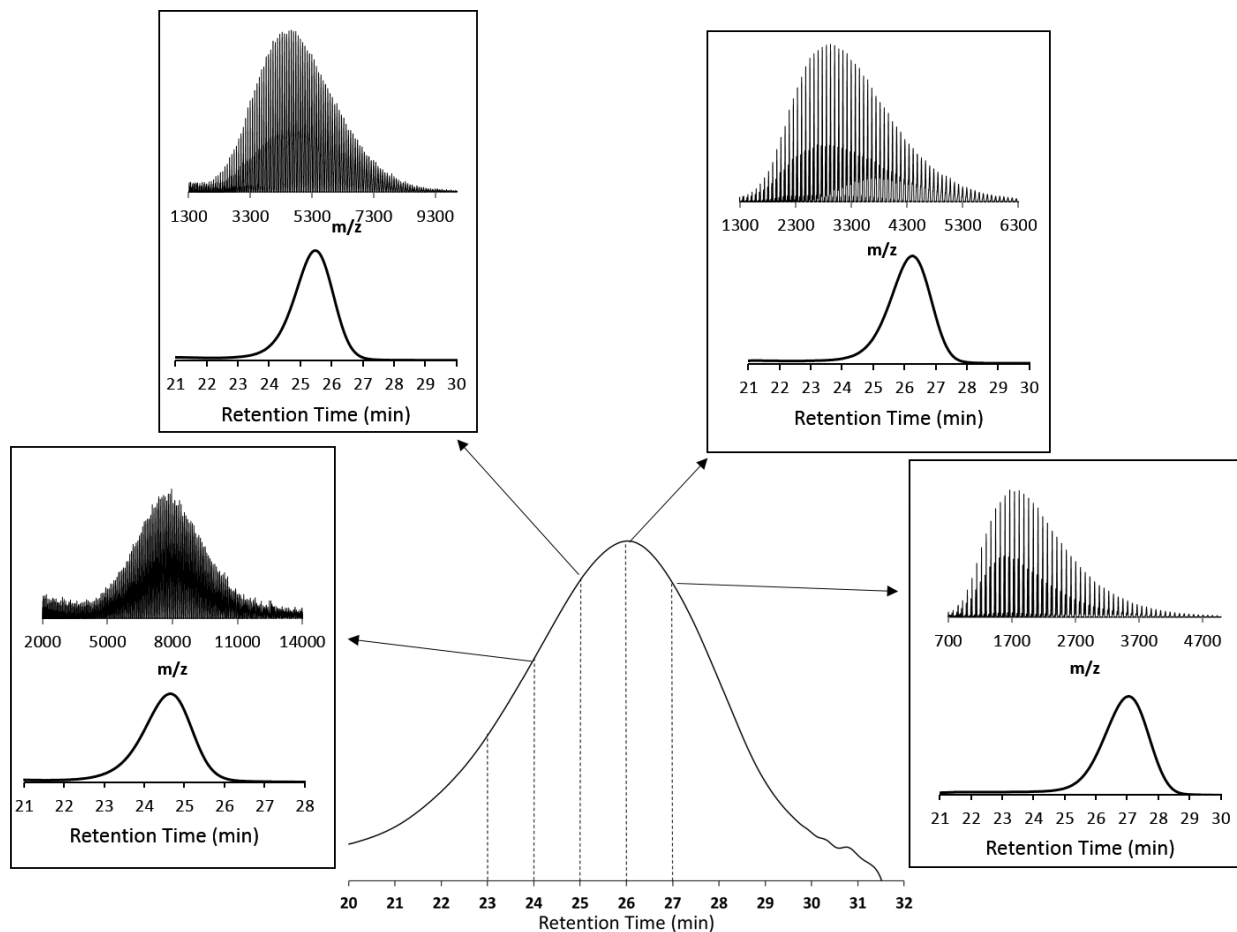


**Figure II-8.** SEC chromatogram of semi-branched poly(glycidol) homopolymer. The insets display the SEC chromatograms (bottom) and the MALDI-ToF MS spectra (top) of the selected fractions.

The molecular weight of each fraction was calculated from their MS spectra by assuming that the mole ratio of each individual species is proportional to the MS detector response. This is a reasonable assumption for samples with narrow molecular weight distribution. The data obtained was compared to GPC analysis of the same fractions using conventional poly(styrene) standards in addition to poly(ethylene glycol) standards (Table II-4). The fractions were reinjected in the GPC equipment in order to determine their elution time. Surprisingly, the molar mass at peak maximum of each fraction determined by MALDI-ToF MS is very close to the value determined by GPC using poly(ethylene glycol) standards (Table II-4). This method also shows that the



**Table II-4.** SEC analysis of semi-branched poly(glycidol) fractions showing a comparison between using polystyrene and polyethylene glycol calibration versus absolute molar-mass calibration with MALDI-ToF MS.

Fraction	elution time (min)	Polystyrene Calibration		PEG Calibration		MALDI-TOF MS Analysis	
		$M_{\text{peak}}$	PDI	$M_{\text{peak}}$	PDI	$M_{\text{peak}}$	PDI
24	24.6	44,764	1.06	8502	1.08	7965	1.10
25	25.5	30,787	1.07	5647	1.09	4636	1.06
26	26.3	22,078	1.08	3864	1.09	2933	1.05
27	27.1	15,784	1.09	2614	1.11	1673	1.08

conventional GPC calibration method using poly(styrene) standards leads to a significant overestimation of branched poly(glycidol) average molecular weights.

The molecular weight at peak maximum ( $M_p$ ) were used to plot the calibration curves corresponding to each polymer. For comparison purposes, the conventional polystyrene calibration curve along with the poly(ethylene glycol) calibration curve, were included (Figure II-9). The line corresponding to poly(ethylene glycol) and MALDI-ToF MS calibration were well below the poly(styrene) calibration line, showing that the poly(styrene) calibration method leads to an overestimation of branched poly(glycidol) average molecular weight. The calibration curve for MALDI-ToF MS is not straight due to the polydispersity of the fractionated samples used for MALDI-TOS MS. This issue can be corrected by using an autosampler to collection fractions at shorter time intervals to get standards that are more monodisperse. However, because of the similarity of the MALDI-ToF MS calibration curve to the PEG calibration curve, we decided to use PEG standards for average molecular weight determination of branched poly(glycidol).

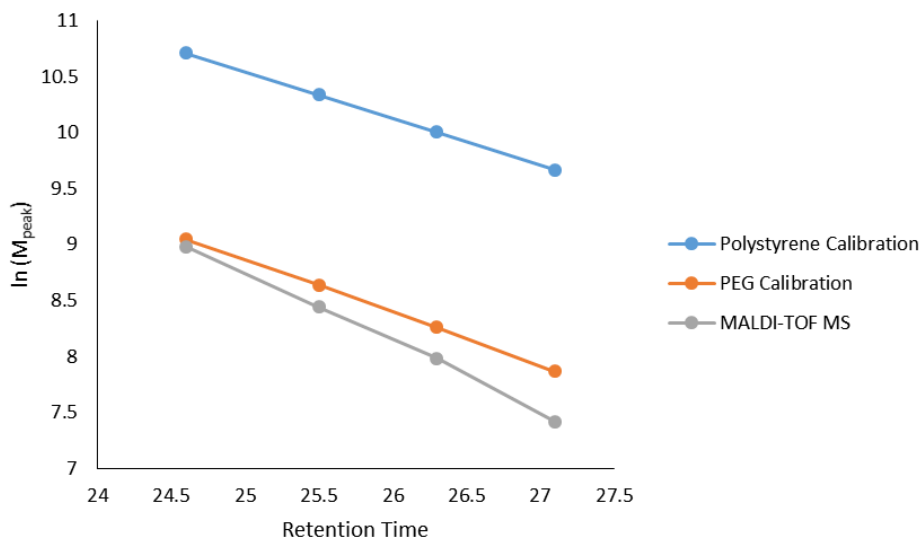


**Figure II-9.** SEC calibration curves obtained with polystyrene standards, polyethylene glycol standards and SEC/MALDI-ToF fractions (24-27). This illustrates that PEG standards are suitable enough for relative molar-mass determination of semi-branched poly(glycidol) by SEC, while polystyrene standards are not ideal.

The molecular weight ( $M_n$ ) and the molecular weight distribution ( $M_w/M_n$ ) obtained from GPC calibrated with PEG standards show good agreement with that calculated from MALDI-ToF MS (Table II-5). Additionally, the molecular weights obtained from NMR were in good agreement with the molecular weights obtained from GPC with PEG calibration. This illustrates that PEG standards are suitable enough for relative molecular weight determination of branched poly(glycidol). As a result,  $M_n$  was calculated mainly with GPC calibrated with PEG standards.

**Table II-5.** Summary of characterization data for optimum branched poly(glycidol) synthesis.

Sample	Ratio (Gly/IAOH)	DP by $^1\text{H}$ NMR	Degrees of Branching	Relative % of Dendritic Carbons	GPC of PG		MALDI-ToF MS	
					$M_n$	$M_w/M_n$	$M_n$	$M_w/M_n$
PGly-11	80	160	0.53	25.2	3715	1.43	-	-
PGly-12	67	165	0.48	22.5	3412	1.38	2969	1.28
PGly-13	53	86	0.46	21.2	2831	1.42	2829	1.34
PGly-14	40	84	0.45	20.8	2265	1.44	2161	1.36
PGly-15	26	52	0.45	20.3	1452	1.38	1771	1.33

## Cytotoxicity of Branched Poly(glycidol)

The cytotoxicity of poly(glycidol)s against mouse fibroblast cells were studied using the MTT assay and LIVE/DEAD assay. The cells were incubated with increasing concentrations of polymer 1, 5 and 10 mg/mL for 24 h before undertaking the MTT assay. The branched poly(glycidol) showed very little toxicity towards fibroblasts cells, with about 98% cell viability observed even at a high concentration of 10 mg/mL after 24 h of incubation (Figure II-10). The data shows that the cells are proliferating at all concentrations tested as indicated by the increased reduction of MTT observed after 96 h. These results indicate that the method used to synthesize these polymers result in biocompatible building blocks for the preparation of biomaterials.

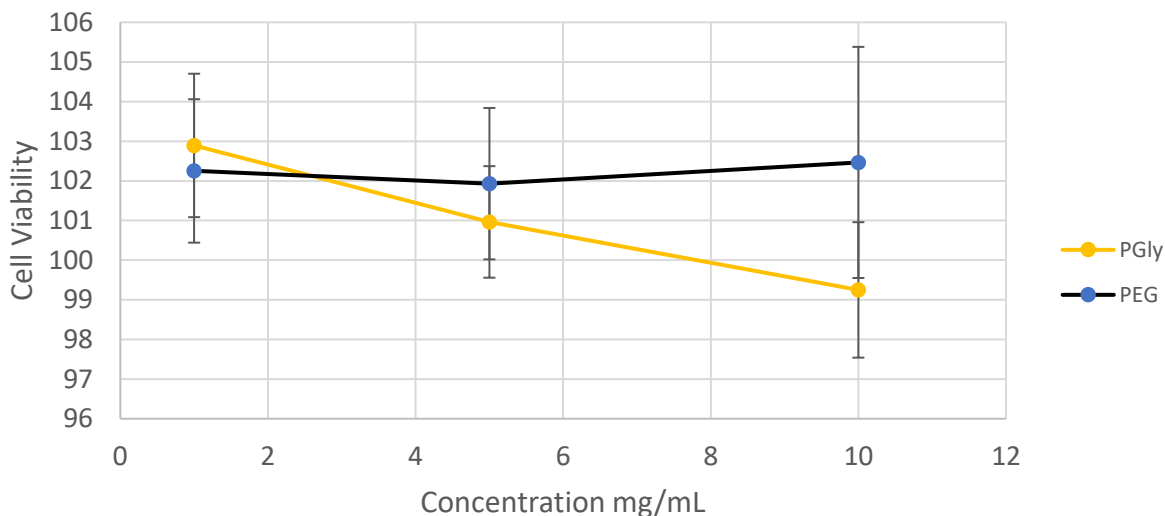


**Figure II-10.** MTT assay of branched poly(glycidol) against NIH 3T3 cells for 24 hrs.

LIVE/DEAD staining of mouse fibroblast cells with branched poly(glycidol) correlates to the data obtained from the MTT assay and give a physical view of the cells in contact with branched poly(glycidol) (Figure II-11). Despite the low cytotoxicity, the fibroblast cells display a change in cellular morphology due to loss of cellular attachment to the bottom of the tissue culture

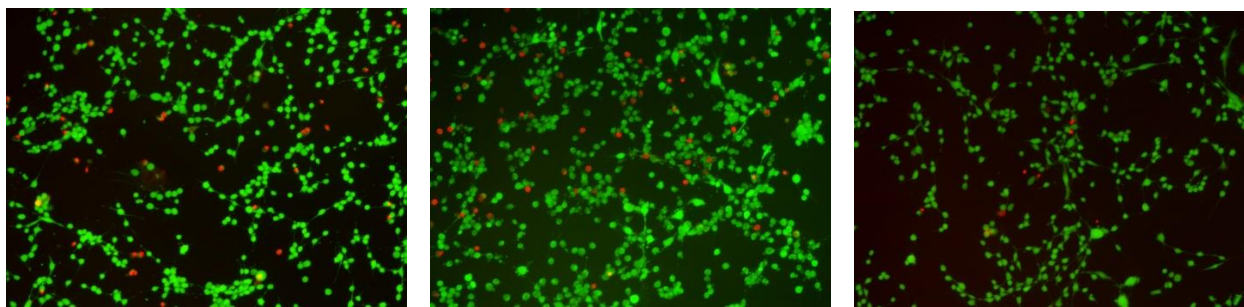


**Figure II-11.** LIVE/DEAD staining of NIH 3T3 cells in contact with PEG and poly(glycidol) (5 mg/mL). (left) PEG, (middle) poly(glycidol), (right) control.

plate. It is believed that the poly(glycidol) is interacting with surface and while this interaction is not killing the cell immediately, the ability for the cell to form attachment is lost. This could have a negative impact on some cellular processes. From this observation, we can deduce that biomedical applications involving cell encapsulation would require a molecular unit to promote cellular attachment.

## CONCLUSION

Tin triflate-mediated ring opening polymerization of glycidol results in branched poly(glycidol) with molecular weights up to 4000 g/mol. Fairly narrow molecular weight distributions ( $1.30 \leq \text{PDI} \leq 1.40$ ) were achieved by slow monomer addition at room temperature, which also led to increased initiations from the isoamyl alcohol initiator, and a decrease in the abundance of macrocyclic species. Reasonable control over molecular weight was achieved by varying the monomer/initiator ratio, and reducing the number of macrocyclic species, however this caused a significant rise in the degree of branching. Characterization of branched poly(glycidol) by inverse-gated proton-decoupled  $^{13}\text{C}$  NMR showed an increase in the number of  $\text{L}_{1,3}$  units and the presence of a  $\text{T}_2$  unit which differs in comparison to hyperbranched poly(glycidol) synthesized by anionic polymerization. Although MALDI-ToF mass spectroscopy allowed for the detection of macrocyclic species, average molecular weight determined by MALDI-ToF were not a true representation of the whole polymer sample due to the polydispersity of the polymer being greater than 1.1. The offline coupling of SEC and MALDI-ToF MS gave a more accurate representation of the average molecular weight ( $M_n$ ) and the molecular weight distribution (PDI) in a polydisperse polymer sample. The SEC/MALDI-ToF MS study of branched poly(glycidol) shows that GPC calibrated with poly(ethylene glycol) standards gave a relatively accurate determination of the average molecular weight, and hence will be used for all future analysis of this polymer. Branched poly(glycidol) synthesized by tin triflate-mediated ring opening polymerization displayed low cytotoxicity similar to FDA approved poly(ethylene glycol) and hence can be used for various biomedical applications as a viable alternative to poly(ethylene glycol).

## EXPERIMENTAL

### Materials

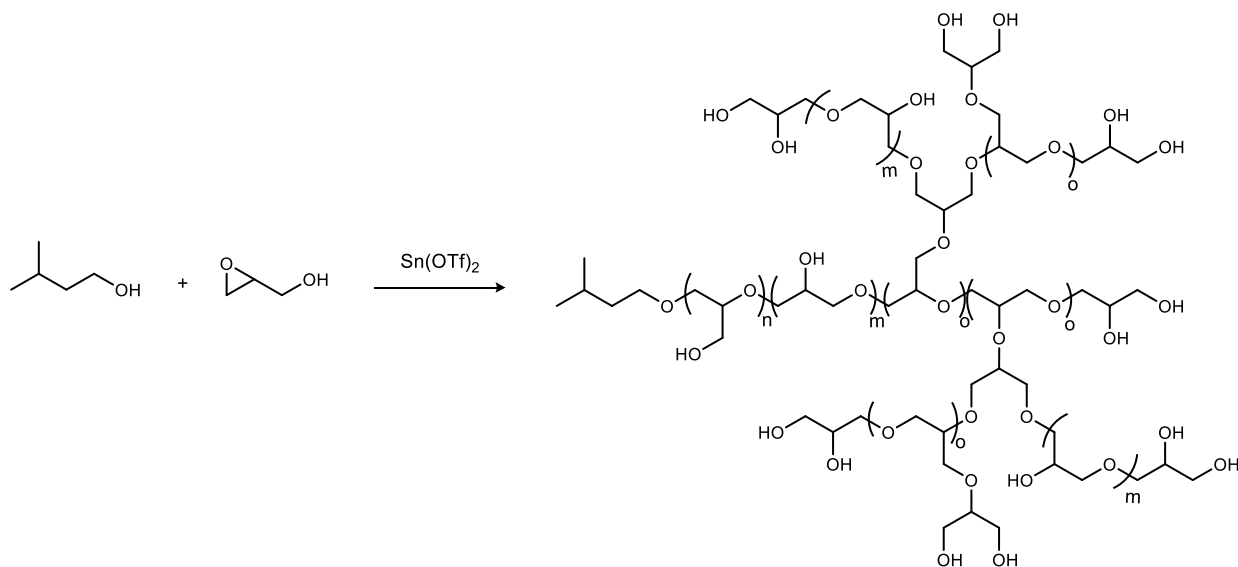
Glycidol (Aldrich, 96%) was freshly distilled from calcium hydride prior to use. 3-Methyl-1-butanol (Aldrich, anhydrous, 99%), Tin (II) trifluoromethanesulfonate (Strem Chemicals, 99%), methanol (Acros, anhydrous, 99.8%), dichloromethane (Aldrich, anhydrous, 99.8%). Dialysis membrane were obtained from spectrum laboratories (Spectra/Por 7, molecular weight cut-off (MWCO) of 1000 Da). PTFE syringe filters were obtained from Thermo Scientific (0.45  $\mu\text{m}$ , 30 mm, Teflon plus glass). All reactions were carried out under argon unless otherwise noted.

### Instrumentation

Nuclear magnetic resonance (NMR) were acquired on a Bruker DRX-500 (500 MHz), Bruker AV-400 (400 MHz) or Bruker AV II-600 (600 MHz) instrument (equipped with a 5 mm Z-gradient TCI cryoprobe). Chemical shifts are measured relative to residual solvent peaks as an internal standard set to  $\delta$  3.31 and  $\delta$  49.0 ( $\text{CD}_3\text{OD}$ ) and  $\delta$  2.50 and  $\delta$  39.52 ( $(\text{CD}_3)_3\text{SO}$ ). Quantitative  $^{13}\text{C}$  NMR was performed by using inverse-gated proton decoupled  $^{13}\text{C}$  NMR with a delay time of 10 seconds. A sample concentration of approximately 150 mg/mL was used for analysis. FT-IR spectra were recorded on a Thermo Nicolet IR 100 spectrophotometer and are reported in wavenumbers ( $\text{cm}^{-1}$ ). Compounds were analyzed as neat films on a NaCl plate (transmission). Size exclusion chromatography (SEC) were performed using a Waters 1525 binary high pressure liquid chromatography pump equipped with a refractive index detector (Waters 2414) and Styragel HR columns (7.8 $\times$ 300 mm Styragel HR 5, Styragel HR 4E, Styragel HR 3). SEC analysis was carried out in DMF (containing 1 mg/mL LiBr) with a flow rate of 1.0 mL/min at 45  $^\circ\text{C}$ . Water SEC was

carried out using Waters Ultrahydrogel™ columns (7.8×300 mm, Ultrahydrogel™ 120, Ultrahydrogel™ DP 120Å, Ultrahydrogel™ 250). HPLC grade water (containing 1 mg/mL LiBr) was used as the eluent at a flowrate of 1 mL/min at 45 °C. Molecular weights ( $M_n$  and  $M_w$ ) and molecular weight distribution were calculated from poly(ethylene glycol) standards provided by Varian. Matrix-assisted laser desorption and ionization time-of-flight mass spectroscopy (MALDI-ToF MS) was carried out on a Voyager DE-STR mass spectrometer equipped with a nitrogen gas laser (337 nm).  $\alpha$ -Cyanohydroxycinnamic acid was used as the matrix and NaI was used as the cationization agent. The samples (5 mg/mL in methanol), matrix (20 mg/mL in methanol) and cationization agent (20 mg/mL) were mixed in a 1:1:0.1 ratio respectively and spotted onto a stainless-steel sample plate. The accelerating voltage was set to 23,000 and measurements took place in reflector mode. Poly(ethylene glycol) was used for external calibration immediately before the measurement. The data was processed using Data Explorer. All spectra were processed (baseline correction, noise filter and Gaussian smooth) before importing mass list into an excel spreadsheet for data analysis.

## Synthesis of Branched Poly(glycidol) homopolymer (PGly-15)



To a 50 mL jacketed three-neck round bottom flask fitted with an argon balloon was added isoamyl alcohol (441  $\mu$ L, 4.05 mmol) and tin (II) trifluoromethanesulfonate (42.0 mg, 0.101 mmol). The mixture was stirred for ten minutes using a mechanical stirrer to form a homogeneous suspension. The jacketed flask was connected to a chiller and cooled to 5  $^{\circ}$ C. Glycidol (13.5 mL, 202.5 mmol) was added via syringe pump (0.7 mL/hr) and the mixture was stirred for 24 hrs at which time stirring was no longer possible due to the viscosity of the reaction mixture. Methanol (15 mL) was added to the reaction to dissolve the polymer and sodium bicarbonate solution (5 mL of a 1 mg/mL) was added. The reaction was filtered (if necessary) and precipitated twice in acetone to isolate the polymer. Further purification by dialysis with Spectra/Por dialysis membrane (MWCO = 1000 Da) in water was performed if needed to furnish the desired polymer PGLY-15 in 80% yield. IR (film) 3390, 1263, 1115  $\text{cm}^{-1}$ .  $^1\text{H}$  NMR (600 MHz,  $(\text{CD}_3)_3\text{SO}$ )  $\delta$  4.73-4.45 (br m, 1H, -OH), 3.69-3.25 (br m, 5H, PGly-scaffold), 1.63 (sept,  $J = 6.5$  Hz, 1H), 1.37 (q,  $J = 6.5$  Hz, 2H), 0.85 (d,  $J = 6.7$  Hz, 6H).  $^{13}\text{C}$  NMR (600 MHz,  $(\text{CD}_3)_3\text{SO}$ ) ppm 82.3-81.6 (-CH( $\text{CH}_2\text{OH}$ )<sub>2</sub>), 80.3-79.4 (-CH( $\text{CH}_2\text{OH}$ ) $\text{OCH}_2$ -), 78.5-77.3 (-CH( $\text{CH}_2\text{O}$ -) $\text{OCH}_2$ -), 73.2 (2C, -CH<sub>2</sub>CH(OH)CH<sub>2</sub>-),



71.9-70.9 (4C,  $-\underline{\text{C}}\text{H}_2\text{CH}(\text{OCH}_2-)\underline{\text{C}}\text{H}_2\text{O}-$ ,  $-\underline{\text{C}}\text{H}_2\underline{\text{C}}\text{H}(\text{OH})\text{CH}_2\text{OH}$ ), 69.5 ( $-\text{O}\underline{\text{C}}\text{H}_2\text{CH}(\text{OCH}_2-)\text{CH}_2\text{OH}$ ), 69.2 ( $-\text{CH}_2\underline{\text{C}}\text{H}(\text{OH})\text{CH}_2-$ ), 63.5 ( $-\text{CH}_2\text{CH}(\text{OH})\underline{\text{C}}\text{H}_2\text{OH}$ ), 62.0-61.8 (2C,  $-\text{CH}(\underline{\text{C}}\text{H}_2\text{OH})_2$ ), 61.4-61.2 ( $-\text{CH}(\underline{\text{C}}\text{H}_2\text{OH})\text{OCH}_2-$ ), 39.5, 25.9, 23.0.

The DB was calculated from the integration of signal intensities in the IG  $^{13}\text{C}$  NMR spectrum using the following equation derived by Holter and Frey:<sup>30</sup>

$$DB = \frac{2D}{2D + L_{1,3} + L_{1,4}}$$

DB represents degrees of branching,  $L_{1,3}$ ,  $L_{1,4}$ , and D represents the signal intensities in the IG  $^{13}\text{C}$  NMR corresponding to one carbon of the linear 1,3, linear 1,4 and dendritic units respectively. The relative abundance of the linear 1,4 structural unit was calculated from the integration of the signal intensities in the IG  $^{13}\text{C}$  NMR using the equation below;

$$Ra (\%) = \left( \frac{(L_{1,4}/2)}{D + L_{1,3} + (L_{1,4}/2) + T_1 + T_2} \right) \times 100$$

The relative abundance of the other structural units was calculated in a similar fashion.

**Table II-6.** Summary of characterization data for semi-branched poly(glycidol) synthesis.

Sample	Ratio (Gly/IAOH)	DP by $^1\text{H}$ NMR	Degrees of Branching	Relative % of Dendritic Carbons	GPC of PG		MALDI-ToF MS	
					Mn	Mn/Mw	Mn	Mn/Mw
PGly-1	80	160	0.53	25.2	3715	1.43	-	-
PGly-2	67	165	0.48	22.5	3412	1.38	2969	1.28
PGly-3	53	86	0.46	21.2	2831	1.42	2829	1.34
PGly-4	40	84	0.45	20.8	2265	1.44	2161	1.36
PGly-5	26	52	0.45	20.3	1452	1.38	1771	1.33

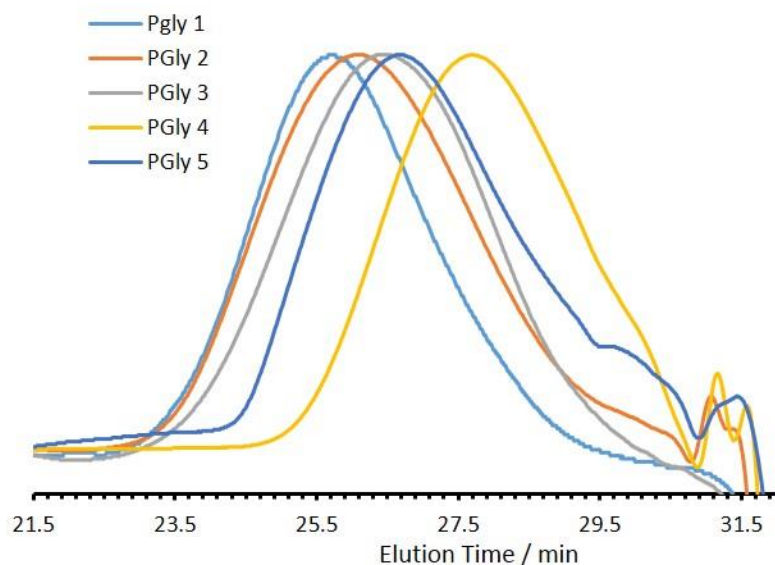


**Figure II-12.** Showing GPC chromatograph of different semi-branched Poly(glycidol)s.

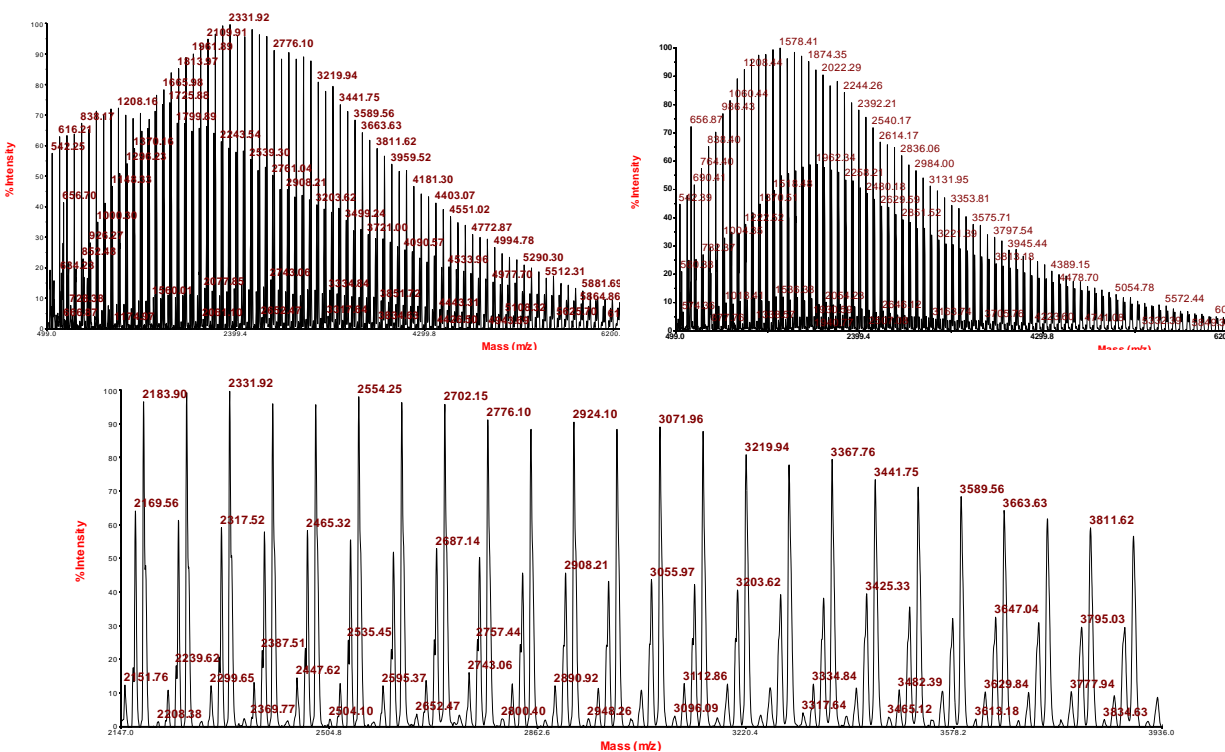


**Figure II-13.** MALDI-ToF MS analysis of semi-branched poly(glycidol) samples. PGly-2 (Top-right), PGly-5 (top-left) and PGly-2 magnified portion (bottom-center).

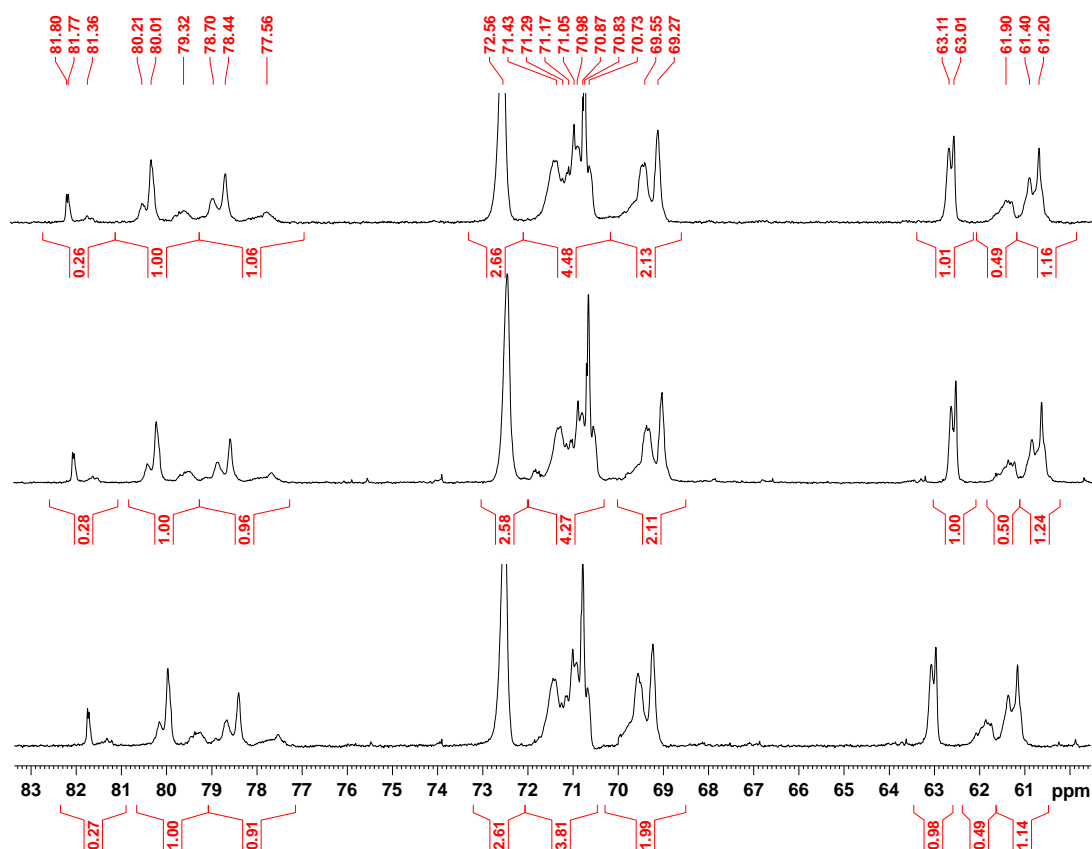
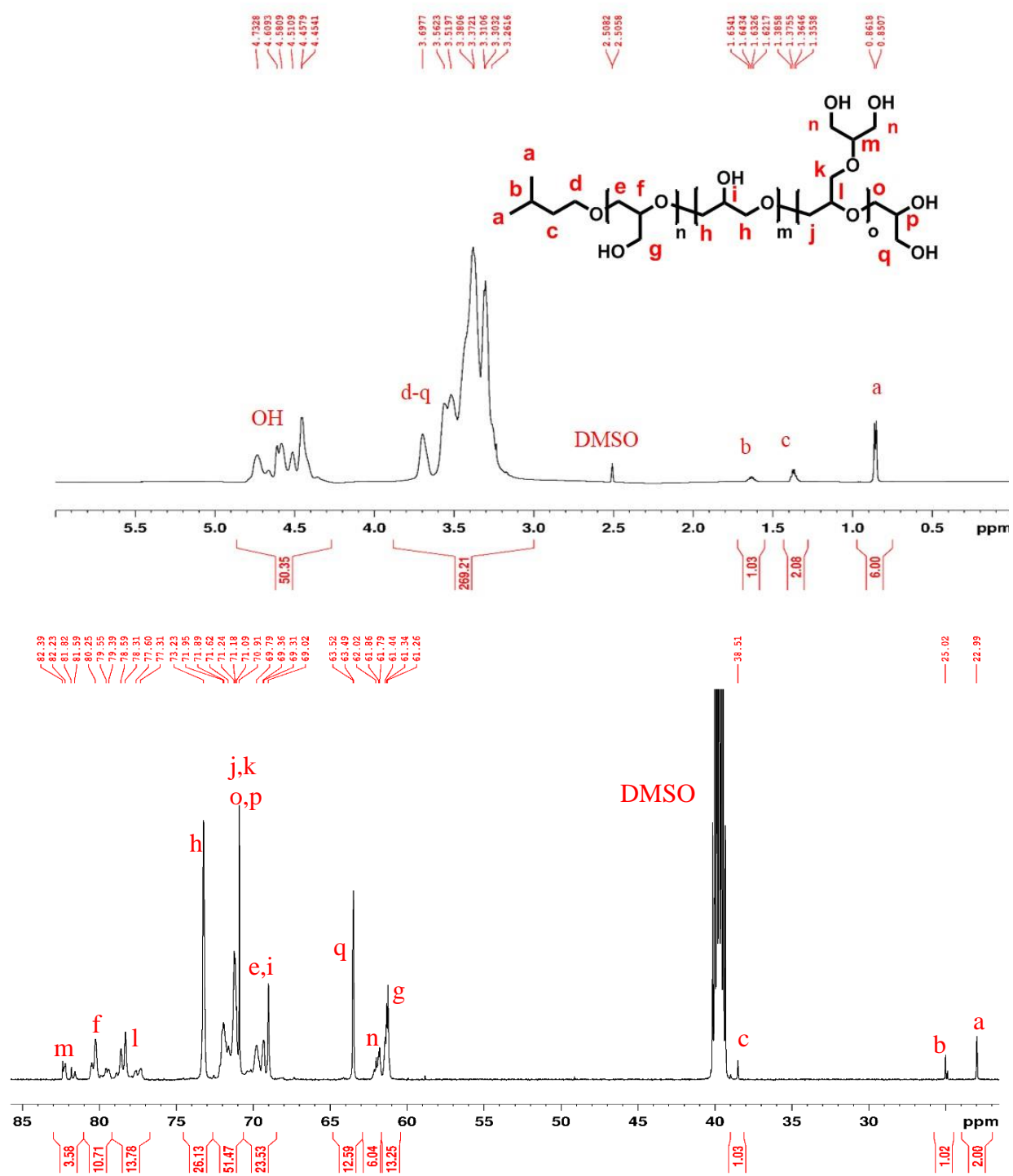


**Figure II-14.** The inverse-gated proton decoupled  $^{13}\text{C}$  NMR for samples PGly-2, PGly-3 and PGly-4 showing the methine carbon of the Linear 1,3 structural unit as the reference for integration.

**Table II-7.** Interpretation of the inverse gated (IG) proton-decoupled  $^{13}\text{C}$  NMR of several branched poly(glycidol) samples.

Structural Unit	Chemical Shift (ppm)	Relative Integrals				
		PGly-1	PGly-2	PGly-3	PGly-4	PGly-5
T <sub>2</sub> (CH)	83.2-82.3	0.34	0.26	0.28	0.27	0.28
L <sub>1,3</sub> (CH)	81.6-80.2	1.00	1.00	1.00	1.00	1.00
D (CH)	80.2-78.1	1.33	1.06	0.96	0.91	0.87
2 L <sub>1,4</sub> (CH <sub>2</sub> )	74.1-73.2	2.60	2.66	2.58	2.61	2.15
2 D (CH <sub>2</sub> ), 2 T <sub>1</sub> (CH, CH <sub>2</sub> )	72.9-71.6	4.95	4.48	4.27	3.81	3.66
L <sub>1,3</sub> (CH <sub>2</sub> ), L <sub>1,4</sub> (CH), I (CH <sub>2</sub> )	71.2-69.8	2.17	2.13	2.11	1.99	1.74
T <sub>1</sub> (CH <sub>2</sub> )	64.5-63.9	1.21	1.01	1.00	0.98	0.94
2 T <sub>2</sub> (CH <sub>2</sub> )	63.5-62.7	0.55	0.49	0.50	0.49	0.49
L <sub>1,3</sub> (CH <sub>2</sub> )	62.7-61.8	1.21	1.16	1.24	1.14	1.21
Structural Unit	Chemical shift (ppm)	Relative abundance (%)				
Linear 1,3 (L <sub>1,3</sub> )	81.6-80.2	19.3	21.5	22.1	22.4	24.1
Linear 1,4 (L <sub>1,4</sub> )	74.1-73.2	25.1	28.6	28.5	29.2	25.9
Dendritic (D)	80.2-78.1	25.7	22.8	21.2	20.3	20.8
Terminal I (T <sub>1</sub> )	64.5-63.9	23.4	21.7	22.0	22.0	22.6
Terminal II (T <sub>2</sub> )	83.2-82.3	6.6	5.4	6.2	6.1	6.6



## SEC/MALDI-ToF MS Off-Line Coupling

SEC/MALDI-ToF MS off-line coupling was performed according to a modified literature procedure. Size exclusion chromatography (SEC) measurements were performed using a Waters 1525 binary high pressure liquid chromatography pump equipped with a refractive index detector (Waters 2414) and Styragel HR columns (7.8×300 mm Styragel HR 5, Styragel HR 4E, Styragel HR 3). SEC analysis was carried out in DMF with a flow rate of 1.0 mL/min at 45 °C and injection volumes of 200 µL of 20 mg/mL solutions. Fractions were collected by hand every minute starting at 21 minutes and finishing at 33 minutes. The fractions were evaporated under vacuum and the absolute molar mass and PDI was determined by matrix-assisted laser desorption and ionization time-of-flight mass spectroscopy (MALDI-ToF MS) analysis on a Voyager DE-STR mass spectrometer equipped with a nitrogen gas laser (337 nm).  $\alpha$ -Cyanohydroxycinnamic acid was used as the matrix and NaI was used as the cationization agent. The samples (5 mg/mL in methanol), matrix (20 mg/mL in methanol) and cationization agent (20 mg/mL) were mixed in a 1:1:0.1 ratio respectively and spotted onto a stainless-steel sample plate. The accelerating voltage was set to 23,000 and measurements took place in reflector mode. Poly(ethylene glycol) was used for external calibration immediately before the measurement. The data was processed using Data Explorer. All spectra were processed (baseline correction, noise filter and Gaussian smooth) before importing mass list into an excel spreadsheet for data analysis. Afterwards, 20 µL of each fraction were reinjected in the SEC apparatus as semi-branched poly(glycidol) standards for absolute molar mass calibration.

## **Cells**

NIH 3T3 cells were purchased from sigma Aldrich and cultured in Dulbecco's modified eagle medium with 10% bovine growth serum and 1% penicillin/streptomycin. They were cultured at 37 °C with 5% CO<sub>2</sub> using standard protocol.

## **MTT Cell Viability and Proliferation Assay**

The cell compatibility of the poly(glycidol) to NIH 3T3 cells was evaluated using a MTT assay. The cells were cultured as described above. Cells were then seeded in a 48 well plate at a density of 7000 cells per well. After 24 hrs, 20 µL of poly(glycidol) was added at concentrations of 1, 5 and 10 mg/mL. The cells were incubated for 24 and 96 hrs. At the end of each period, 20 µL of MTT solution (5 mg/mL) was added to each well and incubate at 37 °C for 3 hours. 200 µL of 10% sodium dodecyl sulfate was added to each well and incubate overnight at 37 °C. Absorbance was measured at 570 nm and subtract the background absorbance read at 690 nm.

## REFERENCES

1. Sandler, S. R.; Berg, F. R., Room temperature polymerization of glycidol. *Journal of Polymer Science Part A: Polymer Chemistry* **1966**, *4* (5), 1253-1259.
2. Vandenberg, E. J., Polymerization of glycidol and its derivatives: A new rearrangement polymerization. *Journal of Polymer Science: Polymer Chemistry Edition* **1985**, *23* (4), 915-949.
3. Taton, D.; Le Borgne, A.; Sepulchre, M.; Spassky, N., Synthesis of chiral and racemic functional polymers from glycidol and thioglycidol. *Macromolecular Chemistry and Physics* **1994**, *195* (1), 139-148.
4. Stiriba, S.-E.; Kautz, H.; Frey, H., Hyperbranched Molecular Nanocapsules: Comparison of the Hyperbranched Architecture with the Perfect Linear Analogue. *Journal of the American Chemical Society* **2002**, *124* (33), 9698-9699.
5. Sunder, A.; Hanselmann, R.; Frey, H.; Mülhaupt, R., Controlled Synthesis of Hyperbranched Polyglycerols by Ring-Opening Multibranching Polymerization. *Macromolecules* **1999**, *32* (13), 4240-4246.
6. Wilms, D.; Schömer, M.; Wurm, F.; Hermanns, M. I.; Kirkpatrick, C. J.; Frey, H., Hyperbranched PEG by Random Copolymerization of Ethylene Oxide and Glycidol. *Macromolecular Rapid Communications* **2010**, *31* (20), 1811-1815.
7. Schömer, M.; Seiwert, J.; Frey, H., Hyperbranched Poly(propylene oxide): A Multifunctional Backbone-Thermoresponsive Polyether Polyol Copolymer. *ACS Macro Letters* **2012**, *1* (7), 888-891.
8. Tokar, R.; Kubisa, P.; Penczek, S.; Dworak, A., Cationic polymerization of glycidol: coexistence of the activated monomer and active chain end mechanism. *Macromolecules* **1994**, *27* (2), 320-322.
9. Bednarek, M.; Biedron, T.; Kubisa, P.; Penczek, S., Activated monomer polymerization of oxiranes. Micro-structure of polymers vs. kinetics and thermodynamics of propagation. *Makromolekulare Chemie. Macromolecular Symposia* **1991**, *42-43* (1), 475-487.
10. Dworak, A.; Walach, W.; Trzebicka, B., Cationic polymerization of glycidol. Polymer structure and polymerization mechanism. *Macromolecular Chemistry and Physics* **1995**, *196* (6), 1963-1970.
11. Kubisa, P., Hyperbranched polyethers by ring-opening polymerization: Contribution of activated monomer mechanism. *Journal of Polymer Science Part A: Polymer Chemistry* **2003**, *41* (4), 457-468.

12. Magnusson, H.; Malmström, E.; Hult, A., Influence of Reaction Conditions on Degree of Branching in Hyperbranched Aliphatic Polyethers from 3-Ethyl-3-(hydroxymethyl)oxetane. *Macromolecules* **2001**, *34* (17), 5786-5791.
13. Royappa, A. T., On the copolymerization of epichlorohydrin and glycidol. *Journal of Applied Polymer Science* **1997**, *65* (10), 1897-1904.
14. Royappa, A. T.; Dalal, N.; Giese, M. W., Amphiphilic copolymers of glycidol with nonpolar epoxide comonomers. *Journal of Applied Polymer Science* **2001**, *82* (9), 2290-2299.
15. Royappa, A. T.; McDaniel, R. L., Copolymerization of glycidol with functionalized phenyl glycidyl ethers. *Journal of Applied Polymer Science* **2005**, *97* (4), 1462-1466.
16. Pale-Grosdemange, C.; Simon, E. S.; Prime, K. L.; Whitesides, G. M., Formation of self-assembled monolayers by chemisorption of derivatives of oligo(ethylene glycol) of structure HS(CH<sub>2</sub>)<sub>11</sub>(OCH<sub>2</sub>CH<sub>2</sub>)<sub>m</sub>OH on gold. *Journal of the American Chemical Society* **1991**, *113* (1), 12-20.
17. Kodera, Y.; Matsushima, A.; Hiroto, M.; Nishimura, H.; Ishii, A.; Ueno, T.; Inada, Y., Pegylation of proteins and bioactive substances for medical and technical applications. *Progress in Polymer Science* **1998**, *23* (7), 1233-1271.
18. Kainthan, R. K.; Janzen, J.; Levin, E.; Devine, D. V.; Brooks, D. E., Biocompatibility Testing of Branched and Linear Polyglycidol. *Biomacromolecules* **2006**, *7* (3), 703-709.
19. Kainthan, R. K.; Muliawan, E. B.; Hatzikiriakos, S. G.; Brooks, D. E., Synthesis, Characterization, and Viscoelastic Properties of High Molecular Weight Hyperbranched Polyglycerols. *Macromolecules* **2006**, *39* (22), 7708-7717.
20. Kainthan, R. K.; Hester, S. R.; Levin, E.; Devine, D. V.; Brooks, D. E., In vitro biological evaluation of high molecular weight hyperbranched polyglycerols. *Biomaterials* **2007**, *28* (31), 4581-4590.
21. Kainthan, R. K.; Brooks, D. E., In vivo biological evaluation of high molecular weight hyperbranched polyglycerols. *Biomaterials* **2007**, *28* (32), 4779-4787.
22. Kainthan, R. K.; Janzen, J.; Kizhakkedathu, J. N.; Devine, D. V.; Brooks, D. E., Hydrophobically derivatized hyperbranched polyglycerol as a human serum albumin substitute. *Biomaterials* **2008**, *29* (11), 1693-1704.
23. Türk, H.; Haag, R.; Alban, S., Dendritic Polyglycerol Sulfates as New Heparin Analogues and Potent Inhibitors of the Complement System. *Bioconjugate Chemistry* **2004**, *15* (1), 162-167.
24. Siegers, C.; Biesalski, M.; Haag, R., Self-Assembled Monolayers of Dendritic Polyglycerol Derivatives on Gold That Resist the Adsorption of Proteins. *Chemistry – A European Journal* **2004**, *10* (11), 2831-2838.



25. Wyszogrodzka, M.; Haag, R., Study of Single Protein Adsorption onto Monoamino Oligoglycerol Derivatives: A Structure–Activity Relationship. *Langmuir* **2009**, *25* (10), 5703-5712.
26. Stevens, D. M.; Watson, H. A.; LeBlanc, M.-A.; Wang, R. Y.; Chou, J.; Bauer, W. S.; Harth, E., Practical polymerization of functionalized lactones and carbonates with Sn(OTf)<sub>2</sub> in metal catalysed ring-opening polymerization methods. *Polymer Chemistry* **2013**, *4* (8), 2470-2474.
27. Spears, B. R.; Waksal, J.; McQuade, C.; Lanier, L.; Harth, E., Controlled branching of polyglycidol and formation of protein-glycidol bioconjugates via a graft-from approach with "PEG-like" arms. *Chemical Communications* **2013**, *49* (24), 2394-2396.
28. Mancilla, G.; Femenía-Ríos, M.; Macías-Sánchez, A. J.; Collado, I. G., Sn(OTf)<sub>2</sub> catalysed regioselective styrene oxide ring opening with aromatic amines. *Tetrahedron* **2008**, *64* (51), 11732-11737.
29. Sunder, A.; Mulhaupt, R.; Haag, R.; Frey, H., Hyperbranched polyether polyols: A modular approach to complex polymer architectures. *Advanced Materials* **2000**, *12* (3), 235-+.
30. Frey, H., Degree of branching in hyperbranched polymers. 2. Enhancement of the db: Scope and limitations. *Acta Polymerica* **1997**, *48* (8), 298-309.

## CHAPTER III

### SYNTHESIS AND CHARACTERIZATION OF BRANCHED POLY(GLYCIDOL)

#### DERIVATIVES

#### INTRODUCTION

Advanced polymeric materials greatly depend on the availability of functionalized building blocks to facilitate novel properties and applications.<sup>1</sup> Polymers with reactive groups on their side chain that can be easily modified in high yield are important building blocks.<sup>1-2</sup> For many applications, post-polymerization modification avoids the need to determine new polymerization conditions for each unique monomer, yet at the same time allowing comparison of a series of macromolecules without complications due to different molecular weight backbones. Ideally, the modification reactions are highly efficient and occur without the use of harsh reaction conditions and reagents.<sup>3</sup>

Branched poly(glycidol) have the make-up to be an ideal candidate for post-polymerization modification strategies,<sup>3-4</sup> providing unprecedented diversity and value for the synthesis of desired hydrophilic and functionalized building blocks. Developed as an alternative to hyperbranched poly(glycidol)s as previously reported,<sup>5</sup> it allows for an increased number of hydroxyl groups available, while still possessing the advantages associated with its branched structure. The branching and shorter molecular weight can provide a reduced toxicity and immunogenicity in contrast to linear, high molecular weight PEG units<sup>6-7</sup> and also guaranties a facile modification and implementation into more complex systems. Furthermore, these *bPGs*

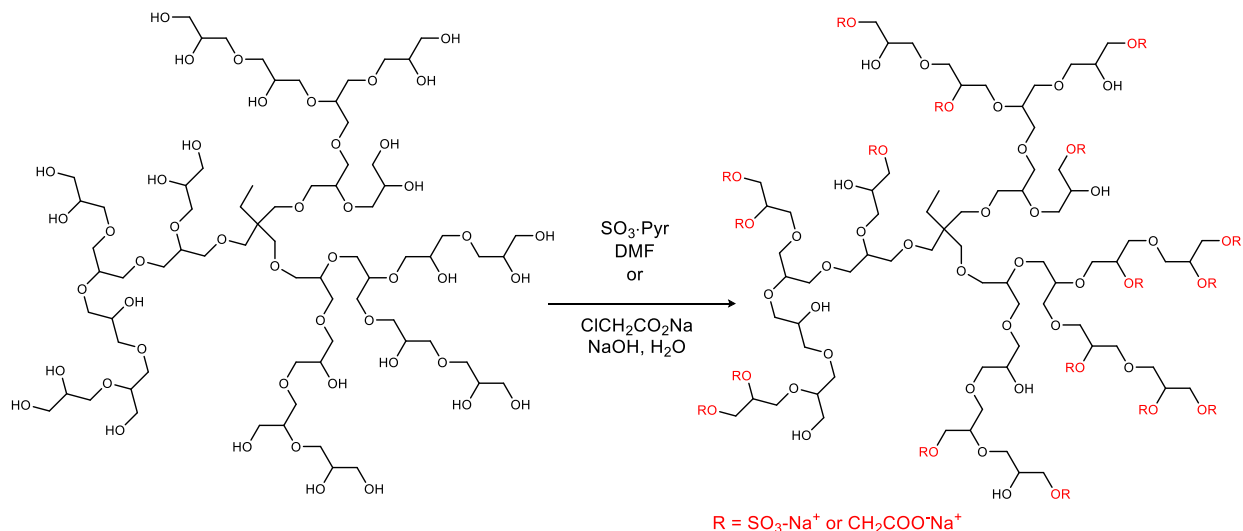
display hydroxyl groups in close proximity and different connectivity, offering a more selected placement of functional groups throughout the structure than possible with linear counterparts.

Poly(glycidol) has numerous primary and secondary hydroxyl groups that can be functionalized to give various derivatives that can be used to for a variety of biological application. However, due to the high density of hydroxyl groups, poly(glycidol) is soluble only in water, lower alcohols such as methanol and ethanol, polar aprotic solvents such as N,N-dimethylformamide, dimethyl sulfoxide and pyridine. As a result, only a limited number of functionalization is possible.

Functionalization of poly(glycidol), in most cases, is a straight forward way to access various poly(glycidol) derivatives, each with their own unique biomedical properties. Sulfonation, esterification, and etherification are a few of some of the hydroxyl group chemistries employed, providing access to variety to polymer with has been shown to possess physical and chemical properties suited to various application.

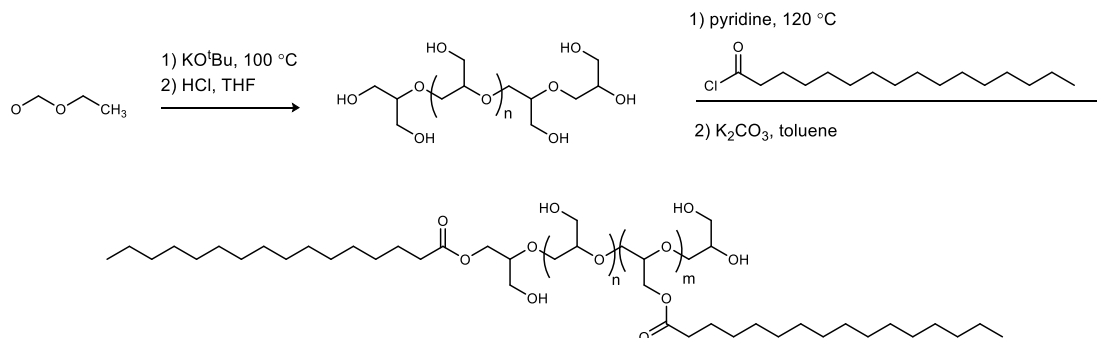
Haag et al.<sup>8</sup> reported the synthesis of highly branched polysulfonated and polycarboxylated branched poly(glycidol). Highly branched poly(glycidol) with molecular weight ranges 2000-10,000 g/mol was sulfonated using SO<sub>3</sub>/pyridine complex as the sulfating reagent and dry dimethylformamide as the solvent (Scheme III-1). The poly(glycidol) sulfates were obtained in good yields and high purity due to dialysis in water. Despite using stoichiometric (with respect to the number of OH groups) amounts of the sulfating reagent only about 85% was sulfonated. This demonstrate how easily accessible the hydroxyl groups are compared to other polymers, for example polysaccharides. Poly(glycidol) carboxylate was synthesise under basic conditions using sodium chloroacetate as the carboxylating reagent. A three-fold excess of sodium chloroacetate was used but only 26% of hydroxyl groups was carboxylated. No observable degradation of polymer backbone was observed under basic conditions. Biological evaluations showed that

poly(glycidol) sulfate exhibited both anticoagulant and anti-inflammatory activities compared to unmodified poly(glycidol) and its carboxylate.



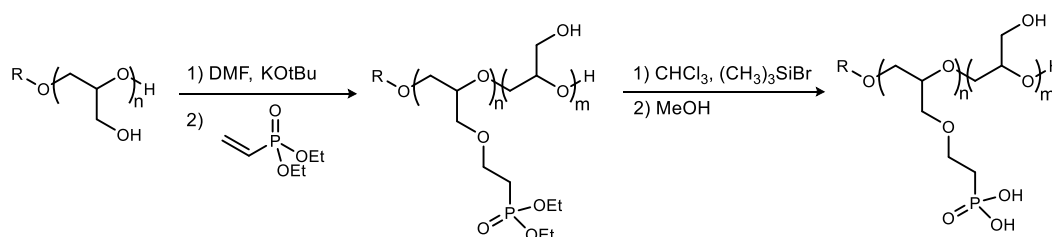
**Scheme III-1.** Synthesis of poly(glycidol) sulfate and poly(glycidol) carboxylate.

Frey et al.<sup>9</sup> reported the esterification of linear and hyperbranched poly(glycidol). Esterification of 60% of the hydroxyl groups of poly(glycidol) was accomplished with pyridine and palmitoyl chloride dissolved in toluene (Scheme III-2). The product was purified by dialysis with benzylated cellulose tubing (MWCO 1,000) in chloroform. No observable decomposition of polymer backbone was observed and there was good agreement between the feed ratio of hydroxyl groups to palmitoyl chloride and the actual incorporation of palmitoyl chloride. Hyperbranched esterified poly(glycidol) was compared to its linear counterparts and shown to be more suited for supramolecular guest encapsulation and phase transfer and hence has huge potential as a drug delivery vehicle.



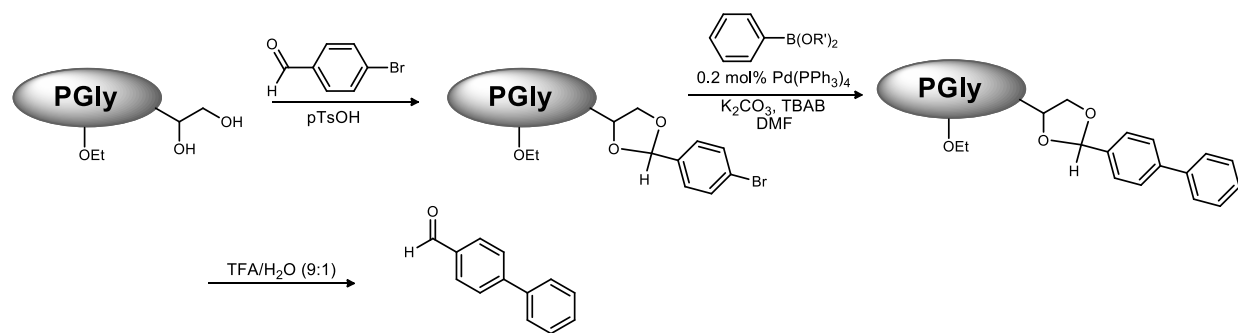
**Scheme III-2.** Synthesis of linear esterified poly(glycidol).

Post-polymerization modification of linear poly(glycidol) with diethyl vinylphosphonate was reported by Moller et al.<sup>10</sup> Their synthetic approach involves the partial phosphonoethylation of poly(glycidol) with diethyl vinylphosphonate in a Michael-type addition under basic condition (Scheme III-3). The phosphonic acid derivative could also be obtained by saponification of the phosphonate groups with bromotrimethylsilane. Purification of the phosphonate was accomplished by precipitation in pentane, while the phosphonic acid was purified by evaporation and centrifugation. The amount of functionalization obtained was in good agreement with the ratio adjusted in the feedstock. These phosphonated poly(glycidol) can be used to coat the surfaces of devices in contact with bodily fluids. The phosphonic acid groups act as anchor groups for covalent binding to different surfaces.



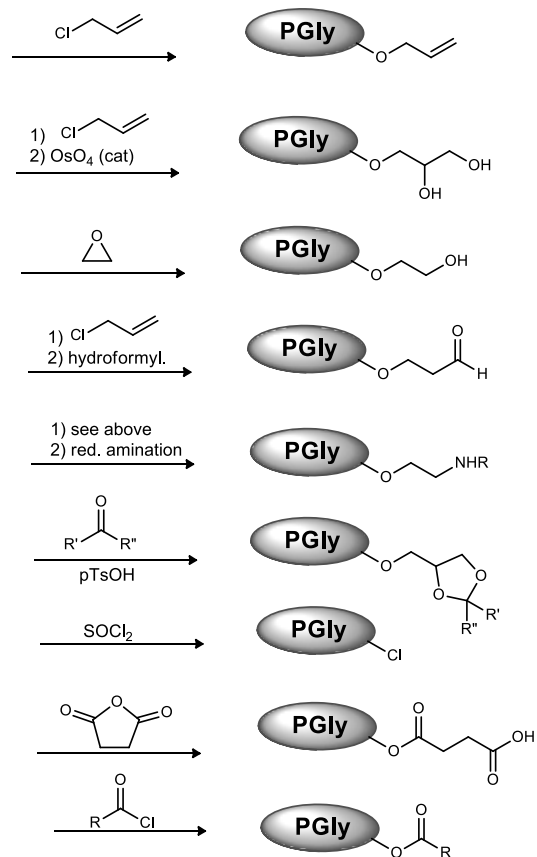
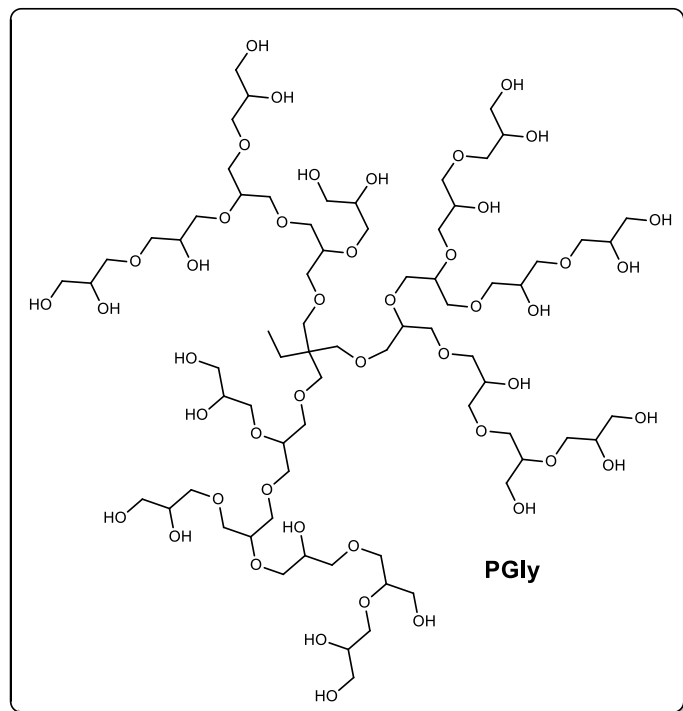
**Scheme III-3.** Synthesis of poly(glycidol) phosphonate and phosphonic acid derivatives.

The terminal 1,2 diols in hyperbranched poly(glycidol) can be transformed by acid catalyzed reaction with carbonyl compounds into acetals. The polymer obtained can be used as a high loading polymer support for some synthetic application.<sup>11</sup> Haag et al.<sup>12</sup> demonstrated this utility by coupling a functional aldehyde onto the polymer support (Scheme III-4), transformed the functionality of the polymeric acetal by nucleophilic substitution as well as palladium-catalyzed cross-coupling and finally cleaved the acetal from the polymer support. All intermediates were purified by dialysis, and the support can be recycled. The remaining hydroxyl groups are still available and can be used to tune the solubility of the polymer in various organic solvents. To increase the scope of possible reaction on this support, the hydroxyl group can be converted into various other linker functionalities.<sup>13-14</sup>



**Scheme III-4.** Poly(glycidol) supported Suzuki coupling applied to the synthesis of biphenylaldehyde

Currently, many groups are further exploring a wide range of orthogonal functional groups that can easily be incorporated in the poly(glycidol) scaffold either by copolymerization or by post-polymerization modification. Scheme III-5 summarizes some of the current functionalities that have been and continue to be explored and developed for a variety of applications in material science and medicine.<sup>14</sup>



**Scheme III-5.** Some postpolymerization modification of polyglycidol reported to date.

## RESULTS AND DISCUSSION

The degree to which poly(glycidol) is modified or functionalized is determined by the number of hydroxyl groups that has been transformed into the desired functionality. To determine the average number of hydroxyl groups per polymer we employed the use of NMR and GPC, and MALDI-ToF mass spectroscopy. Inverse-gated proton-decoupled  $^{13}\text{C}$  NMR gives the relative integrals which can be used to calculate the relative abundance of each structural unit of a polymer in a poly(glycidol) sample. The relative number of each structural unit in a polymer can be determined from the relative abundance calculated from NMR and the number average molecular weight calculated from MALDI-ToF mass spectroscopy. The average number of hydroxyl groups per polymer in a poly(glycidol) sample can then be determined from the relative number of each hydroxyl containing structural units (i.e.  $L_{1,3}$ ,  $L_{1,4}$ ,  $T_1$ ,  $T_2$ ). The average number of hydroxyl groups per polymer is calculated by the equation below:

$$\text{average \# of OHs} = nL_{1,3} + nL_{1,4} + 2(nT_1) + 2(nT_2) \quad (1)$$

$$\text{\# of primary OH} = nL_{1,3} + nT_1 + 2(nT_2) \quad (2)$$

Where  $n$  is the relative number of units which is calculated from the number average molecular weight obtained from GPC analysis. Additionally, the ratio of primary to secondary hydroxyl group can be calculated.  $^{29}\text{Si}$  NMR can also be used to determine the ratio of primary to secondary hydroxyl groups in a polymer. Poly(glycidol) samples synthesized as described in the previous chapter were analyzed to determine the average number of hydroxyl groups.  $^{29}\text{Si}$  NMR was carried out for the trimethylsilyl ethers of the synthesized poly(glycidol) samples to determine



the ratio of primary and secondary hydroxy groups (Figure III-1). The results are summarized in Table III-1. The data obtained from both  $^{13}\text{C}$  and  $^{29}\text{Si}$  NMR was in close agreement.

**Table III-1.** Distribution of primary and secondary hydroxy groups in polyglycidol calculated from  $^{13}\text{C}$  NMR structural data and measured from  $^{29}\text{Si}$  NMR of the trimethylsilyl ethers of polyglycidol.

Sample	$M_n$ from MALDI-ToF	# of units	# of OH groups	# of primary OH	# of secondary OH	Ratio from $^{13}\text{C}$ NMR	Ratio from $^{29}\text{Si}$ NMR
PGly-6	1943	26	28	16	12	1.3:1	1.1:1
PGly-7	2353	32	33	19	14	1.3:1	1.2:1
PGly-8	2012	27	29	16	13	1.2:1	1.1:1
PGly-9	2568	35	36	20	16	1.2:1	1.3:1

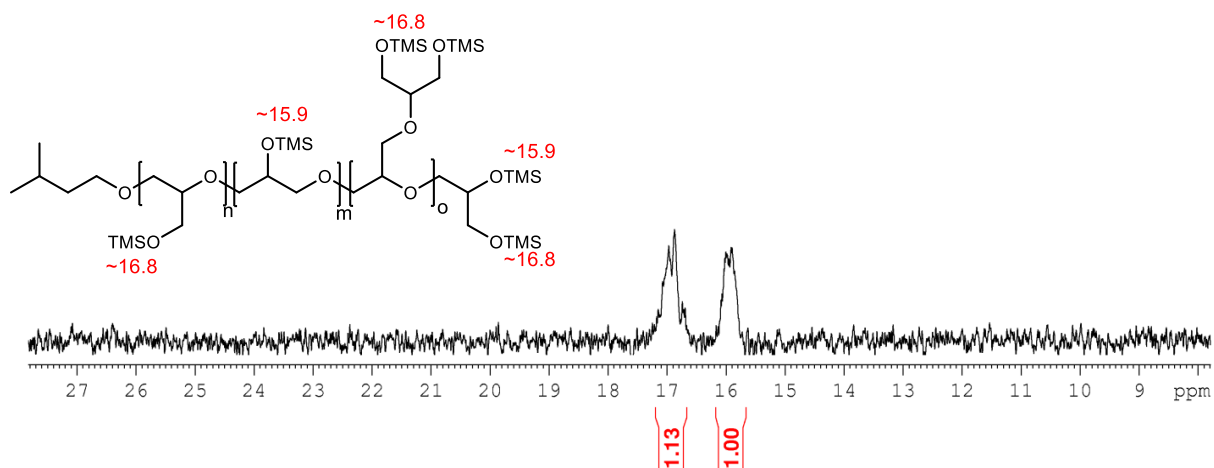


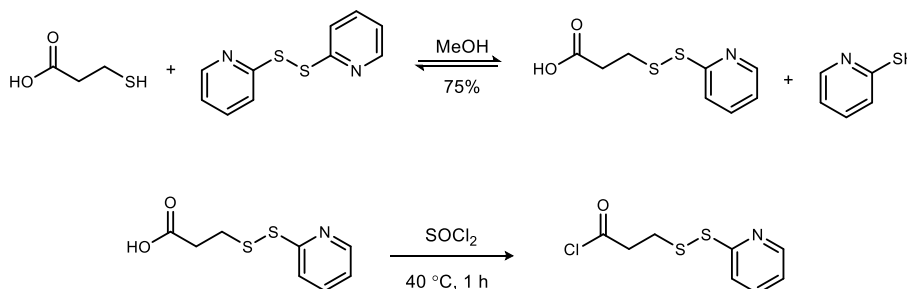
**Figure III-1.**  $^{29}\text{Si}$  NMR (501 MHz,  $(\text{CD}_3)_2\text{SO}$ ) of the trimethylsilyl ethers of poly(glycidol).

Functionalize poly(glycidol) also has the ability to crosslink with different reactive groups to form materials such as nano and micro particles, and hydrogels. These materials have been vastly exploited as drug delivery vehicles due to their ability for controlled release of small and macromolecules. Here we present the synthesis of novel functionalities of poly(glycidol) which has the ability to crosslink to form hydrogels.

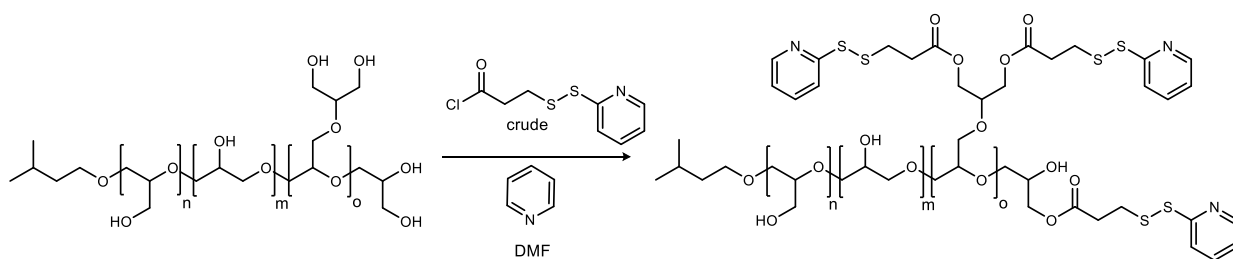
## Synthesis of Thiol-Functionalized Branched Poly(glycidol)

A few research groups have investigated the incorporation of an ester moiety on to the polyether polyol backbone of poly(glycidol). Burgath et al.<sup>15</sup> demonstrated the polymerization of  $\epsilon$ -caprolactone, initiated by poly(glycidol) with tin catalyst to give a polyether polyol with biodegradable poly( $\epsilon$ -CL) arms. This material has properties that are suited for controlled release of small and large bioactive molecules. Additionally, the esterified poly(glycidol) reported by Frey et al., was used to make nanocapsules and nanoparticles that were capable to releasing their guest molecules by hydrolysis of the ester bonds.<sup>9</sup> Since the polyether structure of poly(glycidol) is not biodegradable, the incorporation of an ester functionality generally results in a material that is both biocompatible and biodegradable.

The incorporation of an ester and a thiol functionality into branched poly(glycidol) would make it a viable candidate for the synthesis of biocompatible and biodegradable hydrogels via thiol-ene click reaction. To synthesize hydrogel via thiol-ene click chemistry, alkene and thiol-terminated branched poly(glycidol) derivatives are needed. To synthesize the thiol-terminated branched poly(glycidol) (poly(glycidol-*co*-glycidyl 3-mercaptopropanoate)), two different routes were explored. The first route involved nucleophilic acyl substitution of a thiol-disulfide acyl chloride with branched poly(glycidol), followed by reduction with DTT to produce the free thiol.



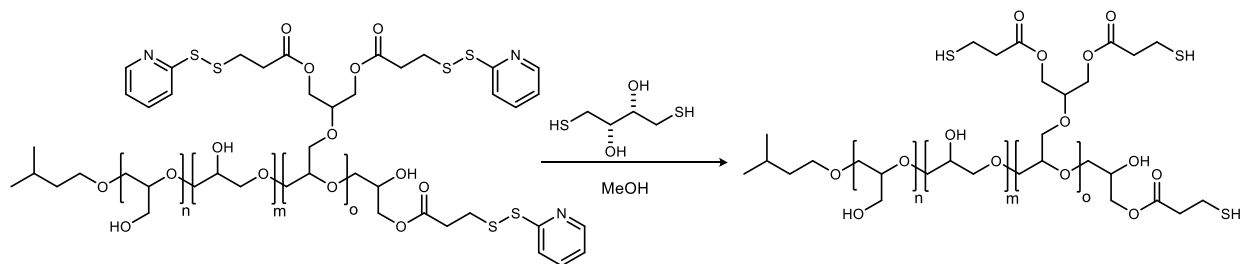
**Scheme III-6.** Synthesis of thiol-disulfide reagent for thiol functionalization of branched poly(glycidol)



**Scheme III-8.** Synthesis of thiol-terminated branched polyglycidol via nucleophilic acyl substitution.

The second is a direct one step synthesis via a modified fisher esterification with 3-mercaptopropionic acid and poly(glycidol).

3-mercaptopropionic acid was subjected to thiol-disulfide exchange with pyridinium disulfide in methanol, according to literature procedures,<sup>16</sup> to furnish the desired disulfide in good yield. The disulfide carboxylic acid was then treated with thionyl chloride for 1 h at 40 °C, which yielded a crude mixture of the desired acyl chloride and the starting material, which was used without further purification (Scheme III-6). Branched poly(glycidol) was then subjected to esterification with the crude acyl chloride in the presence of pyridine. The functionalized polymer was isolated by repeated precipitation in ethyl acetate/ether mixture followed by dialysis in methanol (MWCO 1000). The desired polymer was isolated in moderate yield (Scheme III-8).



**Scheme III-7.** Reduction of the thiol-disulfide poly(glycidol) derivative to form a thiol-terminated branched poly(glycidol) derivative.

The disulfide polymer was then subjected to dithiothreitol (DDT) reduction in methanol (Scheme III-7). The reaction was degassed to reduce oxidation of the dithiothreitol. Purification by dialysis (MWCO 1000) in methanol yielded the desired free thiol.  $^1\text{H}$  and  $^{13}\text{C}$  NMR was used to characterize the desired product and intermediates (Figure III-2).

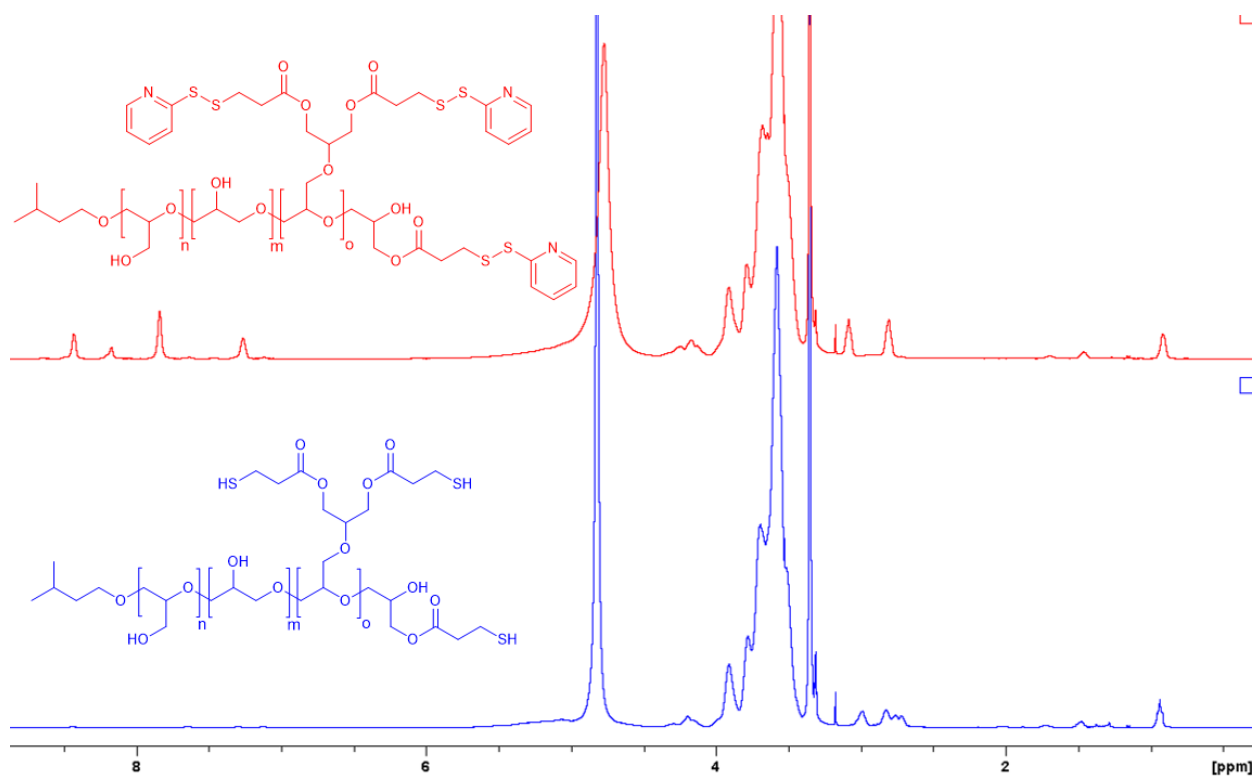
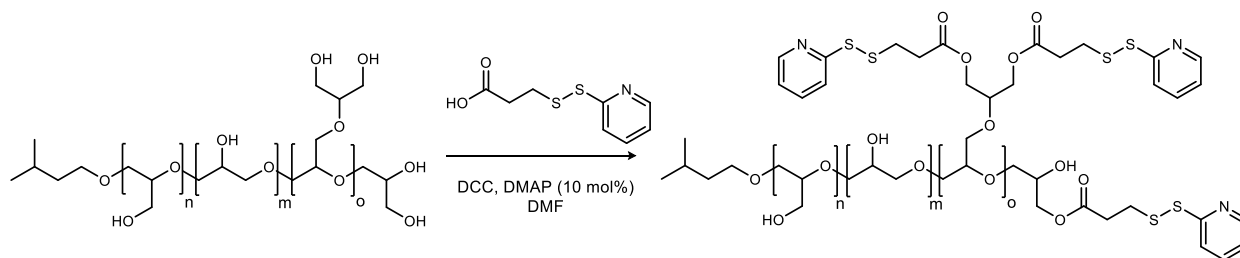


**Figure III-2.**  $^1\text{H}$  NMR (400 MHz,  $\text{CD}_3\text{OD}$ ) of thiol-terminated branched poly(glycidol) derivatives.

The free thiol groups showed a strong tendency to form dithiol linkages when in high concentration i.e. when all solvent has been removed. As a result, the thiolated poly(glycidol) had to be stored in solution for short periods.  $^1\text{H}$  NMR indicates that there was no correlation between the desired degree of functionalization and the actual degree of functionalization. This is due to the crude disulfide reagent that was used. To get better correlation, an alternate approach was explored.

While this synthetic route provides access to the desired thiol-terminated functionalized poly(glycidol), there still exist a need for a reproducible and efficient alternative. Hence, the use of Steiglich esterification was explored as an alternative to the nucleophilic acyl substitution of an acyl chloride. The requisite disulfide was reacted with branched poly(glycidol) in the presence of dicyclohexylcarbodiimide (DCC) and dimethyl aminopyridine (DMAP) (Scheme III-9). The desired product was obtained after 6 h at rt. The reaction was monitored by  $^1\text{H}$  NMR, which showed no change in the ratio of product to starting material after 6 h. The conversion of the starting material was however limited to 40% with yields averaging 60% after dialysis (MWCO 1000) in methanol for 12 h. Improved correlation between the desired and actual degree of functionalization was also not achieved with this method.



Sample <sup>a</sup>	Mn <sup>b</sup>	Mn <sup>c</sup>	% Thiol <sup>d</sup>	% Thiol <sup>e</sup>	PDI <sup>f</sup>
Thiol-Pgly-1	1700	1800	10	5	1.35
Thiol-Pgly-2	1700	1950	20	9	1.31

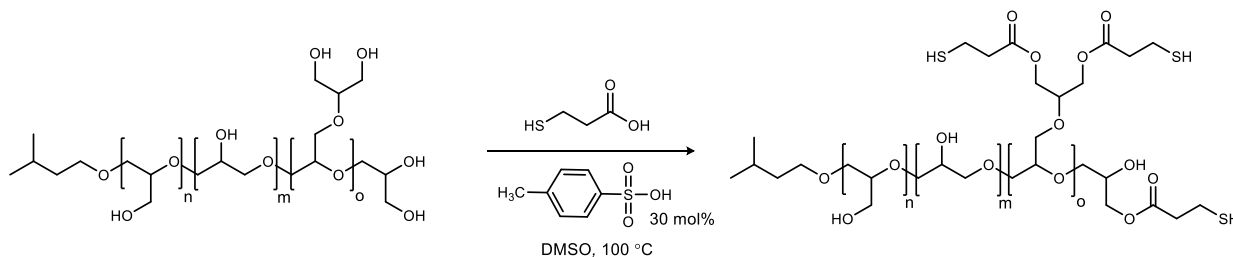
<sup>a</sup>Selected samples. <sup>b</sup>Number average molecular weight by MALDI-ToF of unmodified poly(glycidol). <sup>c</sup>Number average molecular weight by MALDI-ToF of protected 3-mercaptopyropionyl poly(glycidol). <sup>d</sup>Desired functionalization. <sup>e</sup>Actual functionalization. <sup>f</sup>By GPC in DMF calibrated with poly(ethylene glycol) standards.

**Scheme III-9.** Synthesis of thiol-terminated branched poly(glycidol) by Steiglich esterification.

The Steiglich esterification route provides access to the desired thiol-terminated functionalized poly(glycidol) however, there still exist a need for a more concise and effective alternative. Toward this end, a modified Fisher esterification protocol was developed. This involves

the use of drying agent to remove the aqueous byproduct, and a polar aprotic solvent to serve as the reaction medium. 4A molecular sieves was used as the drying agent. Dimethyl sulfoxide proved to be a suitable solvent and was used as the reaction medium. Poly(glycidol) was subjected to esterification with 3-mercaptopropionic acid in the presence of catalytic amounts of p-toluenesulfonic acid (pTSA) in DMSO. After 2 hrs at 110 °C, a gel was formed. This is believed to be the result of disulfide formation. By lowering the concentration and temperature of the reaction medium the desired product was isolated in moderated yield repeatedly precipitating the product in ethyl acetate followed by dialysis (MWCO 1000) in methanol. Varying degrees of ester functionality was installed by changing the amount of reagents added to poly(glycidol) (Table III-2). The isolated polymer was characterized by  $^1\text{H}$  and  $^{13}\text{C}$  NMR. The isolated polymer had similar NMR peaks to the functionalized polymer previously synthesized by an indirect route.

**Table III-2.** Synthesis of 3-mercaptopropionyl polyglycidol by a modified fisher esterification route. Table showing the targeted composition and the actual composition of thiol-terminated branched poly(glycidol) determined by  $^1\text{H}$  NMR.

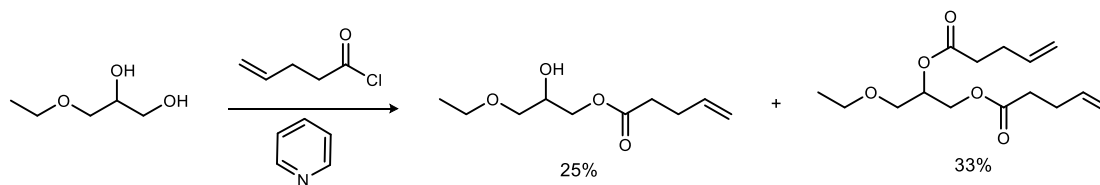


Sample <sup>a</sup>	Mn <sup>b</sup>	Mn <sup>c</sup>	% 3-MP <sup>d</sup>	% 3-MP <sup>e</sup>	PDI <sup>f</sup>
3-MP-Pgly-1	1800	1359	10	7.5	1.29
3-MP-Pgly-2	1800	1489	20	16	1.28

<sup>a</sup>Selected samples. <sup>b</sup>Number average molecular weight by MALDI-ToF of unmodified polyglycidol. <sup>c</sup>Number average molecular weight by MALDI-ToF of 3-mercaptopropionyl polyglycidol. <sup>d</sup>Desired functionalization. <sup>e</sup>Actual functionalization. <sup>f</sup>By GPC in DMF calibrated with poly(ethylene glycol) standards.

## Synthesis of Alkene-Terminated Branched Poly(glycidol)

In an effort to develop reaction condition to functionalized branched poly(glycidol) to its alkene-terminated derivative, 3-ethoxy-1,2-propanediol was used to conduct a model study. 3-Ethoxy-1,2-propanediol was reacted with pyridine and 4-pentenoyl chloride under dilute and concentrated reaction conditions. When stoichiometric amounts of reagents were used under concentrated condition the reaction yielded the desired monoester in 25% yield. The undesired diester was isolated in 33% yield in addition to some starting material. Full conversion of the starting material was observed. This would suggest that both the primary and secondary hydroxy groups of the polymer would be converted to the ester. By integrating and comparing the signals in the  $^1\text{H}$  NMR, it was found that the primary hydroxy group is only slightly more selective than the secondary hydroxy group toward nucleophilic acyl substitution. Under sub-stoichiometric conditions, the selectivity increase. Hence it is expected that branched poly(glycidol) might react in a similar fashion to the model system.



**Scheme III-10.** Esterification of 3-ethoxy-1,2-propanediol

Poly(glycidol) was then subjected to acylation conditions using sub-stoichiometric amounts of reagents. The desired polymer was isolated by repeated precipitation in an ether/ethyl acetate (1:1) mixture followed by dialysis (MWCO 1000).  $^1\text{H}$  and  $^{13}\text{C}$  NMR analysis was used to confirm successful functionalization of the polymer (Figure III-3). In the  $^1\text{H}$  NMR spectrum the peaks at 2.38 and 2.48 ppm corresponds to the two methylene protons of the pentenoyl moiety

while the three diastereotopic protons of the monosubstituted double bond, occurred at 5.03, 5.10 and 5.87 ppm. In the  $^{13}\text{C}$  NMR spectrum peaks at 28.6 and 33.1 ppm corresponds the methylene carbons. The shape of the signal corresponding to the  $\alpha$  methylene carbon is broad and less intense in comparison to the  $\beta$  methylene carbon. This could be due to the reaction of both primary and secondary hydroxyl groups.

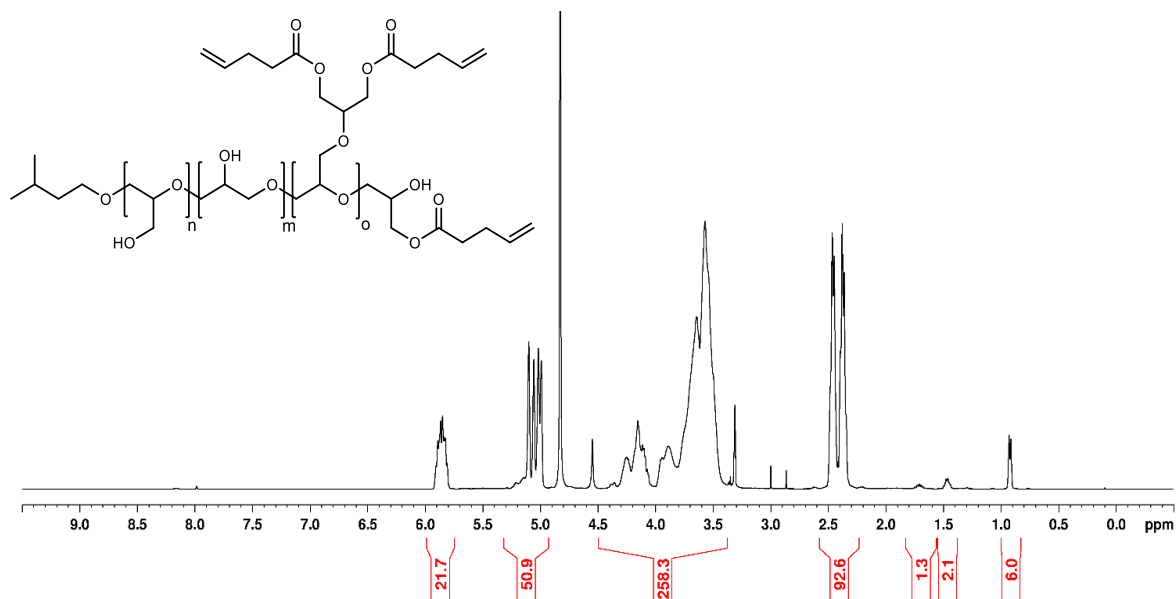
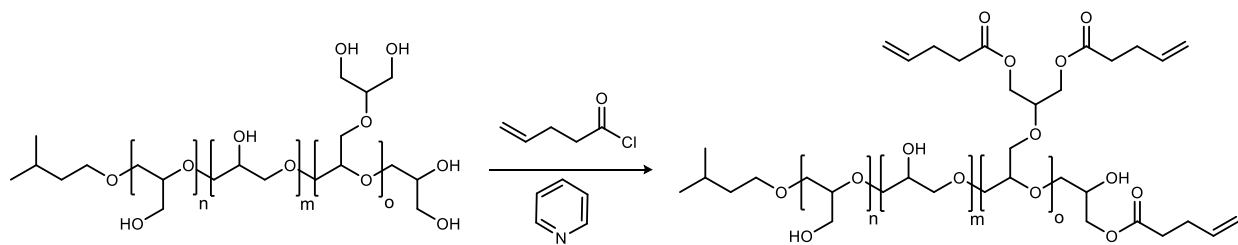


**Figure III-3.**  $^1\text{H}$  NMR (400 MHz,  $\text{CD}_3\text{OD}$ ) of the alkene-terminated derivative of polyglycidol.

For all samples, a good agreement was found between the targeted and actual compositions indicating good conversion of the starting polymer to the desired functionalize polymer (Table III-3). This enables the tailoring of the functionalized polymer by varying the amounts of reagent added to the reaction. The molecular weight determined by MALDI-ToF for both starting poly(glycidol) and the derivative differed only slightly. This further demonstrate that MALDI-ToF data is only accurate for polymer with very narrow molecular weight distribution. The molecular weight distribution was however similar to that of the starting poly(glycidol).



**Table III-3.** Showing the targeted functionalization and the actual functionalization of branched poly(glycidol) determined by  $^1\text{H}$  NMR.



Sample <sup>a</sup>	Mn <sup>b</sup>	Mn <sup>c</sup>	% Alkene <sup>d</sup>	%Alkene <sup>e</sup>	PDI <sup>f</sup>
alkene-Pgly-1	1220	1200	20	16	1.33
alkene-Pgly-2	1220	1300	40	50	1.39

<sup>a</sup>Selected samples. <sup>b</sup>Number average molecular weight by MALDI-ToF of unmodified poly(glycidol). <sup>c</sup>Number average molecular weight by MALDI-ToF of the alkene-terminated poly(glycidol). <sup>d</sup>Desired functionalization. <sup>e</sup>Actual functionalization. <sup>f</sup>By GPC in DMF calibrated with poly(ethylene glycol) standards.

The water solubility of the alkene and thiol-terminated branched polyglycidol was evaluated. It is essential that the poly(glycidol) derivatives that are to be used for hydrogel synthesis is soluble in water. The thiol-terminated branched poly(glycidol) was water soluble at all degrees of functionalization. However, as the degree of functionalization of the alkene-terminated poly(glycidol) was increased from 20% to 30% to 40% the solubility of the polymer derivative decreased. At 20% the alkene-terminated derivative is soluble in water, however at 30% and above the alkene-terminated poly(glycidol) was insoluble in water at all concentrations. As a result, an alternative alkene-terminated derivative was needed for the synthesis of hydrogel via thiol-ene click chemistry. We then hypothesize that the combination of a water-soluble alkene-terminated carboxylic acid with branched poly(glycidol) would give an alkene functionalized polymer that is soluble in water. Hence, we explored the use of acrylic acid for the functionalization of branched poly(glycidol) with terminal alkene groups.

## Synthesis of Acrylate Functionalized Poly(glycidol)

Acrylate functionalized branched poly(glycidol) is a very versatile functional derivative as it can be used for a variety of different applications. However, Due to the toxicity of acrylates, the biomedical applications are limited. We envision that the incorporation of an acrylate moiety into the branched poly(glycidol) side-chains would provide a water-soluble acrylate that can be combined with thiol-terminated branched poly(glycidol) to form hydrogels. Furthermore, hydrogel formation can occur via a Thiol-Michael reaction rather than a thiol-ene reaction.

Since the acrylate derivative of polyglycidol has never been reported, we employed the conditions developed for previous alkene functionalization to access the desired acrylate

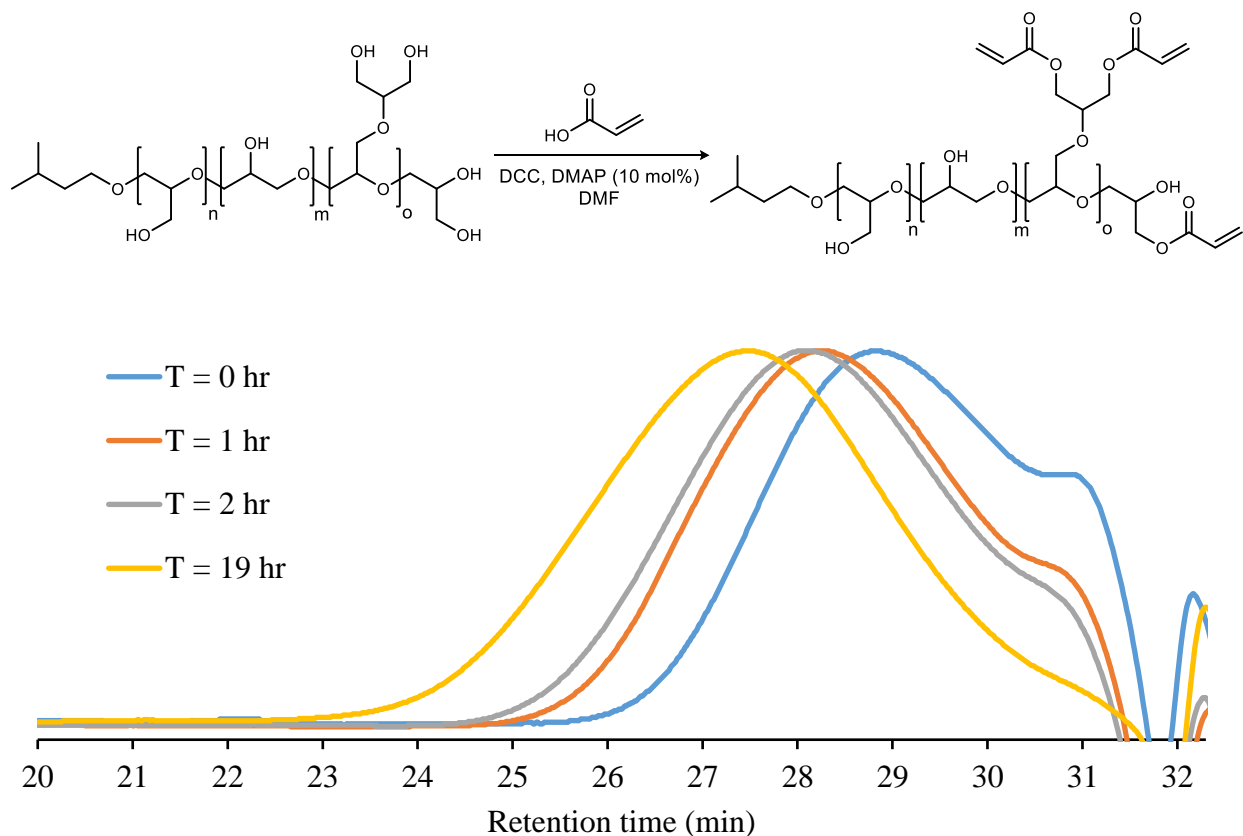


**Figure III-4.** GPC chromatograph showing the evolution of molecular weight during the esterification of poly(glycidol) with acrylic acid.

functionalized polyglycidol. Branched poly(glycidol) was subjected to esterification condition for 24 hrs at rt. Due to the overlapping of peaks in the  $^1\text{H}$  NMR, GPC was used to monitor and track the progress of the reaction (Figure III-3). GPC showed an increase in molecular weight with time. After 24 hrs, no further increase in the molecular weight was observed. The reaction was then filtered and dialyzed in methanol to remove small molecule impurities. After dialysis, we attempted to remove the volatile solvent under rotatory evaporation, at which time the material formed an in-situ gel. We believe the gel formation is most likely due to the polymerization of the acrylates on the polymer due to their high functional group density and the absence of any inhibitor.

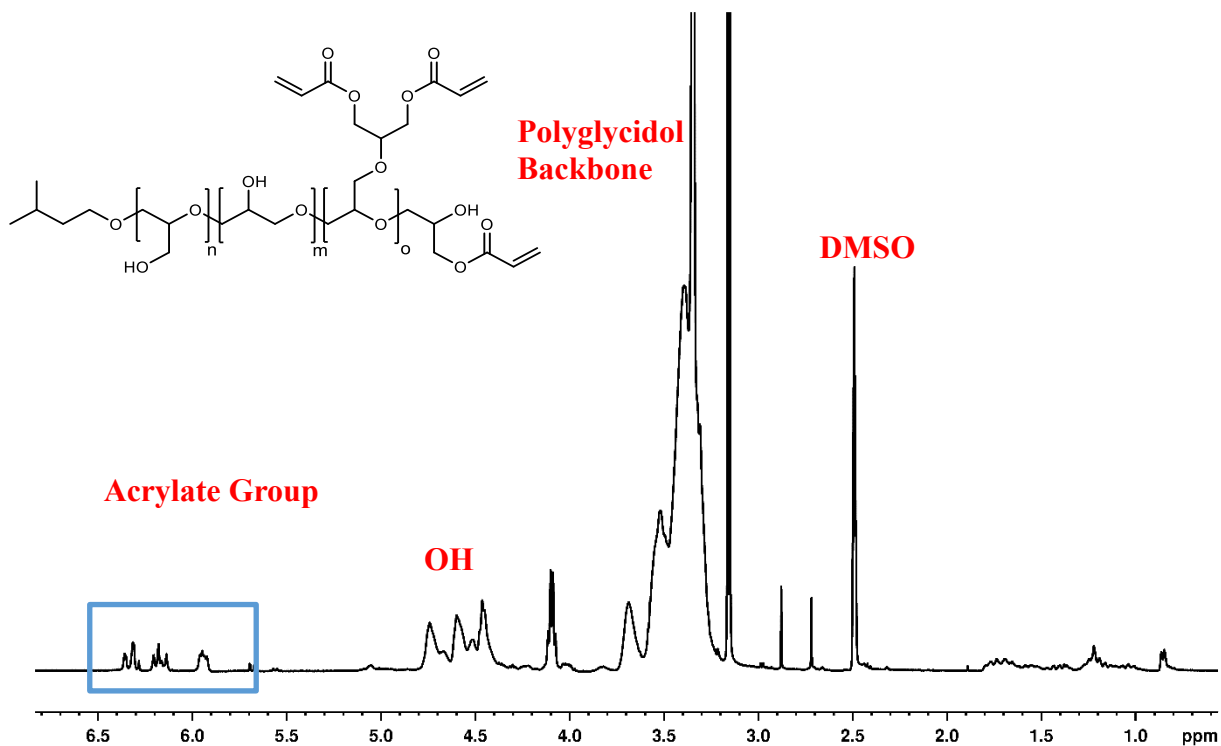


**Figure III-5.**  $^1\text{H}$  NMR (400 MHz,  $(\text{CD}_3)_3\text{SO}$ ) of acrylate-terminated branched polyglycidol.

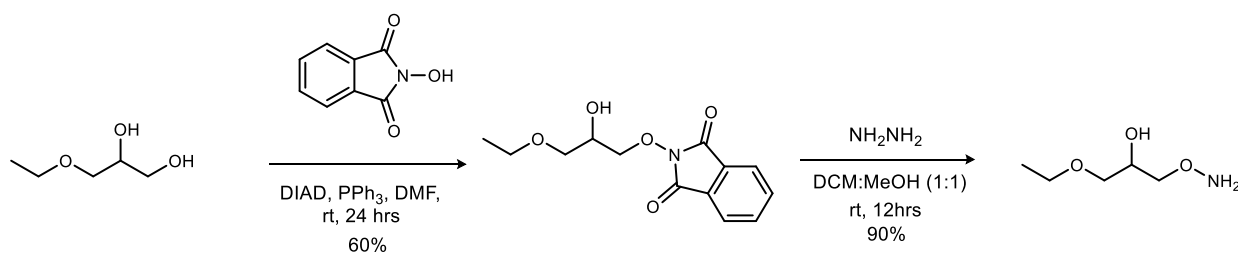
While we were able to synthesize the acrylate functionalized poly(glycidol) (Figure III-5), the side reaction observed during isolation, made this derivative difficult to work with and performed further studies. As a result, the synthesis of poly(glycidol) based hydrogels via thiol-ene click was only possible with alkene-terminated derivatives with degrees of functionalization of less than 20%. Hence, the search continues for more versatile derivatives that are novel and can be easily synthesized in one-two step. The derivative need to be reactive in click chemistry, water soluble and bio-inert. After a review of the literature, we hypothesis that poly(glycidol) functionalized with an aminoxy and a keto-group would have the ability to form hydrogels via oxime click chemistry. Hence, we then pursue the synthesis of these two poly(glycidol) derivatives.

### **Synthesis of Aminoxy Functionalized Branched Poly(glycidol)**

Aminoxy groups are of interested due to their enhanced nucleophilicity compared to the amino group<sup>17</sup> and reacts chemoselectively with aldehydes and ketones to form oximes under mild conditions in the presence of a catalyst<sup>18</sup> or even at physiological pH. The high chemospecificity makes this functionality well suited as orthogonal unit for conjugation to proteins and peptides to polymers,<sup>19-20</sup> synthesis of drug conjugates<sup>21</sup> and various conjugates of carbohydrates,<sup>22-24</sup> and the detection of carbonyl compounds in environmental water samples.<sup>25</sup> To this extend, aminoxy functional groups have also been utilized in the synthesis of oxime hydrogels for drug delivery and tissue engineering applications<sup>26-27</sup> as Maynard<sup>28</sup> and Sumerlin<sup>29</sup> among others have reported and underlines the importance of this reactive group. The aminoxy functionality has been synthesized by utilizing a Mitsunobu reaction to incorporate the N-hydroxyphthalimide moiety followed by cleavage with hydrazine to furnish the desired aminoxy

functionality.<sup>27</sup> Other methods such as the alkylation of ethyl N-hydroxyacetimidate with alkyl methanesulfonates followed by deprotection of the aminoxy group,<sup>30</sup> base catalyzed alkylation of alkyl halides with N-hydroxyphthalimide followed by subsequent hydrazinolysis,<sup>26</sup> and coupling of Boc protected aminoxy acetic acid followed by deprotection of the Boc group<sup>19, 31-32</sup> have also been utilized to install the aminoxy group. However, none of these methods have been applied to the functionalization of hydrophilic, branched structures such as the branched poly(glycidol).

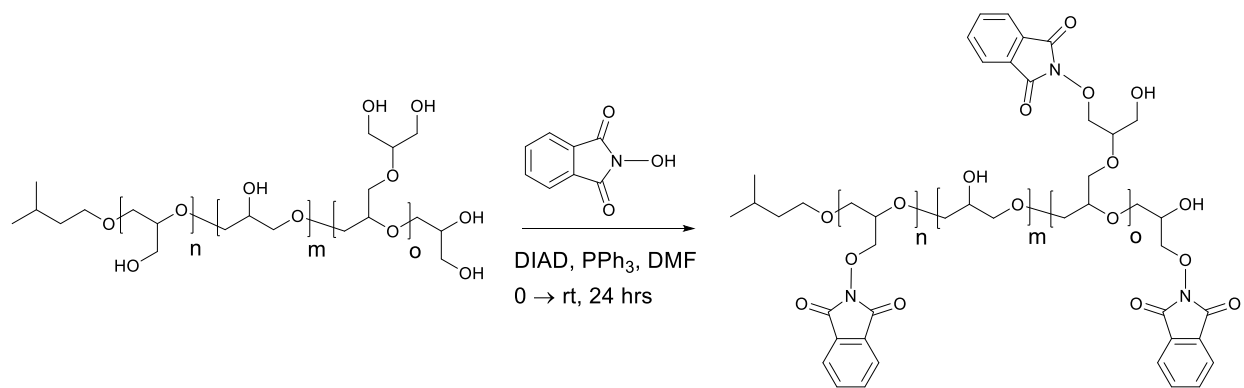
To ascertain valuable information about the Mitsunobu reaction of N-hydroxyphthalimide with poly(glycidol), N-hydroxyphthalimide was reacted with 3-ethoxy-1,2-propanediol in a model reaction (Scheme III-11). 3-ethoxy-1,2-propanediol was stirred in the presence of excess triphenylphosphine and diisopropylazodicarboxylate for 24 hrs at room temperature. The desired product was isolated in moderate yield. Full conversion was observed by thin layer chromatography analysis and <sup>1</sup>H NMR shows that only the primary hydroxy group reacted.



**Scheme III-11.** Mitsunobu reaction of 3-ethoxy-1,2-propanediol followed by hydrazinolysis

The reaction of only the primary hydroxy indicates that under reaction condition, nucleophilic attack on the secondary carbon bearing the hydroxy substituent is hindered by the size of the nucleophile. An increase in temperature however, will most likely increase the

probability of nucleophilic substitution of the secondary hydroxy groups. Subsequent reduction with hydrazine furnishes the desired primary aminoxy in good yields.



Sample	Ratio [NHP]/[OH]	Degree of Functionalization by <sup>1</sup> H NMR / %	GPC of NHP- PG		MALDI-ToF MS		Yield / %
			Mn	Mn/Mw	Mn	Mn/Mw	
1a	0.25	17	2673	1.39	2855	1.30	62
1b	0.40	33	3143	1.35	3205	1.32	72
1c	0.55	43	3314	1.33	3233	1.32	68
1d	0.70	63	3464	1.33	3216	1.33	76

**Figure III-6.** Mitsunobu reaction of branched poly(glycidol) with *N*-hydroxyphthalimide.

The poly(glycidol) was reacted with substoichiometric amounts of *N*-hydroxyphthalimide, triphenylphosphine and diisopropylazodicarboxylate (DIAD) with targeted ratios of reagents to hydroxyl groups being 0.25, 0.40, 0.55 and 0.70 to achieve a degree of functionalization of 17%, 33%, and 43% and 63% (Figure III-6). The desired polymers were isolated by multiple precipitation in a mixture of ethyl acetate and ethyl ether prior to analysis by size exclusion chromatography (SEC), MALDI-ToF mass spectroscopy, <sup>1</sup>H, <sup>13</sup>C and <sup>31</sup>P NMR spectroscopy.

SEC analysis using DMF as the eluent showed that significant aggregation was observed when SEC analysis was conducted in the absence of lithium bromide (LiBr) as an additive. The aggregation was due to hydrogen bonding between the hydroxyl and carbonyl groups of different

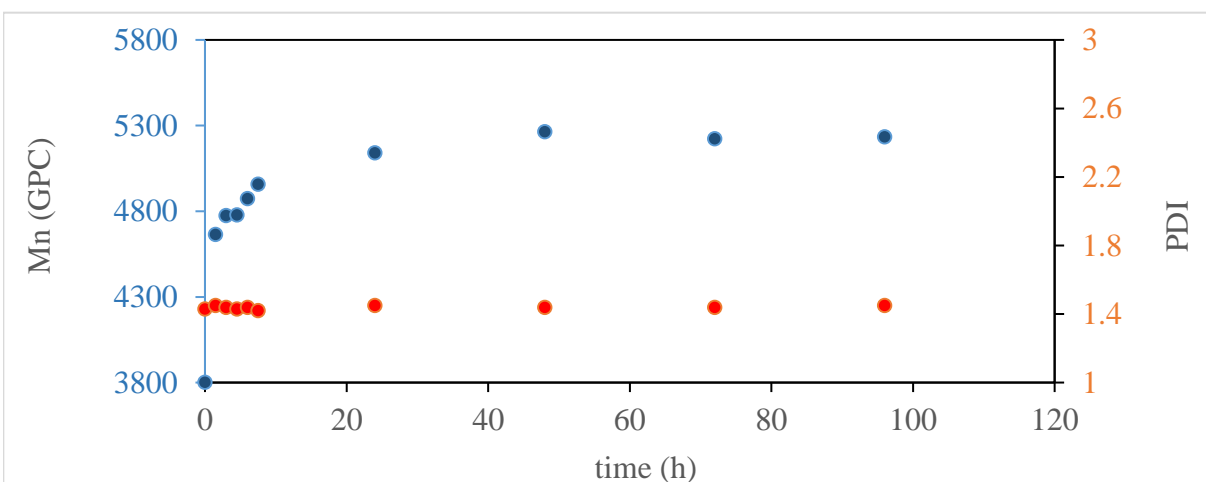
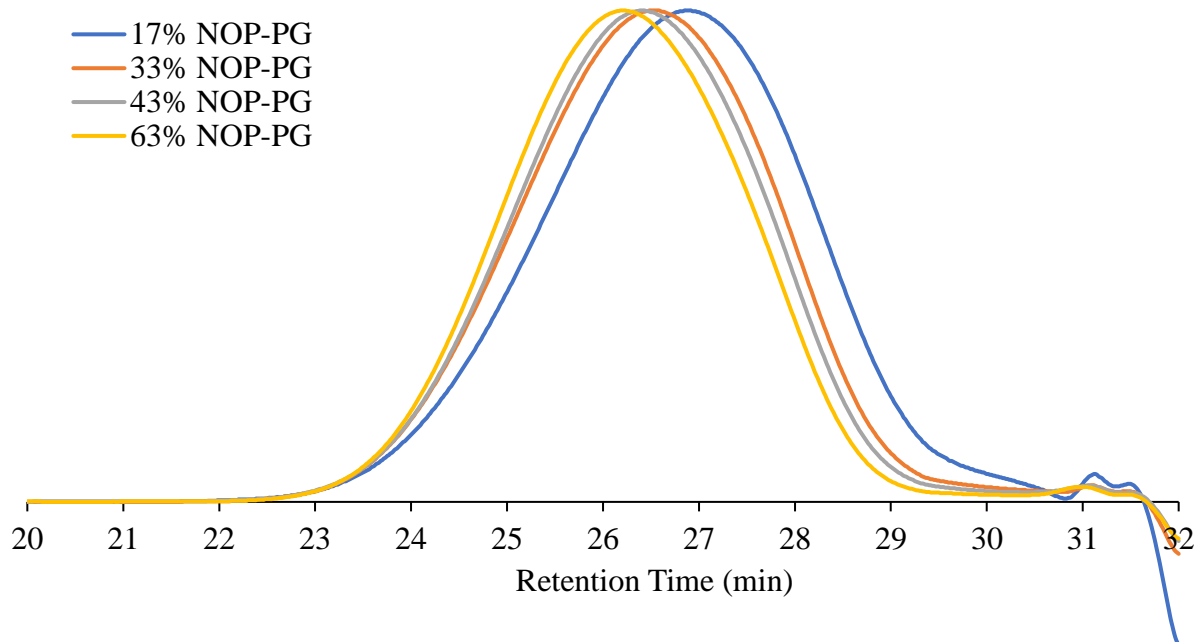


**Figure III-7.** SEC chromatographs of branched poly(glycidol) functionalized with N-hydroxyphthalimide. Analysis was carried out in DMF (LiBr) at 45 °C. The plot of  $M_n$  vs time shows changes in molecular weight and molecular weight distribution over the course of the reaction.

polymer chains. In fact, aggregation could be seen in the SEC analysis of the branched poly(glycidol) in DMF without LiBr added, due to hydrogen bonding between hydroxyl groups (Figure III-7).

Both  $^1\text{H}$  and  $^{13}\text{C}$  NMR spectra of poly[(glycidol-*N*-oxyphthalimide)-*co*-glycidol] (P[(G<sup>NOP</sup>)-*co*-G]) exhibit characteristic signals for the phenyl protons attached the *N*-oxyphthalimide moiety indicating successful incorporation of the desired functionality. In the  $^1\text{H}$  NMR (Figure III-8), this signal appears as a broad singlet at 7.76 ppm due to significant overlapping of the neighboring peaks. In  $^{13}\text{C}$  NMR, the signal corresponding to the carbon of the carbonyl groups can be seen at 164 ppm and the carbons of the phenyl ring appears at 135, 129 and 124 ppm. There was noticeable shifting of the signals in the polymer backbone region of the  $^{13}\text{C}$  NMR spectrum. Moreover, we could observe significant shifting of the signals corresponding to the terminal 1 (T<sub>1</sub>), terminal 2 (T<sub>2</sub>) and linear 1,3 structural unit (L<sub>1,3</sub>) while the linear 1,4

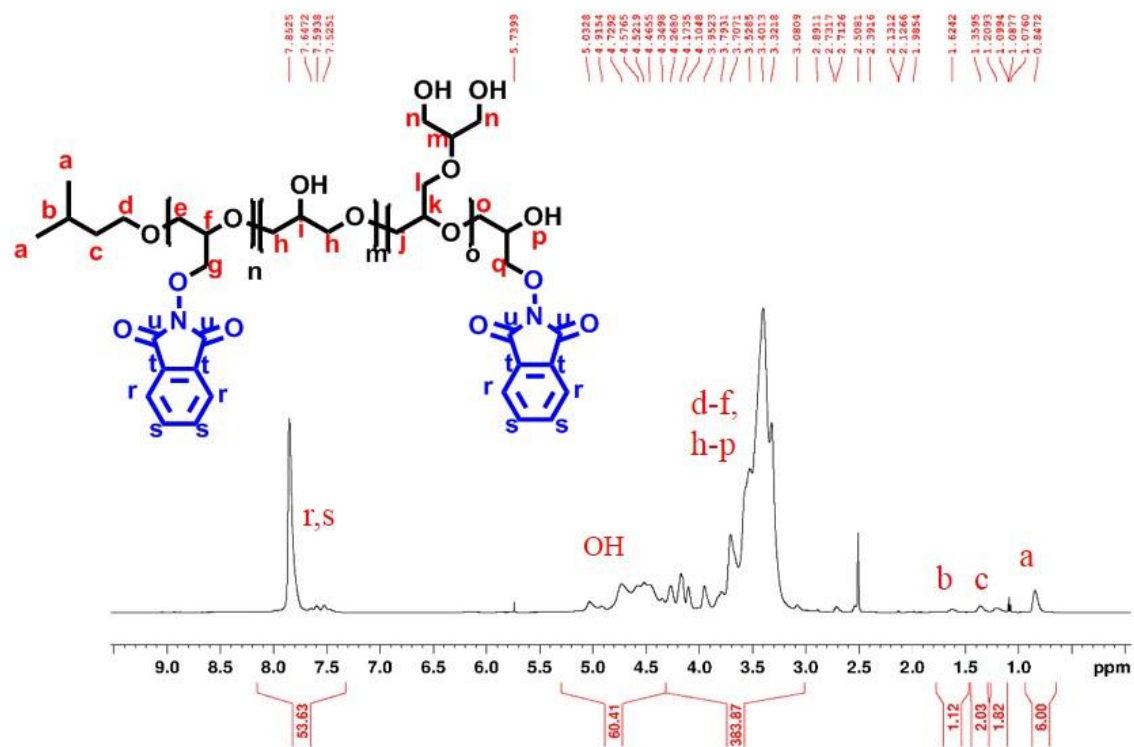


**Figure III-8.**  $^1\text{H}$  NMR (400 MHz,  $(\text{CD}_3)_2\text{SO}$ ) of branched poly(glycidol) functionalized with *N*-hydroxy phthalimide.



structural unit (L<sub>1,4</sub>) appears to be unmodified. The resulting decrease in the signal intensity for the primary hydroxyl groups corresponded to an increase in the ratio of NHP to hydroxyl group in the feed. This would indicate that majority of the primary hydroxyl groups (L<sub>1,3</sub>) participated in the reaction. Due to extensive overlapping, specific assignment of all the peaks was difficult.

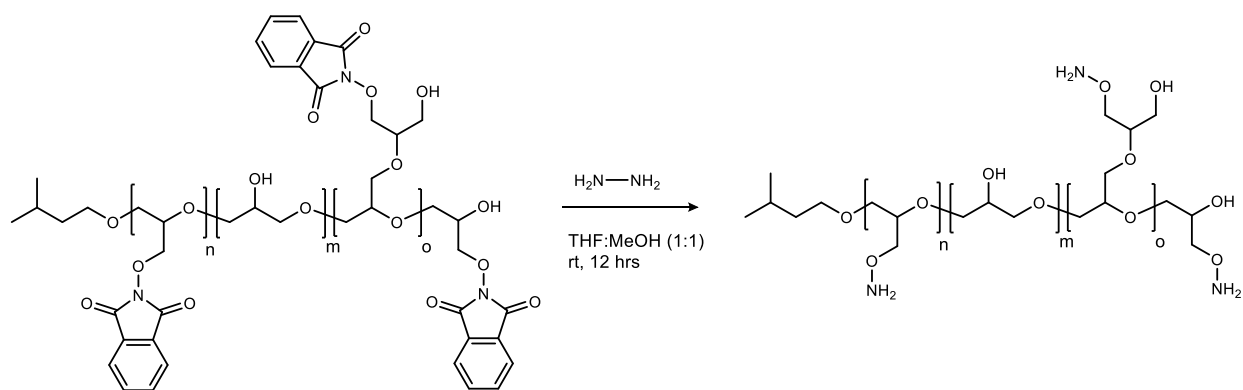
In <sup>31</sup>P NMR, peaks corresponding to triphenyl phosphine oxide was observed as a singlet at 28 ppm. This suggested that trace amounts of triphenylphosphine oxide was present and was removed during purification in the next step. It was also observed that some of the triphenylphosphine (PPh<sub>3</sub>) had reacted with the poly(glycidol) as indicated by broad peaks at 31 ppm. This side reaction was reduced by cooling the reaction to 0 °C and adding the DIAD immediately after the addition of PPh<sub>3</sub>, then allowing the reaction to warm to room temperature and stir over the course of 24 hrs.

The degree of functionalization was calculated by comparing the signal intensity of the phenyl groups on the N-oxyphthalimide moiety to that of the semi-branched poly(glycidol) backbone consulting both the <sup>1</sup>H and <sup>13</sup>C NMR. For <sup>13</sup>C NMR an inverse-gated proton decoupled pulse sequence was used with a relaxation delay of 10 sec. This allowed for integration of the signal intensities in the <sup>13</sup>C NMR spectrum. For the series of experiments carried out, the degree of functionality was in good agreement with the ratios adjusted in the feed reaching from 0.25, 0.40, 0.55, to 0.70 (Figure III-6).

In contrast to the unmodified branched poly(glycidol), the solubility of the N-oxyphthalimide derivative varied based on the degree of functionality. Derivatives with ratio of functionalization of [NHP]/[OH] with less than 0.20 had solubilities similar to that of the parent poly(glycidol). However, polymers with degrees of functionalization between 0.20 and 0.45 was neither soluble in alcoholic nor chlorinated solvents. For these polymers, a mixed solvent system

had to be used to fully dissolve the polymers. Polymers with a degree of functionalization greater than 0.45 were soluble in chlorinated solvents along with tetrahydrofuran and 1,4-dioxane. This variation of solubility supports the successful incorporation of the desired functionality into branched poly(glycidol) with the ability to tailor the polymer to the desired degree of functionalization.

The N-oxyphthalimide functionalized polymer was then subjected to hydrazinolysis to yield the poly[(glycidol-N-aminoxy)-co-glycidol] (P[(G<sup>AO</sup>)-co-G]). This reaction was carried out as a suspension in methanol or as a solution in a mix solvent system of methanol and tetrahydrofuran (1:1) (Figure III-9). The white solid byproduct was removed by filtration and the



Sample	Degree of Functionalization by <sup>1</sup> H NMR/%	GPC		MALDI-ToF MS		Yield / %
		Mn	Mn/Mw	Mn	Mn/Mw	
2a	17	2542	1.64	1635	1.59	69
2b	33	2152	2.01	1985	1.24	53
2c	43	1708	2.52	2546	1.36	55
2d	63	1933	2.08	2610	1.37	52

**Figure III-9.** Hydrazinolysis of the branched poly(glycidol) N-oxyphthalimide derivatives to provide aminoxy functionalized poly(glycidol).

reaction was stirred for an additional 6 hrs. The excess hydrazine was removed by rotary evaporation followed by dialysis. This furnished the desired aminoxy functionalized semi-branched poly(glycidol) in 50-70% yield.

The lack of the phenyl protons in the  $^1\text{H}$  NMR (Figure III-10) as well as the carbon atoms of the phthalimide moiety in the  $^{13}\text{C}$  NMR indicates the reaction was successful. It was observed that when a methanol/dichloromethane mixture was used, signals corresponding to an  $\text{sp}^2$  methylene group was observed in both the  $^1\text{H}$  and  $^{13}\text{C}$  NMR spectrum. This was attributed to the reaction of the aminoxy group with dichloromethane. Therefore, we used tetrahydrofuran instead of dichloromethane to circumvent this problem. The solubility of the final product, the aminoxy poly(glycidol) was observed to be similar to the unmodified polymer.

Additionally, supporting a strong hydrogen bonding effect, the aminoxy poly(glycidol) would take a long time to dissolve in methanol and water, and analysis by SEC in water showed significant aggregation. The addition of LiBr did not solve this problem and added a challenge to the analysis of molecular weight and molecular weight distribution by gel permeation chromatography (Figure III-10). However, MALDI-ToF MS analysis showed a correlation with the molecular weights obtained from SEC analysis. The molecular weight distribution did not correlate as well possibly due to the aggregation of the polymer during SEC analysis.

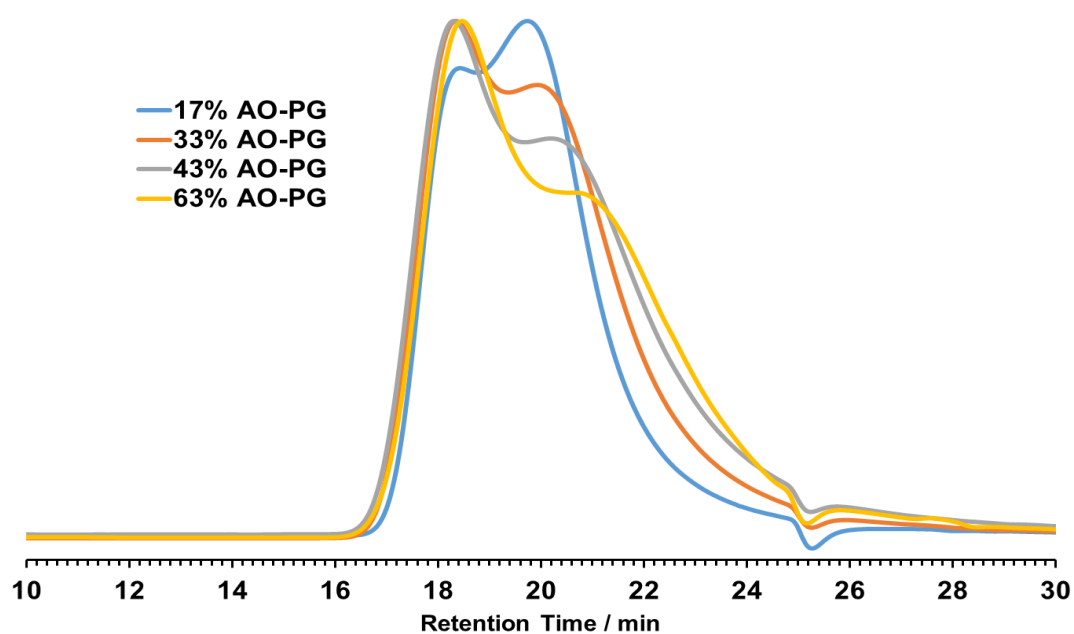
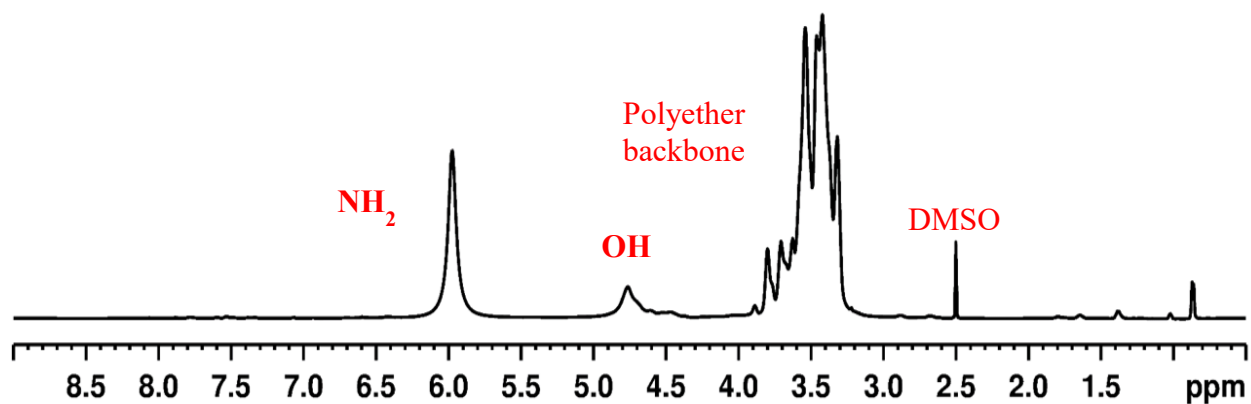


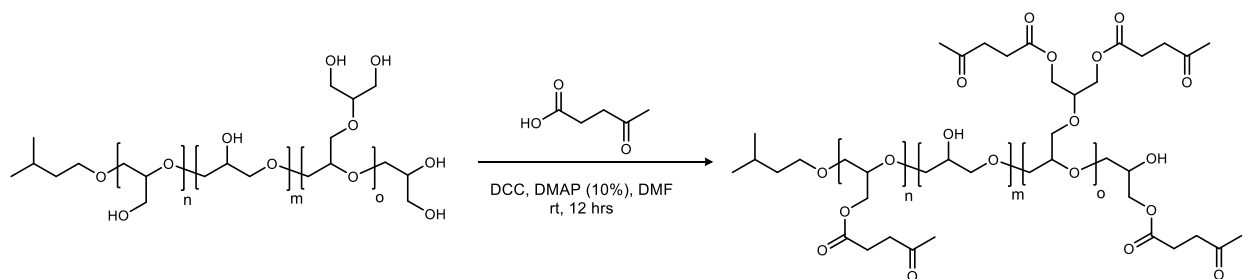
**Figure III-10.**  $^1\text{H}$  NMR (top) and GPC (bottom) of aminoxy-functionalized branched poly(glycidol)

We have successfully synthesized the aminoxy-functionalized branched poly(glycidol) derivatives needed for the oxime-click reaction. The ability to tailor the degree of functionalization will allow for the tuning of the properties of the resulting materials. The next step is to synthesize

the keto-functionalized poly(glycidol) derivative, and in likewise manner, create ratio-controlled keto-functionalized derivatives for crosslinking with the aminoxy poly(glycidol) derivatives.

### Synthesis of $\gamma$ -Keto-Ester Derivative of Branched Poly(glycidol)

The synthesis of  $\gamma$ -keto-ester derivative of poly(glycidol) was accomplished using a Steiglich esterification (Scheme III-12).<sup>16</sup> This involves the formation of an ester from a carboxylic acid, levulinic acid, and the alcohol groups attached to the polyether backbone of branched poly(glycidol) using dimethylaminopyridine (DMAP) as a nucleophilic catalyst and dicyclohexylcarbodiimide (DCC) as the coupling reagent. Branched poly(glycidol) was reacted with substoichiometric amounts of levulinic acid, DCC and DMAP with targeted ratios of reagents to hydroxy group being 0.28, 0.38, 0.53 and 0.68 to achieve a degree of functionalization of 20%, 30%, 45%, and 60%. The desired polymers were isolated by dialysis in water for 24-48 h, followed by evaporation under reduce pressure. The final product, a colorless viscous liquid, was analyzed by gel permeation chromatography (GPC), <sup>1</sup>H, and <sup>13</sup>C NMR spectroscopy.



**Scheme III-12.** Synthesis of keto-functionalized branched poly(glycidol) via esterification with levulinic acid.

The progress of the reaction was monitored by GPC and NMR. The peaks in the  $^1\text{H}$  NMR corresponding to the terminal methyl of the levulinic acid (Figure III-13) was compared to that of the desired polymer product to determine percent conversion of the starting material. Additionally, no side reaction or decomposition of the polymer backbone was observed under the reaction conditions. For all reactions performed, only 55-70% of the levulinic acid in the feed was converted to ester groups, however, the degree of functionalization does not reflect this. This could be due to the polydispersity of the starting polymer. The lower molecular weight polymers have a higher degree of functionalization while the larger polymers have a lower degree of

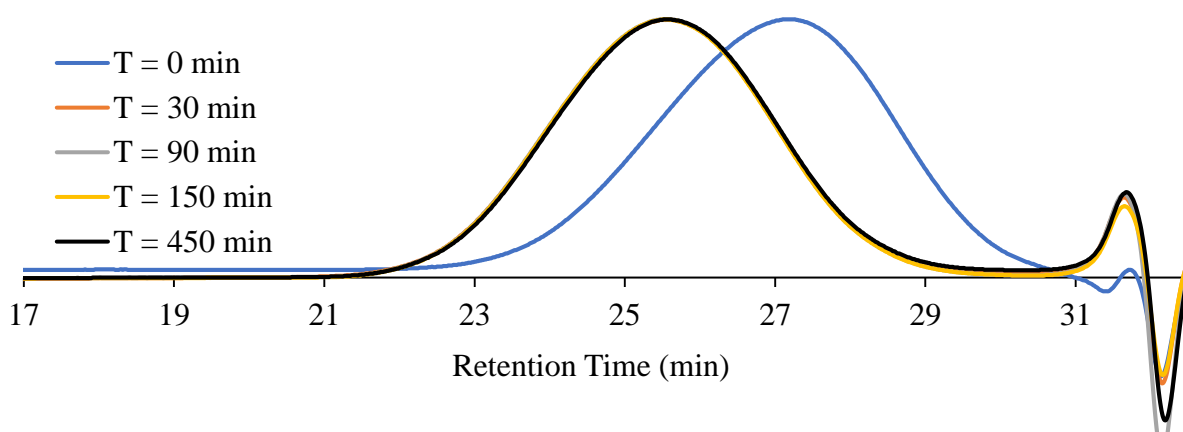
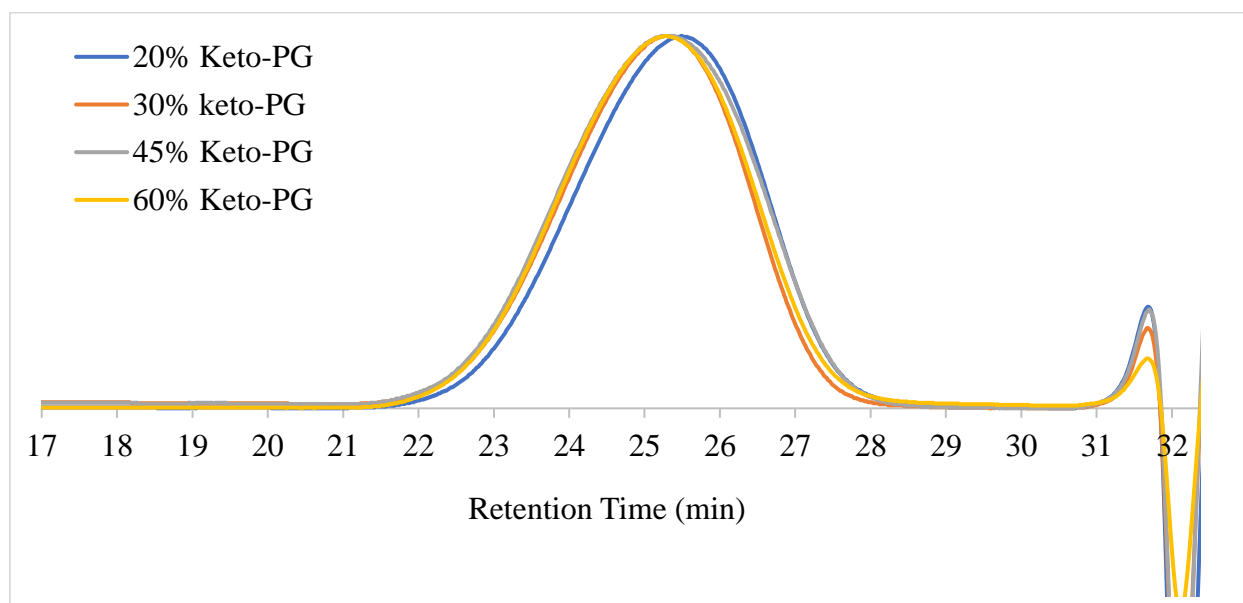


**Figure III-11.** GPC monitoring of the synthesis of keto-functionalized branched polyglycidol showing no change in molecular weight or molecular weight distribution after 30 min of reaction time.

functionalization. The degree of functionalization calculated from NMR is an average representation of the sample. Furthermore, the reaction has a high degree of reproducibility which enabled us to work out a formula for functionalization of poly(glycidol) with levulinic acid. Generally, the degree of functionalization calculated for in the feed, must be 5-8% more than the desired degree of functionalization, therefore If a 30% functionalization is required, the you should aim for 38%. GPC monitoring of the reaction showed that the reaction is complete in 30-60

minutes (Figure III-11). Slight increases in reaction time was observed as when the desired degree of functionalization was increased. GPC analysis using DMF as the eluent (Figure III-12), showed that the synthesized keto-functionalized poly(glycidol)s have fairly narrow polydispersities ( $1.27 \leq \text{PDI} \leq 1.32$ ) and increased number average molecular weights ( $M_n$ ) compared to the unfunctionalized starting polymer. Furthermore, the molecular weights determined from GPC increased moderately with increasing number of keto-ester groups introduced into the branched poly(glycidol). The narrow polydispersities and the moderate increases in molecular weights could be attributed to the uneven reaction rate between the different polymers lengths in solutions.



Sample	Ratio [keto-acid]/[OH]	Degree of Functionalization by $^1\text{H}$ NMR / %	GPC of starting PG		GPC of Keto-PG		Yield / %
			$M_n$	$M_n/M_w$	$M_n$	$M_n/M_w$	
<b>3a</b>	0.28	20	2729	1.58	3100	1.30	52
<b>3b</b>	0.38	30	2729	1.58	3300	1.27	41
<b>3c</b>	0.53	45	2729	1.58	3700	1.32	53
<b>3d</b>	0.68	60	2729	1.58	4100	1.31	64

**Figure III-12.** GPC traces of keto-functionalized branched poly(glycidol).

$^1\text{H}$  NMR analysis of the isolated product reveals that the selected reaction condition results in the successful incorporation of the levulinoyl groups onto the polymer yielding  $\gamma$ -keto-ester functionalized branched poly(glycidol) (Figure III-13). The  $^1\text{H}$  NMR shows broad resonances corresponding to one methyl and two methylene groups of levulinoyl moiety at 1.89, 2.26 and 2.29 ppm respectively. The methylene and methine protons of branched poly(glycidol) appear as one very broad peak between 3.12–4.00 ppm while the protons of the various hydroxyl groups appear as broad peaks between 4.21–4.83 ppm. The signals observed at 0.65, 1.16, and 1.43 ppm corresponds to the methyl, methylene and methine group, respectively, of the initiator isoamyl alcohol used in the synthesis of branched poly(glycidol). The degree of functionalization of branched poly(glycidol) with levulinoyl groups was determined from the  $^1\text{H}$  NMR, by comparing the normalized integrals of the methyl protons of the levulinoyl groups at 1.89 ppm, with the methylene and methine protons of branched poly-glycidol between 3.12–4.00 ppm. It was observed that the degree of functionalization can be tailored by varying the feed ratio of levulinic acid to the branched poly(glycidol).

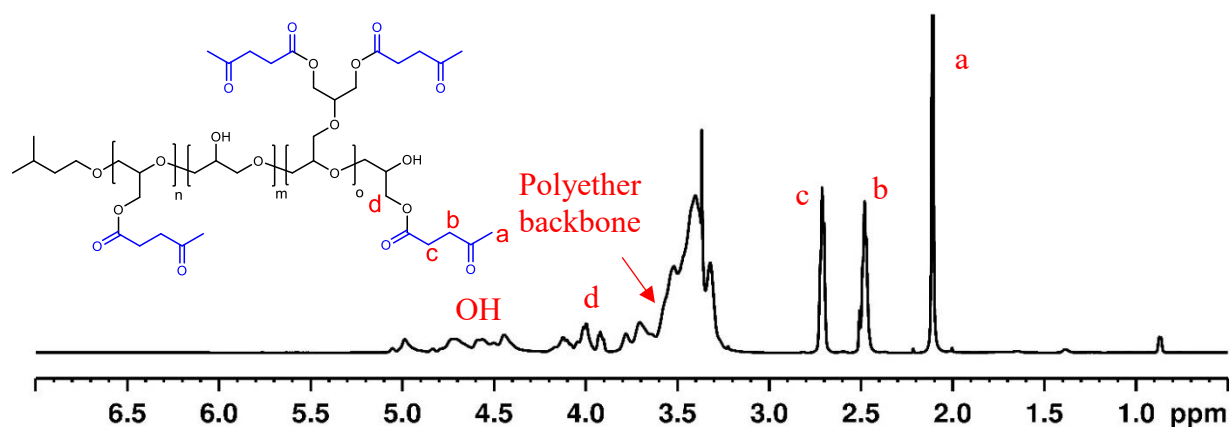


**Figure III-13.**  $^1\text{H}$  NMR (400 MHz,  $(\text{CD}_3)_2\text{SO}$ ) of branched poly(glycidol) functionalized with levulinic acid.



## Cytotoxicity of Branched Poly(glycidol) Derivatives

Brooks and coworkers reported extensively on the biocompatibility of unmodified branched poly(glycidol).<sup>33-43</sup> However, there are no reports of the biocompatibility or cytotoxicity of functionalized poly(glycidol). To investigate their potential uses for biomedical application, the cytotoxicity of aminoxy and keto-functionalized poly(glycidol)s were evaluated. Aminoxy and keto-functionalized poly(glycidol) with 20%, 30% and 60% degree of functionalization were tested for their toxicity against mouse fibroblast cells using the MTT assay. The cells were incubated with increasing concentrations of polymer (0.1, 1, 5 and 10 mg/mL) for 48 h before undertaking the MTT assay (Figure III-14). Both functionalized branched poly(glycidol) showed very little toxicity towards the fibroblasts cells. Furthermore, increasing the amount of the

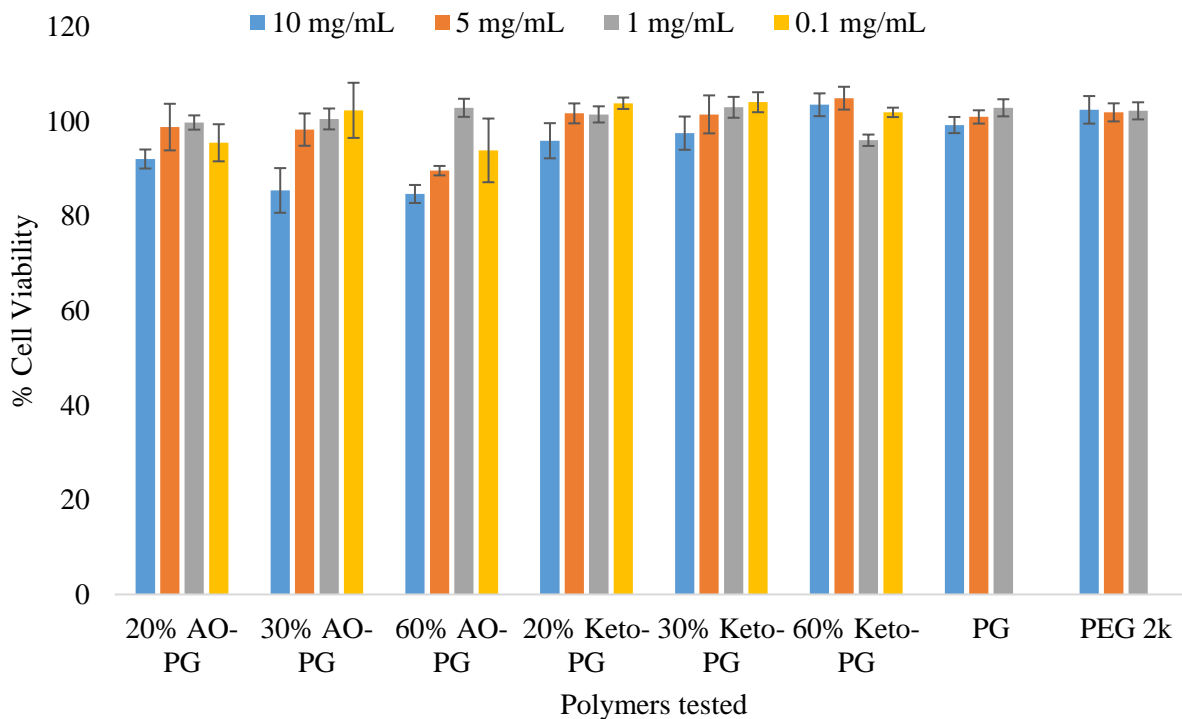


**Figure III-14.** Cytotoxicity of aminoxy and keto-ester functionalized polyglycidols.

aminoxy and keto functionality on the polymer showed very little effect on toxicity. PEG and unmodified poly(glycidol) was also tested alongside the functional poly(glycidol) and was found to have similar cytotoxicity to the functional derivatives tested. These results indicate that the methodology used to functionalize these polymers result in biocompatible building blocks for the preparation of biomaterials.

## CONCLUSION

Functionalized branched poly(glycidol) has numerous applications in the field of regenerative medicine and drug delivery. The derivatives can be synthesized in a simple straight forward manner for the desired application. Esterification has the advantages of incorporating degradable ester bonds which can be exploited in tissue engineering and drug release systems. We have successfully added a number of additional poly(glycidol) derivatives to the stockpile. 4-pentenoyl poly(glycidol) was synthesized by esterification of the corresponding acyl chloride with poly(glycidol). 3-mercaptopropionyl poly(glycidol) was synthesized by a modified Fischer esterification with the corresponding acid and also by esterification with the corresponding disulfide acid followed by reduction of the disulfide. Aminoxy functionalized branched poly(glycidol)s were prepared by a postpolymerization modification using the Mitsunobu reaction for this purpose. The hydroxyl side groups are functionalized with N-hydroxy phthalimide and the hydrazinolysis of this group furnishes a new class of branched poly(glycidol)s with pendant aminoxy groups. Keto-functionalized poly(glycidol) were prepared via Steiglich esterification. Reproducible functionalization degrees of 20%, 30% 45% and 60% can be obtained via the developed methodology. MTT assays demonstrated the cell compatibility of aminoxy and keto-functionalized materials. With this, the prepared structural motifs are valuable precursors for the synthesis biomaterials, bioconjugates and hydrogels where orthogonal strategies are desired. These derivatives are valuable due to the biocompatibility extended by poly(glycidol), and their biodegradability extended by their ester functionality.

## EXPERIMENTAL

### Materials

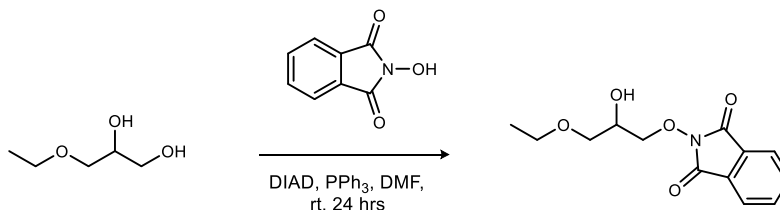
Glycidol (Aldrich, 96%) and N,N-dimethylformamide (Aldrich, 99.8%) was freshly distilled from calcium hydride prior to use. 3-methyl-1-butanol (Aldrich, anhydrous, 99%), Tin (II) trifluoromethanesulfonate (Strem Chemicals, 99%), methanol (Acros, anhydrous, 99.8%), dichloromethane (Aldrich, anhydrous, 99.8%), triphenylphosphine (Aldrich, 99%), N-hydroxyphthalimide (Aldrich, 97%), diisopropyl azodicarboxylate (Aldrich, 98%), and hydrazine (Aldrich, anhydrous, 98%) were used as received. Dialysis membrane were obtained from spectrum laboratories (Spectra/Por 7, molecular weight cut-off (MWCO) of 1000 Da). PTFE syringe filters were obtained from Thermo Scientific (0.45  $\mu\text{m}$ , 30 mm, Teflon plus glass). All reactions were carried out under argon unless otherwise noted.

### Instrumentation

Nuclear magnetic resonance (NMR) were acquired on a Bruker DRX-500 (500 MHz), Bruker AV-400 (400 MHz) or Bruker AV II-600 (600 MHz) instrument (equipped with a 5 mm Z-gradient TCI cryoprobe). Chemical shifts are measured relative to residual solvent peaks as an internal standard set to  $\delta$  7.26 and  $\delta$  77.0 ( $\text{CDCl}_3$ ),  $\delta$  3.31 and  $\delta$  49.0 ( $\text{CD}_3\text{OD}$ ) and  $\delta$  2.50 and  $\delta$  39.52 ( $(\text{CD}_3)_3\text{SO}$ ). Quantitative  $^{13}\text{C}$  NMR was performed by using inverse-gated proton decoupled  $^{13}\text{C}$  NMR with a delay time of 10 seconds. A sample concentration of approximately 150 mg/mL was used for analysis. FT-IR spectra were recorded on a Thermo Nicolet IR 100 spectrophotometer and are reported in wavenumbers ( $\text{cm}^{-1}$ ). Compounds were analyzed as neat films on a NaCl plate (transmission). Size exclusion chromatography (SEC) were performed using a Waters 1525 binary

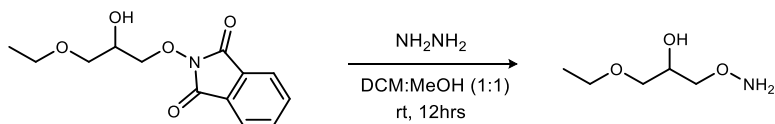
high pressure liquid chromatography pump equipped with a refractive index detector (Waters 2414) and Styragel HR columns (7.8×300 mm Styragel HR 5, Styragel HR 4E, Styragel HR 3). SEC analysis was carried out in DMF (containing 1 mg/mL LiBr) with a flow rate of 1.0 mL/min at 45 °C. Water SEC was carried out using Waters Ultrahydrogel™ columns (7.8×300 mm, Ultrahydrogel™ 120, Ultrahydrogel™ DP 120Å, Ultrahydrogel™ 250). HPLC grade water (containing 1 mg/mL LiBr) was used as the eluent at a flowrate of 1 mL/min at 45 °C. Molecular weights ( $M_n$  and  $M_w$ ) and molecular weight distribution were calculated from poly(ethylene glycol) standards provided by Varian. Matrix-assisted laser desorption and ionization time-of-flight mass spectroscopy (MALDI-ToF MS) was carried out on a Voyager DE-STR mass spectrometer equipped with a nitrogen gas laser (337 nm).  $\alpha$ -Cyanohydroxycinnamic acid was used as the matrix and NaI was used as the cationization agent. The samples (5 mg/mL in methanol), matrix (20 mg/mL in methanol) and cationization agent (20 mg/mL) were mixed in a 1:1/0.1 ratio respectively and spotted onto a stainless-steel sample plate. The accelerating voltage was set to 23,000 and measurements took place in reflector mode. Poly(ethylene glycol) was used for external calibration immediately before the measurement. The data was processed using Data Explorer. All spectra were processed (baseline correction, noise filter and Gaussian smooth) before importing mass list into an excel spreadsheet for data analysis.

## Synthesis of 2-(3-Ethoxy-2-hydroxypropoxy)isoindoline-1,3-dione.



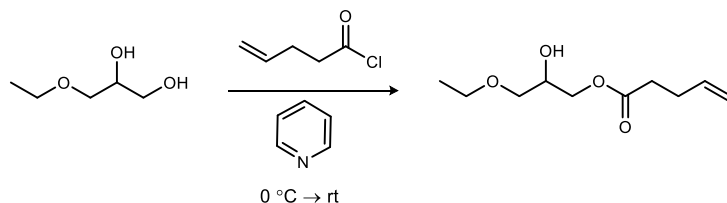
To a 50 mL round bottom flask fitted with an argon balloon and containing a solution of 3-ethoxy-1,2-propanediol (1.00 g, 8.3 mmol) in dichloromethane (5 mL) was added *N*-hydroxyphthalimide (1.3 g, 8.3 mmol) followed by triphenylphosphine (2.2 g, 8.3 mmol) at rt. diisopropylazodicarboxylate (1.6 mL, 8.3 mmol) was then added dropwise and the resulting mixture was stirred at rt for 24 hrs. The reaction was concentrated under reduced pressure and purified by flash column chromatography (SiO<sub>2</sub>, 5-30% ethyl acetate in hexanes) to furnish the desired product as a yellow oil (1.3 g, 60%).  $R_f = 0.5$  (60% EtOAc/hexanes); IR (film) 3455, 3061, 2919, 1789, 1730, 1373, 1127, 731 cm<sup>-1</sup>; <sup>1</sup>H NMR (600 MHz, CDCl<sub>3</sub>)  $\delta$  7.86 (dd,  $J = 5.6, 3.0$  Hz, 2H), 7.78 (dd,  $J = 5.6, 3.0$  Hz, 2H), 4.35 (dd,  $J = 11.3, 3.1$  Hz, 1H), 4.19 (dd,  $J = 11.3, 8.2$  Hz, 1H), 4.13-4.07 (m, 1H), 3.89-3.78 (m, 1H), 3.61-3.51 (m, 3H), 1.19 (t,  $J = 7.1$ , 3H); <sup>13</sup>C NMR (600 MHz, CDCl<sub>3</sub>) ppm 162.8, 134.7, 128.0, 123.4, 79.2, 77.8, 76.6, 74.9, 72.1, 71.4, 67.3, 65.2, 63.1, 61.2, 38.1, 24.7, 21.8.

### Synthesis of 1-(Aminoxy)-3-ethoxypropan-2-ol.



To a 50 mL round bottom flask equipped with a stir bar and an argon balloon was added a solution of 2-(3-ethoxy-2-hydroxypropoxy)isoindoline-1,3-dione (500 mg, 1.88 mmol) in dichloromethane (5 mL). Excess of anhydrous hydrazine (2.49 mL, 78.5 mmol) was added and the reaction was allowed to stir for 12 hrs at rt. The reaction mixture was filtered through 0.2  $\mu\text{m}$  PTFE filter to remove the white solid byproduct. Further purification by flash column chromatography ( $\text{SiO}_2$ , 40-90% ethyl acetate in hexanes) furnished the desired product as a pale-yellow oil (230 mg, 90%).  $R_f = 0.3$  (60% EtOAc/hexanes); IR (film) 3407, 2873, 1373, 1113  $\text{cm}^{-1}$ ;  $^1\text{H}$  NMR (400 MHz,  $\text{CDCl}_3$ )  $\delta$  4.76 (br s, 3H), 3.97-3.91 (m, 1H), 3.65 (dd,  $J = 11.2, 3.5$  Hz, 1H), 3.58 (dd,  $J = 11.2, 6.7$  Hz, 1H), 3.46-3.38 (m, 2H), 3.36 (dd,  $J = 9.9, 4.8$  Hz, 1H), 3.31 (dd,  $J = 9.9, 6.2$  Hz, 1H), 1.09 (t,  $J = 7.0$ , 3H);  $^{13}\text{C}$  NMR (600 MHz,  $\text{CDCl}_3$ ) ppm 76.5, 71.5, 69.4, 66.7, 14.9.

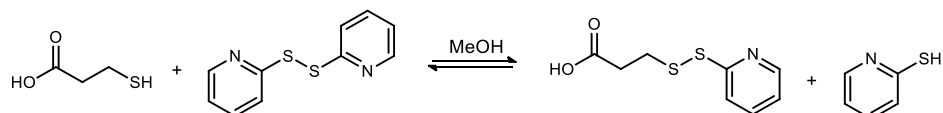
### Synthesis of 3-Ethoxy-2-hydroxypropyl Pent-4-enoate.



To a flame dried 25 mL round bottom flask equipped with a stir bar and argon balloon was added 3-ethoxy-1,2-propanediol (1.00 g, 8.3 mmol) and pyridine (670  $\mu\text{L}$ , 8.3 mmol). The reaction

mixture was stirred at rt for 10 min then cooled to 0 °C. 4-Pentenoyl chloride (900  $\mu$ L, 8.3 mmol) was added dropwise to the reaction. The reaction was allowed to warm up to rt and stirred for 12 hrs. Reaction was then diluted with dichloromethane (2 mL) and washed with 1M HCl, dried and concentrated. Purification by flash column chromatography furnished the desired product as a pale-yellow oil (870 mg, 52%).  $R_f$  = 0.6 (60% EtOAc/hexanes); IR (film) 3407, 2873, 1373, 1113  $\text{cm}^{-1}$ ;  $^1\text{H}$  NMR (400 MHz,  $\text{CDCl}_3$ )  $\delta$  5.78 (dddd,  $J$  = 16.7, 10.2, 6.4, 6.4 Hz, 1H), 5.02 (dddd,  $J$  = 17.2, 1.6, 1.6, 1.6 Hz, 1H), 4.96 (dddd,  $J$  = 10.3, 1.4, 1.4, 1.4 Hz, 1H), 4.14 (dd,  $J$  = 11.5, 4.5 Hz, 1H), 4.08 (dd,  $J$  = 11.5, 6.1 Hz, 1H), 3.96 (dddd,  $J$  = 6.2, 6.2, 4.4, 4.4 Hz, 1H), 3.51 (dd,  $J$  = 7.0, 1.4 Hz, 1H), 3.47 (dd,  $J$  = 7.1, 1.3 Hz, 1H), 3.45 (dd,  $J$  = 9.7, 4.3 Hz, 1H), 3.39 (dd,  $J$  = 9.6, 6.2 Hz, 1H), 2.43-2.31 (m, 4H), 1.17 (t,  $J$  = 7.0 Hz, 3H).  $^{13}\text{C}$  NMR (600 MHz,  $\text{CDCl}_3$ ) ppm 173.1, 136.4, 115.5, 71.2, 68.6, 66.8, 65.5, 33.3, 28.7, 14.9.

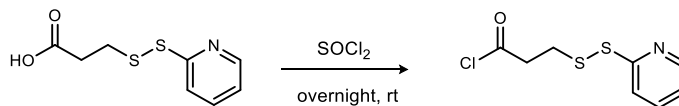
### Synthesis of 3-(2-Pyridinyldisulfanyl)propanoic Acid



To a solution of 3-mercaptopropionic acid (1.22g, 11.5 mmol) in methanol (10mL) was added aldrithiol-2 (3.78 g, 17.25 mmol). The mixture was stirred at room temperature for 3 hrs. The solvent was evaporated and the residue was purified by flash chromatography on silica gel with 30% ethyl acetate in hexanes to give the title compound as a yellow solid (2.44g, 98%).  $^1\text{H}$  NMR (400 MHz,  $\text{CDCl}_3$ )  $\delta$  2.80 (t,  $J$  = 6.8 Hz, 2H), 3.07 (t,  $J$  = 6.8 Hz, 2H), 7.16 (ddd,  $J$  = 7.8, 5.2, 1.6 Hz, 1H), 7.64 (dd,  $J$  = 7.8, 1.6 Hz, 1H), 7.67 (dt,  $J$  = 7.8, 1.6 Hz, 1H), 8.48 (dd,  $J$  = 5.2, 1.6 Hz, 1H).

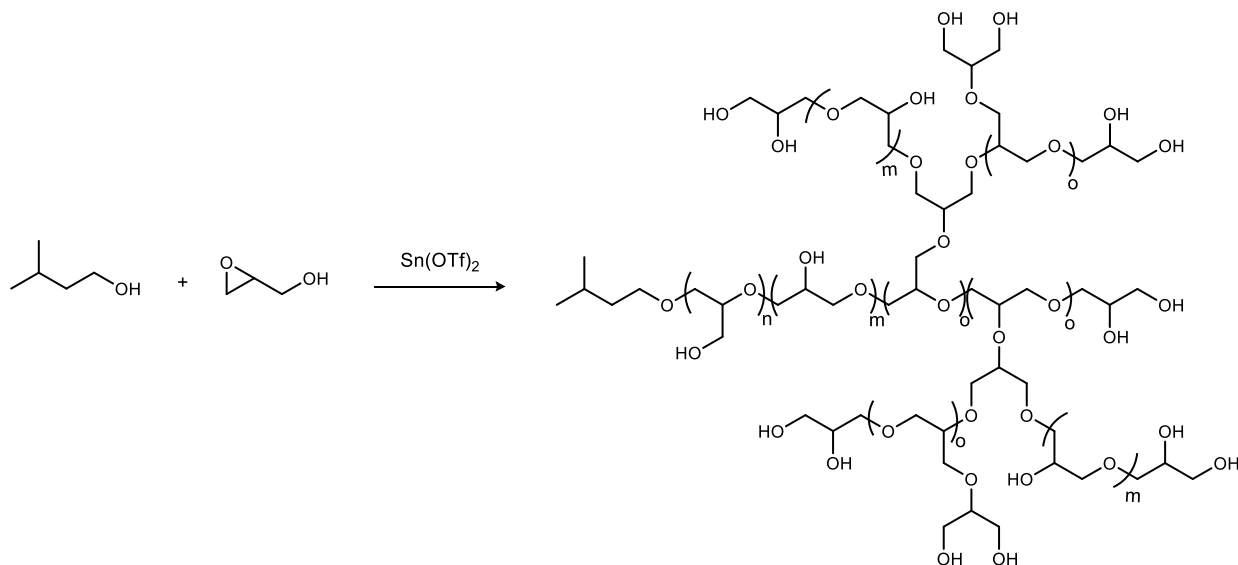


### Synthesis of 3-(pyridin-2-yl)disulfanylpropanoyl chloride



To a flame dried 25 mL round bottom flask equipped with a stir bar and argon balloon was added 3-(2-pyridinyl)disulfanylpropanoic acid (2.00 g, 9.28 mmol) and thionyl chloride (10 mL, 138 mmol). The reaction mixture was stirred at rt for 5 hrs. The bright yellow solution was evaporated under reduced pressure to give a yellow solid. No further purification was desired. <sup>1</sup>H NMR (400 MHz, CDCl<sub>3</sub>) δ 5.78 (dddd, *J* = 16.7, 10.2, 6.4, 6.4 Hz, 1H), 5.02 (dddd, *J* = 17.2, 1.6, 1.6, 1.6 Hz, 1H), 4.96 (dddd, *J* = 10.3, 1.4, 1.4, 1.4 Hz, 1H), 4.14 (dd, *J* = 11.5, 4.5 Hz, 1H), 4.08 (dd, *J* = 11.5, 6.1 Hz, 1H), 3.96 (dddd, *J* = 6.2, 6.2, 4.4, 4.4 Hz, 1H), 3.51 (dd, *J* = 7.0, 1.4 Hz, 1H), 3.47 (dd, *J* = 7.1, 1.3 Hz, 1H), 3.45 (dd, *J* = 9.7, 4.3 Hz, 1H), 3.39 (dd, *J* = 9.6, 6.2 Hz, 1H), 2.43-2.31 (m, 4H), 1.17 (t, *J* = 7.0 Hz, 3H). <sup>13</sup>C NMR (600 MHz, CDCl<sub>3</sub>) ppm 173.1, 136.4, 115.5, 71.2, 68.6, 66.8, 65.5, 33.3, 28.7, 14.9.

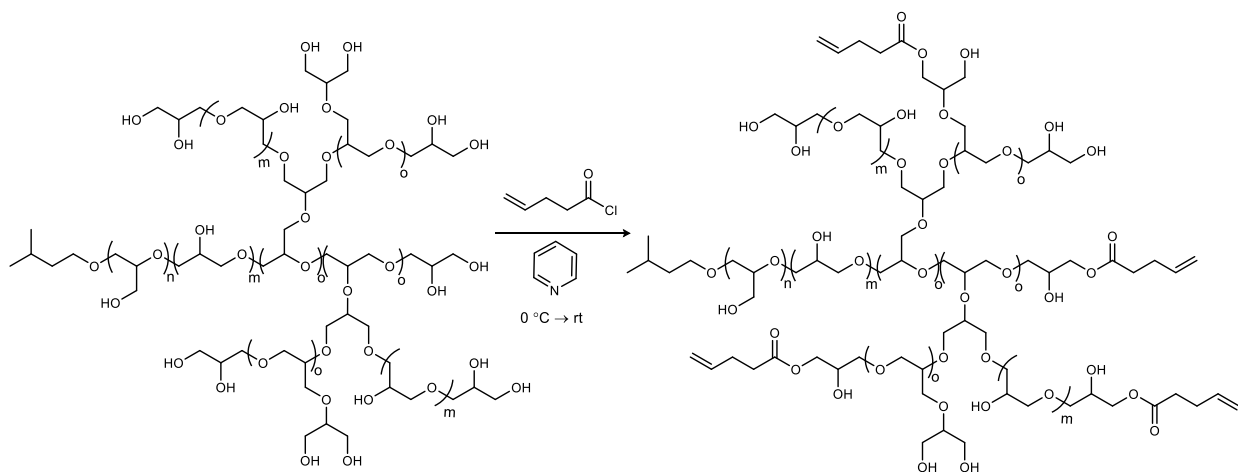
## Synthesis of branched poly(glycidol) homopolymer



To a 50 mL jacketed three-neck round bottom flask fitted with an argon balloon was added isoamyl alcohol (441  $\mu\text{L}$ , 4.05 mmol) and tin (II) trifluoromethanesulfonate (42.0 mg, 0.101 mmol). The mixture was stirred for ten minutes using a mechanical stirrer to form a homogeneous suspension. The jacketed flask was connected to a chiller and cooled to 5  $^{\circ}\text{C}$ . Glycidol (13.5 mL, 202.5 mmol) was added via syringe pump (0.7 mL/hr) and the mixture was stirred for 24 hrs at which time stirring was no longer possible due to the viscosity of the reaction mixture. Methanol (15 mL) was added to the reaction to dissolve the polymer and sodium bicarbonate solution (5 mL of a 1 mg/mL) was added. The reaction was filtered (if necessary) and precipitated twice in acetone to isolate the polymer. Further purification by dialysis with Spectra/Por dialysis membrane (MWCO = 1000 Da) in water was performed if needed to furnish the desired polymer **PGly-15** in 80% yield. IR (film) 3390, 1263, 1115  $\text{cm}^{-1}$ .  $^1\text{H}$  NMR (600 MHz,  $(\text{CD}_3)_3\text{SO}$ )  $\delta$  4.73-4.45 (br m, 1H, -**O****H**), 3.69-3.25 (br m, 5H, PGly-scaffold), 1.63 (sept,  $J = 6.5$  Hz, 1H), 1.37 (q,  $J = 6.5$  Hz, 2H), 0.85 (d,  $J = 6.7$  Hz, 6H).  $^{13}\text{C}$  NMR (600 MHz,  $(\text{CD}_3)_3\text{SO}$ ) ppm 82.3-81.6 (-**C****H**( $\text{CH}_2\text{OH}$ ) $_2$ ), 80.3-79.4 (-**C****H**( $\text{CH}_2\text{OH}$ ) $\text{OCH}_2$ -), 78.5-77.3 (-**C****H**( $\text{CH}_2\text{O}$ -) $\text{OCH}_2$ -), 73.2 (2C, -**C****H** $_2$ **CH**(**OH**)**C****H** $_2$ -),

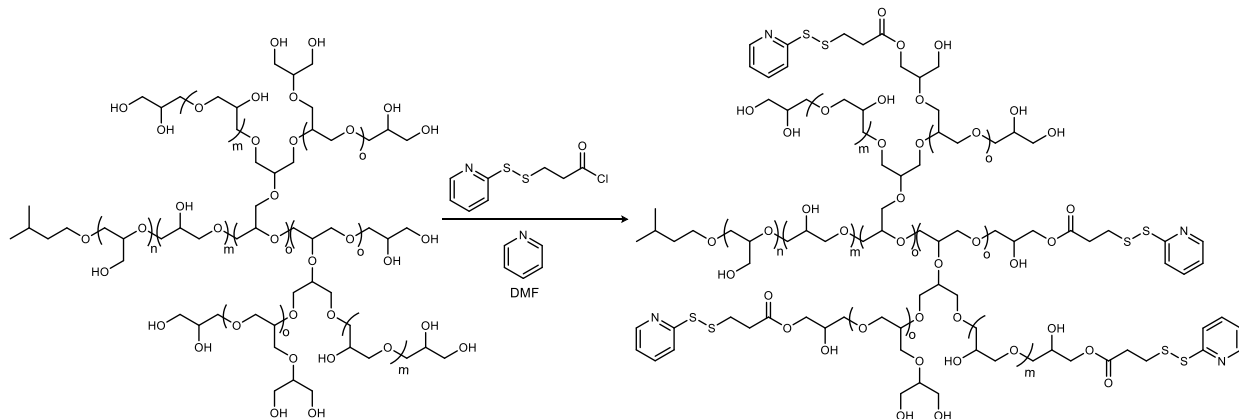
71.9-70.9 (4C,  $-\underline{\text{C}}\text{H}_2\text{CH}(\text{OCH}_2-)\underline{\text{C}}\text{H}_2\text{O}-$ ,  $-\underline{\text{C}}\text{H}_2\underline{\text{C}}\text{H}(\text{OH})\text{CH}_2\text{OH}$ ), 69.5 ( $-\text{O}\underline{\text{C}}\text{H}_2\text{CH}(\text{OCH}_2-)\text{CH}_2\text{OH}$ ), 69.2 ( $-\text{CH}_2\underline{\text{C}}\text{H}(\text{OH})\text{CH}_2-$ ), 63.5 ( $-\text{CH}_2\text{CH}(\text{OH})\underline{\text{C}}\text{H}_2\text{OH}$ ), 62.0-61.8 (2C,  $-\text{CH}(\underline{\text{C}}\text{H}_2\text{OH})_2$ ), 61.4-61.2 ( $-\text{CH}(\underline{\text{C}}\text{H}_2\text{OH})\text{OCH}_2-$ ), 39.5, 25.9, 23.0.

### Synthesis of 4-Pentenyl Poly(glycidol)

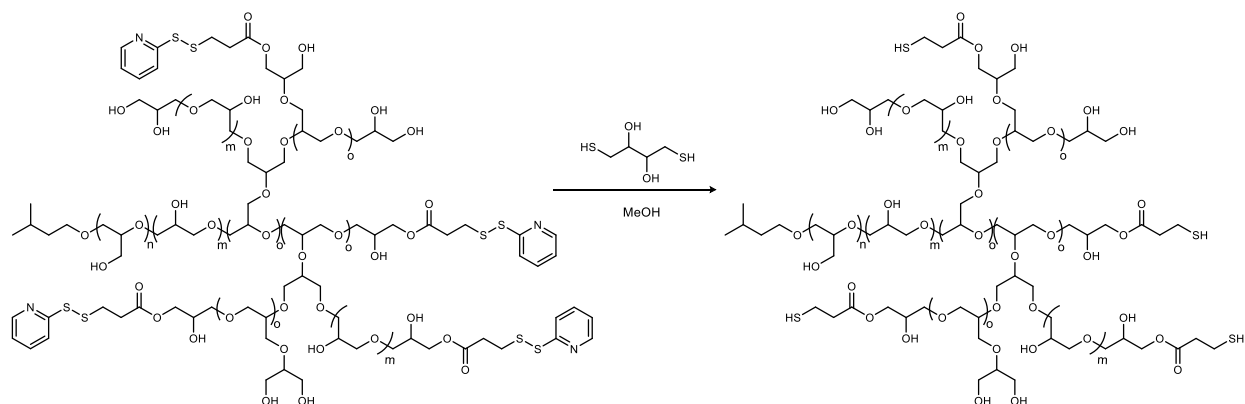


To a flame dried 25 mL round bottom flask equipped with a stir bar and argon balloon was added poly(glycidol) (1 g) and pyridine (2 mL, 25 mmol). The reaction mixture was stirred at rt for 10 min then cooled to 0 °C. Pentenoyl chloride (607  $\mu\text{L}$ , 5.50 mmol) was added dropwise to the reaction. The reaction was allowed to warm up to rt and stirred for 12 hrs. Reaction was then diluted with *N,N*-dimethylformamide (2 mL) and precipitated in a mixture of diethyl ether and ethyl acetate (1:1) to give the desired product as a pale-yellow oil (520 mg, 52%).  $^1\text{H}$  NMR (400 MHz,  $\text{CD}_3\text{OD}$ )  $\delta$  6.07-5.70 (br m,  $\text{CH}_2=\underline{\text{C}}\text{H}-$ ), 5.21-5.01 (br m,  $\underline{\text{C}}\text{H}_2=\text{CH}-$ ), 4.96-4.50 (br s,  $-\text{OH}$ ), 4.40-4.03 (br m,  $-\text{CH}\underline{\text{C}}\text{H}_2\text{OC}(\text{O})\text{CH}_2-$ ), 4.02-3.86 (br m,  $-\text{CH}\underline{\text{C}}\text{H}_2\text{OH}$ ), 3.82-3.22 (br m,  $-\text{OCH}\underline{\text{C}}\text{H}_2\text{CHO}-$ ), 2.60-2.23 (br m,  $-\text{C}(\text{O})\underline{\text{C}}\text{H}_2\underline{\text{C}}\text{H}_2\text{CH}=\text{CH}_2$ ), 1.71-1.66 (br m,  $(\text{CH}_3)_2\underline{\text{C}}\text{H}-$ ), 1.50-1.39 (br m,  $(\text{CH}_3)_2\text{CH}\underline{\text{C}}\text{H}_2-$ ), 0.95-0.81 (br m,  $(\underline{\text{C}}\text{H}_3)_2\text{CH}-$ ).  $^{13}\text{C}$  NMR (600 MHz,  $\text{CD}_3\text{OD}$ ) ppm 173.2, 136.8, 115.2, 80.5-60.4 (PG-scaffold), 38.2, 33.1, 28.6, 24.8, 22.2.

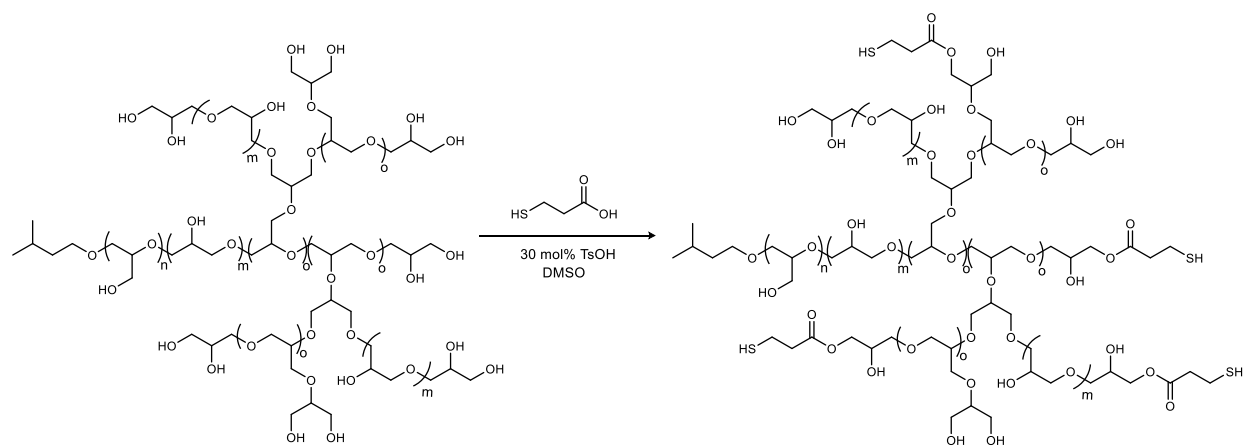
## Synthesis of 3-Mercaptopropanoyl Poly(glycidol)



To a flame dried 25 mL round bottom flask equipped with a stir bar and argon balloon was added polyglycidol (1 g), pyridine (2 mL, 25 mmol) and *N,N*-dimethylformamide (5 mL). The reaction mixture was stirred at rt for 10 mins then cooled to 0 °C. Crude 3-(pyridin-2-yl)disulfanylpropanoyl chloride (1.00 g, 4.28 mmol) in *N,N*-dimethylformamide (2 mL) was added dropwise to the reaction. The reaction was allowed to warm up to rt and stirred for 12 hrs. Reaction was then diluted with *N,N*-dimethylformamide (8 mL) and precipitated in a mixture of diethyl ether and ethyl acetate (1:1) to give 1.4 mg of pale yellow crude viscous polymer. Further purification by dialysis with Spectra/Por dialysis membrane (MWCO = 1000 Da) in methanol furnished 800 mg of the desired product. <sup>1</sup>H NMR (400 MHz, CD<sub>3</sub>OD) δ 8.43 (br s, 1H), 7.84 (br s, 4H), 7.26 (br s, 1H), 4.77 (br s, -OH), 4.40-4.05 (br m, -CHCH<sub>2</sub>OC(O)CH<sub>2</sub>-), 4.01-3.40 (br m, -CHCH<sub>2</sub>OH), 3.17 (br s, -C(O)CH<sub>2</sub>CH<sub>2</sub>S-), 2.81 (br s, -C(O)CH<sub>2</sub>CH<sub>2</sub>S-), 1.78-1.66 (br m, (CH<sub>3</sub>)<sub>2</sub>CH-), 1.52-1.42 (br m, (CH<sub>3</sub>)<sub>2</sub>CHCH<sub>2</sub>-), 0.98-0.87 (br m, (CH<sub>3</sub>)<sub>2</sub>CH-). <sup>13</sup>C NMR (600 MHz, CD<sub>3</sub>OD) ppm 172.6, 160.6, 150.4, 139.1, 122.4, 121.02, 82.8-61.3 (PG-scaffold), 39.3, 34.4, 32.7, 25.8, 23.0.

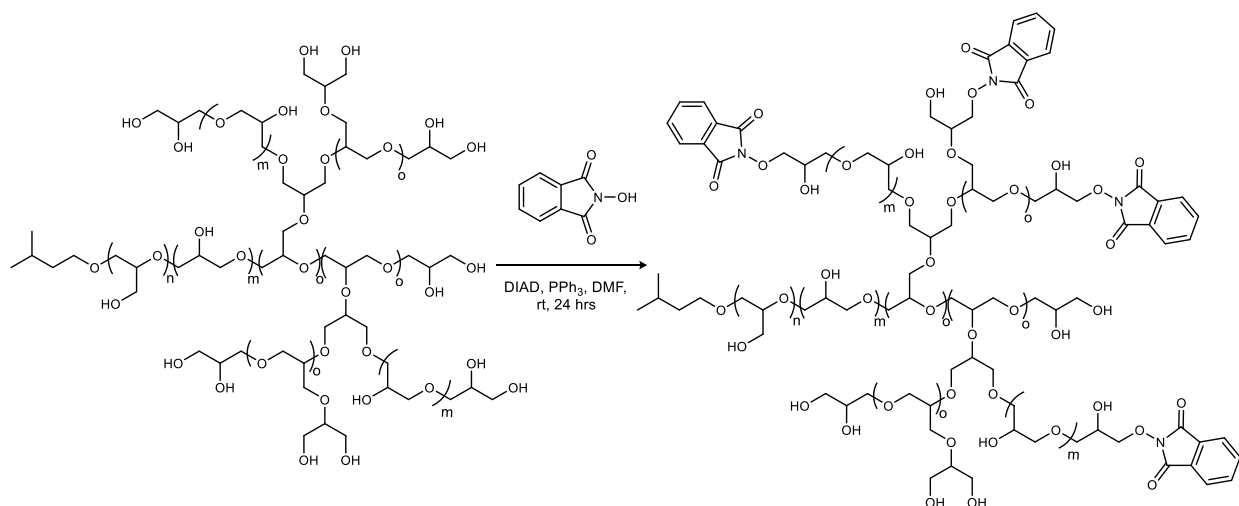


To a 25 mL round bottom flask, flame dried and equipped with a stir bar and argon balloon, was added a solution of poly(glycidol) 3-(pyridin-2-yl disulfanyl)propanoyl derivative (800 mg) in methanol (10 mL), and DL-dithiothreitol (30 mg, 0.19 mmol). The mixture was stirred at rt for 24 hrs. The crude product was further purified by dialysis with Spectra/Por dialysis membrane (MWCO = 1000 Da) in methanol to furnish 350 mg of the desired product.  $^1\text{H}$  NMR (400 MHz,  $\text{CD}_3\text{OD}$ )  $\delta$  4.93 (br s,  $-\text{OH}$ ), 4.46-4.08 (br m,  $-\text{CHCH}_2\text{OC}(\text{O})\text{CH}_2-$ ), 4.01-3.81 (br m,  $-\text{CHCH}_2\text{OH}$ ), 3.85-3.41 (br m,  $-\text{OCHCH}_2\text{CHO}-$ ), 2.81-2.63 (br m,  $-\text{C}(\text{O})\text{CH}_2\text{CH}_2\text{SH}$ ), 1.78-1.66 (br m,  $(\text{CH}_3)_2\text{CH}-$ ), 1.52-1.42 (br m,  $(\text{CH}_3)_2\text{CHCH}_2-$ ), 0.98-0.87 (br m,  $(\text{CH}_3)_2\text{CH}-$ ).  $^{13}\text{C}$  NMR (600 MHz,  $\text{CD}_3\text{OD}$ ) ppm 172.2, 171.8, 81.5-60.4 (PG-scaffold), 38.4, 33.4, 32.7, 24.8, 21.7.



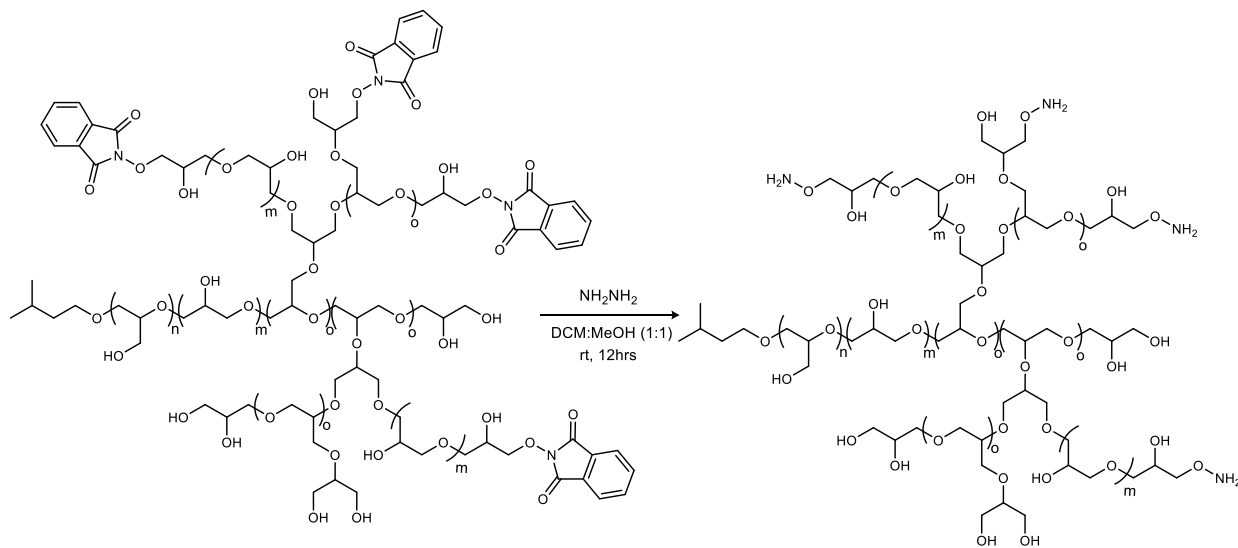
To a 25 mL round bottom flask, flame dried and equipped with a stir bar and argon balloon, was added a solution of polyglycidol (1 g) in dimethyl sulfoxide (1 mL), 3-mercaptopropionic acid (1.4 mL, 16.6 mmol), and *p*-toluenesulfonic acid (34 mg, 0.2 mmol). The mixture was stirred at 100 °C for 24 hrs. The mixture was diluted with *N,N*-dimethylformamide (2 mL), and precipitated in ether. Further purification by dialysis with Spectra/Por dialysis membrane (MWCO = 1000 Da) in methanol furnished 200 mg of the desired polymer.  $^1\text{H}$  NMR (400 MHz,  $\text{CD}_3\text{OD}$ )  $\delta$  4.93 (br s, -OH), 4.46-4.08 (br m, -CHCH<sub>2</sub>OC(O)CH<sub>2</sub>-), 4.01-3.81 (br m, -CHCH<sub>2</sub>OH), 3.85-3.41 (br m, -OCHCH<sub>2</sub>CHO-), 2.81-2.63 (br m, -C(O)CH<sub>2</sub>CH<sub>2</sub>SH), 1.78-1.66 (br m, (CH<sub>3</sub>)<sub>2</sub>CH-), 1.52-1.42 (br m, (CH<sub>3</sub>)<sub>2</sub>CHCH<sub>2</sub>-), 0.98-0.87 (br m, (CH<sub>3</sub>)<sub>2</sub>CH-).  $^{13}\text{C}$  NMR (600 MHz,  $\text{CD}_3\text{OD}$ ) ppm 172.2, 171.8, 81.5-60.4 (PG-scaffold), 38.4, 33.4, 32.7, 24.8, 21.7.

## Synthesis of *N*-oxyphthalimide poly(glycidol) derivative (P(G<sup>NOP</sup>-*co*-G)) (**1a**).



To a 100 mL round bottom flask fitted with an argon balloon and containing a solution of poly(glycidol) (PGly-5, 1.7 g, 1.17 mmol) in DMF (20 mL) was added *N*-hydroxyphthalimide (0.954 g, 5.85 mmol) followed by triphenylphosphine (1.53 g, 5.85 mmol) at rt. Diisopropyl azodicarboxylate (1.15 mL, 5.85 mmol) was then added dropwise at 0 °C. The resulting mixture was allowed to warm up to rt and stirred for 24 hrs. The reaction was concentrated under reduced pressure and precipitated twice in ether:ethyl acetate (1:1) to obtain 1.9 g of the desired polymer **1a** as an off-white amorphous solid. IR (film) 3455, 3061, 2919, 1789, 1730, 1373, 1127, 731 cm<sup>-1</sup>. <sup>1</sup>H NMR (600 MHz, (CD<sub>3</sub>)<sub>3</sub>SO) δ 7.74-7.48 (br m, 4H), 4.86 (br s, 1H, OH), 4.50-3.31 (br m, 5H, PG-scaffold), 1.76-1.66 (m, 1H), 1.47 (q, *J* = 7.1, 2H), 0.92 (d, *J* = 7.1, 6H); <sup>13</sup>C NMR (600 MHz, (CD<sub>3</sub>)<sub>3</sub>SO) ppm 162.8, 134.7, 128.0, 123.4, 79.2, 77.8, 76.6, 74.9, 72.1, 71.4, 71.5-68.0 (br overlapping), 67.3, 65.2, 63.1, 61.2, 38.1, 24.7, 21.8.

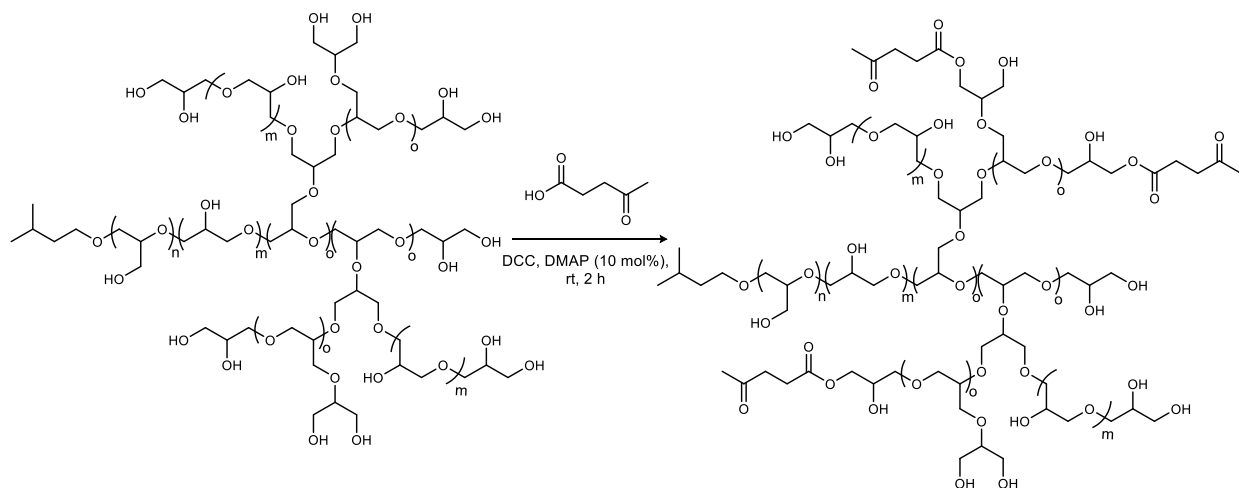
## Synthesis of Aminoxy Poly(glycidol) Derivative



To a 100 mL round bottom flask equipped with a stir bar and an argon balloon was added *N*-oxyphthalimide poly(glycidol) **1a** (1.0 g). Methanol (25 mL) followed by an excess of anhydrous hydrazine (4.5 mL, 140 mmol) was added and the reaction was allowed to stir for 12 hrs at rt. The reaction mixture was filtered through 0.45  $\mu\text{m}$  PTFE filter to remove the white solid byproduct and allowed to stir for an additional 6 hrs at rt. All volatile components were removed under rotary evaporation. The residue was suspended in methanol and filtered a second time. The filtrate was transferred to a dialysis tubing (MWCO = 1000 Da), and was dialyzed against water for 36 hrs. After dialysis, the product was concentrated to furnish 690 mg of the desired polymer. IR (film) 3407, 2873, 1373, 1113  $\text{cm}^{-1}$ .  $^1\text{H}$  NMR (600 MHz,  $(\text{CD}_3)_3\text{SO}$ )  $\delta$  4.86 (br s, 1H,  $\text{OH}$ ), 4.50-3.31 (br m, 5H, PG-scaffold), 1.76-1.66 (m, 1H), 1.47 (q,  $J = 7.1$ , 2H), 0.92 (d,  $J = 7.1$ , 6H).  $^{13}\text{C}$  NMR (600 MHz,  $(\text{CD}_3)_3\text{SO}$ ) ppm 79.9, 79.4, 78.6, 77.7, 74.7, 72.6, 72.0, 71.9-70.4 (br overlapping peaks), 70.0-68.8 (br, overlapping peaks), 66.2, 63.0, 61.9, 61.3, 38.1, 24.7, 21.8.



## Synthesis of 4-Oxopentanoyl Poly(glycidol) Derivative



To a 100 mL round bottom flask fitted with an argon balloon and containing a solution of polyglycidol (2.5 g, 0.66 mmol) in DMF (30 mL) was added levulinic acid (2.8 g, 23.8 mmol) followed by dimethyl aminopyridine (290 mg, 2.38 mmol) at rt. Dicyclohexylcarbodiimide (4.9 g, 23.8 mmol) was then added to the reaction and the resulting mixture was allowed to stir for 24 hrs. The reaction was filtered to remove the white precipitate followed by dialysis in deionized water to obtain 3.5 g of the desired polymer.  $^1\text{H}$  NMR (600 MHz,  $(\text{CD}_3)_3\text{SO}$ )  $\delta$  4.86 (br s, 1H, OH), 4.50-3.31 (br m, 5H, PG-scaffold), 2.49 (br s, 2H), 2.26 (br s, 2H), 1.88 (s, 3H), 1.42 (br s, 1H), 1.16 (br s, 2H), 0.64 (br s, 6H);  $^{13}\text{C}$  NMR (600 MHz,  $(\text{CD}_3)_3\text{SO}$ ) ppm 207.3, 172.5, 79.2, 77.8, 76.6, 74.9, 72.1, 71.4, 71.5-68.0 (br overlapping), 67.3, 65.2, 63.1, 61.2, 38.1, 37.8, 30.0, 28.1, 24.7, 21.8.

## REFERENCES

1. Hawker, C. J.; Wooley, K. L., The Convergence of Synthetic Organic and Polymer Chemistries. *Science* **2005**, *309* (5738), 1200-1205.
2. Coessens, V.; Pintauer, T.; Matyjaszewski, K., Functional polymers by atom transfer radical polymerization. *Progress in Polymer Science* **2001**, *26* (3), 337-377.
3. Liu, J.; Li, R. C.; Sand, G. J.; Bulmus, V.; Davis, T. P.; Maynard, H. D., Keto-Functionalized Polymer Scaffolds as Versatile Precursors to Polymer Side-Chain Conjugates. *Macromolecules* **2013**, *46* (1), 8-14.
4. Theato, P.; Klok, H.-A., *Functional polymers by post-polymerization modification: concepts, guidelines and applications*. John Wiley & Sons: 2013.
5. Spears, B. R.; Waksal, J.; McQuade, C.; Lanier, L.; Harth, E., Controlled branching of polyglycidol and formation of protein-glycidol bioconjugates via a graft-from approach with "PEG-like" arms. *Chemical Communications* **2013**, *49* (24), 2394-2396.
6. Magnusson, J. P.; Bersani, S.; Salmaso, S.; Alexander, C.; Caliceti, P., In Situ Growth of Side-Chain PEG Polymers from Functionalized Human Growth Hormone—A New Technique for Preparation of Enhanced Protein–Polymer Conjugates. *Bioconjugate Chemistry* **2010**, *21* (4), 671-678.
7. Gao, W.; Liu, W.; Christensen, T.; Zalutsky, M. R.; Chilkoti, A., In situ growth of a PEG-like polymer from the C terminus of an intein fusion protein improves pharmacokinetics and tumor accumulation. *Proceedings of the National Academy of Sciences* **2010**, *107* (38), 16432-16437.
8. Türk, H.; Haag, R.; Alban, S., Dendritic Polyglycerol Sulfates as New Heparin Analogues and Potent Inhibitors of the Complement System. *Bioconjugate Chemistry* **2004**, *15* (1), 162-167.
9. Stiriba, S.-E.; Kautz, H.; Frey, H., Hyperbranched Molecular Nanocapsules: Comparison of the Hyperbranched Architecture with the Perfect Linear Analogue. *Journal of the American Chemical Society* **2002**, *124* (33), 9698-9699.
10. Kohler, J.; Keul, H.; Moller, M., Post-polymerization functionalization of linear polyglycidol with diethyl vinylphosphonate. *Chemical Communications (Cambridge, United Kingdom)* **2011**, *47* (28), 8148-8150.
11. Frey, H.; Haag, R., Dendritic polyglycerol: a new versatile biocompatible material. *Reviews in Molecular Biotechnology* **2002**, *90* (3), 257-267.
12. Haag, R.; Sunder, A.; Hebel, A.; Roller, S., Dendritic Aliphatic Polyethers as High-Loading Soluble Supports for Carbonyl Compounds and Parallel Membrane Separation Techniques. *Journal of Combinatorial Chemistry* **2002**, *4* (2), 112-119.

13. Sunder, A.; Türk, H.; Haag, R.; Frey, H., Copolymers of Glycidol and Glycidyl Ethers: Design of Branched Polyether Polyols by Combination of Latent Cyclic AB<sub>2</sub> and ABR Monomers. *Macromolecules* **2000**, *33* (21), 7682-7692.
14. Sunder, A.; Mulhaupt, R.; Haag, R.; Frey, H., Hyperbranched polyether polyols: A modular approach to complex polymer architectures. *Advanced Materials* **2000**, *12* (3), 235-241.
15. Burgath, A.; Sunder, A.; Neuner, I.; Mülhaupt, R.; Frey, H., Multi-arm star block copolymers based on  $\epsilon$ -caprolactone with hyperbranched polyglycerol core. *Macromolecular Chemistry and Physics* **2000**, *201* (7), 792-797.
16. Hattori, Y.; Nagaoka, Y.; Kubo, M.; Yamasaku, H.; Ishii, Y.; Okita, H.; Nakano, H.; Uesato, S.; Maitani, Y., Antitumor Effect of Liposomal Histone Deacetylase Inhibitor-Lipid Conjugates in Vitro. *Chemical & Pharmaceutical Bulletin* **2011**, *59* (11), 1386-1392.
17. Isaacs, N. S., *Physical organic chemistry*. Longman Scientific & Technical; Wiley & Sons: 1995.
18. Rashidian, M.; Mahmoodi, M. M.; Shah, R.; Dozier, J. K.; Wagner, C. R.; Distefano, M. D., A Highly Efficient Catalyst for Oxime Ligation and Hydrazone-Oxime Exchange Suitable for Bioconjugation. *Bioconjugate Chemistry* **2013**, *24* (3), 333-342.
19. Stukel, J. M.; Li, R. C.; Maynard, H. D.; Caplan, M. R., Two-Step Synthesis of Multivalent Cancer-Targeting Constructs. *Biomacromolecules* **2010**, *11* (1), 160-167.
20. Lee, S. C.; Parthasarathy, R.; Botwin, K.; Kunneman, D.; Rowold, E.; Lange, G.; Klover, J.; Abegg, A.; Zobel, J.; Beck, T.; Miller, T.; Hood, W.; Monahan, J.; McKearn, J. P.; Jansson, R.; Voliva, C. F., Biochemical and Immunological Properties of Cytokines Conjugated to Dendritic Polymers. *Biomedical Microdevices* **2004**, *6* (3), 191-202.
21. Szabo, I.; Manea, M.; Orban, E.; Csampai, A.; Bosze, S.; Szabo, R.; Tejada, M.; Gaal, D.; Kapuvari, B.; Przybylski, M.; Hudecz, F.; Mezo, G., Development of an oxime bond containing daunorubicin-gonadotropin-releasing hormone-III conjugate as a potential anticancer drug. *Bioconjugate Chemistry* **2009**, *20* (4), 656-665.
22. Davis, B. G., Synthesis of Glycoproteins. *Chemical Reviews* **2002**, *102* (2), 579-602.
23. Carrasco, M. R.; Nguyen, M. J.; Burnell, D. R.; MacLaren, M. D.; Hengel, S. M., Synthesis of neoglycopeptides by chemoselective reaction of carbohydrates with peptides containing a novel N'-methyl-aminooxy amino acid. *Tetrahedron Letters* **2002**, *43* (33), 5727-5729.
24. Rodriguez, E. C.; Winans, K. A.; King, D. S.; Bertozzi, C. R., A strategy for the chemoselective synthesis of O-linked glycopeptides with native sugar-peptide linkages. *Journal of the American Chemical Society* **1997**, *119* (41), 9905-9906.
25. Houdier, S.; Perrier, S.; Defrancq, E.; Legrand, M., A new fluorescent probe for sensitive detection of carbonyl compounds: sensitivity improvement and application to environmental water samples. *Analytica Chimica Acta* **2000**, *412* (1-2), 221-233.

26. Lin, F.; Yu, J.; Tang, W.; Zheng, J.; Defante, A.; Guo, K.; Wesdemiotis, C.; Becker, M. L., Peptide-Functionalized Oxime Hydrogels with Tunable Mechanical Properties and Gelation Behavior. *Biomacromolecules* **2013**, *14* (10), 3749-3758.
27. Grover, G. N.; Lam, J.; Nguyen, T. H.; Segura, T.; Maynard, H. D., Biocompatible Hydrogels by Oxime Click Chemistry. *Biomacromolecules* **2012**, *13* (10), 3013-3017.
28. Heredia, K. L.; Tolstyka, Z. P.; Maynard, H. D., *Macromolecules* **2007**, *40*, 4772.
29. Mukherjee, S.; Hill, M. R.; Sumerlin, B. S., Self-healing hydrogels containing reversible oxime crosslinks. *Soft Matter* **2015**, *11* (30), 6152-6161.
30. Khomutov, M. A.; Mandal, S.; Weisell, J.; Saxena, N.; Simonian, A. R.; Vepsalainen, J.; Madhubala, R.; Kochetkov, S. N., Novel convenient synthesis of biologically active esters of hydroxylamine. *Amino Acids* **2010**, *38* (2), 509-17.
31. Dufour, E.; Moni, L.; Bonnat, L.; Chierici, S.; Garcia, J., 'Clickable' 2,5-diketopiperazines as scaffolds for ligation of biomolecules: their use in A beta inhibitor assembly. *Organic & Biomolecular Chemistry* **2014**, *12* (27), 4964-4974.
32. Mezo, G.; Szabo, I.; Kertesz, I.; Hegedus, R.; Orban, E.; Leurs, U.; Bosze, S.; Halmos, G.; Manea, M., Efficient synthesis of an (aminoxyl) acetylated-somatostatin derivative using (aminoxyl)acetic acid as a 'carbonyl capture' reagent. *Journal of Peptide Science* **2011**, *17* (1), 39-46.
33. Du, C.; Guan, Q.; Gao, S.; Chafeeva, I.; Brooks, D.; Ngan, C.; Kizhakkedathu, J., A Novel Hyperbranched Polyglycerol-Based Solution for Donor Organ Preservation: A Comparison With University of Wisconsin Solution in Hypothermic Preservation of Mouse Donor Hearts. *Transplantation* **2014**, *98*, 369-369.
34. El Accaoui, R. N.; Gould, S. T.; Hajj, G. P.; Chu, Y.; Davis, M. K.; Kraft, D. C.; Lund, D. D.; Brooks, R. M.; Doshi, H.; Zimmerman, K. A.; Kutschke, W.; Anseth, K. S.; Heistad, D. D.; Weiss, R. M., Aortic valve sclerosis in mice deficient in endothelial nitric oxide synthase. *American Journal of Physiology-Heart and Circulatory Physiology* **2014**, *306* (9), H1302-H1313.
35. Gao, S. H.; Guan, Q. N.; Chafeeva, I.; Brooks, D. E.; Ngan, C. Y. C.; Kizhakkedathu, J. N.; Du, C. G., Hyperbranched Polyglycerol as a Colloid in Cold Organ Preservation Solutions. *PLOS ONE* **2015**, *10* (2), 1-22.
36. Kainthan, R. K.; Gnanamani, M.; Ganguli, M.; Ghosh, T.; Brooks, D. E.; Maiti, S.; Kizhakkedathu, J. N., Blood compatibility of novel water soluble hyperbranched polyglycerol-based multivalent cationic polymers and their interaction with DNA. *Biomaterials* **2006**, *27* (31), 5377-5390.
37. Kainthan, R. K.; Janzen, J.; Kizhakkedathu, J. N.; Devine, D. V.; Brooks, D. E., Hydrophobically derivatized hyperbranched polyglycerol as a human serum albumin substitute. *Biomaterials* **2008**, *29* (11), 1693-1704.

38. Kainthan, R. K.; Janzen, J.; Levin, E.; Devine, D. V.; Brooks, D. E., Biocompatibility Testing of Branched and Linear Polyglycidol. *Biomacromolecules* **2006**, *7* (3), 703-709.
39. Li, S. D.; Bin, L.; Guan, Q. N.; Chafeeva, I.; Brooks, D. E.; Nguan, C. Y. C.; Kizhakkedathu, J. N.; Du, C. G., Cold preservation with hyperbranched polyglycerol-based solution improves kidney functional recovery with less injury at reperfusion in rats. *American Journal of Translational Research* **2017**, *9* (2), 429-441.
40. Li, S. D.; Constantinescu, I.; Guan, Q. N.; Kalathottukaren, M. T.; Brooks, D. E.; Nguan, C. Y. C.; Kizhakkedathu, J. N.; Du, C. G., Advantages of replacing hydroxyethyl starch in University of Wisconsin solution with hyperbranched polyglycerol for cold kidney perfusion. *Journal of Surgical Research* **2016**, *205* (1), 59-69.
41. Liu, Z. H.; Janzen, J.; Brooks, D. E., Adsorption of amphiphilic hyperbranched polyglycerol derivatives onto human red blood cells. *Biomaterials* **2010**, *31* (12), 3364-3373.
42. Nimmo, C. M.; Brooks, P. J., Process for Implementing, Structuring, and Evaluating Pharmacy Practice Residency Experiences. *American Journal of Hospital Pharmacy* **1992**, *49* (9), 2166-2174.
43. Wen, J. Y.; Weinhart, M.; Lai, B.; Kizhakkedathu, J.; Brooks, D. E., Reversible hemostatic properties of sulfobetaine/quaternary ammonium modified hyperbranched polyglycerol. *Biomaterials* **2016**, *86*, 42-55.

## CHAPTER IV

### SYNTHESIS AND CHARACTERIZATION OF NOVEL POLY(GLYCIDOL) HYDROGELS

#### INTRODUCTION

Hydrogels are three-dimensional crosslinked polymeric networks capable of holding water or biological fluids within the spaces available between polymer chains.<sup>1-2</sup> Their ability to absorb water is attributed to the presence of hydrophilic functional groups, such as hydroxyls, carboxylic acids, sulfonic acids, amines and amides, while their resistance to dissolution arises from physical and chemical crosslinks between network polymer chains. The greater the number of hydrophilic groups, the greater the water holding capacity of the hydrogel. However, an increase in the number of crosslinks tends to decrease the hydrophilicity and elasticity of the polymeric network. Their ability to swell and retain water enables them to have a degree of flexibility similar to natural tissues. Many natural and synthetic material fit the definition of a hydrogel. Hydrogels have received considerable attention over the past 50 years due to their many diverse potential applications in material science and medicine.<sup>3-8</sup>

The first reported use of hydrogel for biomedical application dates back to the 1960s when Wichterle and coworkers<sup>9</sup> developed crosslinked poly(hydroxymethyl methacrylate) hydrogels for biological uses. Since then a huge number of efforts and studies has been devoted to advancing and extending the potential attributed to hydrogels. In addition to synthetic polymers, natural polymers have also been used for the development of hydrogels. For example, Lim and others<sup>10</sup> demonstrated the successful application of calcium alginate microcapsules for cell encapsulation. Hydrogels prepared from natural polymer has advantageous properties such as inherent

biocompatibility, biodegradability and biologically recognizable moieties that support cellular activities.<sup>11-15</sup> However, these types of hydrogel may contain pathogens or evoke immune/inflammatory responses. Additionally, they lack batch to batch consistency and tuning properties. The well-defined structure of synthetic polymers may lead to hydrogels with well-defined and fine-tunable degradation kinetic as well as mechanical properties.

Hydrogels may be categorized into two groups based on the chemical or physical nature to the cross-linkage between polymeric chains.<sup>2</sup> Chemically crosslink networks results from the formation of covalent bonds between polymer chains. Physically crosslinked networks result from physical interaction, such as molecular entanglement, ionic interaction and hydrogen bonding, between polymer chains. Hydrogels can also be characterized as conventional or stimuli responsive. Conventional hydrogels do not change their equilibrium swelling in response to stimuli such as pH, temperature, electric field etc., while stimuli responsive hydrogel response to change in its environment brought on by an external stimuli.<sup>16-20</sup> Other properties such as the nature of the polymer side groups, mechanical and structural features, methods of preparation (homo or copolymer), and physical structure (amorphous, semicrystalline or crystalline) are also used to classify hydrogel.<sup>21</sup> The ability of hydrogel to imbibe water is key in determining the overall characteristic of any hydrogel. Hydrogels made from hydrophilic polymers typically have a high water content in their structures while hydrogels made form hydrophobic polymers have low water content in their structures.

Due to the development of an ever-increasing spectrum of functional polymers, innovative hydrogel technologies have emerged, and has advanced many fields including regenerative medicine and drug delivery. In regenerative medicine, hydrogels are used as matrices for repairing and regenerating a wide variety of tissue and organs. For example, Hydrogels has been used for

the regeneration of damage nerves. Injury to any part of the central nervous system (CNS) tends to be permanent due to its limited capacity for repair or regeneration.<sup>22</sup> This is because CNS injury results in cell death, glial scar formation, and pseudocyst formation at the lesion site and this restrict nerve regeneration. In spinal cord injury repair, the hydrogel acts as a scaffold to bridge the gap between lesion sites and deliver nerve growth factors and other therapeutic agents can change the environment at the lesion site and promote nerve regeneration.<sup>23-24</sup>

The use of synthetic polymers in the development of polymeric scaffolds or hydrogel for regenerative medicine application is necessary, if the material is to possess properties similar to the native tissues it is intended to help regenerate. As a result, research is ongoing to create novel polymers that will produce hydrogels with a variety of properties. For example, for the repair or regeneration of tissues that are typically subjected to load such as cartilage, the hydrogel has to possess adequate mechanical properties to offer mechanical support and stimulate regeneration. to this end, a variety of polyethylene glycol hydrogels have been developed for use in cartilage tissue engineering.

Scaffolds for the regeneration of cartilage typically consist of poly(ethylene glycol) (PEG) derivatives. PEG-based hydrogels have been found to possess a biocompatible 3-D network that is sufficiently similar to that of native cartilage.<sup>25-26</sup> These PEG hydrogels typically consist of covalently bonded PEG chains formed from different functional linear PEG precursors. Some PEG hydrogels have been synthesized by photopolymerization of PEG precursors modified with acrylate or methacrylates groups in the presence of photoinitiators.<sup>27</sup> These photo initiators fragment to form free radicals in the presence of UV light. The alkene group of the acrylate functionalized polymer reacts with the free radicals to initiate polymerization and form a hydrogel



network. When immersed in water, these gels are capable of swelling to various degrees based on the strength of the retractile forces arising from chemical crosslinking.

Other PEG hydrogels have been fabricated for different regenerative medicine and drug delivery applications, through the use of a variety of novel crosslinking reactions known as “click chemistry”.<sup>28</sup> The term click chemistry was first introduced by Sharpless and co-workers, and defines a set of nearly perfect reactions that resemble natural biochemical ligations.<sup>29</sup> The most commonly employed reaction are the reactions of thiols with activated disulfides, maleimides, acrylates, alkynes, and vinyl sulfones.<sup>30</sup> In addition to these Michael addition reaction, the thiol-ene click has been utilized by reacting thiolated PEG, with alkene and acrylate functionalized crosslinkers in the presence of a photoinitiator.<sup>31</sup> The copper-catalyzed Huisgen cycloaddition has also been employed in the synthesis of PEG hydrogels.<sup>32</sup> The copper free azide-alkyne Click reactions has been used as an alternative for the copper catalyzed variant of this reaction.<sup>33</sup>

While the thiol chemistry has been extensively use for hydrogel synthesis, it is sensitive to oxygen, resulting in disulfides. Additionally, the native cystine residue on many proteins can compete and result in undesired protein conjugation and immobilization within the hydrogel network. To circumvent this issue a novel oxime click reaction has emerged as a biorthogonal alternative thiol based click chemistries.<sup>34</sup> Oxime Click chemistry is the reaction between an aminoxy group and an aldehyde or ketone. The reaction has been shown to be fast, orthogonal to biological functionalities, produces water as a biproduct, and requires no catalyst or external stimuli. Additionally, the aminoxy, aldehyde and ketone functionalities have increased stability in aqueous solvent compared to thiols. The oxime click reaction has been used to synthesized PEG hydrogel which were demonstrated to possess the unique able to support cell encapsulation and

proliferation through the incorporation of attachment promoting peptide, conjugated to the polymer network via an oxime bond.<sup>34</sup>

Branched poly(glycidol) (*b*PG) (typically called poly(glycerol) by the Germans) is a viable alternative to PEG for the synthesis of diverse hydrogel networks. The branched nature of *b*PG and to presence to multiple hydroxyl groups along the backbone of the polymer make this polyether polyol more versatile than its PEG counterpart. PEG possess only two hydroxy groups per polymer which limits its applications in hydrogel with low polymer concentration but high strength. Poly(glycidol) hydrogel has been synthesized by the use of difunctionalized boronic acids as crosslinkers. Already these hydrogels were shown to possess mechanical strength and elasticity not reported for PEG based systems.<sup>35-37</sup> Additionally poly(glycidol) hydrogels have been synthesized by ring-opening reaction of epichlorohydrin. This hydrogel showed a novel temperature-responsible swelling behavior which could be implemented into drug delivery systems.<sup>38</sup> Furthermore, disulfide crosslinked poly(glycerol) hydrogels were prepared by the ring-opening crosslinking polymerization of glycidol and PEG-based polyepoxides and disodium disulfide. Multivalent poly(glycerol) hydrogels were prepared by acid-catalyzed hydrolysis of remaining epoxide functionalities. These hydrogels were shown to be interesting scaffolds for bioactive substances, where drug release is triggered by the hydrogel degradation. Poly(glycidol) hydrogels had huge potential for applications in regenerative medicine due to its biocompatibility. Recently, an enzymatically crosslinked poly(glycidol) hydrogel was shown to be capable to encapsulating cells under gelation conditions.<sup>39</sup>

The use of click reactions in the formation of poly(glycidol) networks has been largely unexplored. It is envisioned that the formation of a poly(glycidol) hydrogel network by utilizing the novel oxime click chemistry would create a hydrogel with a unique set of properties.

Additionally, this hydrogel would be biocompatible and can be used for regenerative medicine and drug delivery applications.

## RESULTS AND DISCUSSION

The initial motivation for the synthesis of an oxime-hydrogel system came as a result of a previous study involving the delivery of the protein Bone Morphogenetic Protein 2 (BMP2). Harth and others<sup>40</sup> showed that pure uncrosslinked branched poly(glycidol) (*bPG*) could be used as a matrix for the local dual delivery of a polyester nanoparticle loaded with a hydrophobic small molecule and the growth factor BMP2 (Figure IV-1). The viscosity of the *bPG* polymer reduced the diffusion of the protein and increased its concentration at the delivery site. However, diffusion of the protein was still at a rapid rate and so a crosslinked *bPG* network was needed to have more reproducible control over the diffusion of BMP2 at the delivery site. For this purpose, water soluble aminoxy and ketone functionalized poly(glycidol) was synthesized and evaluated.

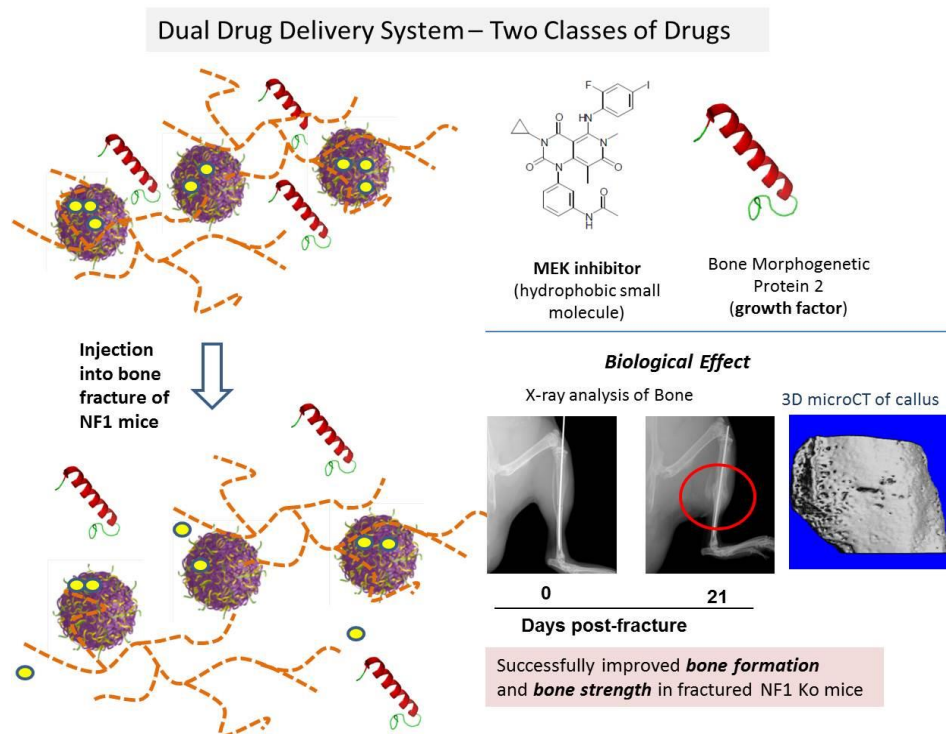


**Figure IV-1.** Dual drug delivery system. The MEK loaded nanosponges and the growth factor stabilized in the *bPG* “matrix” results in the only successful callus formation and bone strength of all treatment groups.

## Synthesis of Poly(glycidol) Hydrogels by Oxime Click Chemistry

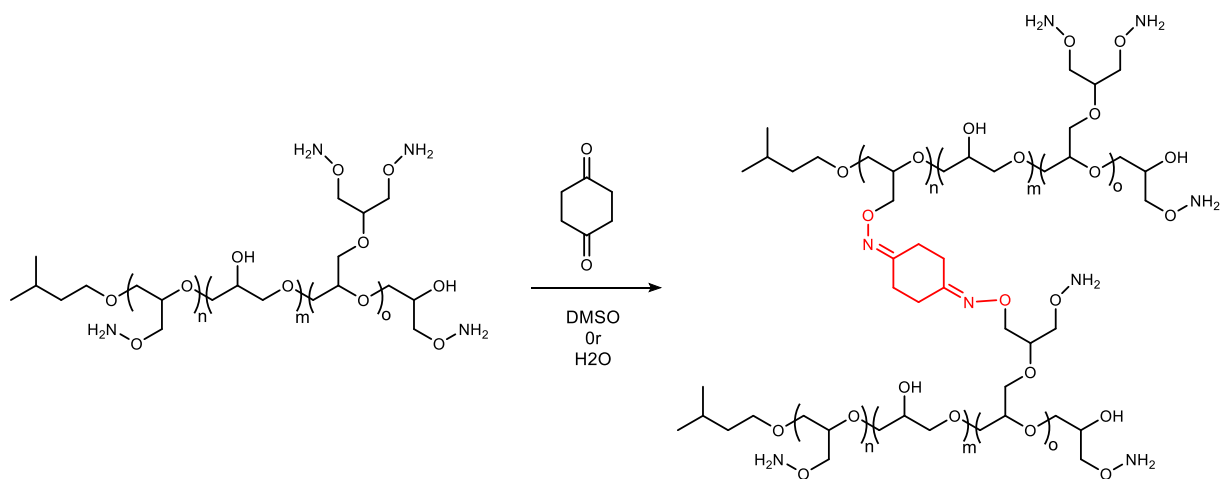
The reaction between an aminoxy group and an aldehyde or ketone is termed “oxime click”. The oxime click reaction has the advantages of been fast, orthogonal to many biological functionalities, works without a catalyst and produces water as a byproduct. Despite these advantages, oxime-click was only recently applied to the synthesis of eight-arm PEG hydrogel. We envision that the oxime-click chemistry can be used to crosslink branched poly(aminoxy glycidol) via a ketone group to form a biocompatible *bPG* hydrogel to be used for biomedical applications.

Branched poly(glycidol) (*bPG*) is a suitable scaffold material for the desired hydrogel due to its biocompatibility. *bPG* was synthesized by utilizing the cationic  $\text{Sn}(\text{OTf})_2$  mediated ring-opening polymerization (CROP) of glycidol as described in Chapter I. Polymers with an average molecular weight of 2000 Da and a molecular weight distribution of 1.4 was used for this study. By varying the ratio of N-hydroxysuccinimide to the average number of OH groups in *bPG*, degree of aminoxy functionalization of 20%, 30%, and 60% were obtained.

Initial studies began with the synthesis of a ketone functionalized polyester via the  $\text{Sn}(\text{OTf})_2$ -mediated ring-opening polymerization of  $\delta$ -valerolactone (VL) and 2-oxepane-1,5-dione (OPD). It was hypothesized that the OPD content of this polyester would make the polymer water soluble, while the ester functionality would make the result hydrogel hydrolytically and enzymatically degradable. OPD is not commercially available and was synthesized by the Bayer-villager oxidation of 1,4-cyclohexanedione. After synthesizing the VL-OPD copolymer, the water solubility was tested. Unfortunately, the polymer was insoluble. We increased the OPD content of the copolymer up to 40% and varied the length of the polymer in the range 1500-4000 Da, but still

the polyester copolymer was not water solubility. Attempts were made to synthesize an OPD homopolymer and perform a sodium borohydride reduction in methanol, however the polymer degraded under the reaction conditions. We then envision that a monomer with a free hydroxyl group could be created to replace VL in the copolymerization with OPD. However, attempts to synthesized such monomer was not successful. Nevertheless, the VL-OPD copolymer was indeed soluble in dimethyl sulfoxide(DMSO), and so the synthesis of *b*PG -polyester hybrid hydrogels in DMSO was explored in collaboration with another group member, Kelly Gilmore.

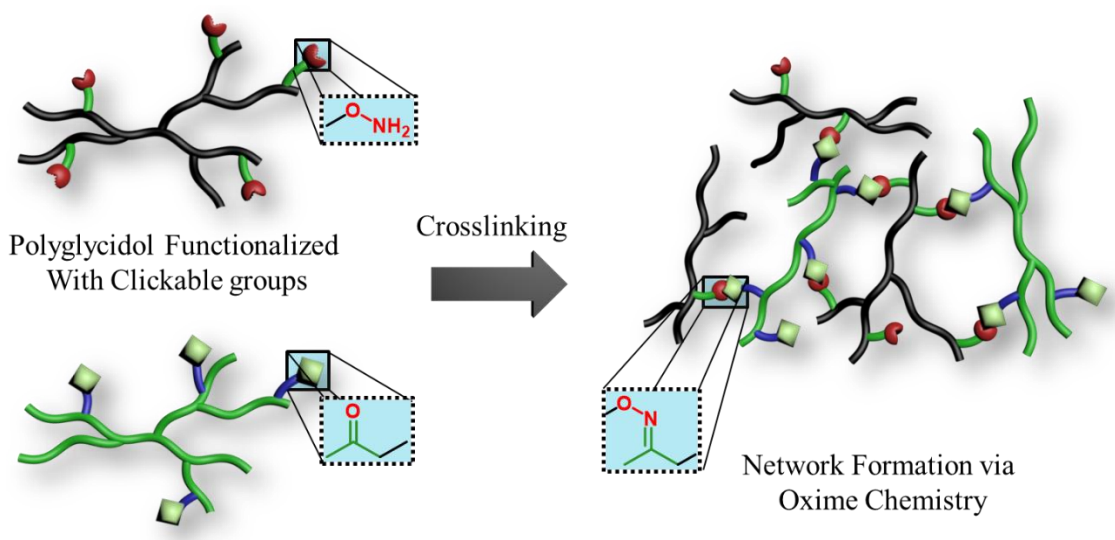
In light of the low water solubility of the proposed ketone functionalized polyester, the search for a water soluble crosslinker to pair with the aminoxy functionalized *b*PG continued. During the synthesis of OPD, it was discovered that the precursor 1,4-cyclohexanedione was soluble in water. Therefore, the synthesis of *b*PG hydrogels with the use of poly(aminoxy glycidol) (AO-*b*PG) that was previously synthesized and 1,4-cyclohexanedione as the diketone linker was explored (Scheme IV-1). Dimethyl sulfoxide and water was used as the gelation medium. Upon addition of a solution of the diketone linker to AO-PG hydrogel formation was observed. The gelation kinetic varied based on the solvent used as well as the pH. In dimethyl



**Scheme IV-1.** Reaction of aminoxy *b*PG with 1,4-cyclohexanedione to form hydrogels

sulfoxide (DMSO), hydrogel formation was observed within 15-20 minutes. When gelation was carried out in distilled water, hydrogel formation was immediately observed. The rapid gelation that occurred in water did not allow for a homogeneously crosslinked hydrogel. It was observed that some areas of the hydrogel had a higher crosslink density than other regions of the hydrogel. Gelation was also investigated in phosphate buffer at different pH. At pH 6, gelation again was instantaneous. Increasing the pH to 7.4 slowed the rate resulting in gel formation within 2 minutes. At a pH of 8, hydrogel formation was observed within 10 minutes. These results suggest that the rate of gelation can be controlled by the type of solvent used and the pH. The influence of pH on gelation kinetic is most likely due to the acid-catalyzed nature of oxime-bond formation.

Since the small molecule diketone linker did not allow for the formation of homogeneous hydrogel networks in an aqueous environment, in addition to its potential toxicity towards cells, an alternative approach was investigated. It was then proposed that the attachment of the ketone groups to biocompatible *bPG* would create a bioinert derivative with comparable structure to the



**Scheme IV-2.** Showing the combination of the aminoxy and the ketone derivative of branched *bPG* to form a network via Oxime Click chemistry.

aminoxy derivative which will allow for the formation of a more homogeneous hydrogel (Scheme IV-2). The synthesis of the ketone functionalized *b*PG was described in Chapter II.

In situ forming *b*PG hydrogels were prepared by simply mixing solutions containing the aminoxy and ketone functionalized polyglycidol. The two functionalized polymers were combined in a 1:1 mole ratio of ketone:aminoxy polymer precursors in phosphate buffered saline (PBS) solution at pH 7.4. The polymer content was kept at 25 wt. % and injected into silanized glass vials to prepare hydrogels for testing. The nomenclature for each hydrogel was determined by the degree of functionalization of the aminoxy and ketone functionalized *b*PG. For example, a 20% hydrogel is a hydrogel formed from the combination of a 20% aminoxy functionalized *b*PG with a 20% ketone functionalized *b*PG in a (1:1) mole ratio, while a 30/60% hydrogel was formed by combining a 30% aminoxy functionalized *b*PG with a 60% ketone functionalized *b*PG (Figure IV-2).

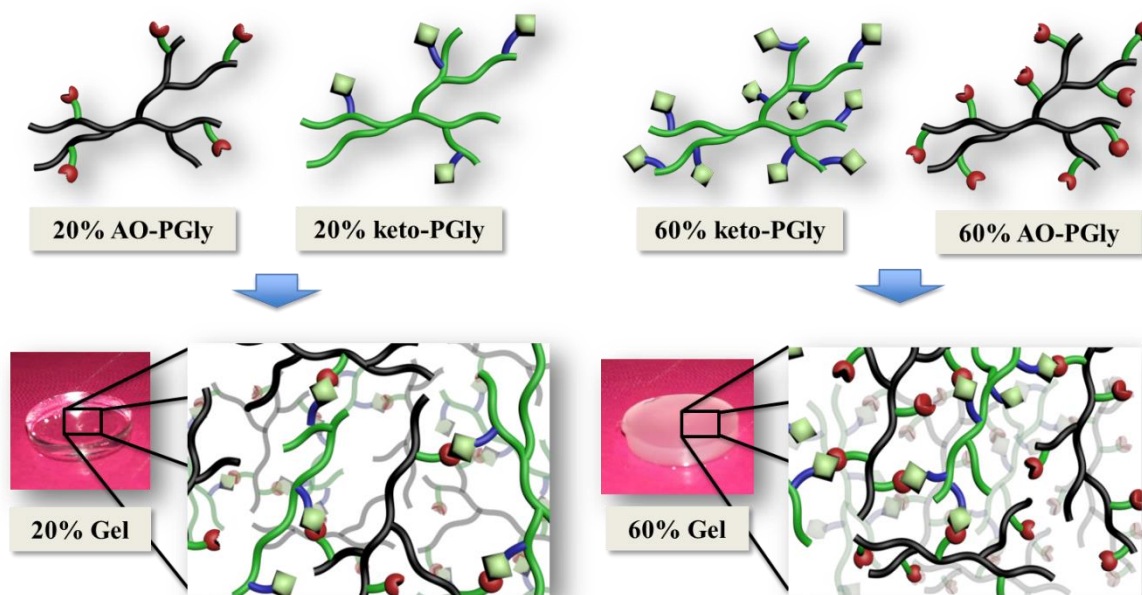


**Figure IV-2.** Formation of 20% and 60% *b*PG hydrogels showing changes in crosslinking density.



Four combinations (20%, 30%, 60% and 30/60%) of aminoxy and ketone functionalized *b*PG were investigated for their hydrogel formation and resultant properties. The rate of gelation was monitored by the vial tilt method<sup>41</sup> and by rheology. As determined by the vial tilt method, all hydrogels were formed within ten minutes of mixing. The gelation time for the 20%, 30% and 60% was 10 min, 2 min, and 30 seconds respectively. It was observed that all hydrogel network investigated show a 5 to 20 % shrinking in the diameter of the hydrogel approximately 1 hr after hydrogel formation. The branched nature of the *b*PG allow functional groups to be in close proximity to each other. Even though there is reduced mobility of the polymer chains upon gelation, additional mobility is due to the magnetic-like effect of reactive groups proximity. As each crosslink is established, it creates tension which cause the polymer chains to move and form new crosslinks.

The kinetics of the gelation was further examined by monitoring the evolution of storage modulus with time via rheometer (Figure IV-3). The results show that the degree of

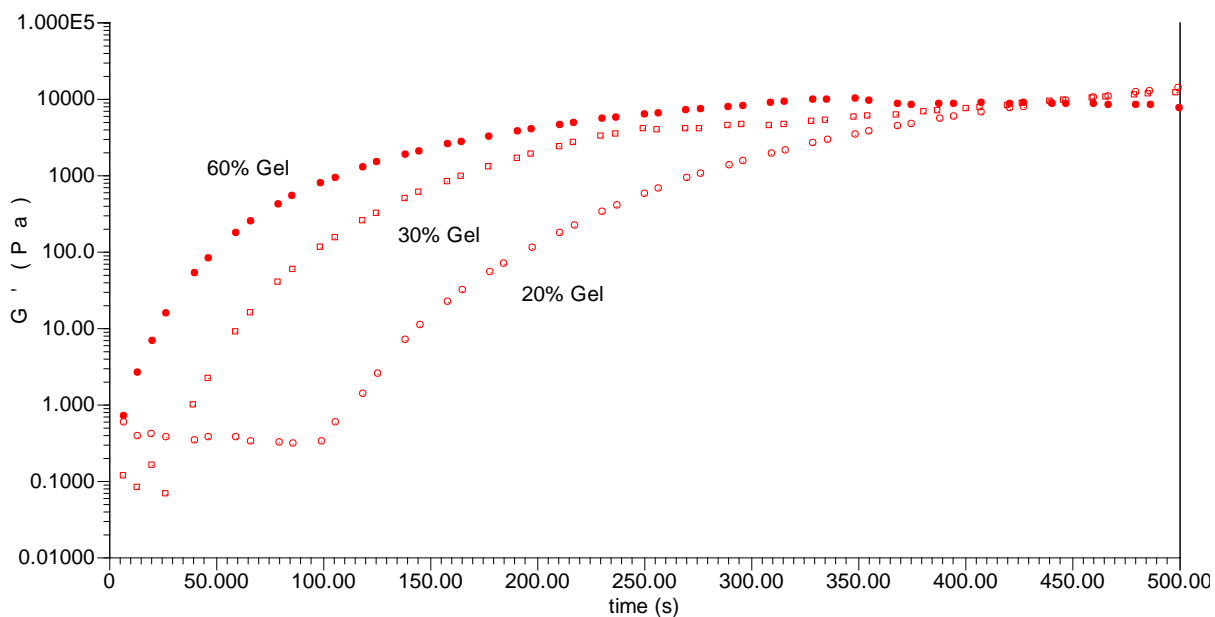


**Figure IV-3.** Showing the influence of degrees of functionalization of gelation kinetics at pH 7.4. Higher degree of functionalization increases the rate of gelation.

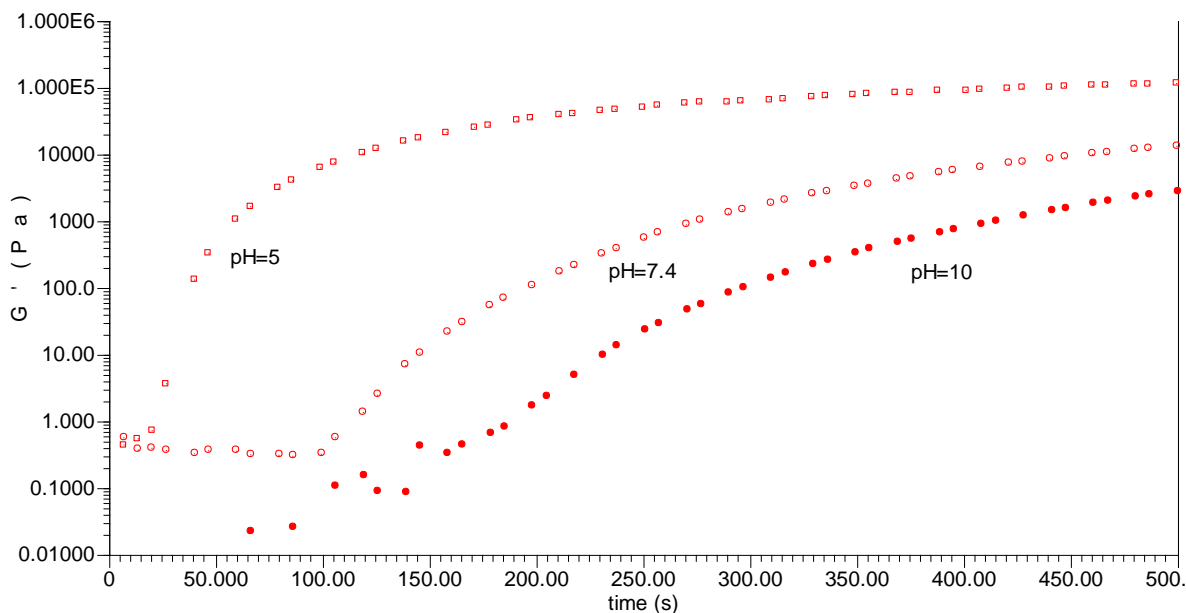


**Figure IV-4.** pH dependence of hydrogel gelation kinetics determined by rheometry.

functionalization strongly influences the gelation kinetics. The higher the degree of functionalization of the hydrogel precursors, the greater the reaction rate. The rate of reaction was also investigated by this method (Figure IV-4). The results indicate that the higher the pH of the buffer solution, the slower the reaction rate. This finding is important because it indicates that for the highly functionalized derivatives, the rate of hydrogel formation can be tailor to get different crosslinked materials.

Scanning electron microscopy was employed to study the morphology of the hydrogel network. The images suggest that the 20% and 30% hydrogels have a homogeneous and porous structure, while the 60% hydrogel has a rather heterogeneous structure with less pores. The observed differences could be attributed to the high degree of functionalization of the polymer precursors of the 60% hydrogel and the fast rate of gelation (Figure IV-5).

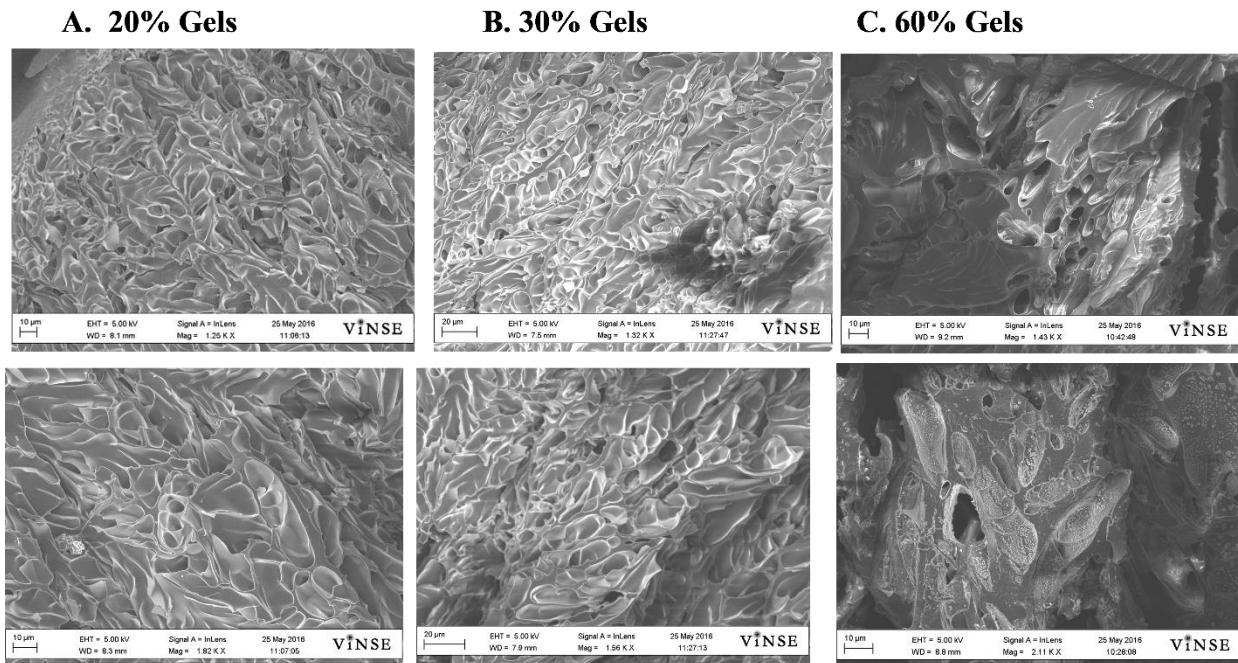


**Figure IV-5.** Scanning electron microscopy (SEM) images of various poly(glycidol) hydrogel formulations.

### Mechanical Studies of Poly(glycidol) Oxime Hydrogels

The relationship between network composition and the mechanical properties (elasticity and strength) of the poly(glycidol)-based hydrogels were evaluated by compression testing. The compressive modulus of the hydrogel can provide information on the impact of the structure of the material on the tightness and crosslinking density of the hydrogel network. The compressive modulus of the hydrogels was determined from the initial linear region of the stress-strain data. The first set of hydrogels were made from aminoxy and keto- functionalized polymers with degrees of functionalization of 20%, 30% and 60%. The hydrogels were found to be robust with fracture stress values in the range from 0.5–0.8 MPa and compression modulus values in the range 1.35–1.56 MPa (Figure IV-6). As the degrees of functionalization of the poly(glycidol) derivatives increased from 20% to 30%, the stiffness of the hydrogel network increased. This was indicated

by the increase in the compression modulus from 1.35 to 1.44 MPa. This trend continued when the degrees of functionalization was increased from 30% to 60%, as indicated by the change in the compression modulus from 1.45 to 1.57 MPa. The increase in the stiffness of the hydrogel network can be attributed to a decrease in the average molecular weight between the crosslinks. When the degree of functionalization was increased from 20% to 30%, there was an increase in the rate of gelation which resulted in reduced mobility of the polymer chains as the sol-gel transition occurred. This reduced mobility reduced the average number of potential crosslinking reaction per polymer which caused only a slight increase in stiffness of the 30% hydrogel compared to the 20% hydrogel. The increased stiffness can mainly be attributed to the increase in crosslinking density. This phenomenon was more pronounced when the degrees of functionalization was increased from 30% to 60%. At 60% functionalization, there is a significant number of functional groups that are available for crosslinking in a small volume. This results in an increase in the crosslinking density compared to the 20% and 30% hydrogels. The increase in functional group density also causes a significant decrease in the gelation time, with gelation occurring under 30 seconds. This create an inhomogeneous network which cause the network to fracture more easily than the 20% and 30% hydrogel. The range of poly(glycidol) hydrogel compression modulus covers much of the range of the mechanical properties of cartilaginous biological tissues, such as articular cartilage in the immature (0.1-0.3 MPa)<sup>42</sup> and mature state (0.19-2.1 MPa)<sup>42-46</sup> and also meniscus (0.38-0.49 MPa)<sup>47</sup> and intervertebral Disc (IVD) (0.38-1.01 MPa).<sup>48-50</sup>

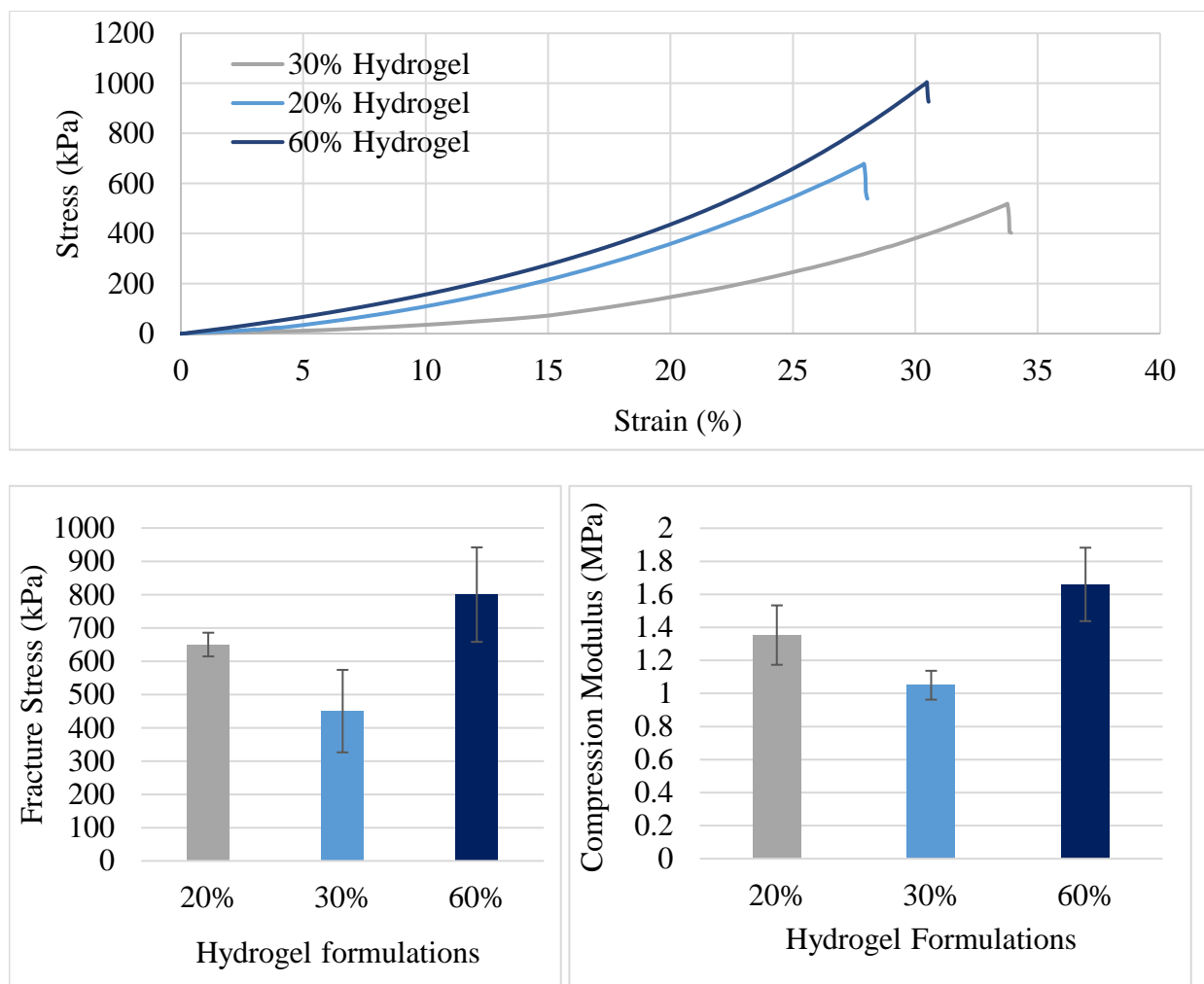


**Figure IV-6.** Stress/strain data for the poly(glycidol) oxime hydrogel formulations at pH 7.4.

The rate of ketoxime formation is influenced by pH. The reaction rate is rapid at low pH, and slow at high pH. By varying the pH of the buffer solution containing the functionalized poly(glycidol) hydrogel precursors, we were able to moderate the rate of gelation. The impact of reaction rate on the mechanical properties were explored with the poly(glycidol) hydrogels. To this end, 20%, 30% and 60% hydrogels were synthesized at pH 7.4 and 9 (Figure IV-7). For the 60% hydrogel network, As the pH of the precursor solutions increased from 7.4 to 9, the compression modulus of the 60% hydrogel increased from 1.56 to 2.00 MPa, while the compressive strength increase from 0.53 to 0.95 MPa. This increase in strength and stiffness is due

to the increase in the number of cross linkages formed as a result of the high functional group density and increased mobility of the polymer chains due to decreased gelation time. The decrease in gelation time is due to the reduced rate of formation of the oxime linkages due to the increase in pH.

The increased strength and stiffness observed for the 60% hydrogel network is opposite to that observed for the 20% and 30% hydrogel network. For the 30% hydrogel network, the compressive modulus decreased from 1.45 MPa at pH 7.4 to 0.86 MPa at pH 9, while the compressive strength decreased from 0.73 MPa at pH 7.4 to 0.52 MPa at pH 9. The compressive

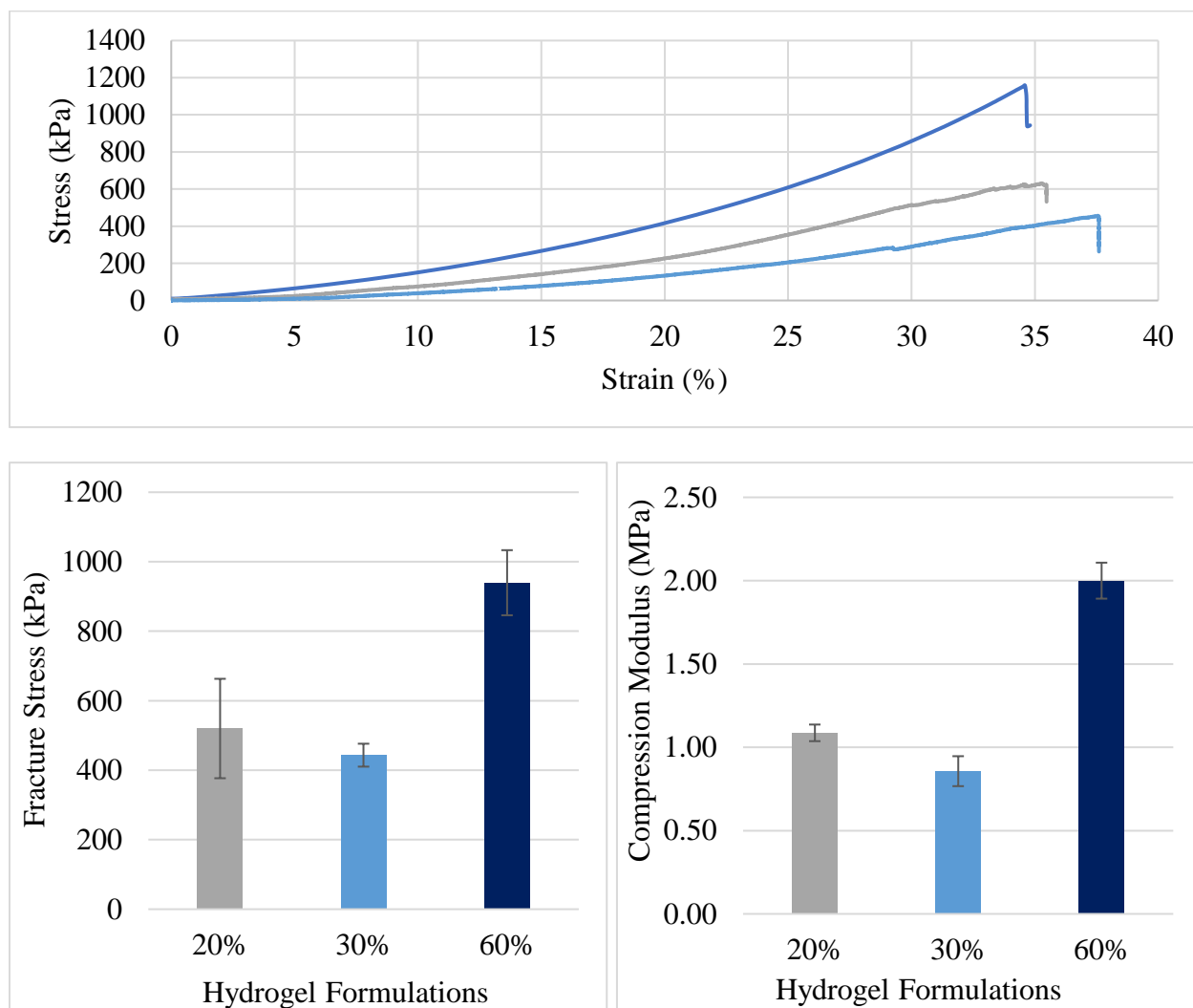


**Figure IV-7.** Stress/strain data for three poly(glycidol) oxime hydrogel formulations at pH 9.

modulus for the 30% hydrogel decreased from 1.35 MPa at pH 7.4 to 1.09 MPa at pH 9, while its compressive strength decreased from 0.73 MPa at pH 7.4 to 0.52 MPa at pH 9. This decrease could be due to the decrease in the rate of crosslinking coupled with the lower functional group density compared to the 60% hydrogel network. Therefore, changing the pH of the gelation buffer can provide access to hydrogels with a different range of mechanical strength and elasticity.

The ability of tailor the mechanical properties of the poly(glycidol) hydrogel by varying the ratio of [ketone]:[aminoxy] groups would add to the versatility of the poly(glycidol) oxime hydrogel network. The ratio of the [ketone]:[aminoxy] groups were then varied to evaluate their effect on the mechanical properties of the poly(glycidol) hydrogel network. 30% and 60% hydrogels were made using a ratio of [ketone]:[aminoxy] of 1:1 and 1:2. It was previously reported<sup>51</sup> that increasing the ratio of [ketone]:[aminoxy] from 1:1 to 1.5:1 had no effect on the mechanical strength of the reported hydrogel system formed from the oxime reaction. We therefore employed a ratio of [ketone]:[aminoxy] of 2:1 to see if we would observe an effect. For both the 30% and the 60% hydrogel system, a significant decreased in the compression modulus and strength was observed. These observations are consistent with a decrease in the crosslinking density. This decrease could be attributed to the excess keto-functionalized poly(glycidol) relative to the aminoxy derivative. In light of these results, a novel approach was devised. The ratio of [ketone]:[aminoxy] of 2:1 could be achieved by combining a 60% functionalized keto-poly(glycidol) with 30% functionalized aminoxy poly(glycidol) in a 1:1 ratio by mass. This way the amount of each polymer is the same while the ratio of [ketone]:[aminoxy] groups on the polymers is 2:1. The resulting material had significantly increased strength and stiffness (Figure IV-8) with values of 3.2 MPa for the compressive modulus and 1.8 MPa for the compressive

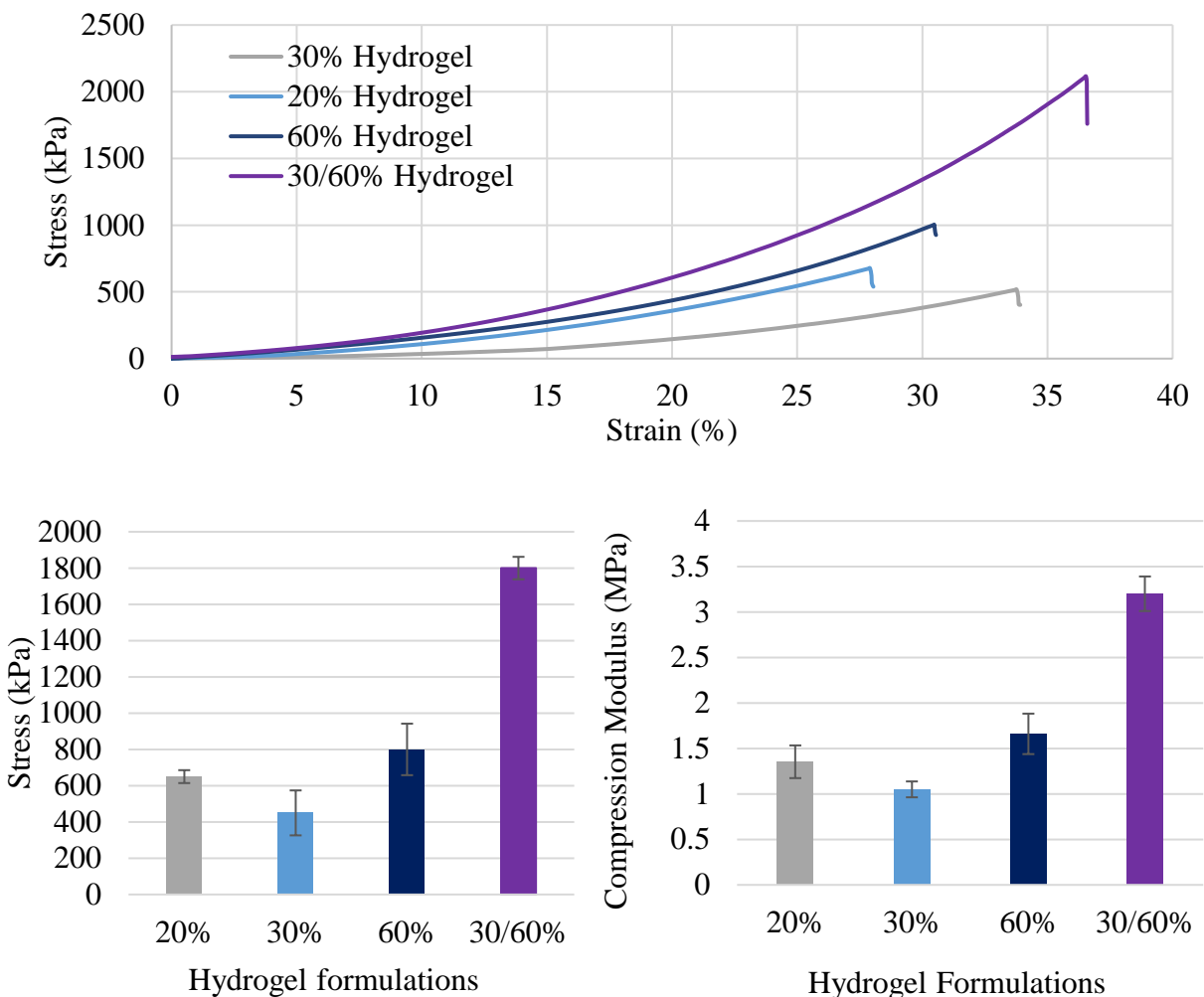


**Figure IV-8.** Stress/strain data for poly(glycidol) hydrogel showing comparison of 30/60% hydrogel with previous hydrogel formulations.

strength. This demonstrates the unique ability to tune the mechanical properties of poly(glycidol) hydrogels by mixing polymer derivatives with different degrees of functionalization.

For some applications such as 3-D cell cultures and protein delivery, it might be necessary to work with hydrogels with a polymer concentration of 10 wt.% or less. Hence, we were interested to see what effect would lowering the hydrogel precursor concentration have on mechanical properties of the poly(glycidol) network. To this end, hydrogels with precursor total polymer concentration of 10 wt.% were synthesized and evaluated. These hydrogels were significantly



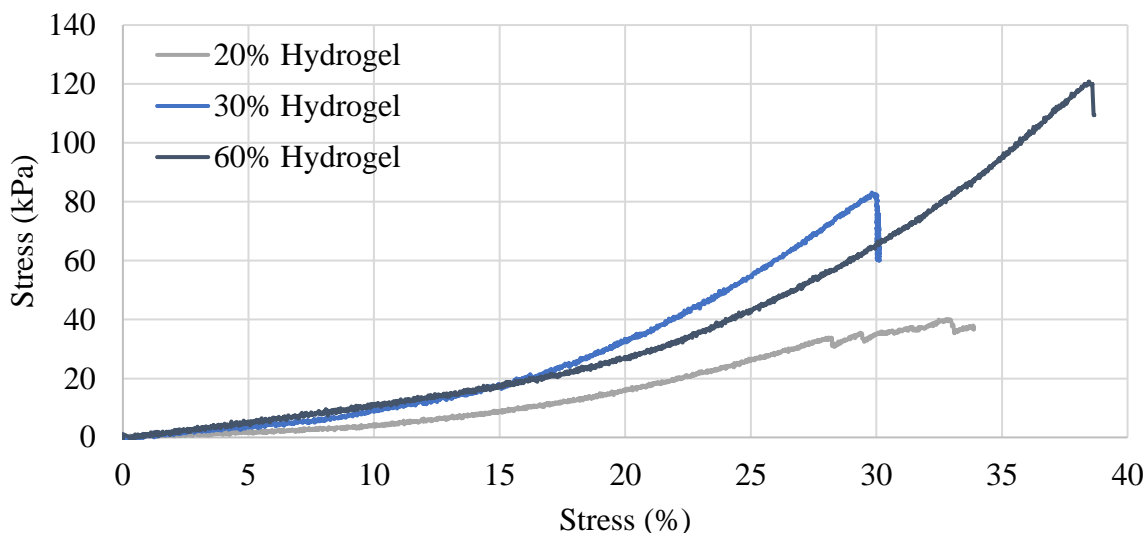


**Figure IV-9.** Stress/strain data for the 10 wt.% poly(glycidol) oxime hydrogel.

weaker compared to the 25 wt.% polymer (Figure IV-9). This is due to reduced functional group density resulting in a weaker network. However, the strain at fracture for these hydrogels were greater than the 25 wt.% hydrogel networks. This is probably due to the increase in molecular weight between the crosslinks, as the more dilute conditions reduces the number of crosslinks.

### **Tailoring and Optimizing the Elasticity and Strength of the Poly(glycidol) Hydrogel**

To increase the versatility of the poly(glycidol) hydrogel network, we seek to develop methods that would allow for tailoring of the hydrogel network to obtain materials with high strength and high elasticity. We have demonstrated that the poly(glycidol) hydrogel network has the potential for high strength and stiffness. However, for some application, hydrogels with low compressive modulus and high compressive strength are desired. To this end, methods to increase the elasticity of the poly(glycidol) oxime hydrogels were explored.

The elastic properties of a polymeric network can be improved by incorporating supramolecular structures capable of forming physical crosslinks through adsorption with the polymer network<sup>52-53</sup>. Recently, Leibler and other demonstrated a novel approach toward the adhesion of hydrogels using an aqueous solution of silica nanoparticles. The method involves adding a droplet of 52 wt. % silica solution (LUDOX TM-50) onto the surface of dimethylacrylamide hydrogel, followed by contact with another dimethylacrylamide hydrogel. The silica nanoparticle acted like connector between the two pieces of dimethylacrylamide hydrogel, gluing the two pieces together.<sup>54-58</sup> Under constraints, the adsorbed layers were able to reorganize, dissipate energy, and prevent interfacial fracture propagation. We envision the use of silica nanoparticles to create a nanocomposite poly(glycidol) hydrogels that possess high elasticity and toughness.

Nanocomposite poly(glycidol) hydrogels were synthesized by adding 10 wt.% silica nanoparticles to the current hydrogel formulations. 30% and 60% hydrogels with 10 wt.% silica was made initially and evaluated. The gelation times for each silica nanocomposite hydrogel was longer than that of the ordinary hydrogels. This could be due to the basic silica solution (ph 9) that was used to fabricate the silica nanocomposite hydrogels. The compressive strength and modulus

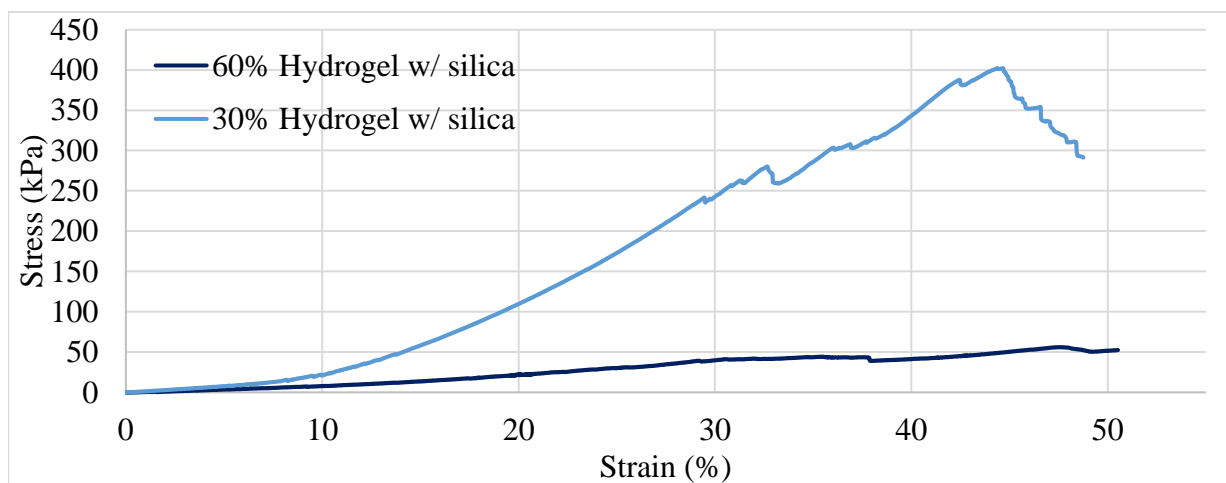


**Figure IV-10.** Stress/strain data for poly(glycidol) hydrogels made with silica nanoparticles incorporated

of the 30% and 60% nanocomposite hydrogels was far less than desired. There was a significant decrease in the strength of the hydrogel, and very little change in the strain at failure compared to the non-composite hydrogels (Figure IV-10). It was envisioned that the silica nanoparticles would serve as a glue to hold the polymer chains together and dissipate energy as the hydrogel is compressed. However, it seems as though the hydrogen bonds that are needed to have this desired effect were not formed. We suspect that the poly(glycidol) derivatives may not be as effective at forming these hydrogen bonds as we initially thought.

It was hypothesized that the hydroxy groups on the poly(glycidol) polymer can serve as good hydrogen bond donors, however the hydrogen bond acceptor ability of poly(glycidol) is less compared to that of a carbonyl group which would explain why polydimethylacrylamide worked so well compared to our poly(glycidol) system. Therefore, to test this hypothesis a series of experiments were devised where unfunctionalized poly(glycidol) was combined with silica in various weight percentages. A 30, 40 and 50 wt.% poly(glycidol) in buffer solution was combined with enough silica to produce a 10 wt.% silica polymer solution. After 48 hrs, no gelation was

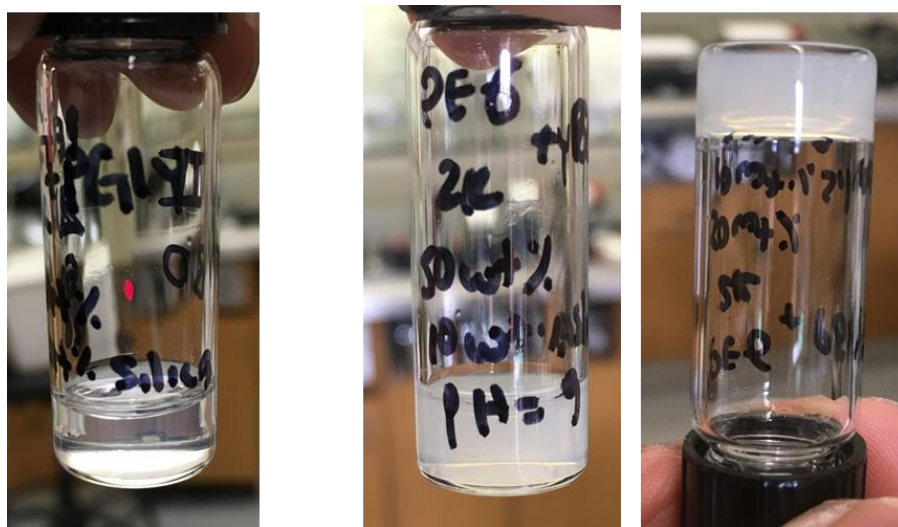


**Figure IV-11.** Showing formation of physically crosslinked network consisting of poly(glycidol) poly(ethylene glycol) and silica nanoparticles via the tilt vial method.

observed. However, when unfunctionalized poly(glycidol) was combined with polyethylene glycol in buffer, and enough silica nanoparticles was added to create a 10 wt.% silica in solution, gelation occurred after 12 hours at room temperature (Figure IV-11). The poly(glycidol)-polyethylene glycol silica nanocomposite hydrogel was based solely on the physical interactions between the polymers and the surface of the silica nanoparticles. When 30, 40 and 50 wt.% poly(ethylene glycol) was combined with 10 wt.% silica no gelation occurred. This experiment illustrates that both polyethylene glycol and poly(glycidol) was needed to form the hydrogel bonded network.

The hydrogen-bonded nanocomposite hydrogel system based on poly(glycidol) and polyethylene glycol was a lot weaker than the poly(glycidol) oxime crosslinked hydrogels. It was then envisioned that since the silica has failed to produce a highly elastic and strong hydrogel, a hybrid hydrogel system between poly(glycidol) and polyethylene glycol would produce the desired hydrogel. It was recently reported that the crosslinking of a 3 arm or 4 arm polyethylene glycol with a linear polyethylene glycol via nucleophilic thiol-yne click reaction resulted in hydrogels with high elasticity and high strength.<sup>59</sup> Hence the branched architecture of poly(glycidol) combined with the linear PEG component should give us a similar type of hydrogel network.

Linear polyethylene glycol aminoxy and ketone derivatives were synthesized by utilizing the same reaction conditions employed for the functionalization of poly(glycidol). Hydrogels were then fabricated by combining the aminoxy functionalized poly(glycidol) with the ketone functionalized linear polyethylene glycol in a 1:1 mole ratio of functional groups, at a total polymer concentration of 25 wt.%. Only 30% and 60% aminoxy functionalized poly(glycidol) was used for this experiment, while polyethylene glycol derivatives with an average molecular weight of 2000 g/mol and 4000 g/mol were used as the crosslinkers. By utilizing a linear crosslinker, the

molecular weight between the cross linkages will be significantly increased with should impart high elasticity into the hydrogel network. However, the crosslinking density will also decrease due to the significantly reduced reactive group density of the linear polyethylene glycol derivatives.

Compression studies was carried out on the poly(glycidol)-polyethylene glycol (PG-PEG) hydrogel network (Figure IV-12). The first set of hydrogels were made from 60% aminoxy-poly(glycidol) and 2000 g/mol polyethylene glycol diketone. These hydrogels had lower compressive strength, averaging 0.14 MPa, compared to 0.73 MPa for the 60% pure poly(glycidol) hydrogels. Despite the decline in strength observed for this hydrogel, the strain at failure for this hydrogel network increased by 50%. This increase in elasticity is further evident by the decrease in the compression modulus from 1.57 MPa for the pure 60% poly(glycidol) hydrogel to 0.12 MPa for the 60% poly(glycidol)-polyethylene glycol hydrogel. By increasing the molecular weight of the polyethylene glycol linker to 4000 g/mol, a greater than 100 % increase was observed in the strain at fracture followed by a significant decrease in the compression modulus. The compressive strength of these hydrogels fabricated with 4000 g/mol polyethylene glycol linkers was lower compared to the hydrogels synthesized from 2000 g/mol polyethylene glycol linkers. It should be

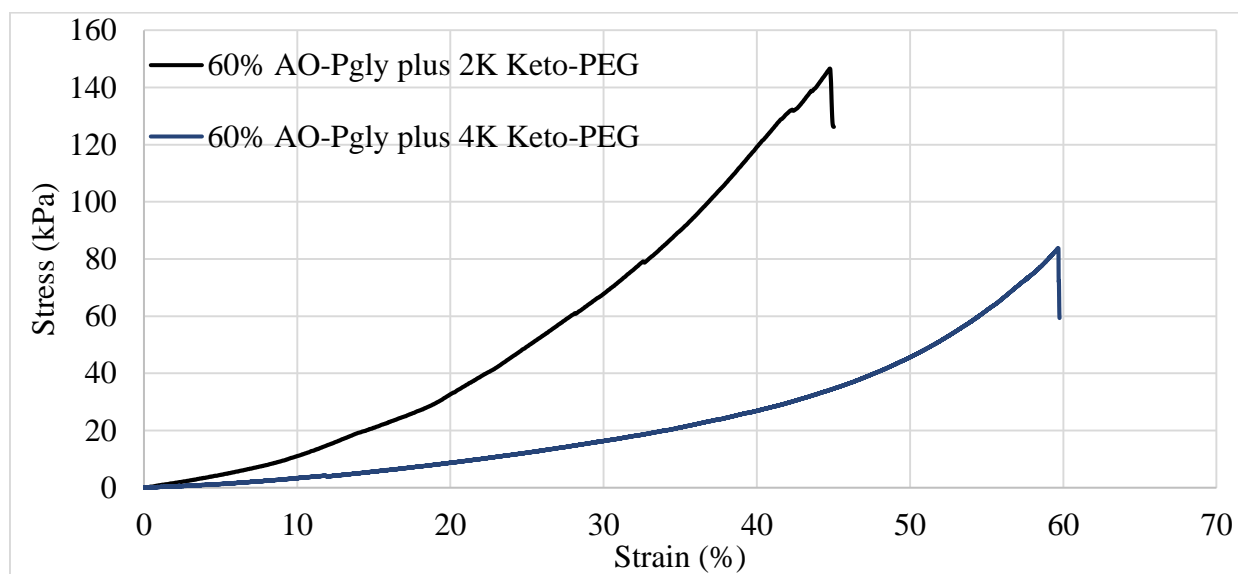


**Figure IV-12.** Stress/strain data for the 60% AO-PG with 2 and 4 kDa Keto-PEG hydrogels.

noted that great effort was required to solubilize the ketone functionalized polyethylene glycol derivatives, due to their limited solubility in buffer. This could have contributed to the significant decrease in the strength of these hydrogel system.

In an effort to circumvent the solubility challenges with the ketone functionalized polyethylene glycol, aminoxy functionalized polyethylene glycol was synthesized and combined with the ketone functionalized poly(glycidol) to make poly(glycidol)-polyethylene glycol hydrogels. Hydrogels synthesized from 60% keto-poly(glycidol) and 2000 g/mol aminoxy-polyethylene glycol showed improved strength and elasticity compared to the previous hydrogel network consisting of aminoxy-poly(glycidol) and keto-polyethylene glycol (Figure IV-13). The compressive strength of the 60% keto-poly(glycidol) - 2000 g/mol aminoxy-polyethylene glycol hydrogel was 0.22 MPa (up from 0.14 MPa) and the compression modulus was 0.23 MPa (up from 0.12 MPa). The stress at failure for the 60% keto-poly(glycidol) - 2000 g/mol aminoxy-polyethylene glycol hydrogel increased by 5% compared to the aminoxy-poly(glycidol) and keto-polyethylene glycol hydrogels. Further increases in the elasticity was observed when the molecular

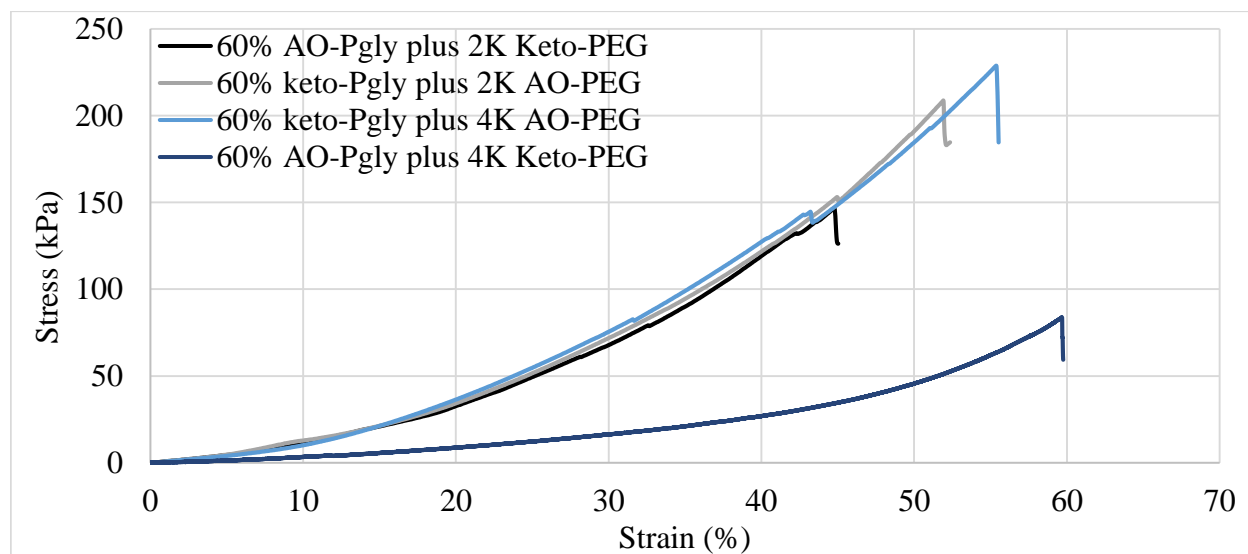


**Figure IV-13.** Stress/strain curves for poly(glycidol)-PEG Hydrogels.

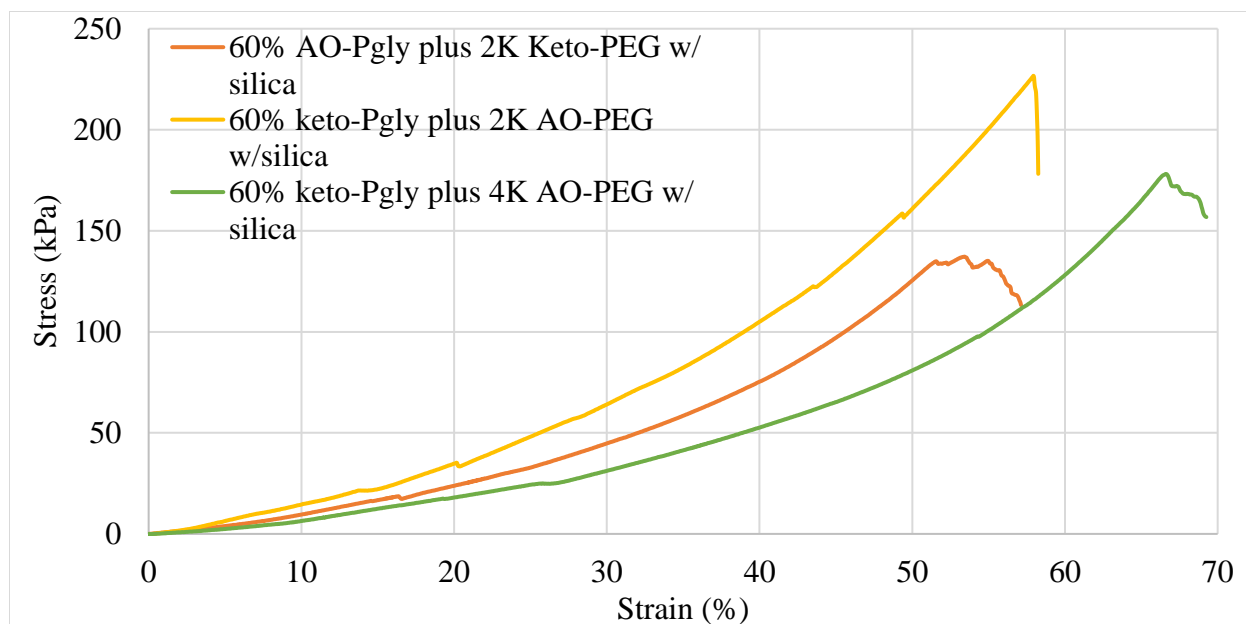


**Figure IV-14.** Stress/strain data for 60% poly(glycidol)-PEG hydrogel with 10 wt.% silica

weight of the aminoxy polyethylene glycol linker was increased from 2000 g/mol to 4000 g/mol, while the compressive strength was relatively unchanged. The increase in elasticity is due to the increase in the molecular weight of crosslinker. Silica nanoparticles were added to the current hydrogel formulations to evaluate its effects on network properties. Compression studies on these nanocomposite hydrogels showed increased elasticity compared to the non-composite hydrogel formulations (Figure IV-14). Additionally, the compressive strength of the hydrogel was statistically similar, which indicates that the crosslinking density is similar for both the silica nanocomposite and non-composite hydrogel systems. Based on these results, it seems that the silica nanoparticles were able to form hydrogel bonds which held the network together, making the networks more elastic without any loss in strength.

Hydrogels were also made from 30% keto-poly(glycidol) and 2000 g/mol aminoxy-polyethylene glycol. These hydrogels showed significantly improved elasticity with a greater than 100% increase in the strain at failure compared to pure 30% poly(glycidol) hydrogel (Figure IV-

15). The strength of these hydrogels was 50% less compared to the pure 30% poly(glycidol) oxime hydrogel network. When the molecular weight of the polyethylene glycol crosslinker was increased, the elasticity increased, as evident by the 10% increase in the strain at failure compared to the pure poly(glycidol) hydrogel network. The increase in molecular weight of the polyethylene glycol linker had no effect on the overall strength of the hydrogel. The addition of silica nanoparticles to hydrogels synthesized with both the 2000 and 4000 g/mol polyethylene glycol linkers showed a remarkable effect on the elasticity and strength of the 30% PG-PEG hybrid hydrogel network. The most significant improvement was seen in the hydrogel network fabricated with 30% keto-poly(glycidol) and 4000 g/mol aminoxy-polyethylene glycol. The addition of 10 wt.% silica nanoparticles resulted in nanocomposite hydrogels with up to 78% strain at failure, and a compressive strength of 0.3 MPa.

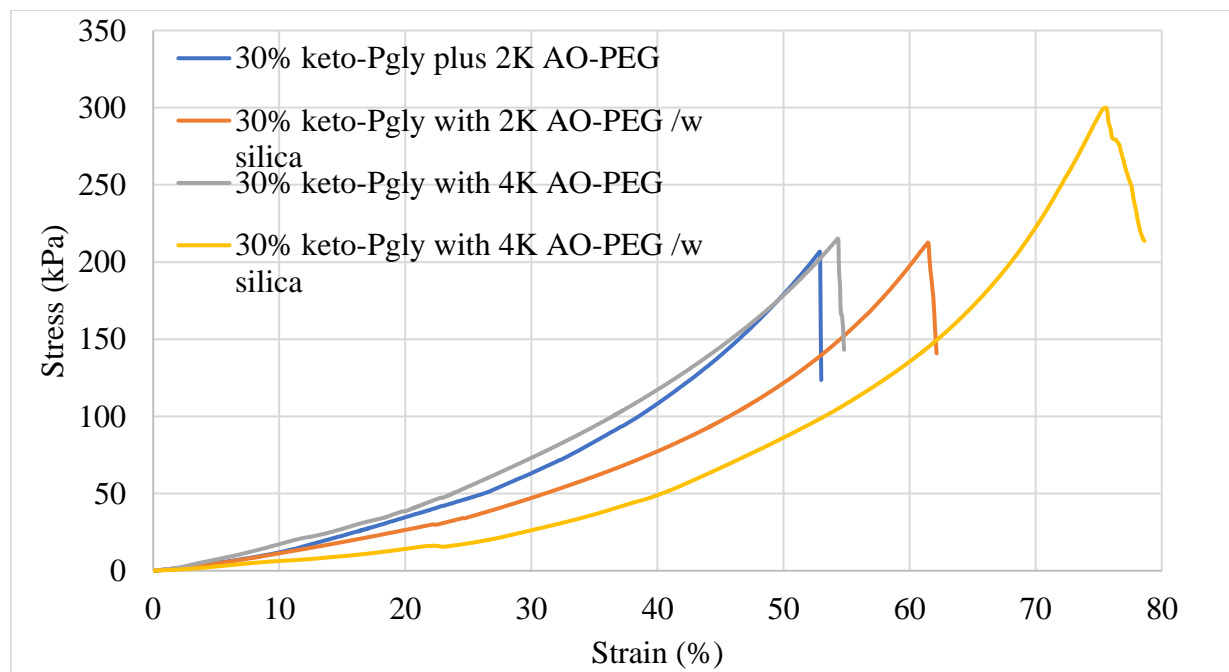


**Figure IV-15.** Stress/strain data for 30% poly(glycidol)-PEG hydrogels with and without silica nanoparticles.



From the above series of experiments, it can be concluded that the poly(glycidol)-based oxime system is very versatile, with mechanical strength and elasticity that can be tuned in various ways to suit a desired application. Furthermore, the range of mechanical strength and elasticity is similar to some biological tissues and can be implemented into tissue regenerative strategies.

### **Biodegradation Studies of Poly(glycidol) Oxime Hydrogels**

Biodegradation refers to the gradual breakdown of a material in a biological environment, mediated by a specific biological activity.<sup>60</sup> biodegradable hydrogels are an attractive approach for regenerative medicine applications because they offer a temporary support structure for encapsulated cells but can degrade as the new tissue is formed. Ideally, a hydrogel would degrade at a rate that allows it to provide adequate support to cells without restricting the production of new tissue. To determine the suitability of the poly(glycidol) hydrogel network for use as a polymeric scaffold and delivery systems in regenerative medicine application, the biodegradation of the hydrogels has to be characterized. Characterization is necessary to assess their clinical applicability. The biodegradation of hydrogels can occur via an oxidative, enzymatic and hydrolytic mechanism. The oxidative, esterolytic and hydrolytic degradation of poly(glycidol) hydrogel was explored and the results presented below.

#### **Oxidative Degradation**

The in-vivo oxidative degradation of polyether has been studied for a wide range of biomaterials containing polyether linkages. The in-vivo degradation can be replicated in vitro by using a combination of cobalt(II) chloride and hydrogen peroxide. The cobalt chloride reacts with  $H_2O_2$  via a Fenton reaction to produce reactive hydroxyl radicals. The hydroxyl radicals abstract a

proton from the methylene carbon to form which initiates the oxidation. Chain scission then occurs by radical-radical combination of the alkyl-polymer radical and another hydroxy radical to form a hemiacetal. Collapse of the hemiacetal cause chain scission and produces an aldehyde and an alcohol end groups.

The oxidative degradation of 20%, 30% and 60% poly(glycidol) oxime hydrogel were evaluated by submerging a weighted dry hydrogel sample in the oxidative media consisting of cobalt chloride and hydrogen peroxide. The three samples were then incubated at 37 °C for three to four days. The in vitro incubation of the poly(glycidol) hydrogel in oxidative media show accelerated degradation compared to buffer control (Figure IV-16). This is in agreement with previous studies reporting that polyethers undergo oxidative degradation.<sup>61-64</sup> The 20% hydrogel degraded after just 1 week while the 30% hydrogel degraded after 22 days. After 30 days, the 60% hydrogel was only 45% degraded. The faster rate of degradation for the 20% hydrogel network can be attributed to the lower crosslinking density, which makes this hydrogel more susceptible to oxidative degradation compared to the 30% and 60% hydrogel networks. This would also indicate that the rate of oxidative degradation can be tuned by varying the crosslinking density of the

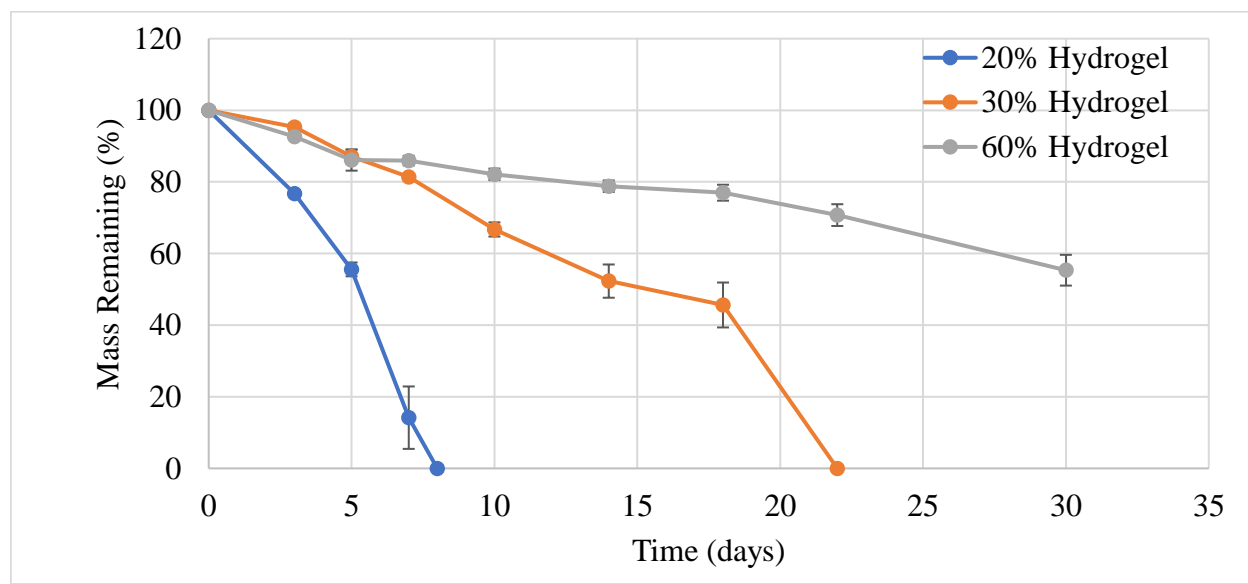


**Figure IV-16.** Oxidative degradation of poly(glycidol) hydrogels

hydrogel network. These observations suggest that in vivo, the reactive oxygen species secreted by macrophages can mediate the oxidative chain scission of the poly(glycidol) hydrogels resulting in the biodegradation of the hydrogel network.

### **Enzymatic Degradation**

The biological environment in vivo is highly complex and can allow for multiple biodegradation pathways acting in parallel or in synergy. Macrophages can secrete reactive oxygen species that can mediate the oxidative biodegradation. They can also secrete hydrolytic enzymes such as carboxyl esterases, lipase, and cholesterol esterase that can facilitate the enzymatic cleavage of ester groups. Cholesterol esterase was shown to be the most effective of the hydrolytic enzymes in the degradation of poly(ester urethanes).<sup>65</sup>

The enzymatic degradation of poly(glycidol) hydrogels was evaluated using cholesterol esterase. An enzyme concentration of 1 U/mL cholesterol esterase was used, and the media was changed every 3 to 5 days to maintain enzyme activity, verified with a nonspecific activity assay based on the enzymatic conversion of *p*-nitrophenyl butyrate into *p*-nitrophenol.<sup>66-67</sup> Enzymatic biodegradation of poly(glycidol) hydrogels mediated by the hydrolytic enzyme cholesterol esterase, show significantly slower degradation compared to oxidative biodegradation (Figure IV-17). Very little degradation was observed after 18 days. This could be due to the accessibility of the ester groups. It is envisioned however, that if the enzyme concentration was increased to 400 U/mL, a concentration that is significantly larger than the estimated physiological level, faster degradation would be observed. Hence enzymatic degradation is not only affected by the crosslinking density of the hydrogel network, but also by the concentration of the active enzyme present in solution. It should be mentioned that the initial degradation of the 60% hydrogel was

faster than then 30% and 20% hydrogel, possibly due to the higher concentration of loosely crosslinked polymer on the outside of the hydrogel. The faster gelation rate of the 60% hydrogel create inhomogeneities in the hydrogel network.

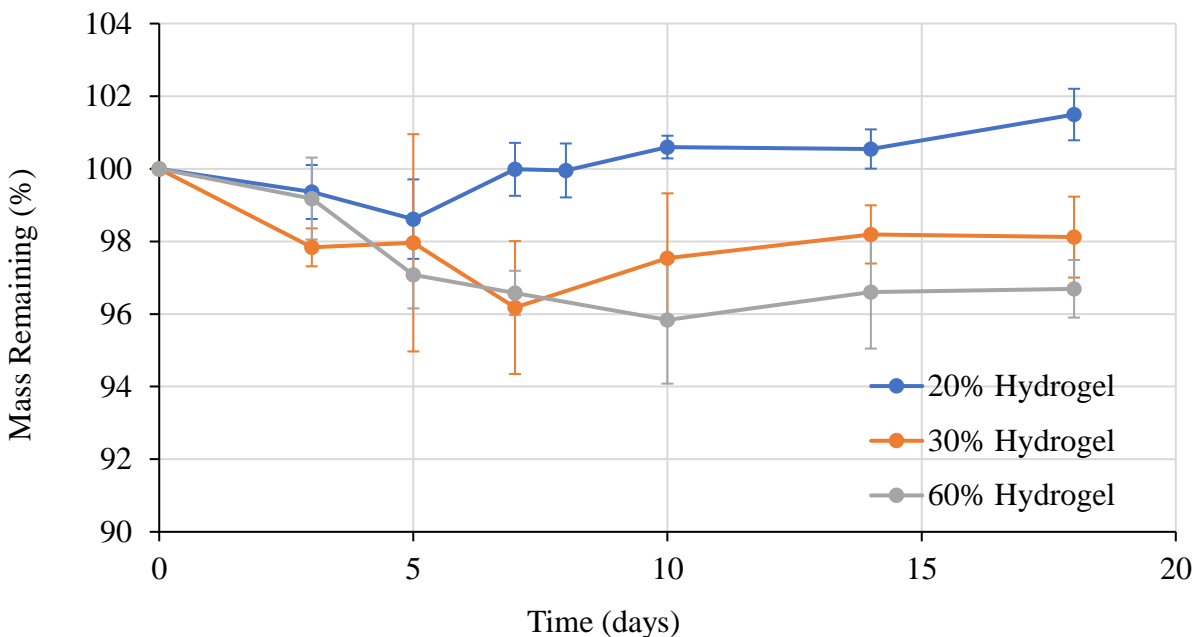


**Figure IV-17.** Showing the enzymatic degradation of various poly(glycidol) hydrogels with 1 U/mL cholesterol esterase.

### Hydrolytic Degradation

Hydrolytic degradation of the poly(glycidol) hydrogel occurs thru the cleavage of the ester linkages with water. The resulting product is an alcohol and a carboxylic acid which can then lower the pH of the medium and accelerate the rate of degradation. For this reaction, the media has to be change frequently to ensure constant degradation conditions. While, hydrolytic degradation can be mediated with enzymes, it can also occur in the absence of enzymes.

The hydrolytic degradation of the poly(glycidol) hydrogels were evaluated by soaking the hydrogels in buffer and recording the mass lost over a period of 30 days. The rate of hydrolytic

degradation was very slow for the 20%, 30% and the 60% (Figure IV-18). However, we did observe that the 60% hydrogel seems to be degrading faster than the 20% and 30%.

Given that the crosslinking density of the 60% hydrogels is higher compared to the 30% and 20% this was an unexpected observation. A similar observation was seen in the enzymic degradation of these poly(glycidol) hydrogels. In light of this result, an experiment was designed to evaluate the swelling behavior of the hydrogel as it degrades. In this experiment, the hydrogel that degrades the fastest will swell the fastest due to increases in pore size as the gel degrades. The 20% hydrogels were expected to degrade the fastest, as it possesses the lowest crosslinking density. This was observed for the 20% poly(glycidol) hydrogel network (Figure IV-19). The 30% hydrogel had a slower hydrolytic degradation rate, while the 60% hydrogel exhibited the slowest rate of hydrolysis. This observation is in agreement with previous observations which shows that hydrogels with higher crosslinking density tends to degrade slower than hydrogels with lower

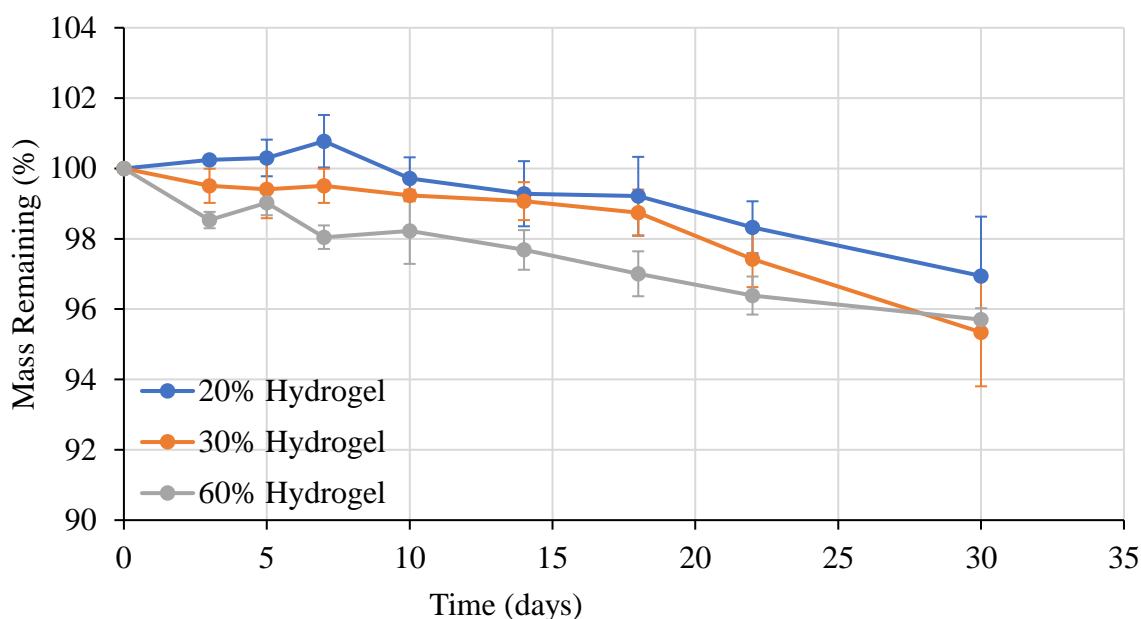


**Figure IV-18.** Hydrolytic degradation of poly(glycidol) oxime hydrogels in PBS buffer pH 7.4.

crosslinking densities. This observation also indicates that the rate of hydrolytic degradation can be tailored to changing the crosslinking density with the hydrogel network.

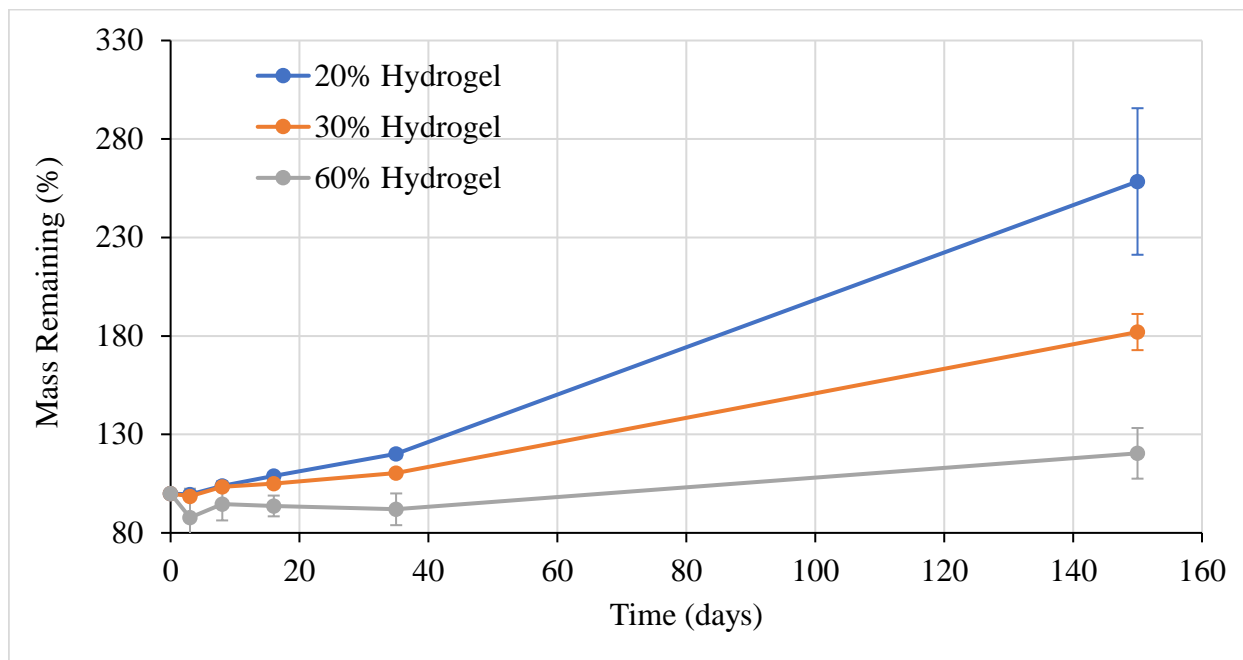


**Figure IV-19.** Changes in mass during hydrolytic degradation of poly(glycidol) oxime hydrogels

### **Biocompatibility Studies of Poly(glycidol) Oxime Hydrogels**

The ability to encapsulate cell within the hydrogel network was explored. NIH 3T3 mouse fibroblast cells were selected as a starting point due the relatively high abundance of fibroblast cells in the human body. The fibroblast cells were incubated in the presence of 20% functionalized poly(glycidol) in media at 37 °C. The gelation time was longer compared to buffer with gelation occurring within 1 hour after mixing the cells and the hydrogel precursors together. The cell laden hydrogels were incubated for 24 hrs. LIVE/DEAD staining of the cell-laden hydrogel showed that the encapsulation process had low toxicity toward these cells, as indicated by the high viability compared to control (Figure IV-20). The rounded shape of the cell indicate that the cells are not

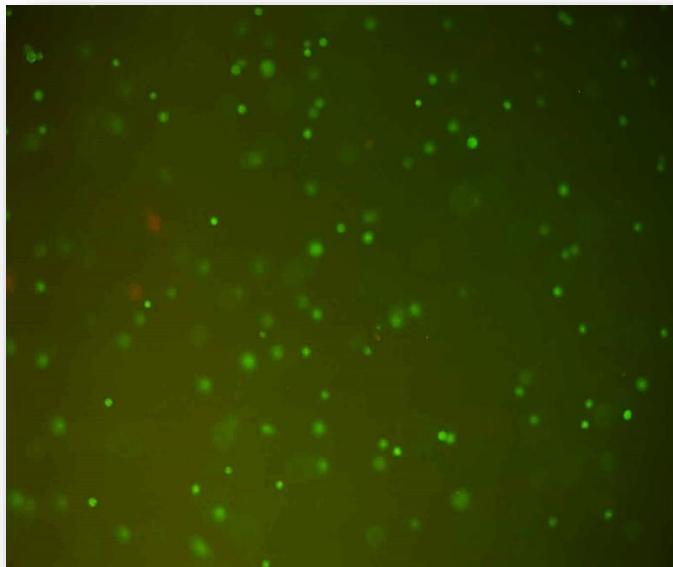


**Figure IV-20.** Fluorescent image showing LIVE/DEAD staining of the encapsulated NIH 3T3 cell after 24 h in swollen 20% poly(glycidol) hydrogel.

attaching to the poly(glycidol) hydrogel network. This is consistent with observations that poly(glycidol), like polyethylene glycol, possess cell repellent properties. In order for the cell to proliferate, peptides that can mediate cell attachment can easily be incorporated into the hydrogel network by an oxime linkage.

### **Swelling Studies of (Polyglycidol) Oxime Hydrogels**

The amount of water absorbed by the hydrogel and the amount that it is able to swell are important properties of hydrogels for use in regenerative medicine and drug delivery applications. For these applications, it is important to evaluate the ability of the hydrogel to swell and retain water as this could influence the diffusional properties of a solute through the hydrogel. The percentage swelling of a hydrogel is directly proportional to the amount of water absorbed within the hydrogel. Generally, the higher the percentage swelling of the hydrogel, the higher the water

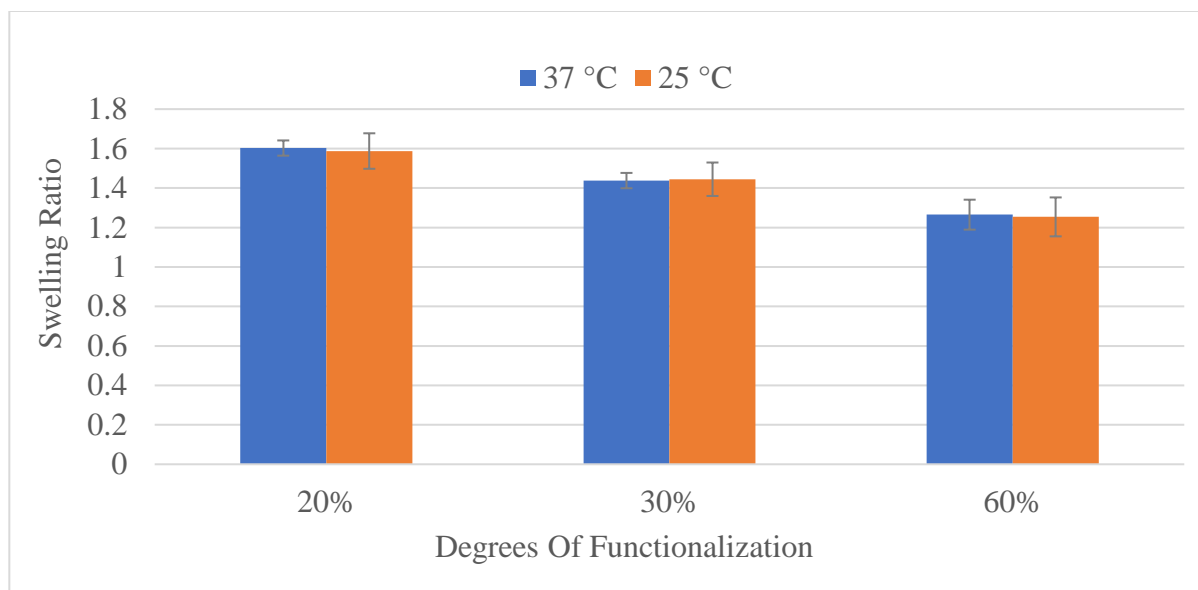


**Figure IV-21.** Showing the ratio of swelling of poly(glycidol) hydrogels.

content of the hydrogel, and hence the greater the diffusion rate into and out of the hydrogel. The water content of a series of hydrogels, with different hydrogel formulation were dividing swollen hydrogel weight by non-swollen hydrogel weight. From the results, it can be seen that as the degrees of functionalization is increased from 20% to 30% to 60% the swelling ratio decreased from 1.6 to 1.4 to 1.2 respectively (Figure IV-21). This indicates that the more tightly crosslinked the hydrogel network is the lower the equilibrium water content and swelling ratio. This result reinforces that seen during the hydrolytic degradation of the 20% hydrogel, where the degradation of the hydrogel loosens up the network crosslinks resulting in greater water content and higher swelling. These results also indicate that the swelling ratio of the hydrogels can be changed by varying the degrees of functionalization of the hydrogel precursors.

### **Protein Release from Poly(glycidol) Hydrogels**

Hence to determine the suitability of the poly(glycidol) hydrogels for the delivery of Bone Morphogenetic Protein 2, model studies using lysozyme (LYZ) and bovine serum albumin (BSA)



to evaluate protein encapsulation efficiency and release profile were performed for the 20%, 30% and 60% poly(glycidol) hydrogels (Figure IV-22). The encapsulation efficiency of the poly(glycidol) hydrogel was affected by the shrinking of the poly(glycidol) as the polymer chains came together, expelling water in the process. Upon initial gelation, 100% of both the LYZ and the BSA was encapsulated in all of the hydrogel formulations. However, after 1 hour at rt the hydrogels shrink by 5 to 10% of its initial diameter expelling water and some of the previously encapsulated protein. These phenomena accounted for the high initial release observed with LYZ and BSA.

Despite the initial burst release of proteins, due to hydrogel shrinking, the release of LYZ and BSA was significantly different. For LYZ, the change in crosslinking density of not have much of an influence on the release rate of LYZ. This observation indicates that the release of LYZ is governed solely by diffusion of the protein from the pores within the hydrogel network. According to the SEM, the pore structure within the different hydrogel formulation are very similar. Hence this explain with the release profile for LYZ form the different hydrogel formulation is so similar. BSA on the other hand did not diffuse out of the hydrogel as expected. This could be as a result of imine formation of the BSA amine groups with the ketone functionalized poly(glycidol). This was not expected as the reaction of the imine with carbonyls is slow and unstable under aqueous conditions. It could be that the hydrogel form binding pockets that helps to stabilize the formation of the protein imine linkage. Further studies are ongoing to determine the nature of the interaction between BSA and poly(glycidol) oxime hydrogels to elucidate the nature of the interaction that cause BSA immobilization in the hydrogel.

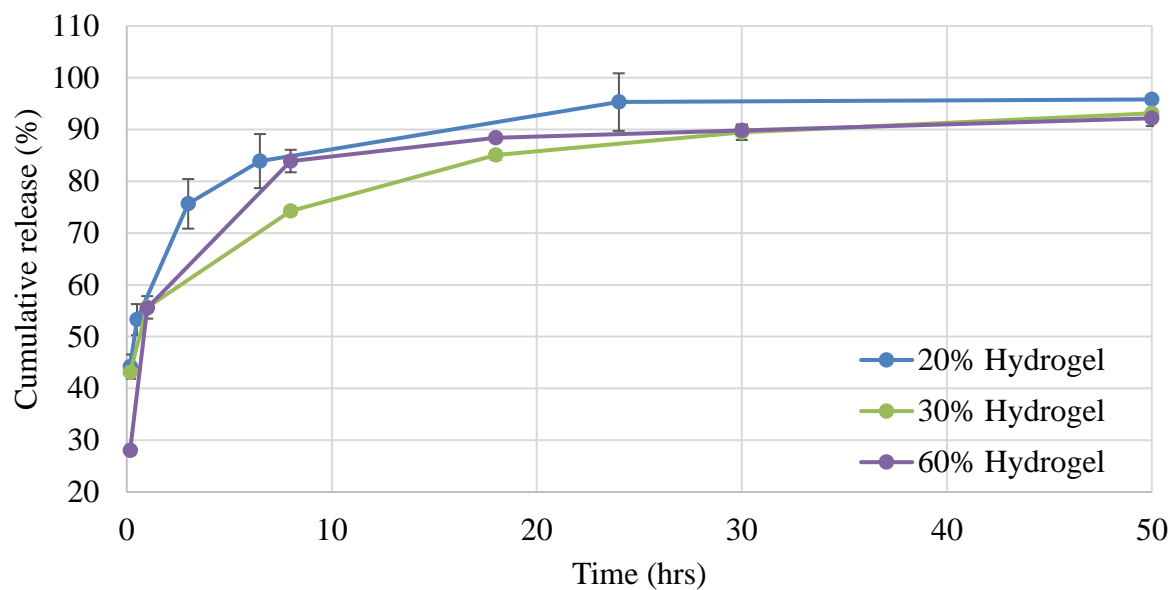


**Figure IV-22.** Showing the release of lysozyme from polyglycidol hydrogel in PBS buffer 7.4 at 37 °C.

Overall, these findings indicate that these poly(glycidol) hydrogels are promising candidates for the synthesis of a biocompatible protein delivery system.

## CONCLUSION

In conclusion, we have prepared a series of polyglycidol hydrogels by oxime bond formation. The hydrogels could be formed readily under ambient conditions and in an aqueous environment within 15 minutes, making the methodology ideal for application in regenerative medicine and drug delivery. The mechanical properties water absorption, and swelling ratio of the polyglycidol hydrogels can be tuned by adjusting the degrees of functionalization of the hydrogel precursors. The gelation kinetics can be tuned by adjusting the pH of the PBS buffer solution within a pH range that is still applicable for tissue engineering applications. The gelation kinetics was can also be tuned by adjusting the degree of functionalization of the polymer precursors. The crosslinking density of the hydrogels network was found to be tunable based on the degree of functionalization of the hydrogel precursors and the pH of the PBS buffer solution. The polyglycidol hydrogel can be made more elastic by incorporating linear polyethylene glycol precursors as well as silica nanoparticles into the system. The ability to tune the properties of the polyglycidol hydrogel in addition to the ability to encapsulate cell will allow this material to be used for stem cell therapies in a research and clinical settings.

## EXPERIMENTAL

### Materials

Glycidol (Aldrich, 96%) and N,N-dimethylformamide (Aldrich, 99.8%) was freshly distilled from calcium hydride prior to use. 3-methyl-1-butanol (Aldrich, anhydrous, 99%), Tin (II) trifluoromethanesulfonate (Strem Chemicals, 99%), methanol (Acros, anhydrous, 99.8%), dichloromethane (Aldrich, anhydrous, 99.8%), triphenylphosphine (Aldrich, 99%), N-hydroxyphthalimide (Aldrich, 97%), diisopropyl azodicarboxylate (Aldrich, 98%), and hydrazine (Aldrich, anhydrous, 98%) were used as received. Dialysis membrane were obtained from spectrum laboratories (Spectra/Por 7, molecular weight cut-off (MWCO) of 1000 Da. PTFE syringe filters were obtained from Thermo Scientific (0.45  $\mu\text{m}$ , 30 mm, Teflon plus glass). All reactions were carried out under argon unless otherwise noted.

### Instrumentation

Nuclear magnetic resonance (NMR) were acquired on a Bruker DRX-500 (500 MHz), Bruker AV-400 (400 MHz) or Bruker AV II-600 (600 MHz) instrument (equipped with a 5 mm Z-gradient TCI cryoprobe). Chemical shifts are measured relative to residual solvent peaks as an internal standard set to  $\delta$  2.50 and  $\delta$  39.52 ((CD<sub>3</sub>)<sub>2</sub>SO). Quantitative <sup>13</sup>C NMR was performed by using inverse-gated proton decoupled <sup>13</sup>C NMR with a delay time of 10 seconds. A sample concentration of approximately 150 mg/mL was used for analysis. FT-IR spectra were recorded on a Thermo Nicolet IR 100 spectrophotometer and are reported in wave-numbers (cm<sup>-1</sup>). Compounds were analyzed as neat films on a NaCl plate (transmission). Size exclusion chromatography (SEC) were performed using a Waters 1525 binary high pressure liquid

chromatography pump equipped with a refractive index detector (Waters 2414) and Styragel HR columns (7.8×300 mm Styragel HR 5, Styragel HR 4E, Styragel HR 3). SEC analysis was carried out in DMF (containing 1 mg/mL LiBr) with a flow rate of 1.0 mL/min at 45 °C. Water SEC was carried out using Waters Ultrahydrogel™ columns (7.8×300 mm, Ultrahydrogel™ 120, Ultrahydrogel™ DP 120Å, Ultrahydrogel™ 250). HPLC grade water (containing 1 mg/mL LiBr) was used as the eluent at a flowrate of 1 mL/min at 45 °C. Molecular weights ( $M_n$  and  $M_w$ ) and molecular weight distribution were calculated from poly(ethylene glycol) standards provided by Varian. Stress-strain measurements were performed using a Instron 5944 mechanical testing system.

#### **Synthesis of Branched Poly(glycidol) Homopolymer.**

Branched poly(glycidol) homopolymer was prepared using procedures similar to methods published previously.<sup>68</sup>

#### **Synthesis of Branched Poly(glycidyl aminoxy-co-glycidol) copolymer (Large Scale).**

To a 100 mL round bottom flask fitted with an argon balloon and containing a solution of branched polyglycidol (PG, 12.6 g, 3.31 mmol) in DMF (150 mL) was added N-hydroxyphthalimide (19.5 g, 119 mmol) followed by triphenylphosphine (31.5 g, 119 mmol) at rt. The reaction was cooled with an ice-bath and diisopropylazodicarboxylate (24.4 mL, 119 mmol) was then added dropwise. The resulting mixture was allowed to slowly warm up to rt and stirred for 36 hrs. The reaction was then concentrated under reduced pressure and precipitated twice in ether:ethyl acetate (1:1) to obtain 29.8 g of the desired polymer as an off-white powdery solid. <sup>1</sup>H

NMR (600 MHz, (CD<sub>3</sub>)<sub>3</sub>SO)  $\delta$  7.74-7.48 (br m, 4H), 4.86 (br s, 1H, OH), 4.50-3.31 (br m, 5H, PG-scaffold), 1.76-1.66 (m, 1H), 1.47 (q,  $J = 7.1$  Hz, 2H), 0.92 (d,  $J = 7.1$  Hz, 6H).

To a 500 mL round bottom flask equipped with a stir bar and an argon balloon was added N-oxyphthalimide poly(glycidol) (18.5 g). THF/Methanol (150 mL, (1:1)) followed by an excess of anhydrous hydrazine (9 mL, 280 mmol) was added and the reaction was allowed to stir for 18 hrs at rt. The reaction mixture was filtered through 0.45  $\mu$ m PTFE filter to remove the white solid byproduct and allowed to stir for an additional 6 hrs at rt. All volatile components were removed under rotary evaporation. The residue was suspended in methanol and filtered a second time. The filtrate was transferred to a dialysis tubing (MWCO = 1000 Da), and was dialyzed against water for 36-48 hrs. After dialysis, the product was concentrated to furnish 8.6 g of the desired polymer. <sup>1</sup>H NMR (600 MHz, (CD<sub>3</sub>)<sub>3</sub>SO)  $\delta$  4.86 (br s, 1H, OH), 4.50-3.31 (br m, 5H, PG-scaffold), 1.76-1.66 (m, 1H), 1.47 (br s, 2H), 0.92 (br s, 6H).

### **Synthesis of Levulinic acid Poly(glycidol) Derivative.**

To a 100 mL round bottom flask fitted with an argon balloon and containing a solution of poly(glycidol) (12.5 g, 3.30 mmol) in DMF (150 mL) was added levulinic acid (14 g, 119 mmol) followed by dimethyl aminopyridine (1.45 g, 11.9 mmol) at rt. Dicyclohexylcarbodiimide (24.5 g, 119 mmol) was then added to the reaction and the resulting mixture was allowed to stir for 24 hrs. The reaction was filtered to remove the white precipitate followed by dialysis in deionized water to obtain 19 g of the desired polymer. <sup>1</sup>H NMR (600 MHz, (CD<sub>3</sub>)<sub>3</sub>SO)  $\delta$  4.86 (br s, 1H, OH), 4.50-3.31 (br m, 5H, PG-scaffold), 2.49 (br s, 2H), 2.26 (br s, 2H), 1.88 (s, 3H), 1.42 (br s, 1H), 1.16 (br s, 2H), 0.64 (br s, 6H); <sup>13</sup>C NMR (600 MHz, (CD<sub>3</sub>)<sub>3</sub>SO) ppm 207.3, 172.5, 79.2, 77.8, 76.6,

74.9, 72.1, 71.4, 71.5-68.0 (br overlapping), 67.3, 65.2, 63.1, 61.2, 38.1, 37.8, 30.0, 28.1, 24.7, 21.8.

### **Hydrogel Formation.**

A 1:1 molar ratio between the side chain aminoxy and  $\gamma$ -keto ester functional groups was used for all hydrogel preparation. In a typical procedure, p(G<sup>AO</sup>-co-G) and p(G<sup>KE</sup>-co-G) were each dissolve in PBS buffer to a concentration of 250 mg/mL. 200  $\mu$ L of each derivative was added to separate side of to double syringe. The solutions were injected into a glass vial (with sigmacote) at which time gel formation was observed. The gel was then extracted from the vial for further characterization. To determine gel fraction, the synthesized gel was immersed in deionized water for three days with frequent changes. The hydrogels were then lyophilized and weighted. The gel fraction was calculated as the weight percentage of dry gel over total weight of the polymer precursors.

### **Hydrogel Water Uptake Studies.**

The prepared gels were soaked in PBS overnight immediately following their gelation. The weight was then recorded and the gels were lyophilized to dryness and the dry weight recorded. The equilibrium water content was calculated by dividing the gels total water weight by the gels total weight.

### **Hydrogel Degradation Studies.**

The prepared gels were placed in PBS pH 7.4 and incubated at 37 °C. The PBS solution was replaced every three days to prevent the build-up of solute. At pre-set time intervals, gels were

removed, blotted dry and weighted. The degradation was monitored by the percentage of weight remaining.

### **Rheological Characterization.**

To measure the time course of gelation, the gel precursor solution was injected onto the bottom plate of the rheometer. The modulus was measured under a constant strain of 1% at a frequency of 1/s at 37 °C for 10 minutes. Gels were made in triplicates.

### **Uniaxial Compressive Testing**

Stress-strain measurements were performed using a Instron 5944 mechanical testing system. The hydrogel samples were prepared in a 10 mL glass vial previously salinized with sigmacote, to prevent gels from adhering to the glassware. After 1-2 h of gelation, the hydrogels were removed and placed between two parallel platens for measurements. Each specimen had a cylindrical geometry with a diameter of 12 mm and a thickness of 7 mm. The machine was operated at a compression velocity of 5 mm min<sup>-1</sup> with a load cell of 2000 N and the force-displacement data were acquired at a frequency of 10 kHz. The elastic modulus was defined as the slope of the initial linear modulus.

### **Cell Viability and Proliferation Studies.**

The cell compatibility of the poly(glycidol) hydrogel precursors to NIH 3T3 cells was evaluated using a MTT assay. NIH 3T3 cells were purchased from Sigma Aldrich and cultured in Dulbecco's modified eagle medium with 10% bovine growth serum and 1% penicillin/streptomycin. They were cultured at 37 °C with 5% CO<sub>2</sub> using standard protocol. The



cells were seeded in a 96 well plate at a density of 7000 cell per well. After 24 hrs, 20  $\mu$ L of each poly(glycidol) hydrogel precursors was added at concentrations of 0.1, 1, 5 and 10 mg/mL. The cells were incubated for 24, 48 and 72 hrs. At the end of each time period, 20  $\mu$ L of MTT solution (5 mg/mL) was added to each well and incubate at 37 °C for 3 hours. 150  $\mu$ L of 10% sodium dodecyl sulfate was added to each well and incubate overnight at 37 °C. Absorbance was measured at 570 nm.

### **Cell Encapsulation with 3T3 cells.**

p(G<sup>AO</sup>-co-G) and p(G<sup>KE</sup>-co-G) were each dissolved in modified DMEM to a concentration of 250 mg/mL. a 200  $\mu$ L solution of each derivative was added to separate side of a double-barrel syringe. The solutions were injected into a 24 well plate. 100  $\mu$ L of DMEM containing 20,000 cells were added to each well and stirred. After gel formation, encapsulated cells were incubated at 37 °C for 24 hrs.

### **Gel Imaging.**

The cell viability was determined by a LIVE/DEAD viability/cytotoxicity kit. 1  $\mu$ L of ethidium homodimer-1 and 0.25  $\mu$ L of calcein AM from the kit were diluted with 500  $\mu$ L of DMEM to make the staining solution. Each gel was stained with 150  $\mu$ L of staining solution and incubated at 37 °C for 1 h. The stained gels were then washed with fresh medium prior to imaging with a fluorescent micro-scope. The cell viability was quantified by calculating the percentage of live cells relative to total number of cells.

## REFERENCES

1. Peppas, N.; Mikos, A., Preparation methods and structure of hydrogels. *Hydrogels in medicine and pharmacy* **1986**, *1*, 1-27.
2. Ahmed, E. M., Hydrogel: Preparation, characterization, and applications: A review. *Journal of Advanced Research* **2015**, *6* (2), 105-121.
3. Hamidi, M.; Azadi, A.; Rafiei, P., Hydrogel nanoparticles in drug delivery. *Adv Drug Deliv Rev* **2008**, *60* (15), 1638-49.
4. Hoffman, A. S., Hydrogels for biomedical applications. *Advanced Drug Delivery Reviews* **2002**, *54* (1), 3-12.
5. Wu, M.; Ni, C. H.; Yao, B. L.; Zhu, C. P.; Huang, B.; Zhang, L. P., Covalently cross-linked and hydrophobically modified alginic acid hydrogels and their application as drug carriers. *Polymer Engineering and Science* **2013**, *53* (8), 1583-1589.
6. Sun, S. H.; Cao, H.; Su, H. J.; Tan, T. W., Preparation and characterization of a novel injectable in situ cross-linked hydrogel. *Polymer Bulletin* **2009**, *62* (5), 699-711.
7. Peng, H. T.; Martineau, L.; Shek, P. N., Hydrogel-elastomer composite biomaterials: 1. Preparation of interpenetrating polymer networks and in vitro characterization of swelling stability and mechanical properties. *Journal of Materials Science-Materials in Medicine* **2007**, *18* (6), 975-986.
8. Coviello, T.; Matricardi, P.; Marianecchi, C.; Alhaique, F., Polysaccharide hydrogels for modified release formulations. *Journal of Controlled Release* **2007**, *119* (1), 5-24.
9. Wichterle, O.; Lim, D., Hydrophilic Gels for Biological Use. *Nature* **1960**, *185* (4706), 117-118.
10. Lim, F.; Sun, A. M., Microencapsulated Islets as Bioartificial Endocrine Pancreas. *Science* **1980**, *210* (4472), 908-910.
11. Ungerleider, J. L.; Christman, K. L., Concise Review: Injectable Biomaterials for the Treatment of Myocardial Infarction and Peripheral Artery Disease: Translational Challenges and Progress. *Stem Cells Translational Medicine* **2014**, *3* (9), 1090-1099.
12. Rane, A. A.; Christman, K. L., Biomaterials for the Treatment of Myocardial Infarction. *Journal of the American College of Cardiology* **2011**, *58* (25), 2615-2629.
13. Christman, K. L.; Lee, R. J., Biomaterials for the treatment of myocardial infarction. *Journal of the American College of Cardiology* **2006**, *48* (5), 907-913.

14. Wang, H. B.; Zhou, J.; Liu, Z. Q.; Wang, C. Y., Injectable cardiac tissue engineering for the treatment of myocardial infarction. *Journal of Cellular and Molecular Medicine* **2010**, *14* (5), 1044-1055.
15. Zhao, W.; Jin, X.; Cong, Y.; Liu, Y. Y.; Fu, J., Degradable natural polymer hydrogels for articular cartilage tissue engineering. *Journal of Chemical Technology and Biotechnology* **2013**, *88* (3), 327-339.
16. Ekenseair, A. K.; Boere, K. W. M.; Tzouanas, S. N.; Vo, T. N.; Kasper, F. K.; Mikos, A. G., Synthesis and Characterization of Thermally and Chemically Gelling Injectable Hydrogels for Tissue Engineering. *Biomacromolecules* **2012**, *13* (6), 1908-1915.
17. Therien-Aubin, H.; Wang, Y. H.; Nothdurft, K.; Prince, E.; Cho, S.; Kumacheva, E., Temperature-Responsive Nanofibrillar Hydrogels for Cell Encapsulation. *Biomacromolecules* **2016**, *17* (10), 3244-3251.
18. Lin, G. Y.; Cosimbescu, L.; Karin, N. J.; Tarasevich, B. J., Injectable and thermosensitive PLGA-g-PEG hydrogels containing hydroxyapatite: preparation, characterization and in vitro release behavior. *Biomedical Materials* **2012**, *7* (2).
19. Prabhakar, M. N.; Sudhakara, P.; Subha, M. C. S.; Rao, K. C.; Song, J. I., Novel Thermoresponsive Biodegradable Nanocomposite Hydrogels for Dual Function in Biomedical Applications. *Polymer-Plastics Technology and Engineering* **2015**, *54* (16), 1704-1714.
20. Klouda, L., Thermoresponsive hydrogels in biomedical applications A seven-year update. *European Journal of Pharmaceutics and Biopharmaceutics* **2015**, *97*, 338-349.
21. Khanlari, A.; Suekama, T. C.; Gehrke, S. H., Structurally Versatile Glycosaminoglycan Hydrogels for Biomedical Applications. *Macromolecular Symposium* **2015**, *358* (1), 67-77.
22. Silver, J.; Miller, J. H., Regeneration beyond the glial scar. *Nature Reviews Neuroscience* **2004**, *5* (2), 146-156.
23. Jain, A.; Kim, Y. T.; McKeon, R. J.; Bellamkonda, R. V., In situ gelling hydrogels for conformal repair of spinal cord defects, and local delivery of BDNF after spinal cord injury. *Biomaterials* **2006**, *27* (3), 497-504.
24. Van Tomme, S. R.; Storm, G.; Hennink, W. E., In situ gelling hydrogels for pharmaceutical and biomedical applications. *International Journal of Pharmaceutics* **2008**, *355* (1-2), 1-18.
25. Bryant, S. J.; Anseth, K. S.; Lee, D. A.; Bader, D. L., Crosslinking density influences the morphology of chondrocytes photoencapsulated in PEG hydrogels during the application of compressive strain. *Journal of Orthopaedic Research* **2004**, *22* (5), 1143-1149.
26. Nicodemus, G. D.; Bryant, S. J., Mechanical loading regimes affect the anabolic and catabolic activities by chondrocytes encapsulated in PEG hydrogels. *Osteoarthritis and Cartilage* **2010**, *18* (1), 126-137.

27. Peppas, N. A.; Bures, P.; Leobandung, W.; Ichikawa, H., Hydrogels in pharmaceutical formulations. *European Journal of Pharmaceutics and Biopharmaceutics* **2000**, *50* (1), 27-46.
28. Nimmo, C. M.; Shoichet, M. S., Regenerative Biomaterials that "Click": Simple, Aqueous-Based Protocols for Hydrogel Synthesis, Surface Immobilization, and 3D Patterning. *Bioconjugate Chemistry* **2011**, *22* (11), 2199-2209.
29. Kolb, H. C.; Finn, M. G.; Sharpless, K. B., Click chemistry: Diverse chemical function from a few good reactions. *Angewandte Chemie-International Edition* **2001**, *40* (11), 2004-+.
30. Hoyle, C. E.; Lowe, A. B.; Bowman, C. N., Thiol-click chemistry: a multifaceted toolbox for small molecule and polymer synthesis. *Chemical Society Reviews* **2010**, *39* (4), 1355-1387.
31. Yang, T.; Long, H.; Malkoch, M.; Gamstedt, E. K.; Berglund, L.; Hult, A., Characterization of Well-Defined Poly(ethylene glycol) Hydrogels Prepared by Thiol-ene Chemistry. *Journal of Polymer Science Part a-Polymer Chemistry* **2011**, *49* (18), 4044-4054.
32. Yang, J. Y.; Jacobsen, M. T.; Pan, H. Z.; Kopecek, J., Synthesis and Characterization of Enzymatically Degradable PEG-Based Peptide-Containing Hydrogels. *Macromolecular Bioscience* **2010**, *10* (4), 445-454.
33. DeForest, C. A.; Anseth, K. S., Cytocompatible click-based hydrogels with dynamically tunable properties through orthogonal photoconjugation and photocleavage reactions. *Nature Chemistry* **2011**, *3* (12), 925-931.
34. Grover, G. N.; Lam, J.; Nguyen, T. H.; Segura, T.; Maynard, H. D., Biocompatible Hydrogels by Oxime Click Chemistry. *Biomacromolecules* **2012**, *13* (10), 3013-3017.
35. Kim, B. S.; Im, J. S.; Baek, S. T.; Lee, J. O.; Azuma, Y.; Yoshinaga, K., Synthesis and characterization of crosslinked hyperbranched polyglycidol hydrogel films. *Journal of Macromolecular Science Part a-Pure and Applied Chemistry* **2006**, *43* (4-5), 829-839.
36. Kim, B. S.; Im, J. S.; Baek, S. T.; Lee, J. O.; Sigeta, M.; Yoshinaga, K., Synthesis of polyglycidol hydrogel films crosslinked with carboxyl-terminated poly(ethylene glycol). *Polymer Journal* **2006**, *38* (4), 335-342.
37. Gosecka, M.; Gosecki, M.; Kazmierski, S., DOSY NMR as a tool for predicting optimal conditions for hydrogel formation: The case of a hyperbranched polyglycidol cross-linked with boronic acids. *Journal of Polymer Science Part B-Polymer Physics* **2016**, *54* (21), 2171-2178.
38. Yang, Q. Z.; Fan, C. J.; Yang, X. G.; Liao, L. Q.; Liu, L. J., Facile synthesis of biocompatible polyglycerol hydrogel based on epichlorohydrin. *Journal of Applied Polymer Science* **2016**, *133* (21).
39. Wu, C. Z.; Strehmel, C.; Achazi, K.; Chiapisi, L.; Dervede, J.; Lensen, M. C.; Gradzielski, M.; Ansoerge-Schumacher, M. B.; Haag, R., Enzymatically Cross-Linked Hyperbranched Polyglycerol Hydrogels as Scaffolds for Living Cells. *Biomacromolecules* **2014**, *15* (11), 3881-3890.

40. Ndong, J. D.; Stevens, D. M.; Vignaux, G.; Uppuganti, S.; Perrien, D. S.; Yang, X. L.; Nyman, J. S.; Harth, E.; Elefteriou, F., Combined MEK Inhibition and BMP2 Treatment Promotes Osteoblast Differentiation and Bone Healing in Nf1(Osx)(-/-) Mice. *Journal of Bone and Mineral Research* **2015**, *30* (1), 55-63.
41. Mazunin, D.; Broguiere, N.; Zenobi-Wong, M.; Bode, J. W., Synthesis of Biocompatible PEG Hydrogels by pH-Sensitive Potassium Acyltrifluoroborate (KAT) Amide Ligations. *ACS Biomaterials Science & Engineering* **2015**, *1* (6), 456-462.
42. Williamson, A. K.; Chen, A. C.; Sah, R. L., Compressive properties and function-composition relationships of developing bovine articular cartilage. *Journal of Orthopaedic Research* **2001**, *19* (6), 1113-1121.
43. Chen, A. C.; Bae, W. C.; Schinagl, R. M.; Sah, R. L., Depth- and strain-dependent mechanical and electromechanical properties of full-thickness bovine articular cartilage in confined compression. *Journal of Biomechanics* **2001**, *34* (1), 1-12.
44. Mow, V. C.; Kuei, S. C.; Lai, W. M.; Armstrong, C. G., Biphasic Creep and Stress-Relaxation of Articular-Cartilage in Compression - Theory and Experiments. *Journal of Biomechanical Engineering-Transactions of the Asme* **1980**, *102* (1), 73-84.
45. Schinagl, R. M.; Gurskis, D.; Chen, A. C.; Sah, R. L., Depth-dependent confined compression modulus of full-thickness bovine articular cartilage. *Journal of Orthopaedic Research* **1997**, *15* (4), 499-506.
46. Frank, E. H.; Grodzinsky, A. J., Cartilage Electromechanics .2. A Continuum Model of Cartilage Electrokinetics and Correlation with Experiments. *Journal of Biomechanics* **1987**, *20* (6), 629-639.
47. Proctor, C. S.; Schmidt, M. B.; Whipple, R. R.; Kelly, M. A.; Mow, V. C., Material Properties of the Normal Medial Bovine Meniscus. *Journal of Orthopaedic Research* **1989**, *7* (6), 771-782.
48. Johannessen, W.; Elliott, D. M., Effects of degeneration on the biphasic material properties of human nucleus pulposus in confined compression. *Spine* **2005**, *30* (24), E724-E729.
49. Best, B. A.; Guilak, F.; Setton, L. A.; Zhu, W. B.; Saednejad, F.; Ratcliffe, A.; Weidenbaum, M.; Mow, V. C., Compressive Mechanical-Properties of the Human Anulus Fibrosus and Their Relationship to Biochemical-Composition. *Spine* **1994**, *19* (2), 212-221.
50. Iatridis, J. C.; Setton, L. A.; Foster, R. J.; Rawlins, B. A.; Weidenbaum, M.; Mow, V., Degeneration affects the anisotropic and nonlinear behaviors of human anulus fibrosus in compression. *Journal of Biomechanics* **1998**, *31* (6), 535-544.
51. Mukherjee, S.; Hill, M. R.; Sumerlin, B. S., Self-healing hydrogels containing reversible oxime crosslinks. *Soft Matter* **2015**, *11* (30), 6152-6161.

52. Han, J. Q.; Lei, T. Z.; Wu, Q. L., High-water-content mouldable polyvinyl alcohol-borax hydrogels reinforced by well-dispersed cellulose nanoparticles: Dynamic rheological properties and hydrogel formation mechanism. *Carbohydrate Polymers* **2014**, *102*, 306-316.
53. Cordier, P.; Tournilhac, F.; Soulie-Ziakovic, C.; Leibler, L., Self-healing and thermoreversible rubber from supramolecular assembly. *Nature* **2008**, *451* (7181), 977-980.
54. Rose, S.; PrevotEAU, A.; Elziere, P.; Hourdet, D.; Marcellan, A.; Leibler, L., Nanoparticle solutions as adhesives for gels and biological tissues. *Nature* **2014**, *505* (7483), 382-+.
55. Meddahi-Pelle, A.; Legrand, A.; Marcellan, A.; Louedec, L.; Letourneur, D.; Leibler, L., Organ Repair, Hemostasis, and In Vivo Bonding of Medical Devices by Aqueous Solutions of Nanoparticles. *Angewandte Chemie-International Edition* **2014**, *53* (25), 6369-6373.
56. Chen, K.; Zhang, Q. S.; Chen, B. J.; Chen, L., Nanocomposite hydrogels with rapid thermal-responsibility by using surfactant detergent as template. *Applied Clay Science* **2012**, *58*, 114-119.
57. Lin, W. C.; Fan, W.; Marcellan, A.; Hourdet, D.; Creton, C., Large Strain and Fracture Properties of Poly(dimethylacrylamide)/Silica Hybrid Hydrogels. *Macromolecules* **2010**, *43* (5), 2554-2563.
58. Rose, S.; Dizeux, A.; Narita, T.; Hourdet, D.; Marcellan, A., Time Dependence of Dissipative and Recovery Processes in Nanohybrid Hydrogels. *Macromolecules* **2013**, *46* (10), 4095-4104.
59. Macdougall, L. J.; Truong, V. X.; Dove, A. P., Efficient In Situ Nucleophilic Thiol-yne Click Chemistry for the Synthesis of Strong Hydrogel Materials with Tunable Properties. *ACS Macro Letters* **2017**, *6* (2), 93-97.
60. Williams, D. F.; Zhong, S. P., Biodeterioration Biodegradation of Polymeric Medical Devices in-Situ. *International Biodeterioration & Biodegradation* **1994**, *34* (2), 95-130.
61. Hafeman, A. E.; Zienkiewicz, K. J.; Zachman, A. L.; Sung, H. J.; Nanney, L. B.; Davidson, J. M.; Guelcher, S. A., Characterization of the degradation mechanisms of lysine-derived aliphatic poly(ester urethane) scaffolds. *Biomaterials* **2011**, *32* (2), 419-429.
62. Christenson, E. M.; Anderson, J. M.; Hittner, A., Biodegradation mechanisms of polyurethane elastomers. *Corrosion Engineering Science and Technology* **2007**, *42* (4), 312-323.
63. Christenson, E. M.; Anderson, J. M.; Hiltner, A., Oxidative mechanisms of poly(carbonate urethane) and poly(ether urethane) biodegradation: In vivo and in vitro correlations. *Journal of Biomedical Materials Research Part A* **2004**, *70a* (2), 245-255.
64. Christenson, E. M.; Dadsetan, M.; Wiggins, M.; Anderson, J. M.; Hiltner, A., Poly(carbonate urethane) and poly(ether urethane) biodegradation: In vivo studies. *Journal of Biomedical Materials Research Part A* **2004**, *69a* (3), 407-416.

65. Christenson, E. M.; Patel, S.; Anderson, J. M.; Hiltner, A., Enzymatic degradation of poly(ether urethane) and poly(carbonate urethane) by cholesterol esterase. *Biomaterials* **2006**, *27* (21), 3920-3926.
66. McBane, J. E.; Santerre, J. P.; Labow, R. S., The interaction between hydrolytic and oxidative pathways in macrophage-mediated polyurethane degradation. *Journal of Biomedical Materials Research Part A* **2007**, *82a* (4), 984-994.
67. Labow, R. S.; Meek, E.; Santerre, J. P., Model systems to assess the destructive potential of human neutrophils and monocyte-derived macrophages during the acute and chronic phases of inflammation. *Journal of Biomedical Materials Research* **2001**, *54* (2), 189-197.
68. Beezer, D. B.; Harth, E., Post-Polymerization Modification of Branched Polyglycidol with N-Hydroxy Phthalimide to Give Ratio-Controlled Amino-Oxy Functionalized Species. *Journal of Polymer Science Part a-Polymer Chemistry* **2016**, *54* (17), 2820-2825.

## CHAPTER V

### CONCLUDING REMARKS AND FUTURE DIRECTIONS

#### GENERAL DISCUSSION AND CONCLUSION

The overall aim of this research was to develop a biocompatible poly(glycidol)-based hydrogel platform that can be used for various applications in the field of regenerative medicine and drug delivery. The potential of poly(glycidol) for these application have been largely unexplored, as the fields are dominated by the use of poly(ethylene glycol). Poly(glycidol) is similar to poly(ethylene glycol), however it has many more hydroxyl groups available. All previous attempts to synthesize poly(glycidol)-based hydrogels involve the use of hyperbranched poly(glycidol) (DB = 0.55-0.70), synthesized by anionic ring-opening polymerization. However, these highly branched materials have significantly less free hydroxyl groups, available for functionalization. We presented a novel series of poly(glycidol)-based hydrogels, synthesized from branched poly(glycidol)s (DB < 0.5) with lower branching and hence more free hydroxyl groups. These lower branched polymers are synthesized using our in-house cationic ring-opening polymerization, and possesses a more linear architecture, which is advantageous for network formation.

The properties of our hydrogels reflected a significant improvement over many currently existing poly(ethylene glycol)-based network technologies. Prior to click chemistry, PEG hydrogels for regenerative medicine applications were mainly synthesized by photopolymerization of various PEG acrylate derivatives. Nguyen and coworkers<sup>1</sup> reported a comprehensive study on the mechanical properties of PEG based hydrogels synthesized from photopolymerization of



poly(ethylene glycol) dimethacrylate. They were able to modulate the mechanical properties of PEG-hydrogels by varying the molecular weight and the concentration of PEG hydrogel precursors. Our study illustrates that branched poly(glycidol) hydrogel precursors, have the ability to tailor the mechanical properties without varying the molecular weight and concentration of hydrogel precursors is one of the advantages of using poly(glycidol) as an alternative to poly(ethylene glycol). The mechanical properties reported by Nguyen and coworkers were similar to the mechanical properties of our novel hydrogels, however again we see that the range over which the mechanical properties can be tailored is larger in our hydrogel network compared to theirs. Compression modulus for PEG hydrogels varied from 0.2 to 0.7 MPa for polymers with molecular weight between 3.4-10 kDa, at concentrations of 10-40 wt. %, whereas the compression modulus of poly(glycidol) hydrogels varied from 1 to 3.5 MPa, for polymers with molecular weight between 2-4 kDa at a concentration of 25 wt. %. In addition to the mechanical properties, the structure and swelling properties of the PEG hydrogels were also modulated by molecular weight and concentration of the precursors. The swelling ratio for most of these PEG hydrogels varied from 10-30 compared to 1.3-1.6 for the poly(glycidol) oxime hydrogels. The range over which the swelling properties of the poly(glycidol) oxime hydrogels can be tuned is a lot smaller compared to most PEG hydrogels.

There are a number of other PEG-based hydrogels that have been synthesized via alkene photopolymerization. Table V-1 summarizes some of these reports, highlighting the mechanical properties of these hydrogels. By comparing the data in this table to the data in Chapter IV, we can see that the use of branched poly(glycidol) in conjunction with the oxime click reaction produced hydrogels with comparable and better mechanical properties than most PEG-based hydrogels.

**Table V-1.** Mechanical properties of PEG-based hydrogels in compression studies.

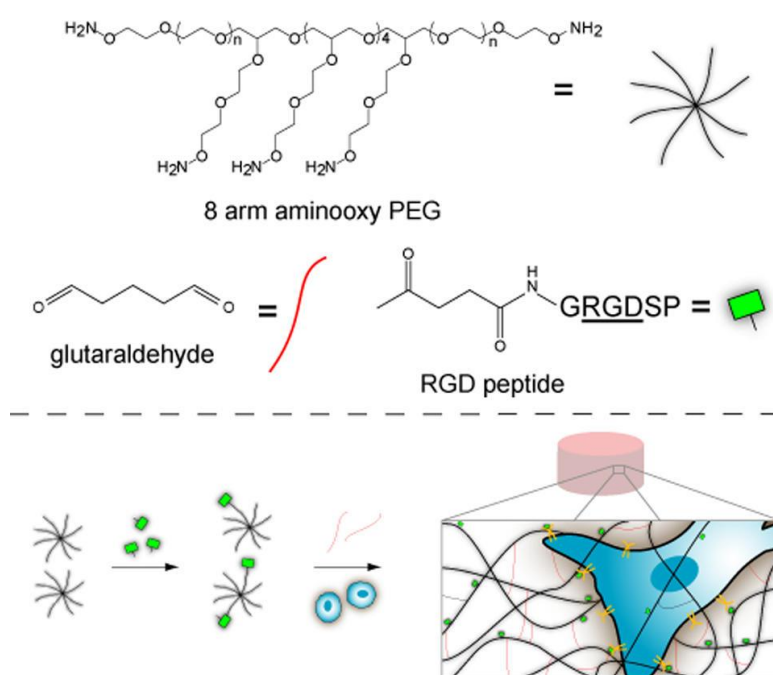
PEG Derivative	Concentration	Molecular Weight	Methods	Mechanical Property	Results
PEG-DM <sup>2</sup>	10	3000	unconfined compression testing	compressive modulus, compressive strength	0.06 MPa, 0.0084 MPa
	20	3000			0.67 MPa, 0.12 MPa
PEG-DM <sup>3</sup>	10	3400	Unconfined compression testing	Compressive modulus	0.034 MPa
	20	3400			0.36 MPa
	30	3400			0.94 MPa
	40	3400			1.37 MPa
PEG-DM and PEG-LA <sup>4</sup>	10	3000	Unconfined compression testing	Compressive modulus	0.06 MPa
	15	3000			0.17 MPa
	20	3000			0.49 MPa
PEG-DA <sup>5</sup>	15	2000	Unconfined compression testing	Compressive modulus, stress and strain at failure	0.036 MPa, 0.36 MPa, 0.71
PEG- <i>b</i> -PLA <sup>6</sup>	25	4600	Unconfined compression testing	Compressive modulus	0.25 MPa
	50	4600			0.7 MPa
	70	4600			0.9 MPa
PEG-DM <sup>7</sup>	10	4600	Unconfined compression testing	Compressive modulus	0.05 MPa
	15	4600			0.19 MPa
	20	4600			0.27 MPa

Abbreviations: PEG-dimethacrylate (PEG-DM), PEG-diacrylate (PEG-DA), PEG-lactic acid (PEG-LA), PEG poly lactic acid (PEG-*b*-PLA).

In recent years, the advent of click chemistries and PEG with multiarm, have led to the synthesis of PEG hydrogels that are more suited for regenerative medicine and drug delivery.

Maynard and others<sup>8</sup> reported the use of oxime click chemistry to synthesize PEG-based hydrogels

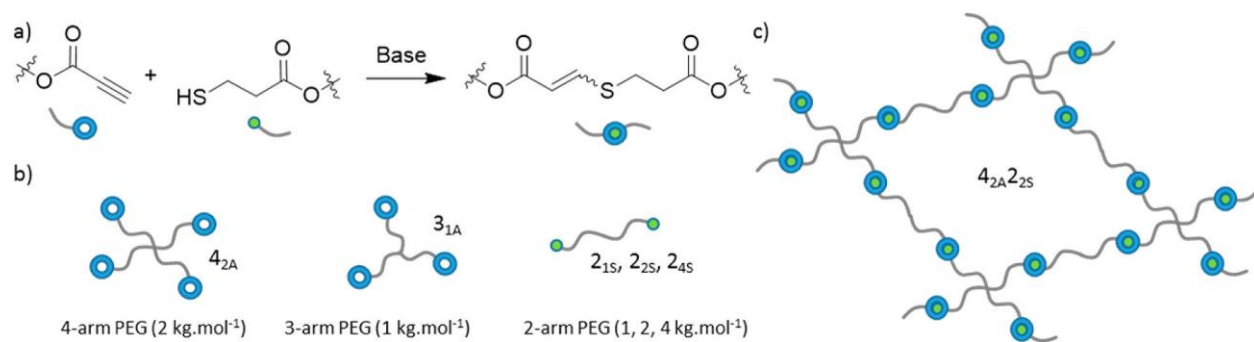
for biomedical applications. While the tunable properties of this hydrogel system were similar to the hydrogels reported here, the range over which the properties can be tuned were significantly larger. Furthermore, their use of glutaraldehyde can be detrimental to their targeted biomedical applications for example, in drug delivery, unreacted glutaraldehyde could degrade the active agents being released or alter the biological activity of the agent.<sup>9</sup> While these hydrogels are biocompatible, no degradation studies were carried out to determine their biodegradability.



**Scheme V-1.** Synthesis and Encapsulation of MSCs within RGD-functionalized Oxime-Crosslinked PEG hydrogels. Adopted from ref. 1.

Dove and others,<sup>10</sup> recently reported a series of PEG-based hydrogel synthesized by an efficient in situ nucleophilic thiol-yne click reaction. To overcome the limitation of linear PEG derivatives, they utilized multiarm PEG for hydrogel synthesis. In comparison to the branched poly(glycidol) oxime hydrogels, these PEG thiol-yne hydrogels have higher water content (90% vs 75%), and similar compressive strength (up to 2.4 MPa). The compression moduli of these



hydrogels are significantly lower due to their viscoelastic properties, while their % strain at failure were higher (> 90%) relative to the branched poly(glycidol) hydrogel. These are the strongest most elastic PEG hydrogels reported to date, and highlights the advantages of using branched polymers to access a wider range of advanced materials.



**Figure V-1.** (a) Nucleophilic base-catalyzed reaction between an alkyne and thiol; (b) Schematic of PEG precursors synthesized for crosslinking; and (c) Schematic of exemplar hydrogel networks. Ref. 10.

A little more than a decade ago, poly(glycidol) was first used to synthesize hydrogels for biomedical application. The initial set of reports, highlighted in chapter 1, utilized hydroxyl group chemistry in addition to photopolymerization to synthesize these hydrogels. While these materials had high potential for uses in regenerative medicine and drug delivery, there were a number of limitations barring their successful integration into biological systems. Table V-2 summarizes some of these limitations, and highlights how the novel branched poly(glycidol) oxime hydrogel overcomes these limitations. Overall, this is the first example of the use of click chemistry to fabricate poly(glycidol)-based hydrogels. Furthermore, these are the only poly(glycidol) hydrogels with cartilage-like mechanical properties. While oxime click chemistry has been used by different groups for PEG hydrogel fabrication, the mechanical properties of the resulting poly(glycidol)-based hydrogel are a significant improvement over currently existing PEG-based hydrogels.

**Table V-2.** Table highlighting the comparison of current hydrogel technologies to the novel branched poly(glycidol) hydrogel technology.

 Current Hydrogel Technologies	<b>Hydrogel Properties</b>	 Novel Hydrogel Technology
COMPARISON OF TECHNOLOGY		
Too high and non-tailorable	<u><i>Swellability</i></u>	Tailorable
Alkene and epoxide containing agents	<u><i>Crosslinkers</i></u>	Aminoxy and ketone containing agents
Hydroxyl group chemistry or radical polymerization	<u><i>Crosslinking Mechanism</i></u>	Oxime Click chemistry
Low strength and stiffness	<u><i>Mechanical Properties</i></u>	High strength and elasticity
Toxic byproducts hinder cell encapsulation	<u><i>Biocompatibility</i></u>	Non-toxic byproducts, water as a byproduct
Non-tailorable	<u><i>Crosslinking Density</i></u>	Tailorable

## FUTURE DIRECTIONS

### Photoacid-mediated ring-opening polymerization of glycidol driven by visible light

We seek to develop a novel methodology of visible light regulated ring opening polymerization of glycidol in the presence of reversible merocyanine-based<sup>11</sup> or similar photoacids. This will create new opportunities for the design and development of advanced polymer materials. Previous work using a reversible merocyanine-based photoacid was unsuccessful. This was attributed to the low acidity of the photoacid. As a future direction, we hope to increase the acidity of the photoacid through chemical modification, or seek out another photoacid with a pKa low enough to promote the ring opening polymerization of glycidol.

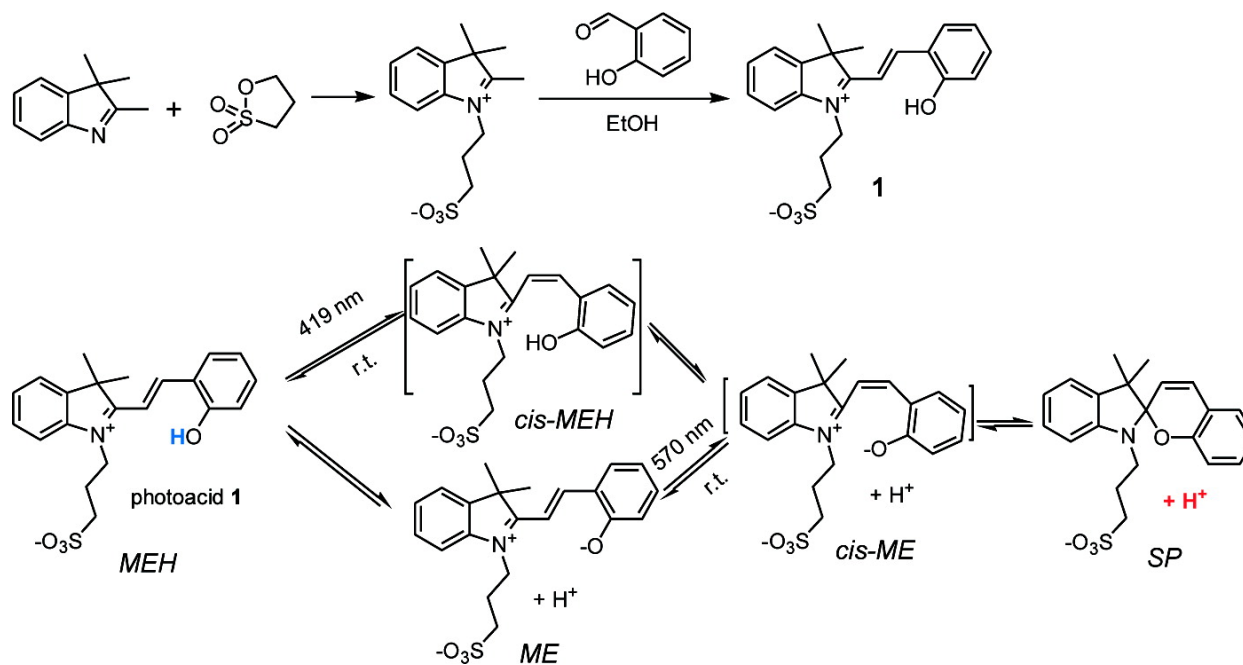


**Figure V-2.** Synthesis and photochemical reaction of the protonated merocyanine (MEH) photoacid 1.

## Poly(glycidol)-based cartilage scaffolds with tunable mechano-responsive behavior

An overriding challenge in regenerative medicine is the development of articular cartilage regenerative materials with the same or similar mechanical properties and mechano-responsive behavior as native cartilage, which allow for an ideal regeneration of the native cartilage over time<sup>12-18</sup>. Among the current difficulties are the integration of growth factors and chondrocytes in a form that can respond to mechanical load and changes in hydrostatic pressure while meeting the mechanical requirements of articular cartilage. To overcome this challenge, we will be testing and optimizing the poly(glycidol) oxime hydrogel platform in order to identify and validate a series of hydrogels which will be successful as cartilage repair materials. We will test the materials in a rabbit model to evaluate their biocompatibility and integration into the articular cartilage. The detailed tests will reveal the regrowth in the defect area, depending on the strength and elasticity of the material with and without MSC cells and growth factors incorporated (Figure V-3).

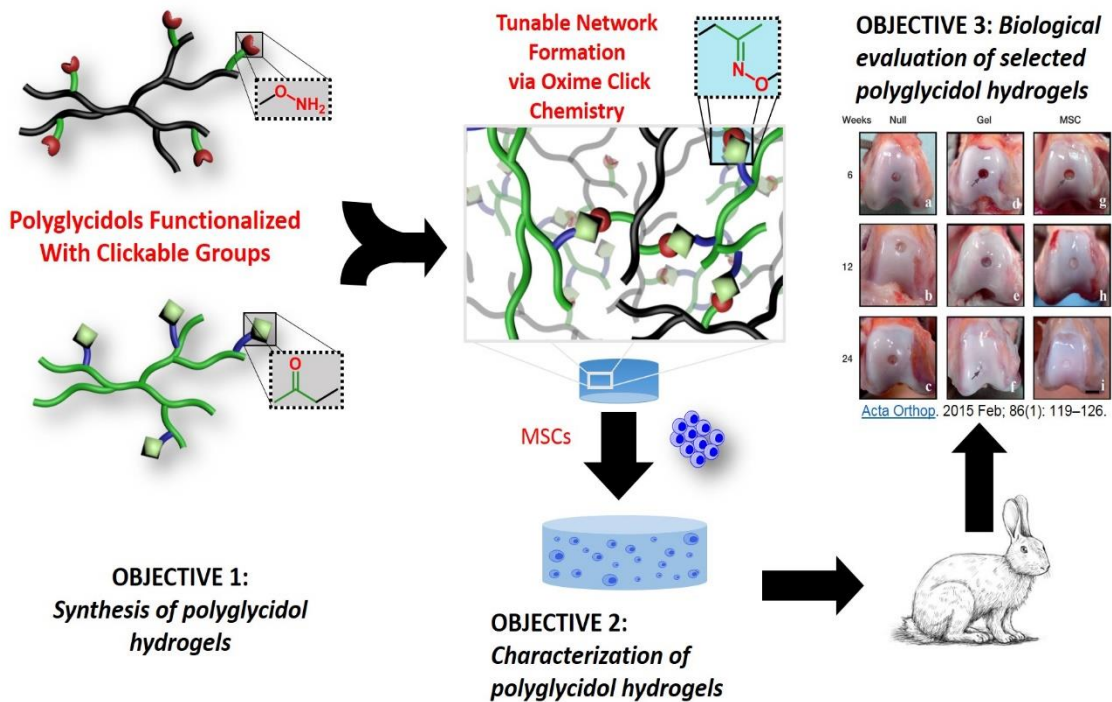


**Figure V-3.** Development of poly(glycidol) hydrogels for cartilage tissue engineering.

Furthermore, because the oxime “click” reaction works rapidly in water, another future direction of this project will involve the construction of layer-by-layer structures using hydrogel precursors with varying degrees of functionalization. These types of hydrogels with a variation in biomechanical strength will be tested to demonstrate their capability to facilitate stem cells growth and differentiation. We plan to implant three examples of the layer-by layer hydrogels, in which the basal layers will have compositions with increased intrinsic stiffness and are developed under (osteogenic) differentiation conditions that permit higher collagen I expression. The layer-by-layer materials will be easily fabricated because of the available amino-oxy and keto-groups on each fabricated hydrogel precursors.



## REFERENCES

1. Nguyen, Q. T.; Hwang, Y.; Chen, A. C.; Varghese, S.; Sah, R. L., Cartilage-like mechanical properties of poly (ethylene glycol)-diacrylate hydrogels. *Biomaterials* **2012**, *33* (28), 6682-90.
2. Bryant, S. J.; Anseth, K. S.; Lee, D. A.; Bader, D. L., Crosslinking density influences the morphology of chondrocytes photoencapsulated in PEG hydrogels during the application of compressive strain. *Journal of Orthopaedic Research* **2004**, *22* (5), 1143-1149.
3. Bryant, S. J.; Anseth, K. S., Hydrogel properties influence ECM production by chondrocytes photoencapsulated in poly(ethylene glycol) hydrogels. *Journal of Biomedical Materials Research* **2002**, *59* (1), 63-72.
4. Bryant, S. J.; Bender, R. J.; Durand, K. L.; Anseth, K. S., Encapsulating chondrocytes in degrading PEG hydrogels with high modulus: Engineering gel structural changes to facilitate cartilaginous tissue production. *Biotechnology and Bioengineering* **2004**, *86* (7), 747-755.
5. DeKosky, B. J.; Dormer, N. H.; Ingavle, G. C.; Roatch, C. H.; Lomakin, J.; Detamore, M. S.; Gehrke, S. H., Hierarchically Designed Agarose and Poly(Ethylene Glycol) Interpenetrating Network Hydrogels for Cartilage Tissue Engineering. *Tissue Engineering Part C: Methods* **2010**, *16* (6), 1533-1542.
6. Metters, A. T.; Anseth, K. S.; Bowman, C. N., Fundamental studies of a novel, biodegradable PEG-b-PLA hydrogel. *Polymer* **2000**, *41* (11), 3993-4004.
7. Roberts, J. J.; Earnshaw, A.; Ferguson, V. L.; Bryant, S. J., Comparative study of the viscoelastic mechanical behavior of agarose and poly(ethylene glycol) hydrogels. *Journal of Biomedical Materials Research Part B: Applied Biomaterials* **2011**, *99B* (1), 158-169.
8. Grover, G. N.; Lam, J.; Nguyen, T. H.; Segura, T.; Maynard, H. D., Biocompatible Hydrogels by Oxime Click Chemistry. *Biomacromolecules* **2012**, *13* (10), 3013-3017.
9. Hassan, C. M.; Peppas, N. A., Structure and Applications of Poly(vinyl alcohol) Hydrogels Produced by Conventional Crosslinking or by Freezing/Thawing Methods. In *Biopolymers · PVA Hydrogels, Anionic Polymerisation Nanocomposites*, Springer Berlin Heidelberg: Berlin, Heidelberg, 2000; pp 37-65.
10. Macdougall, L. J.; Truong, V. X.; Dove, A. P., Efficient In Situ Nucleophilic Thiol-yne Click Chemistry for the Synthesis of Strong Hydrogel Materials with Tunable Properties. *ACS Macro Letters* **2017**, *6* (2), 93-97.
11. Shi, Z.; Peng, P.; Strohecker, D.; Liao, Y., Long-Lived Photoacid Based upon a Photochromic Reaction. *Journal of the American Chemical Society* **2011**, *133* (37), 14699-14703.

12. Huey, D. J.; Hu, J. C.; Athanasiou, K. A., Unlike Bone, Cartilage Regeneration Remains Elusive. *Science* **2012**, 338 (6109), 917-921.
13. Little, C. J.; Bawolin, N. K.; Chen, X., Mechanical Properties of Natural Cartilage and Tissue-Engineered Constructs. *Tissue Engineering Part B: Reviews* **2011**, 17 (4), 213-227.
14. Kon, E.; Filardo, G.; Di Martino, A.; Marcacci, M., ACI and MACI. *J Knee Surg* **2012**, 25 (01), 017-022.
15. Vasara, A. I.; Nieminen, M. T.; Jurvelin, J. S.; Peterson, L.; Lindahl, A.; Kiviranta, I., Indentation Stiffness of Repair Tissue after Autologous Chondrocyte Transplantation. *Clinical Orthopaedics and Related Research* **2005**, 433, 233-242.
16. Mithoefer, K.; McAdams, T.; Williams, R. J.; Kreuz, P. C.; Mandelbaum, B. R., Clinical Efficacy of the Microfracture Technique for Articular Cartilage Repair in the Knee: An Evidence-Based Systematic Analysis. *The American Journal of Sports Medicine* **2009**, 37 (10), 2053-2063.
17. Camarero-Espinosa, S.; Rothen-Rutishauser, B.; Foster, E. J.; Weder, C., Articular cartilage: from formation to tissue engineering. *Biomaterials Science* **2016**, 4 (5), 734-767.
18. Sun, W.; Xue, B.; Li, Y.; Qin, M.; Wu, J.; Lu, K.; Wu, J.; Cao, Y.; Jiang, Q.; Wang, W., Polymer-Supramolecular Polymer Double-Network Hydrogel. *Advanced Functional Materials* **2016**, 26 (48), 9044-9052.